A Tribological assessment of the porous coated anatomic total hip replacement

Alistair Philip David Elfick

A Tribological Assessment of the
Porous Coated Anatomic Total Hip Replacement

by

Alistair Philip David Elfick, BSc MSc

Submitted for the degree of Doctor of Philosophy.

University of Durham,
Centre for Biomedical Engineering,
School of Engineering

January, 1999

Acknowledgements

Abstract

The tribological performance of internal joint prostheses is a fundamental influence on their longevity. The aim of this study is to characterise the tribological performance of the Porous Coated Anatomic total hip replacement by the analysis of 119 explanted prostheses. Investigations of the friction, wear, surface topography and wear debris were made and related to the joint's clinical performance.

The friction of the joints at explant was similar to that of new prostheses. The median total wear volume ($419mm^3$) was found to agree with previous wear studies suggesting the existence of a threshold wear volume which promotes osteolysis. Clinical wear factor for the whole cohort matched that of alternative joint designs.

The femoral head finish was shown to degrade but not in proportion to implant duration. The roughness of the UHMWPE liner was shown to fall but no relationship with any head roughness, or temporal, parameter could be distinguished.

Simulator studies confirmed that the wear factor of a joint is likely to change over its lifespan. Wear models published previously describing the influence of femoral head roughness on wear could not predict the performance of explanted prostheses. An alternative relationship was observed indicating that head roughness is not as powerful a predictor of wear as previously held.

A novel technique for the characterisation of the size distribution of *ex vivo* and *in vitro* wear debris was developed. A Low-Angle Laser Light Scattering Particle Analyser was used to size particles continuously over a range from 0.5 to 1000μm. This technique offers considerable improvement over existing microscope-based methods in terms of the detail of the information and does so with less experimental effort. It was shown to be highly accurate and repeatable in preliminary investigations. Case studies of five tissue samples revealed the potential of this method.

Contents

7. REFERENCES   145

8. APPENDICES

List of Figures

List of Tables

Abstract

A_p	Age at primary surgery (years)
A_r	Age at revision surgery (years)
CDH	Congenital Dysplasia of the Hip
d	Particle diameter – Stoke's equation (m)
DIC	Differential Interference Contrast microscopy
DSC	Differential Scanning Calorimetry
ECD	Equivalent Circle Diameter
EDAX	Energy Dispersive X-ray Analysis
f	Friction factor
F_F	Frictional force (N)
FTIR	Fourier Tranform InfraRed spectroscopy
g	Acceleration due to gravity (ms^{-2})
H	Hardness
^{3}H-TdR	^{3}H-Thymidine
IL-1	Interluekin 1
IL-6	Interluekin 6
JRF	Joint reaction force (N)
k	Wear factor (mm^3/Nm)
k_{clin}	Clinical wear factor (mm^3/Nm)
l	Penetration depth (mm)
L	Load (N)
LDH	Lactose DeHydrogenase
MNGC	Multi-Nuclear Giant Cell
N	Number of wear cycles
OA	Osteoarthritis
PCA	Porous Coated Anatomic
PGE_2	ProstaGlandin E_2
PMMA	PolyMethylMethAcrylate
r	Radius (mm)
RA	Rheumatoid Arthritis
R_N	Normal reaction force (N)
S	Sliding distance (m)
SEM	Scanning Electron Microscopy
T	Torque (Nm)
TEM	Transmission Electron Microscopy
THR	Total Hip Replacement
TKR	Total Knee Replacement
TNFα	Tumour Necrosing Factor α
u	Entraining velocity (ms^{-1})
u_s	Terminal velocity of particle in suspension - Stoke's eqn. (ms^{-1})
UHMWPE	Ultra-High Molecular Weight Polyethylene
W	Patient weight (N)
z	Sommerfeld parameter

ΔV	Wear volume (mm^3)
α	Wear angle relative to anatomical axes
β	Wear angle relative to open face of acetabular socket
γ	Angle between wear angle (α) and the joint reaction force (JRF)
ρ_s	Density of solid in Stokes equation (kg/m^3)
ρ_f	Density of fluid in Stokes equation (kg/m^3)
ε_u	Elongation at failure
η	Viscosity (Pa s)
μ	Co-efficient of friction
σ_u	Ultimate tensile strength (Pa)

* For abbreviations and definitions of topographical parameters see Appendix 3.

1.   Introduction

Arthritis of the hip, be it rheumatoid or osteoarthritis, is a profoundly debilitating condition. Those who suffer from this disease experience considerable pain both during motion and at rest. This toothache-like pain often leads to disrupted sleep patterns and immobility. Concurrent with the pain is a loss of mobility of the joint, creating difficulty with activities such as the clipping of toenails. Unfortunately the damage to the joint which causes the pain is irreversible and conservative treatment with analgesics, steroids, synovectomy and so on, can only serve to alleviate the symptoms.

Joint replacement surgery is by no means a recent development, however the advances in the last 30 years have transformed total hip replacement (THR) into possibly the most common and successful orthopaedic surgical procedure. Part of the success of THR has been in the refinement of the surgical procedures involved to the point were they become accessible to all orthopaedic surgeons. At present in excess of 50,000 primary THR operations are conducted each year[1]. THR replaces the damaged articulating joint surfaces with neuropathologically inert biomaterials. This is intended to relieve the patient from all joint pain. Whilst providing relief from pain and restoring the patient's quality of life, THR also has secondary benefits. It has been observed by Ries *et al.*[2] that the cardiovascular fitness of recent THR recipients increases.

Unfortunately THR is not an absolute solution to the difficulties associated with arthritis, nor is it permanent. For reasons reviewed extensively in Chapter 2 the prosthesis may become loose. If this happens the joint will become painful and is considered a clinical failure. The only solution in this situation is to re-operate and replace the prosthesis. The increase in the numbers of revision procedures performed has important implications for the health care providers. Whilst the cost of the implants used varies little from primary to secondary procedure, the cost of the revision procedure is approximately 40% higher[3]. This is due to the longer operating time and hospital stay, the increased risk of complication, greater post-operative care demands and so on.

There is therefore a strong motivation in terms of economics and patient benefits for reducing revision rates. Wroblewski[4] recently reported that 50% of all Charnley LFA THRs performed at Wrightington Hospital were revision procedures. If the longevity of the primary operation could be optimised the number of costly revision procedures required could be minimised. The prostheses removed at revision surgery hold a vast amount of information on the processes of wear in the body. It is essential that this reservoir of knowledge is fully exploited. The belief that these are failed joints and therefore should be neglected is short-sighted, as is any assertion that joints which are no longer manufactured are not worth studying. It may be argued that the joints that perform inadequately, the failures both clinically and commercially, are precisely the joints to study in order to gain insight into their shortcomings.

The joint on which this thesis focuses is the Porous Coated Anatomic THR (Howmedica, Rutherford, New Jersey). This joint displays a number of developments over the more traditional Charnley prosthesis (both these joints are described in Section 2.3). It is the affect that the subtle variations in design have on the joint's performance which it is the aim of this study to elucidate.

A comprehensive tribological study (from the Greek, tribein, to slide) was undertaken on the PCA prosthesis. This comprised investigations into the wear, friction and lubrication, surface topography and wear debris. The results obtained were analysed and compared to those of the Charnley LFA THR. The Charnley was chosen primarily because it represents an opposing approach to addressing the demands of THR. Also it has been adopted as the industry benchmark and as such has been extensively studied.

2. Literature Review

2.1 Preamble

Sir John Charnley wrote in the British Medical Journal[5] that:

> "This type of surgery (arthroplasty) demands a training in mechanical techniques which, though elementary in practical engineering, are as yet unknown in the training of a surgeon."

His call for a better understanding of "mechanical techniques" might be countered that in order for the optimisation of the THR to continue it is important that the engineer should have an appreciation of cellular biology, anatomy and physiology. Only then shall we master the effect of the complex biological environment in which the THR must perform and the consequences of its presence to the host.

As such this literature review will first investigate the many modes of failure experienced clinically and the mechanisms by which they occur. Attention will then be focused on the two joints which are to be considered in this thesis. A brief overview of the Charnley low-friction arthroplasty will be followed by a more comprehensive study of the PCA hip replacement.

At this point an introduction into the tribology of total hip replacement will be undertaken, followed by a review of the various measurement techniques used to assess the tribological performance of hip joints.

2.2 Motivation for Study

2.2.1 Clinical Failure of the Prosthesis

To deduce which engineering parameters are important in increasing the longevity of THR's we must consider the modes of failure of the joints. The clinical failure of a THR may be defined as the point at which surgical intervention becomes necessary. The reasons for these failures are many and varied. If we discount the few joints revised for sepsis or incorrect implantation, then pain, wear, loosening and bone loss are the principal indicators. These four factors are all interrelated, for example a

3

microscopically loose prosthesis will be painful and would be revised for persistent pain where loosening was the root cause.

The greatest challenge facing contemporary THR is bone resorption, or osteolysis. This is the process by which the bony support necessary for the fixation of the prosthesis is removed. The importance of this condition is twofold, not only compromising the fixation of the present prosthesis, but also that of any subsequent joints.

Two distinct modes of bone loss exist - diffuse or linear, and focal or localised. The typical radiographic appearance of diffuse osteolysis is shown in Figure 2.1. A characteristic feature is the appearance of a slowly progressing radiolucent line around the prosthesis. This form of bone loss is usually associated with a loose prosthesis and therefore pain. Focal osteolytic lesions, as seen in Figure 2.2, may be present despite the patients being asymptomatic and having a well fixed prosthesis.

The observation of bone loss is well documented with Charnley et al.[6] attributing the massive focal bone loss he experienced to sepsis, despite an inability to culture any bacteria from the lesions. The frequency of small, slowly progressing, focal lytic lesions was noted by Jasty et al.[7] in association with well fixed cemented THRs. This became of increasing concern in cemented femoral components as observed by Maloney et al.[8] and Anthony et al.[9]. However, it has become apparent that the occurrence of focal osteolytic lesions is not limited to cemented THR. Santavirta et al.[10,11] described the observation of rapidly progressing "aggressive granulomatous lesions" around cementless prostheses. Attention has since become focused upon cementless femoral components[12]. Focal osteolytic lesions are more common around cementless acetabular components than their cemented counterparts which seem more prone to linear osteolysis[13]. It is therefore clear that osteolysis is a complex condition with distinctive characteristics which can affect any type of prosthesis.

The observation of osteolysis and the increasing threat that it poses to the longevity and continued development of THR have resulted in considerable research focused on the causes of bone resorption. There has been much debate over the stimulus for the resorption of bone and the responsible mechanism. Here the evidence, and the conflicting hypotheses, are investigated.
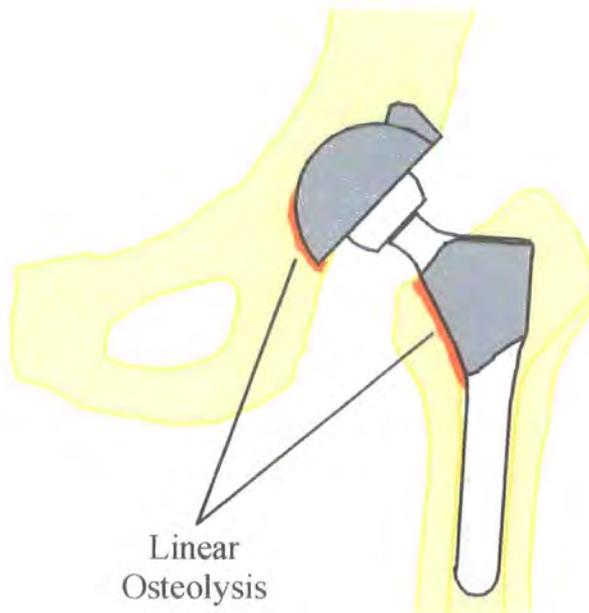
Figure 2.1:   Schematic diagram of linear osteolysis.
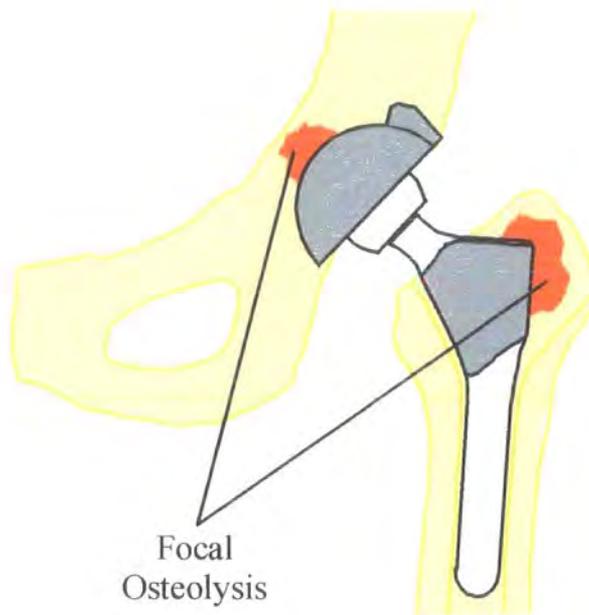
Figure 2.2:   Schematic diagram of focal osteolysis.

2.2.2   Biologically Mediated Bone Loss

Since osteolysis was first reported there has been a growing circumstantial link between bone loss and wear debris. The early hypothesis that osteolysis was caused

as a reaction to PMMA debris, the infamous "cement disease" as it was christened by Jones and Hungerford [14], has been replaced by a growing body of evidence linking all types of wear debris with osteolysis.

All the materials used in total joint replacement have been thoroughly screened for biocompatibility and are inert in their bulk form. However the body's reaction to these materials in particulate form may be very different from that of the bulk. This phenomenon is not without precedent. The reaction of the lung to dust has been studied extensively. The alveolar macrophage is the principal mediator in the tissue response seen in the lung. It has been shown that the composition, morphology, size and number of particulates all influence the response of the macrophage. The release of cellular factors by the alveolar macrophage provokes fibrosis, vascular proliferation and cell necrosis.
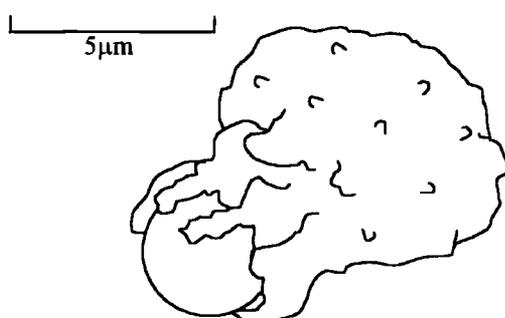
Figure 2.3:   The process of phagocytosis. A macrophage engulfs a yeast cell.

Histological studies of the periprosthetic tissue in THR has shown the presence of particulate wear debris in both well fixed and loose prostheses. The wear debris is observed to reside both in the extracellular fibrous stroma and intracellularly in the cytoplasm of defensive cells. A summary of studies into the histological observations of clinically retrieved tissue is shown in Table 2.1. These defensive cells, or macrophages, are cells with the ability to ingest matter. The function of the macrophage in the body's cellular defence system is to ingest bacteria, dead cells and other foreign particles in order to digest, or dispose, of them. The process of ingestion, or phagocytosis, involves the macrophage extending pseudopodia to wrap around the foreign body and enclose it (Figure 2.3)[15]. Once the particle is ingested the macrophage will attempt to digest it using digestive enzymes, called lysosomes[16]. In the case of the wear debris the lysosomes produced have no effect on the particle

and it will reside in the cytoplasm indefinitely. However, the presence of the intracellular debris will not deter the macrophage from continuing to phagocytose additional particles.

Author	Tissue	Technique	Debris Observed	Effects Observed
Agins et al. 1988 [17]	Periprosthetic	Optical microsc. & atomic absrop. spectroscopy	PMMA, UHMWPE & Ti/6Al/4V	Implant loosening
Bos et al. 1995 [18]	acetabulae at post-mortem	Optical microsc.	PMMA, UHMWPE, metal & ceramic	Thickness of membrane correlated with no.s of particles
Jasty et al. 1986 [7]	Lytic zones	Optical microsc.	PMMA	Bone lysis
Santavirta et al. 1990 [10]	Periprosthetic	Optical microsc.	UHMWPE	Granulomatous lesions
Schmalzried et al. 1992 [19]	Interface lytic zones	Optical & TEM	UHMWPE, cytoplasmic birefringence	Bone resorption, implant loosening
Wang et al. 1996 [20]	periprosthetic metal/metal joint	Optical microsc.	intracellular metal and PMMA	Response less severe than metal on UHMWPE

Table 2.1:   Clinical studies of tissue response to particulates.

Most of the studies in Table 2.1 have utilised standard histological methods to assess the specimens. However, the resolution of the optical microscopes involved will not allow the identification of particles less than approximately 5µm in size. As will be seen in Chapter 2.5.3 the modal size of polyethylene wear debris produced in THR is approximately 0.4µm. Therefore, we may speculate that many of the early investigations into the link between wear debris and osteolysis may have provided false negative, or at least no strong positive, correlation between UHMWPE debris and osteolysis. Schmalzried et al.[19] noted a "cytoplasmic birefringence" and using transmission electron microscopy confirmed that this was due to the presence of intracellular UHMWPE particles of less than one micron in size. Clearly, there is

conclusive evidence that UHMWPE particles infiltrate the pseudocapsule and reside in the fibrous stroma until they are ingested by macrophages.

If we consider the size of the wear debris once more, we can determine that whilst the modal size was indeed 0.4μm the presence of particles as large as 100μm was noted. The maximum size of polymer particle which a mononuclear macrophage can phagocytose is of the order of 10μm[21]. Larger particles, and aggregates of smaller particles, were shown by Howie *et al.*[22] to be found within multinuclear giant cells (MNGC's), or surrounded by MNGC's. MNGC's are a type of macrophage which may be created by either macrophage mitosis in the absence of cytogenesis, or by the fusion of newly arrived monocytes with ageing macrophages[23]. The ratio of MNGC's to macrophages present in the periprosthetic tissue is directly related to the size distribution of the particles found in the tissue. Schmalzried *et al.*[24] demonstrated that in THR the cellular reaction was dominated by monocytes, whereas in TKR the reaction was characterised by a much greater proportion of MNGC's. This was attributable to the wear debris of TKR being of a larger size due to the non-conforming nature of the articulation. Schmalzried *et al.*[19] had previously observed a variability in the number of macrophages present depending on the type of osteolysis, the regions of linear bone loss had a ratio of macrophages to fibroblasts of 1:20, whilst in the lytic lesions he observed a ratio of 20:1.

Notable by their absence from the histological studies of periprosthetic tissue were lymphocytes[19]. These are the cells employed by the immune system to respond to objects recognised as invaders. Santavirta *et al.* observed that the periprosthetic lesion abounded in macrophages, with fewer fibroblasts and very few lymphocytes[11]. This prompted work revealing that wear debris is immunologically inert, soliciting no reaction from cultured human lymphocytes[25]. Similarly Jasty *et al.*[26] using mice with varying degrees of immuno-incompetence showed a similar reaction to a subcutaneous injection of PMMA powder regardless of the degree of immunodeficiency. It is safe to conclude that the response observed in conjunction with wear debris is a severe foreign-body reaction and not an immunological response.

We have established a link between the occurrence of osteolysis and the presence of wear debris, and we have seen that the size of the particle is important to the type of

cell recruited. Why then is the ingestion of particles, and the resultant foreign-body reaction, responsible for the resorption of the adjacent bone and what is the mechanism by which the bone resorption happens?

2.2.3 Why does phagocytosis stimulate osteolysis?

Firstly let us consider why the phagocytosis of particles by macrophages stimulates osteolysis. There are two proposed theories: that the inability of the cell to digest the particles and resultant increasing volume of particles causes the stimulation of osteoclastic activity, or that the recruitment of vast numbers of macrophages requires space which is made by the removal of bone. However before we can investigate this point we must take a brief aside in order to consider how it is possible to assess the macrophage's response to ingesting particles.

2.2.4 Cell Viability and Signalling

Cells, like any living organism, must absorb and secrete chemicals in order to remain healthy, or to communicate with neighbouring cells. It is this phenomenon which allows the appraisal of the cell's viability (or health) and the impact of phagocytosing particulates. The first factor of interest is lactose dehydrogenase (LDH), an intracellular enzyme which is leaked as a result of cellular damage[27]. Also capable of assessing cell viability is ^{3}H-Thymidine (^{3}H-TdR) uptake. This factor is used by cells to create DNA[28]. An important set of factors are known as interleukins, especially IL-1 and IL-6. These lymphokines have a number of roles in immunology, but they are important as mediators of bone resorption[29]. However, bone resorption is believed to be controlled principally by tumour necrosing factor, or TNFα[30]. This cytokine is secreted mainly by macrophages and is also an important component of the complex regulatory system governing immune response and inflammation[15]. Finally, prostaglandin E_2 (PGE$_2$) has been shown by Vaes[31] to stimulate osteoclastic bone resorption.

2.2.5 Cellular damage or mis-communication?

Returning to the question of why the phagocytosis of debris stimulates osteolysis, there is now a substantial body of information on the effect of particle ingestion. A summary of some of this is shown in Table 2.2. The work of Murray et al.[27] indicates that UHMWPE and PMMA are inert at low doses displaying little cellular response. However, the levels of LDH secreted become significant at higher particle concentrations. They concluded that the increase in LDH was not attributable to cell damage but instead was a consequence of leakage as a result of membrane perturbations during phagocytosis. Further, it is shown that different species of particle provoke a different intensity of response. Very high concentrations of latex are required to illicit a cellular reaction, moderate amounts of PMMA and UHMWPE but only small amounts of zymosan, which is considered to have a inflammatory effect. Shanbhag et al.[28] however attributed a decrease in the uptake of ^{3}H-TdR at high particle doses to cellular damage. Also of note in the study of Shanbhag et al.[29] was the effect of particle size. Lower levels of IL-1 were observed for titanium dioxide particles of 0.15μm and 0.45μm than that of 1.76μm particles at the same dose. Green et al.[32] also observed a dependence on particle size asserting that cell viability was not effected by the presence of UHMWPE particles. The most biologically active particles lay within a size range of 0.3-10μm and at particle doses of 100μm^3/macrophage and 10μm^3/macrophage, causing release of IL-1, IL-6 and TNFα. The work of Gelb et al.[33] also points to a relation between particle size and intensity of reaction but they introduce a further variable, the morphology of the particle. They found that irregularly shaped PMMA particles elicited more response than spherical particles. They suggest that these differences may be related to the surface area of exposed particles. As a final confounding factor the work of Tabata et al.[34] has shown that particles with hydrophobic surfaces were more readily phagocytosed than those with hydrophilic surfaces.

Metallic wear debris is capable of affecting the macrophages in two ways. The reaction to metal particles is similar to that for other particles[17]. However, Haynes et al.[35] showed that titanium-aluminium-vanadium particles cause the release of PGE$_2$, IL-1, IL-6 and TNFα, whilst cobalt-chromium alloy particles, of the same size and at the same concentration, illicit a toxic response with decreased PGE$_2$ and IL-6.

Maloney et al.[36] showed that the response to metallic debris was dependant on metal and cell type. The response of fibroblasts and chondrocytes was observed to vary depending on the metal species and concentration at which they were administered. Cobalt was found to be the most toxic metal regardless of cell type as indicated by a fall in ^{3}H-TdR[36,37]. The cytotoxicity of cobalt may be due to the release of metallic ions. Cobalt, and chromium, ions were shown by Wang et al.[20] to be toxic at lower concentrations than titanium ions, stimulating human osteoclasts to release IL-1, IL-6 and TNFα. The effects of metal corrosion with low levels of ion release on the patient are not known. Peters et al.[38] revealed no significant elevation in serum or urine ion levels in subjects with an extensively porous coated prosthesis unless the joint was loose. This concurs with the work of Dorr et al.[39].

Author	Tissue	Material			Cellular Response
		Species	Size Range (μm)	Load	
Bendall et al. 1996 [40]	periprosthetic	CoCr & Ti	0.5 - 50	unknown	Raised IL-1α & TNFα secretion
Green et al. 1997 [32]	mucine peritoneal macrophages & human monocytes	PE dust	0.1 - 100	various	Raised IL-6, IL-1β & TNFα secretion
Haynes et al. 1993 [35]	rat peritoneal macrophages	CoCr & Ti	-	various	Ti raised IL-6, IL-1, PGE$_2$ & TNFα CoCr lowered IL-6 & PGE$_2$, no effect on IL-1 & TNFα
Howie et al. 1993 [22]	rats	UHMWPE	1-200	unknown	Bone loss from cement interface
Murray et al. 1990 [27]	mucine peritoneal macrophages	HDPE PMMA + 2 more	~ 1 for HDPE < 50 for PMMA	various	-
Santavirta et al. 1993 [25]	periprosthetic & human lymphocyte culture	UHMWPE	~30	5mg/ml	Immunologically inert
Shanbhag et al. 1994 [28]	mucine macrophage	Titania Polystyrene	0.15, 0.45, 1.76 0.11, 0.49, 1.61	various	Increased PGE$_2$ & LDH secretion
Wang et al. 1997 [41]	human osteoclasts	Latex Ti PMMA	0.1, 1 & 10 1-3 < 50	-	-

Table 2.2:   Laboratory studies into cellular response to particulate materials.

So we may conclude that different species of particles possess a varying degree of cellular response. In addition to this each species seems to possess a size of particle

which is most biologically reactive. Unfortunately, in the case of UHMWPE, the size that seems most reactive coincides with the size of the wear debris generated by the prosthesis. There also seems to be a volume of intracellular debris which elicits the greatest response. This threshold volume for the stimulation of macrophages is not without precedent. If we again consider the comparison to the reaction of the alveolar macrophage to dust, it was shown by Morrow et al.[42] that a load of $60\mu m^3$/macrophage will produce an overload where clearance of the particles from the lung will cease. Finally, the morphology of the particles may be of influence, the rougher the particle the greater will be the cellular response.

2.2.6 How does phagocytosis stimulate osteolysis?

There are two proposed mechanisms claimed to be responsible for bone resorption. The obvious link between the production of PGE_2 and $TNF\alpha$, both known as osteoclastic activation factors, would suggest that we need look no further. However, in the case of normal healthy bone, the complex cellular communication and feedback mechanisms would ensure that no bone resorption would occur without being accompanied by an increase in bone deposition. Therefore, for a net decrease in the volume of bone surrounding the prosthesis the osteoclastic stimulation has to be coincident with an osteoblastic inhibition. Hence the macrophage must produce factors both to stimulate osteoclasts and inhibit osteoblasts.

The second mechanism for bone resorption is the direct removal of bone by the macrophage. Schmalzried et al.[19] observed that "in sufficient numbers, particles stimulate macrophages to resorb bone directly". Similarly, Amstutz et al.[43] state that in their experience they consider this to be a possible mechanism of osteolysis. Evidence to support this observation comes from Athanasou et al.[44]. By using SEM they where able to show shallow depressions in the surface of bone where macrophages had been resting. They concluded that "macrophages are capable of a type of low-grade bone resorption". This observation was interpreted by Pandey et al.[45] as the macrophage's differentiating to become an osteoclastic cell, he showed that the particle laden cells were positive for the calcitonin. An alternative to this hypothesis is that osteoclasts themselves phagocytose particles and become more

active bone resorbers as a result[20]. It is difficult to distinguish osteoclasts from macrophages morphologically and histochemically and this possibly contributes to the confusion. Also, the phagocytosis of foreign matter is usually not a task which the specialist osteoclast would perform. This probably led Willert *et al.*[46] to state that osteoclasts did not contain wear debris, a view, until recently, widely accepted and affirmed in a recent NIH consensus statement[47].

The hypotheses of direct macrophage resorption and of osteocytic stimulation by macrophages both have their proponents and body of evidence, but the debate is essentially academic as both result in the outcome - bone loss and prosthetic loosening. Indeed there seems no reason why both of these mechanisms cannot contribute to osteolysis.

In summary, macrophages ingest particulate wear debris of all kinds. This initiates a foreign-body reaction resulting in the macrophagic secretion of factors which mediate bone resorption. These factors act on the relevant osteocytes creating a resorption of bone. A contribution to resorption is also made by direct osteoclastic activity by differentiated macrophages and particle bearing osteoclasts. Why then may it take months or years to develop osteolysis and then once initiated why is the progression of the granulomatous lesion often very rapid?

2.2.7 Progression, Hydraulic and Lymphatic Transfer

The rate of progression of bone loss is said to be slow with linear osteolysis and rapid with focal osteolysis. However, due to the different area of the expanding fronts, the volume of expansion of the fibrous layer may be the same for both cases.

Let us consider a hypothetical joint with a femoral head diameter of 22mm, using a UHMWPE acetabular component. A reasonable penetration rate of 0.20mm/year would produce approximately 30mm³ of wear debris per year. If we assume that all the wear particles are of 1μm³ in volume this results in a release of 3×10^{10} particles in one year. The work of Green *et al.*[32] has given us a range of 10-100μm³/macrophage for maximum reactivity, let us assume a load of 50μm³/macrophage for this case (or 50 particles/macrophage). Therefore our wear debris load would necessitate the recruitment of 6×10^9 macrophages. If each macrophage is assumed to be a cube of

$10\mu m$ in length, then the particulate load would require a space of $6cm^3$/year. This is purely the volume of densely packed macrophages required to store the yearly accumulation of particles with no account being taken of fibrous stroma or vessels.

If this load of particles were to be stored in the tissue of the pseudocapsule it would quickly overload the storage potential of this region. However, the observation that osteolysis is not commonly observed until many years post-operatively indicates that there must be transport of debris away from the joint space. Three modes of transport have been suggested: diffusion through the tissue, transfer through the lymphatic system and hydraulic transportation by pressurised synovial fluid.

It has been shown that wear particles can exist in the fibrous stroma of the periprosthetic tissue at sites distant from its source, for example the distal end of the femoral component or superior aspect of the acetabular component. The presence of particles in the fibrous membrane at sites distant to the pseudocapsule but unconnected by any conduit for transfer by the intracapsular fluid, shows that the particles must possess the ability to diffuse through the fibrous stroma. This mechanism, whilst being slow, may allow the debris to travel freely greatly increasing the particle storage capacity of the region. The potential for migration of the particles is likely to be dependent on their size. The work of Noble et al.[48] using the intra-articular injection of radioactive particles of varying size showed that smaller particles leaked from the synovial cavity faster than large particles. This is also expected to be the case for the rate of migration through the fibrous stroma.

The lymph system is the body's mechanism for removing the waste from cells and transporting it back to the circulatory system from where it can be expelled from the body. It also plays a role in the immune response with structures such as the spleen and tonsils producing lymphocytes. The role of the lymph system in the transport of debris away from the joint space has recently been the subject of renewed interest. Concern has been expressed that the deposition of wear debris in soft tissues remote from the prosthesis may possess the potential for long-term complications. The possibility of the accumulation of sizeable concentrations of metallic debris may cause neoplasia since the materials used in prostheses have been shown to be carcinogens in other situations, for example industrial exposure from inhalation[49]. In 1992 an editorial by Goodfellow[50] gave the figure of malignant tumours observed adjacent to

implants as 24. Whilst this number is very small in comparison with the number of THRs undertaken, this complication may become more prevalent as the expected life of the implants increases. Gillespie *et al.*[51] quantified the increased risk of tumour of the lymphatic or heamopoietic system rising from 0.2% to 0.6% after THR. However they qualify this result by saying the increased risk could be due to factors other than the presence of the implant such as drug therapy.

Early reports on the transport of wear debris to the peri-vascular lymph spaces observed accumulations of macrophages containing particles found around the vessels[46]. The work of Langkamer *et al.*[52] detailed studies of tissue from two patients, one obtained at post-mortem, both of which had had THRs. Greying of the lymph tissue in a manner similar to that widely reported in the synovium was observed. The greyness of the tissue fell in intensity the further from the prostheses at which the samples were taken. Metallic particulates were observed as distantly as the spleen. An extension to this work presented by Case *et al.*[49] also showed the presence of significant quantities of metal debris in the spleen and the liver. Further it was stated that the amount of material disseminated seemed higher if the prosthesis had been loose. The most heavily affected lymph nodes showed evidence of fibrosis and necrosis. The effect of polymer particles should not be overlooked whilst focusing on their metallic counterparts, Benz *et al.*[53] comment on the similarities between the histopathological response to polyethylene wear debris seen at the lymph nodes and that seen in the periprosthetic tissue.

The conveyance of wear debris, to areas remote from the joint space, by the synovial fluid may be regarded as the most important transport mechanism. The synovial fluid may become pressurised during gait by implant micromotion and will be forced out into any communicating spaces. The work of Maloney *et al.*[8] and Anthony *et al.*[9] shows that these communicating spaces may be extensive due to fissures in the mantle of cement. Similarly cementless THR may have abundant routes for distribution through screw holes in the acetabular component or through discontinuity of the porous coating around a femoral component. Schmalzried *et al.*[19] suggests that the joint fluid penetrates widely, even along the interface between prosthesis and bone, giving the name "effective joint space" to the areas accessible to the joint fluid. The wear debris may then be deposited preferentially in some areas of the effective joint

space creating lesions in these areas, whilst the lower concentrations of wear debris in the other areas results in linear osteolysis.

It is possible for the pressurised fluid to create communicating bursae in the surrounding soft tissue not contacting the bone[54]. A similar deposition of debris and foreign body reaction would ensue forming a granulomatous body.

The variable time to create osteolysis and the sudden occurrence of focal lesions may then be connected to changes in the flow regime within and around the effective joint space. If we consider a joint that has been well-fixed for a number of years, the migration of debris away from the joint space along the prosthesis bone interface will produce a slow thickening of the fibrous membrane and low grade osteolysis possibly dominated by differentiated macrophages and particle laden osteoclasts. The corresponding transport of debris away from the immediate area will retard the onset of gross loosening. If the flow pattern of the joint fluid changes it could result in the large quantities of debris being deposited in one area. This high concentration will overcome the transport mechanisms and the macrophage load will increase to the threshold stimulating the release of bone resorption mediators and chain of events leading to a focal osteolytic lesion.

A summary diagram showing the three modes of debris transport can be seen in Figure 2.4. The prevalence of each mechanism will dictate when the prosthesis may be expected to fail and by what mechanism. It is likely that all three will make a contribution to the transport of debris in every joint. The proportion of the transport made up by each may well vary over the life of the joint. Transport to the lymphatic system will not directly compromise the joint but may create secondary complications.

Particle Production

hydraulic action pumps to remote

synovial macrophage overload

debris deposition in one area

soft tissue bursa

slow macrophage recruitment

lymph vessels

rapid macrophage recruitment

granuloma

critical macrophage load quickly achieved

macrophage load increases slowly

accumulation in nodes

dilution of sinuses, node enlargement

focal osteolysis

linear osteolysis as concentration of cytokines is low

distant lymph nodes & organs

Figure 2.4: Summary diagram showing the various transport modes away from the joint site for debris particulates.

2.2.8 Mechanically Mediated Bone Loss

There can be no doubt that wear particles are responsible for a foreign body reaction in tissue to which they are exposed. However, concern has been expressed about the hypothesis that this is solely responsible for bone resorption[55,56]. The work of Aspenberg et al.[57] showed no bone resorption in a rat model when exposed to particles alone. This conflicts with the work of Howie et al.[58]. However, when micromotion was simulated in Aspenberg et al.'s model bone loss was observed regardless of the presence of particles. Aspenberg et al.'s model could be criticised in that there was no control of the dosing of the particles and that the movement was not typical of that found in vivo. However the message that osteolysis may rely on more than just the presence of particles cannot be disputed.

The hypothesis independently proposed by Aspenberg et al.[56] and Wroblewski[55] is one of hydraulic osteonecrosis. The elevated bursal fluid pressures during gait act to kill the osteocytes in exposed bone. The dead bone is then resorbed by osteoclasts as for any case of osteonecrosis. The presence of wear debris in these areas is then

coincidental and not causal. This would account for the widely observed foreign body granulomatous lesions in areas of osteolysis and consequently the lack of new bone formation. Neither Aspenberg or Wroblewski dispute that wear debris can cause osteolysis *in vitro* or *in vivo*. However, they suggest that the mechanical hypothesis of loosening best fits clinical observations.

This is essentially a chicken and egg debate over whether loosening causes osteolysis or vice versa. The conflicting hypotheses are both backed by substantial clinical and experimental evidence. A definitive answer as to which is correct may never be achievable.

It is quite conceivable that osteolysis may be stimulated by either mechanism depending on the circumstance. If a prosthesis shows early migration and endosteal cavitation leading to premature failure then this must be a good candidate for mechanically mediated osteolysis. Alternatively if a joint appears well fixed and experiences bone loss coincident with radiographic evidence of wear then debris stimulated osteolysis must be likely.

2.2.9 Mechanical Loosening

The THR as we know it today was conceived to minimise the frictional torque to which the prosthesis bone boundary was subjected (see Chapter 2.3.1). Charnley theorised that the frictional torque was important in the failure of early hip prostheses. This is especially relevant to the acetabular socket as the geometry of the fixation provided for the stem will ensure that it is less susceptible to this form of failure. Yet there is now evidence to suggest that the magnitude of the shear forces exerted on the bone-acetabulum interface is not sufficient to cause loosening without an underlying loss of fixation.

The work of Anderson *et al.*[59] gave a figure of 100Nm for the torque necessary to remove a well-fixed socket from its anchoring. This is greater than one order of magnitude larger than that found in the studies of Hall *et al.* for explanted joints[60,61]. Similarly Mai *et al.*[62] whilst not measuring frictional torque directly did show that larger articulating diameters were negatively correlated with the occurrence of loosening. Clearly friction alone is not sufficient to initiate loosening, but it may be

that the shear forces exerted on the implant-bone interface will contribute to the failure of a prosthesis in which the fixation has already been compromised. Wroblewski[4] asserts that if a prosthesis is secured by a fibrous membrane as opposed to direct bone-implant apposition, then it becomes likely that a joint with higher friction will cause loosening.

There is however one circumstance in which the shear forces imposed may become sufficient to produce loosening. The impingement of the neck of the femoral component against the rim of the socket will produce high magnitudes of torque. Fortunately this will in general only occur at the extremes of motion and as such relatively infrequently. However, impingement will become more prevalent if the components have been malpositioned, or if a substantial penetration of the femoral head into the socket has taken place[63].

2.2.10 Motivation

Failure of the fixation of the prosthesis, be it evidenced as osteolysis, loosening or migration, will account for the majority of clinical failures and revision procedures. It is essential that a complete understanding of the behaviour of a joint *in vivo* is established to complement the knowledge attained through *in vitro* studies.

The overwhelming message from literature studies is that the wear of the prosthesis is seen as a fundamental parameter governing failure. As such the majority of this investigation will focus on the measurement of wear and characterisation of the wear debris. The influence of all quantifiable parameters which may affect the wear will also be considered.

We have seen that clinical failure can be attributed to many different things with large bodies of evidence supporting each hypothesis. Additional complicating factors such as component design and patient parameters adds uncertainty. Explant studies provide a valuable source of information on the prosthesis and its interaction with the host patient. Laboratory based wear tests will never be able to simulate fully the complexity of the demands placed upon a joint during its lifetime.

Retrieval studies have been criticised due to the concern that only poorly functioning prostheses are being evaluated. Whilst this is the case, it is also true to say that these are the important joints as these are the ones that must be remedied.

2.3   Overview of the Joints to be compared

2.3.1   The Charnley Low Friction Arthroplasty

The development of the total hip replacement as we recognise it today may be attributed almost entirely to one man - Sir John Charnley. Whilst he was not the first to carry out total arthroplasty of the hip, he introduced many of the features which are seen commonly among the various designs of joints currently available. In order to appreciate the development of the Charnley hip joint it is convenient to consider its evolution.

The initial motivation for Charnley to consider the development of a novel hip replacement was the observations he made of the Judet prosthesis. The Judet prosthesis comprised an acrylic femoral head which articulated against the bone of the acetabulum. A common complaint was the occurrence of a squeaking noise when the joint articulated. Charnley observed that the cessation of the squeaking coincided with the loosening of the joint and concluded that the friction between the bone and acrylic caused the noise and created the loosening. His conclusion was that the development of a low friction joint replacement was necessary.

Charnley's initial design was in effect a surface replacement prosthesis. Two polytetrafluorethylene (PTFE) components were secured using a press-fit. This design was discarded as it was shown to limit the blood supply to the femoral head causing bone loss. A more radical solution was now adopted using a Thomson stem articulating against a PTFE socket. It was at this point where the use of dental acrylic cement was introduced. The components were secured in place using a polymethylmethacrylate (PMMA) grout that acted as a physical interlock between the prosthesis and the bone. The results of this procedure were said to be "gratifying"[164] but a further series of modifications were undertaken in order to reduce the frictional torque exerted on the cement bone interface. The size of the femoral head was

reduced from the 42mm of the Thomson stem to 28mm, then 25mm and finally 22.25mm. It was decided not to go any smaller as the risk of dislocation became great[65].

Charnley's appreciation of the biomechanics of the hip and his innate appreciation of engineering led him to introduce a modification to the loading regime of his artificial hip. The centre of rotation of the femoral head was moved 9mm medially to give the joint a more valgus position[66]. This had the effect of decreasing the moment arm, reducing the joint reaction force (see Figure 2.5). The reduction in the joint reaction force will produce a corresponding fall in the frictional torque experienced by the joint. A further modification to the biomechanics of the hip replacement was proposed by Tom English[67]. This acted to replace the greater trochanter in its original position thereby restoring its moment arm and again reducing the resultant joint reaction force (Figure 2.5).

Unfortunately these early designs which used PTFE for the acetabular socket suffered from excessive wear. The wear particles of PTFE produced a severe granulomatous reaction, causing the prosthesis to become loose often within two years. Clearly a change in the material used for the socket was necessary. A number of alternatives were investigated including glass fibre reinforced PTFE. However the final choice arrived at by Charnley and his co-workers was ultra-high molecular weight polyethylene (UHMWPE). Extensive testing of this new material was undertaken to ensure that the experiences of PTFE were not repeated. UHMWPE was first implanted at the end of 1962 and is now the universal polymer choice in joint replacement technology.

Subtle changes in the stem and socket continued, and still continue to this day, but essentially the Low Friction Arthroplasty devised by Charnley has remained the same. Manufacture of the prosthesis was originally undertaken by Thackray, Leeds which has since been bought by Depuy International Ltd., Leeds. Charnley's Low Friction arthroplasty has become the industry's gold standard and many of its once novel features are now commonplace.

Clinical Performance

Mr. B. M. Wroblewski of Wrightington Hospital, has a wealth of experience with Low Friction arthroplasty and has in recent years published a number of studies dealing with large numbers of joints which have long implantation periods.

In a study of 193 joints with an average implant duration of 20.75 years 85% were found to be pain free, with a further 11% only experiencing slight discomfort (as defined by the criteria of D'Aubigne & Postel[68]). Also 60% of the joints were said to have normal function and 63% had a normal range of motion[69]. This study also showed an exponential relationship between the depth of the socket wear and the presence of migration: 9% of sockets with less than 1mm wear migrated, 22% of sockets with less than 3mm wear migrated and 100% of sockets with greater than 5 mm wear migrated. In a study of a larger group of 1342 joints with an implant duration of only 10.33 years Wroblewski et al.[70] showed that the incidence of revision due to socket loosening was more than twice that due to stem loosening, being 5.7% and 2.5% respectively. In contrast, dislocation accounted for only 0.2% of revisions.

The ultimate measure of a joint's success is the survivorship rate. This is defined as the percentage of surviving hips with revision as the definition of a failure. The survivorship rate of the two components of the joint have been presented separately giving an insight into how the modifications introduced over the evolution of the joint have influenced its success. If we first consider the socket, a flange was introduced to the rim of the cup in order to retain, and hence pressurise, the cement prior to its setting. This was designed to increase the cement interdigitation with the bone[71]. Wroblewski et al.[72] showed that the flange had increased the survivorship rate of the socket from approximately 90% at 20 years without the flange to 97% at 17 years. The introduction of a bone block at the distal end of the stem was intended to stop the spread of cement down the medullary canal and again facilitate effective pressurisation. In a study of 258 joints Wroblewski et al.[73] gave survivorship rates for the stem of 94.4% at 15 years without the bone block but of 99.2% at 10 years when a bone block was present. These two simple improvements in the cementing technique along with the advances made in the mixing and delivery systems employed have made cemented fixation highly successful.
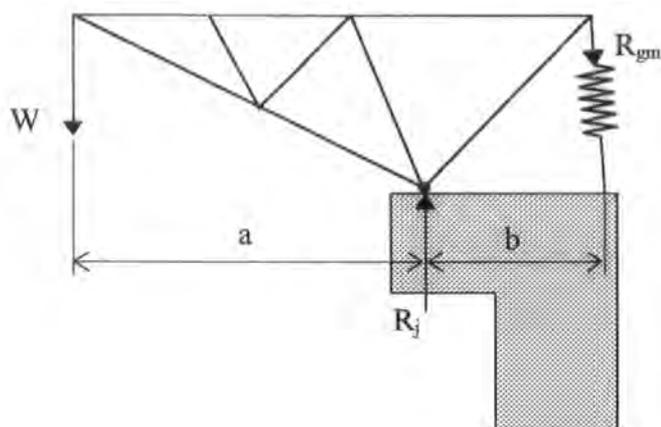
For vertical equilibrium:

Forces acting upwards = Forces acting downwards
$$R_j = W + R_{gm}$$

The body weight of the patient, W, is effectively a constant. Therefore in order to reduce the joint reaction force, R_j, the magnitude of the force imposed by the gluteus medius muscle, R_{gm}, must be reduced.

If we consider moments about A:

$$W.a = R_{gm}.b$$

Charnley achieved this by reducing the moment arm of the body weight, a, by 9mm. The further modification proposed by English was to restore the gluteus medius muscle to its original position effectively increasing the moment arm, b. This is shown below.
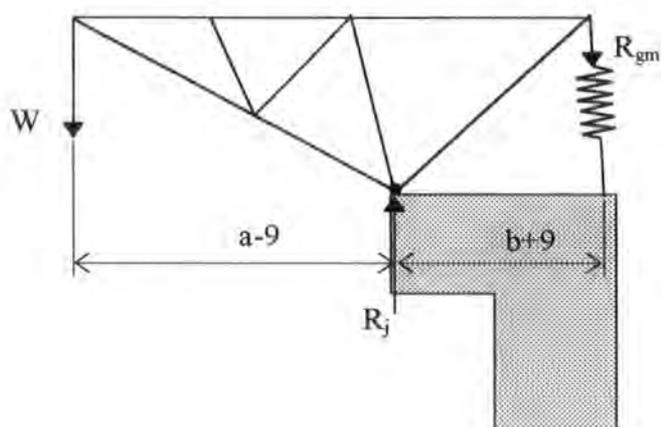
Figure 2.5:   Modifications to the forces imposed upon the LFA hip joint.

2.3.2 The Porous Coated Anatomical Total Hip Replacement

The Porous Coated Anatomical (PCA) total hip replacement was introduced to the market by Howmedica (Rutherford, New Jersey) in 1983. The rapid adoption of this technology is illustrated by the fact that in excess of 160,000 joints were implanted world-wide by 1992[74].

Design Philosophy

The design of the PCA hip system was very different from that of traditional joints, such as the Charnley type. These differences were intended to improve joint life, reduce stock levels and hence cost, and provide more flexibility for the surgeon.

The most notable change came in the mode of fixation employed by the PCA. This was a hip joint which was designed in response to the hypothesis that the polymethylmethacrylate bone-cement was responsible for the loss of bone stock around the prosthesis[14] (see Chapter 2.2.2). Hence, the PCA was one of the first generation of joints to be used without cement. Fixation was instead provided by the ingrowth of bone into a porous layer on the surface of the components. The porous layer was created by sintering a double layer of beads, approximately 300μm in diameter, to the surface of the metallic components. This creates an average pore size of 425μm and porosity of 35%[74]. The porous coating extends over the entire back of the acetabular component and circumferentially on the proximal third of the femoral component, Figures 2.6a & 2.6b.

It takes a finite time for the bone to grow into the pores, so the design utilises an interference fit for primary stability until the ingrowth is complete. This is achieved in the acetabular component by reaming the acetabulum to a smaller diameter than that of the joint. In addition, the acetabular component has two pegs that are intended to counter any rotation. In the case of the femoral component the posterior bow of the design creates a three point locking mechanism which is aided by the metaphyseal filling shape, Figure 2.6.

The next most radical design feature is the extensive use of modularity. The femoral component is a two piece unit in which the head fits to the stem via a Morse taper. The head is available in three diameters (26, 28 and 32mm) and in three neck lengths

(standard, +5 and +10mm). To facilitate these large offsets of the head, a skirt is incorporated into its base. In addition, the 32mm head is available in a fourth neck length of -3mm. The femoral stem is available in three lengths (primary, mid and long) and in nine widths for the primary and eleven for the mid or long versions. The femoral stem is made from cobalt-chromium-molybdenum alloy (CoCrMo) and the femoral head may be either CoCrMo or ceramic (32mm alumina or 28mm zirconia).

The acetabular component is also a two piece unit with an ultra-high molecular weight polyethylene (UHMWPE) liner within a CoCrMo alloy backing. They come in two profiles, low and deep, and in outer diameters from 40mm to 67mm, in 3mm increments. The metal backing is of the form of a truncated sphere with two anti-rotation lugs located at its rim. Early examples of this system used an acetabular design in which the unit was supplied with the liner permanently located in the metal backing (one-piece). The liner was secured in place by a peg at the pole of the cup, with a tab on the rim to stop rotation about the pole (Figure 2.7a). The later snaplock system was introduced in which liners and backings were supplied separately. The liner is available in two versions, neutral and 10° hooded, and locates in a locking mechanism at the rim of the cup which has ten discrete positions (see Figure 2.6a & 2.7b).
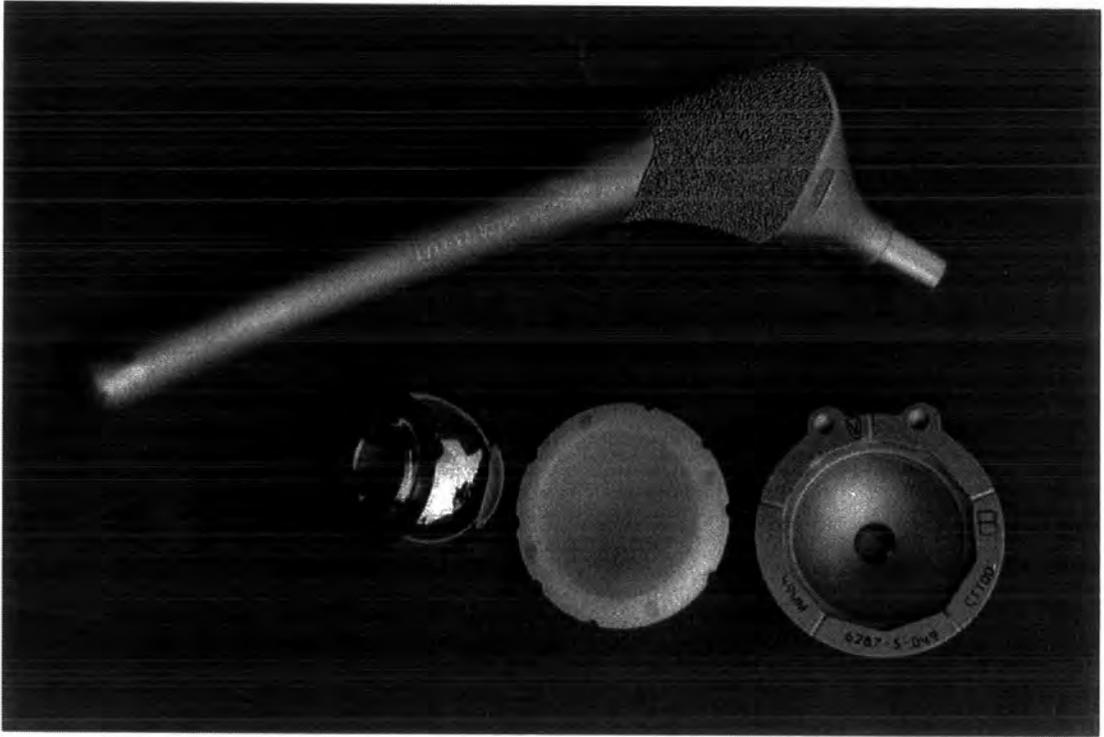
Figure 2.6a: Photograph of PCA total hip replacement.

Figure 2.6b: Photograph of PCA total hip replacement.
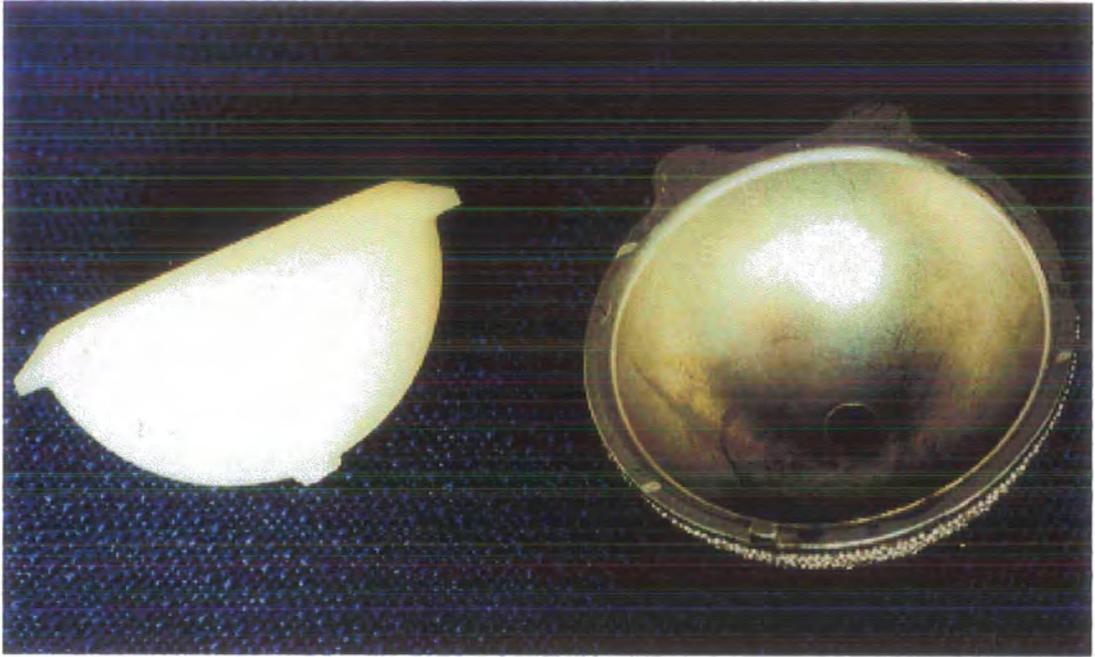
Figure 2.7a: Photograph of one-piece type acetabular component showing profile of the liner.
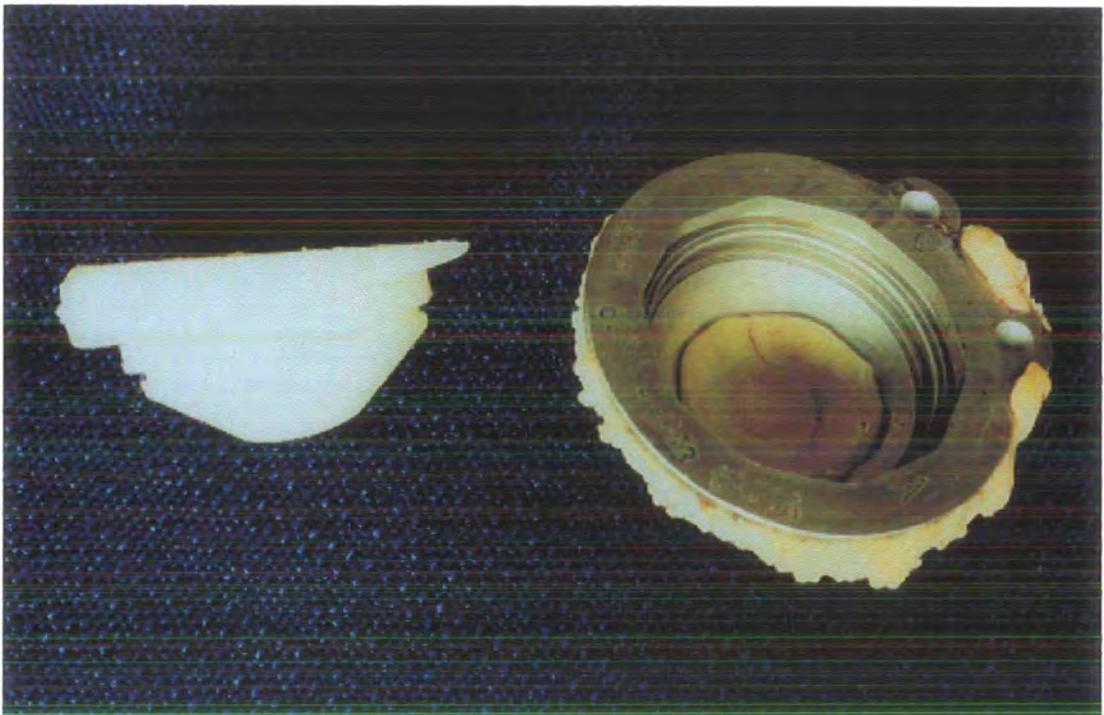
Figure 2.7b: Photograph of snaplock type acetabular component showing locking mechanism. Note the hooded liner.

2.3.3 Clinical Performance

The PCA hip system is well instrumented and is said to be a relatively simple procedure to perform[75,76]. When considering the outcome of the operation it quickly becomes apparent that the early results show a very different picture to that of longer-term studies.

It has been widely reported that the PCA system provides a good functional outcome with impressive hip function scores[77,78,79]. However, this is often concurrent with persistent thigh pain reported to effect 8-39.4% of hips at two years post-operatively[78-83].

The survivorship of the prosthesis is similar to that of other joints in the short term. However, beyond 6 years the revision rates increase dramatically, see Table 2.3. Owen et al.[84] assert that the predominant reason for the late failure of the joint is osteolysis of the acetabular component. Twenty-six of the thirty-two failures in their study were at the acetabular side. This view is reinforced by the work of Kim et al.[85] who in their study of 116 joints observed that osteolysis affected 33% of joints at 7 years. Similarly Astion et al.[86] reported a pronounced increase in the incidence of osteolysis of the acetabular component after five years rising from 2% to become 38% at seven years.

Author	Cohort Size	Follow-up Duration (Years)	Survivorship Rate (%)
Astion et al. [86]	199	4.9	94
Berry et al. [87]	49	6	81
Krismer et al. [88]	60	8	88
Maric et al. [83]	63	2.4	92
Owen et al. [84]	241	6	91
		7	73
		8	57

Table 2.3:   Survivorship studies for PCA hip replacements.

The failure of this design of hip has also been associated with the dissociation of the liner from its metal backing. Case studies have been presented by Brien et al.[89] and Ries et al.[90], reporting 4 and 3 cases respectively, where the peg of the one-piece type

socket has fractured and the liner has been displaced. In some cases this led to the articulation of the femoral head directly on the metal backing of the acetabular component, resulting in metallosis of the capsule.

The use of modularity has also been cited as the source of complications. Barrack *et al.*[91] in a study involving a wide variety of joint types, reported twenty complications including six femoral head detachments, seven liner displacements and most alarmingly four cases of operative error in which an incompatible pairing of components had been used, for example a 26mm femoral head with a 22mm acetabular liner.

The efficacy of the fixation method was assessed by Heekin *et al.*[78] according to the criteria of Engh *et al.*[92]. Fixation of the femoral component at five years was found to be by bony ingrowth in 94% of cases, stable fibrous membrane in 1% and unstable fibrous membrane in 4%. Indeed the early migration of components has also been found to correlate to the late failure of the femoral component[93,94]. Settlement in excess of 3mm was noted by Kim *et al.*[85,95] in twenty-two of a series of 116 hips. This was due to the femoral components being too small and correlated strongly with the development of a fibrous membrane and pain, or loosening. At seven years of the twenty-two hips with migration, twelve had a stable fibrous membrane, nine were loose and only one had any evidence of bone ingrowth. However the poor initial fit of the joints in Kim *et al.*'s study group was due to the variations in the quality of the patient's metaphyseal bone - 57% of patients suffered from avascular necrosis of the femoral head or femoral neck fracture

Migration is of principal concern in relation to the acetabular component and is compounded by the common occurrence of malpositioning of the acetabular component in the pelvis. Learmonth *et al.*[96] comment on the misconception that the anti-rotation lugs should be placed superiorly which subsequently leads to the insertion of the acetabular component in an open (too vertical) position. This is illustrated in Devane *et al.*'s[97] radiographic study of PCA joints were it was shown that the mean angle of the cup relative to the horizontal was 50.9°. The initial fit of the acetabular cup is important and good preparation of the bone with accurate reaming to an appropriate size helps to ensure the apposition of the porous surface to

the bone[98]. Only then will sufficient stability occur to facilitate the ingrowth of bone and hence the long term fixation of the component.

It would seem that when implanted correctly the femoral component of the PCA system is successful and can perform well in the long term. However, if the initial interference fit is not good, the collarless nature of the design allows rapid subsidence. The acetabular component however, is more susceptible to the occurrence of osteolysis and in extreme circumstances may fail catastrophically.

Dislocation

Dislocation of the prosthesis is a well-understood mechanism. It was found with the early Charnley designs that when in the seated position the neck of the femoral component was prone to impingement with the anterior wall of the acetabular component. This problem was reduced by the reduction in diameter of the femoral neck and the introduction of an acetabular component with a long-posterior wall.

In the case of the PCA system, the likelihood of impingement is increased by the modular nature of the femoral component. The presence of a skirt on the heads incorporating an offset increases the effective diameter of the neck. However, the large diameter of the head counteracts this effect. This results in a more complex situation where a skirted 26mm (+10mm offset) diameter head is more likely to impinge than a standard 32mm head.

Also of influence is the presence and orientation of the 10° hood on the UHMWPE liner which is available in the snaplock type design. If the hood is located anteriorly to the coronal plane then impingement is enhanced and if positioned posteriorly then the possibility of impingement is reduced.

Pain

The occurrence of persistent thigh pain will often necessitate the replacement of the joint. Campbell *et al.*[81] found that the persistent thigh pain suffered by many PCA THR recipients correlated with implant migration. Investigations into the cause of pain are inconclusive. The most plausible theory is that the pain is caused by the microscopic movement of the prosthesis relative to the bone. The presence of

sensory nerves in the interface membrane of aseptically loose hip prostheses was established recently by Ahmed et al.[99]. The micromotion will stimulate these nociceptors and it is suggested that this may contribute to the release of neurones capable of stimulating immune cells to release bone resorption mediating cytokines (see Chapter 2.2.5).

Stress-Shielding

Bone is a living medium and as such is responsive to changes in its environment. Wolff[100] found that bone responds to function. An increase in the stresses imposed, within limits, will cause deposition of bone, and vice versa. Hence the introduction of a very stiff femoral component will off-load the surrounding bone and result in the atrophy of the proximal metaphyseal bone. Minuesa et al.[101] and Turan et al.[102] showed that the bone mineral density decreases in Gruen zones 1 and 7[103]. Resorptive bone remodelling of the medial neck cortex was found in 65% of the subjects followed by Gruen et al.[104] at 5.4 years. Indeed bone remodelling changes have been observed in 23% of subjects as early as two years post-operatively[105].

Additionally, at the point were the prosthesis ends, the stresses are raised and there is a corresponding increase in the bone thickness of the distal cortex. This effect was observed in 80% of the patients followed by Gruen et al.[104].

These changes in bone density will affect both the Charnley and the PCA prostheses. The PCA femoral component is of a considerably greater diameter than that of the Charnley and as such will off-load the bone to a greater extent. It may be expected that the PCA should suffer from bone loss associated with stress shielding. However, the changes in bone stock will often take a long time to manifest themselves. It is doubtful whether this mode of failure is an important one for the PCA hip system as the duration of implantation seldom exceeds 10 years.

Sepsis

The occurrence of infection around the prosthesis often leads to failure as it is difficult to eradicate the bacteria without direct access to the area. The fibrous membrane surrounding the prosthesis is vascularly deficient and as such any systemic antibiotics

are ineffective. A great deal of work was undertaken by Charnley[65] to reduce the opportunity for the joint to become infected. The introduction of many novel practices such as clean air enclosure and body-exhaust suits were pioneered during the 60's and 70's. As a result, this mode of failure has been reduced to a tolerably low level.

2.4 Introduction to Tribology

Tribology is the study of how two bearing surfaces interact when they move relative to one another. Tribology may be broken down into three related sub-topics: lubrication, friction and wear. For the purpose of this review attention will be concentrated on hard/soft bearing combinations representative of metal against polyethylene.

2.4.1 Dry Friction

Consider a rectangular block resting on a surface. At the interface between the two there will be some interaction between the microscopic asperities of the two surfaces (Figure 2.8). The force required to move the block is proportional to the load normal to the two surfaces, with the constant of proportionality, μ, being known as the coefficient of friction (Equation 2.1). The value of the coefficient of friction varies depending on the material and topographical properties of the two surfaces. For example polished steel sliding against itself has a coefficient of friction of 0.4, whilst polished steel against polyethylene has a coefficient of friction of 0.04.
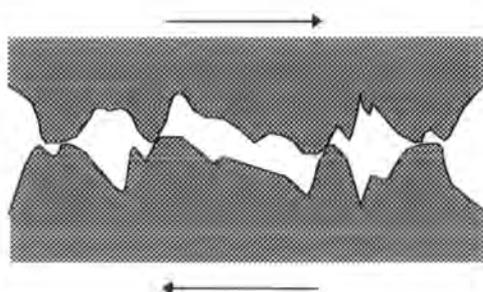
Figure 2.8: Interaction of two microscopically rough surfaces.

Equation (2.1) is the most elementary of tribological relationships, but it does provide the interesting observation that frictional force is independent of the apparent contact area between the two surfaces[106].

$$F_f = \mu R_N \qquad (2.1)$$

This phenomenon requires a little more explanation. Intuitively, it may be expected that if a load were spread over a larger area, then it would be easier to move. However, the 'apparent' area of contact is not in fact the 'true' contact area. The macroscopic apparent area of contact in our example would simply be the length multiplied by the breadth of the block. In contrast, the true area of contact is that between the microscopic asperities. Even at low loads when the two surfaces come together the pressures at the tips of the asperities can be very high. This will cause plastic deformation of the softer material. The area of contact will grow and new asperities will be recruited until the load is supported elastically. Increasing the load would squash the asperities to a greater extent and hence increase the true contact area.

In summary, if the rectangular block above were laid on its smaller side, the apparent area of contact would change, but the true area would not. Alternatively, if another block was laid on top of the first, the apparent contact area with the surface would not change, but the true contact area would increase.

When in contact, a certain amount of force will be required to create a relative motion between the two surfaces. Each individual asperity interaction will contribute to the total frictional force experienced. The observation that frictional force remains constant is attributable to the large number of interactions. At any time the statistical distribution of the contact processes is almost constant[107].

Simple physics tells us that to move a force through a displacement will require work. The two key processes responsible for the dissipation of the frictional energy are adhesion and deformation. These two mechanisms are complex and interactive so we shall distil them to their simplest forms.

If the asperities of the loaded surfaces are considered, then at the junction between the two asperities, because of the high pressures involved, the materials may adhere to one another. To create motion these adhesions would have to be broken. This will occur either at the original junction between the two materials, or in the bulk

material of the softer of the two materials. The release of the adhesions will result in the dissipation of energy.

Similarly the deformation of any portion of the surface, be it elastic or plastic, will also absorb frictional effort. These processes will ultimately lead to an increase in the temperature of the articulating surfaces. Studies attempting to quantifying the increase in temperature both *in vitro*[108] and *in vivo*[109] have been published. They show approximately a 2°C increase in temperature for a number of sampling sites around a THR simulating *in vivo* articulation. However due to the location of the measurement this is the temperature of the joint environment and not that of the surfaces where the heat energy is generated. It is quite possible that the temperature at the asperity interaction points is considerably greater.

2.4.2 Lubrication

An important parameter in the moderation of both friction and wear is the lubrication of the interface. Until now only the interaction of the two surfaces has been considered under dry conditions. However in the case of joint replacement, the prosthesis will always operate with a lubricating medium. A fluid acts as a lubricant by transferring some, or all, of the load through the joint by becoming pressurised. In situations where all the force across a joint is transmitted by the pressurised fluid, with no asperity contact, this is known as fluid-film lubrication. Alternatively, when only a portion of the load is supported in this manner, while the remainder of the load is carried by asperity contact, this situation is called mixed lubrication.

A Stribeck plot is often used to establish the mode of lubrication in which a bearing is operating[125], an idealised representation of which can be seen in Figure 2.9. Friction factor is a modification of the coefficient of friction proposed by Unsworth *et al.*[126] and defined as:

$$f = \frac{T}{rL} \qquad (2.2)$$

where T is the average frictional torque, r is the radius of the femoral head and L is the load across the bearing. The Sommerfeld parameter, z, is calculated using the formula

$$z = \frac{\eta u r}{L}$$ (2.3)

where η is the viscosity of the fluid and u is the entraining velocity. A descending trend in the Stribeck curve is indicative of a mixed lubrication regime. An increase in the viscosity of the lubricant will allow it to become more effective at separating the bearing surfaces. A gently rising trend in the Stribeck curve would suggest fluid film lubrication. Increasing the viscosity of the lubricant when in fluid film lubrication increases the energy absorbed shearing the liquid, raising the force required.

If this diagram is considered in more depth it provides yet more contradiction. Earlier in this section it was suggested that for a given combination of bearing materials a coefficient of friction could be defined such that,

$$F_f = \mu R_N$$ (2.1)
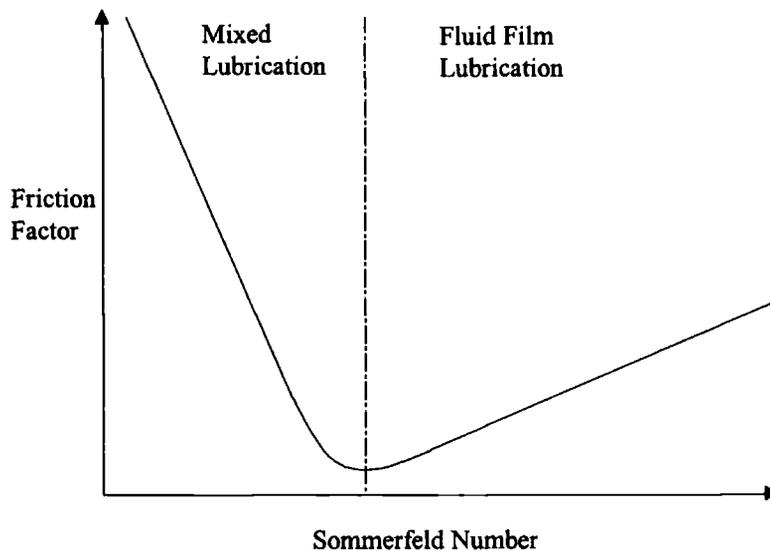
Figure 2.9: An idealised Stribeck plot.

However the Stribeck plot shows that when working in a lubricated environment this no longer holds true. The friction factor between a set of materials can vary as any one of a number of parameters is altered, for instance the lubricant viscosity.

If the effect of varying the load is considered, for a given set of material and tribological parameters, the Stribeck plot is displaced towards the origin by

increasing the load. That increasing load reduces the friction factor seems surprising. This is due to the action of the lubricant. As the bearing takes the increased load the asperities will be compressed as they are elastic, however the lubricant will be effectively incompressible and will become rapidly pressurised. The proportion of the load which is borne by the lubricant will increase, theoretically is capable of establishing the fluid film lubrication regime.

When considering the environment in which joint replacements operate, we must examine the rheological properties of synovial fluid. To summarise the work of Cooke et al.[127], normal synovial fluid has a very high viscosity at low shear rates, reducing exponentially as shear rates increase. In contrast synovial fluid from a diseased patient has moderate viscosities at low shear rates and low viscosity at high shear rates. In simpler terms, diseased synovial fluid is thinner than healthy fluid, especially when the joint is moving slowly. However, at realistic shear rates the viscosity of all types of synovial fluid is low (i.e. 0.005 Pa s).

An alternative mode of lubrication involves the introduction of a third medium between the two articulating surfaces. This third material is adherent to the surfaces and is itself sheared in preference to the softer of the two bearing materials. A very weak form of boundary lubrication, as this is known, is thought to be present in artificial joints. Proteins from the synovial fluid attach to the surfaces and when the asperities contact in the mixed lubrication regime boundary lubrication may also occur.

The presence of protein boundary lubrication is likely to be the mechanism by which the wear rate of Lancaster et al.[117] is so much lower than that reported by Dowson et al.[116] quoted in the previous section on wear. A small contribution will also be made by the marginal increase in the viscosity of the bovine serum lubricant.

2.4.3 Wear

The same processes of interaction between the two surfaces which cause friction and the generation of heat will result in the wear of the bearing surfaces. Wear can be divided into two sub-categories: cohesive and interfacial[110].

If we consider cohesive wear these are the mechanisms which are governed in the main by the cohesive strength of the polymer and may affect the polymer to some depth.

Deformation processes may be divided into two subsets: asperity interaction and macroscopic ploughing. The asperity interaction processes absorb energy through the displacement and deformation of the asperities. When two asperities impinge, the asperities must be compressed, or displaced, in order to pass one another. The repeated deformation of the surfaces due to abrasion can also lead to fatigue wear[111].

The interaction of a single hard asperity drawn across an elastomer was investigated by Shallamach[112]. Sharp needles caused tearing parallel to the direction of motion, while rounded indentors caused cracks and lips perpendicular to the direction of motion[113]. The observation of ripples across the surface of *in vitro* test components and explanted UHMWPE liners by Wang *et al.*[114] was attributed to the accumulation of strain caused by repeated deformation of the asperities. The ripples of Wang *et al.* bear a resemblance to the waves of Shallamach in terms of topography and whilst the elastic modulus of the UHMWPE is greater than that of the rubber used by Shallamach the mode of their formation is likely to be similar.

Macroscopic ploughing involves the harder asperity ploughing a groove into the softer material. This often results in the release of wear particles. This is termed abrasive wear[111].

The second category of wear is interfacial wear. This includes wear as a result of energy dissipation processes in the regions immediately adjacent to the surface. Adhesion is the most important of these in the case of polymers. Clearly the adhesion of the two bearing materials may result in the immediate detachment of material from the softer component. In addition, the breaking of the original boundary will impose a cycle of stresses on the asperity over a number of articulations which may fatigue the asperity. Ultimately the asperity will fail and be removed. These two mechanisms of wear are known simply as adhesive wear and fatigue wear, respectively[107].

If we consider how the wear of the bearing surfaces are affected by their material and topographical properties. In the same way that friction is not dependent on the apparent contact area the amount of wear experienced is also unrelated to apparent

contact area. Friction and wear are both proportional to load across the interface and this implies a relation to the true contact area. If the interaction between the two surfaces is assumed to be that of ideally plastic-elastic materials, to a first approximation, wear is proportional to the load, L and the sliding distance, S and inversely proportional to the hardness H[115].

$$\Delta V \propto \frac{LS}{H} \qquad (2.4)$$

That wear is proportional to sliding distance holds true for a wide range of conditions. However, if load is increased beyond the bulk yield stress of the material the wear will increase greatly.

The roughness of the hard counterface against which the softer bearing surface articulates will also influence the rate of wear. A simple model to predict the affect of counterface roughness on the rate of wear of the UHMWPE was derived by Dowson et al.[116]. Their laboratory based studies suggest that the wear factor, k (mm^3/Nm), could be modelled using the equation

$$k = a(R_a)^b \qquad (2.5)$$

where R_a is the arithmetic mean deviation (μm) from the mean plane of the surface and a and b are dimensionless parameters. Dowson et al. in their study on stainless steel reciprocating against polyethylene in water found a to be 4×10^{-5} and b to be 1.2. By contrast Lancaster et al.[117] using bovine serum as a lubricant found a to be 7.69×10^{-9} and b to be 0.37. This variation is attributable to variations in the lubricating mechanism present and is dealt with in Section 2.4.4. Wang et al.[118] developed a theoretical wear model associated with the microasperity contact between the bearings surfaces. The model predicts the volumetric rate of wear per walking cycle, $\Delta V/N$ ($mm^3/cycle$), as

$$\frac{\Delta V}{N} \propto L^{1.5} R_a^{1.5} \frac{1}{\sigma_u^{1.5} \varepsilon_u} \qquad (2.6)$$

where L is the load (N), σ_u is the ultimate tensile strength (MPa) and ε_u is elongation of the material at failure in a tensile test (mm). This indicates that the roughness of the metallic counterface has a powerful influence over the rate of wear. The empirical studies of Weightman and Light[119] sliding stainless steel and alumina

38

against UHMWPE showed a non-linear relationship between wear rate and surface roughness. Wang *et al.* re-analysed their data and showed that wear rate was proportional to $R_a^{1.4}$. Also the work of Rose and Cimino[120] indicates a similar relationship. Wang *et al.* concluded that these experimental correlations, in addition to their own, strongly supported their proposed model. The inclusion in Wang *et al.*'s model of material parameters allows the theoretical comparison of different material combinations as well as topographical variations.

The above models have been shown to perform well for unidirectional motion but concern has been expressed that this is not capable of extrapolation to the physiological situation[121,122]. Indeed when a rotational motion is applied to a simple unidirectional test the wear rates increases substantially[123]. This has also been shown to be the case for more advanced hip wear simulator testing[114,120,124]. The impact of this phenomenon will be assessed in the Discussion section.

2.4.4 Three Body Wear

An additional wear mechanism is known as three body wear. This involves the presence of a particle between the articulating surfaces which causes further abrasion. This third body must be harder than at least one of the surfaces to cause wear. The third-body will sometimes become embedded in the softer bearing material and will act as a plough as it is dragged over the counterface.

This mode of wear is particularly relevant to artificial joints as there are many sources of third bodies and no possibility of removing them as may happen in other engineering situations. Third bodies come from three sources: bone, cement or metal. These may be released due to abrasion between the implant and the bone or as a result of the surgical procedure.

2.5 Assessment of Tribological Parameters

2.5.1 The Measurement of Wear

There are two sources of data in the investigation of the amount of material removed through wear of the articulating components. One is the examination of clinical radiographs and the other is the study of components retrieved at revision, or those obtained at post-mortem. The different sources of data, and different methods for deducing the wear volume, contribute to a lack of clarity concerning wear.

The Source of Data

The source of the data, on which the calculations of wear are made, has great influence on the interpretation of the results. The most frequently employed method is the use of radiographs. This allows the measurement of wear in clinically well functioning prostheses. The conventional view, in the coronal plane, may be taken with the patient upright, or prone, leading to uncertainty as to whether the femoral head was in contact with the worn surface.

The study of components retrieved at revision surgery is a well documented alternative to radiographs. This source of data allows the direct measurement of wear volume and also enables the investigation of the surface topography of the components. The drawback to this data source is the possibility that the dataset is skewed. Studying a group of failed prostheses raises the possibility that the wear found in these joints is only typical of failed joints not joints in general.

A solution to the problem of studying failed prostheses is to obtain components retrieved at post-mortem. This allows the direct measurement of wear for clinically successful, well-functioning prostheses. These joints are invaluable as they facilitate the exhaustive study of tribology, fixation and histology. However, there are few joints available at post-mortem restricting the size of the dataset attainable.

Methods of Deducing Wear

The study of wear may be regarded in two stages namely assessing the penetration and calculating the wear. The majority of methods commonly used combine these

two stages, though the common exceptions are co-ordinate measuring machines (CMM), gravimetric methods and fluid displacement techniques.

There are various ways to measure the penetration of the femoral head into the acetabular component. The penetration may be regarded as a combination of changes due to wear and those due to creep. This will be addressed later in this chapter.

Early investigations such as those by Charnley and co-workers[128,129] used sequential radiographs of the hip to assess the penetration. This was achieved by measuring the displacement of the head relative to a semicircular wire marker in the coronal plane of the acetabular component. Charnley's early work was criticised by Clarke et al.[130] in two regards. Firstly that the magnification of the radiographs was not accounted for, and second, if the marker did not lie in coronal plane then the penetrations deduced would be in doubt. The problem of magnification was recognised and compensation made, however concerns surrounding the radiographic measurement of penetration still exist despite its acceptance as a performance measure and a diagnostic tool used clinically. The principal doubt remains that the wear direction may not lie in the coronal plane. Therefore traditional radiographic assessment would underestimate the actual wear. This phenomenon was observed in the studies of Wroblewski et al.[131,132] and Hall et al.[133,134]. A review of these and other causes of bias and imprecision in the uni-radiographic assessment of wear was presented by Hall[135]. These issues were addressed by Devane et al.[97] by the development of an alternative radiographic method of measuring wear which utilised two radiographs. These were the conventional coronal plane image and another in the sagittal plane, to create a 3-dimensional image of the true penetration. Devane et al.[97] showed that for a group of 141 PCA joints the 3-dimensional penetration was measured at 0.264mm/year which was almost twice that found in similar studies using coronal plane radiographs alone.

The alternative method for establishing the penetration is used when the components are accessible, after revision or removal at post-mortem. This method was first described by Atkinson et al.[136] and in a modified form by Wroblewski et al.[131] and has become known by the generic title of shadowgraphing. A cast is made of the acetabular component, the profile of this cast is projected onto a screen and measured to ascertain the centre of curvature of the original surface and the worn area (this method is explained fully in Chapter 3.2.3). The distance between the two centres

gives the penetration depth. The angle of penetration can also be deduced relative to the plane of the open face of the socket. Hall *et al.*[133] directly measured the wear using a CMM and assessed the accuracy of both radiographic and shadowgraph methods. The penetration depths found using CMM and shadowgraph were found to be similar, but the radiographic method significantly underestimated penetration. Work by Cunningham *et al.*[137] on the repeatability and reproducibility of measurement using the shadowgraph method revealed that the penetration could be ascertained to a precision of less than 4% and less than 20% for the wear angle.

Once the penetration depth and angle has been found, whether they be in the coronal plane or the plane of wear, they have to be converted into volumes. The formula used by Charnley and co-workers[128,129] assumed that the wear volume was of a cylindrical shape. However, the later work of Kabo *et al.*[132] and Hall *et al.*[133] showed that this is not the case and such an assumption would result in an overestimation of the wear. Table 2.4 shows how the estimated volume of wear can vary and illustrates the caution that is necessary when interpreting results from different authors. Derbyshire[138] commented on the errors in estimation of wear volume which can be introduced through neglecting the initial radial clearance with which the THR is manufactured. The geometry of the PCA joint means that this will result in a small overestimation of wear volume.

In Table 2.5 we see the combined effects of varying methodologies and data sources illustrated. If we examine the penetration rates reported for Charnley type prostheses we can observe a twofold difference between the mean rate reported by different authors (Pedersen *et al.* 0.11mm/yr & Wroblewski *et al.* 0.21mm/yr).

There are alternative ways to assess the wear volume as mentioned above. These methods do not require the use of formulae as they give a measure of the true wear volume directly. The use of CMM requires a good quality reference surface from which the shape of the socket can be deduced. A matrix of points is obtained from which the volume change can be calculated assuming the original geometry is known. This is a complex and time consuming method but has the ability to give highly accurate results[151].

	Formula	Example (mm^3)
Cylindrical[128]	$V = \pi r^2 l$	760.3
Devane[97]	$V = r^2 \left[1.0472 - 0.666 \tan \left[\begin{matrix} (180 - \beta)\frac{2\pi}{360} \\ -0.0116(\beta - 90) \end{matrix} \right] \right] + \pi r^2 l$	896.3
Hashimoto[139]	$V = \frac{r^2 l}{2}(\pi + 2\beta + \sin 2\beta)$	583.8
Kabo[132]	$V = \pi r^2 l - r^2 \left[l \cos^{-1}\left(\frac{l \tan \beta}{r}\right) - \sqrt{\frac{r^2}{\tan^2 \beta} - l^2} + \frac{r}{\tan \beta} \right]$ $- \frac{r^3}{3 \tan \beta}\left[\left(1 - \frac{l^2 \tan^2 \beta}{r^2}\right)^{3/2} - 1 \right]$	616.1

Table 2.4:   Wear Equations - The above equations use the following abbreviations: V for the total wear volume, r for radius of the femoral head, l for the penetration depth and β for the penetration angle. The example calculation uses the equations shown to derive the volume wear caused by a 22mm diameter head with a penetration of 2mm at an angle of 40°.

In gravimetric techniques the weight of an explanted socket is measured, and deducted from the socket's original weight, giving a measure of weight loss and hence, by calculation, volume loss. This relies on the accurate estimation of the socket's weight when implanted. This method is prone to error due to the absorption of water by the polyethylene during its time *in vivo*[152] and the possibility of peripheral surgical damage when removing the prostheses.

A variation on the gravimetric technique is that of measuring the weight of fluid which can be contained in the socket. Again the volume of liquid held by a new component would be taken from that of the explant and the remaining mass would be converted into a volume[139]. This is in effect very similar to the fluid displacement method of Jasty *et al.*[145] where a femoral head of the appropriate size was placed into the explanted socket, abutted to the worn region, and the volume of oil required to fill the remaining volume was measured.

All the methods of deducing wear volume should at best be regarded as estimations of the volume of polyethylene lost. This is because, without the prospective measurement of the sockets prior to implantation, we cannot be sure of the original weight, or exact dimensions, of the components.

The problem of distinguishing the overall change in socket profile into the wear and creep components is negated by the use of gravimetric methods. However, the methods that calculate volumetric wear from a measure of penetration incorporate error due to inclusion of deformation as a result of creep. Creep is the plastic deformation of the polymeric component, also known as "cold-flow". The contribution of creep to the overall penetration has been studied previously[142,153]. In general the contribution of creep is small and primarily restricted to the early life of the prosthesis. Hall et al.[142] proposed that for 22mm diameter femoral heads the creep component was 96 (SE 36)mm^3 which occurred within the first year of implantation. This work is supported by simulator studies which give creep components of approximately 30mm^3 occurring within one million cycles[154]. If we consider the PCA system the larger head sizes used will tend to reduce the occurrence of creep as the stresses imposed on the bulk of the material may be less.

Table 2.5: Comparison of studies on wear. Note total wear may be expressed as either mean or median.

Author	Hip Design	Fixation Method	Cohort Size	Head Diameter	Experimental Method	Wear Equation	Total Wear (linear or volume)	Wear Rate (linear or volume)
Atkinson et al. 1985 [136]	Charnley	cemented	25	22	shadowgraph	-	580 mm³	65 mm³/yr
Cates et al. 1993 [140]	MOSC	cemented	233	28	radiographic	cylindrical	~0.6 mm 363 mm³	0.10 mm/yr 61.6 mm³/yr
Devane et al. 1995 [97]	PCA	cementless	141	32 & 26	3D radiographic	Devane	448 mm³	0.26 mm/yr 79 mm³/yr
Devane et al. 1997 [141]	Mallory-Head	both	70 cem 69 uncem	28	3D radiographic	Devane	-	98.5 mm³/yr 155 mm³/yr
Hall et al. 1996 [142]	Charnley	cemented	129	22	shadowgraph	Kabo (modified)	1.8 mm	0.20 mm/yr 55 mm³/yr
Hashimoto et al. 1995 [139]	PCA	cementless	57	32	gravimetric & shadowgraph	Hashimoto	grav - 551 mm³ shad - 387 mm³	grav - 1162 mm³/yr shad - 544 mm³/yr
Hernandez et al. 1994 [143]	Universal	both	231	28	radiographic	cylindrical	cem - 290 mm³/yr uncem - 449 mm³/yr	cem - 0.15 mm/yr uncem - 0.21 mm/yr
Isaac et al. 1990 [144]	Charnley	cemented	100	22	shadowgraph	-	1.69 mm	0.21 mm/yr
Jasty et al. 1997 [145]	various	cemented	128	-	fluid displacement	-	-	63 mm³/yr
Kabo et al. 1993 [132]	various	both	60	-	shadowgraph	Kabo	-	25.9 mm³/yr (22mm) 88.7 mm³/yr (32mm)
Kesteris et al. 1996 [146]	Scanhip	cemented	67	22 32	radiographic	cylindrical	-	57 mm³/yr 148 mm³/yr
Kusaba et al. 1997 [147]	Muller	cemented	24	32	shadowgraph	-	-	0.21 mm/yr
Pedersen et al. 1995 [148]	Charnley Iowa	cemented both	210	22 28	radiographic	cylindrical	-	0.11 mm/yr 0.12 mm/yr
Sychterz et al. 1996 [149]	various	both	26	32	post-mortem	Hashimoto	245 mm³	0.07 mm/yr 39.8 mm³/yr
Woolson et al. 1995 [150]	Harris-Galante	cementless	80	28	radiographic	-	-	0.14 mm/yr
Wroblewski et al. 1985 [131]	Charnley	cemented	22	22	radiographic shadowgraph	-	-	0.21 mm/yr 0.19 mm/yr

2.5.2 Wear Debris Isolation and Characterisation

The morphology of the wear debris produced has important implications to the biological response solicited from the host (see Chapter 2.2.3). It is therefore important that the size distribution, shape and numbers of particles produced during the articulation of a joint are characterised. This also provides insight into the wear mechanisms which are present. In the laboratory situation it is possible to retain the lubricant used for testing and extract the wear debris at any juncture. However, in the clinical situation the debris will reside in the tissue surrounding the joint and it will only be accessible during revision surgery, or at post-mortem. Further, in this case we have to be able to isolate the debris from the tissue in which it will reside without affecting the data obtained.

Early attempts to characterise the wear debris produced during the articulation of total joint prostheses utilised standard histological techniques to observe the debris *in situ*[19]. The size of particles that this technique could distinguish was limited by the resolution of the optical microscopes used and is reflected by the assertion of Schmalzried *et al.*[19] that most UHMWPE particles were less than 1μm in size as evidenced by a general cytoplsmic birefringence. The early work by Lee *et al.*[155] using tissue digestion to isolate the wear particles also used optical microscopy and therefore suffered from exactly the same limitation.

The work of Lee *et al.* also serves as a good example of the problems which isolation techniques must address. They compare the size range of metallic debris observed in the tissue with that of particles isolated from the tissue. The mean size of the particles was found to be, 0.3μm and 0.8μm, respectively. This is explained by the assertion that the larger particles must be removed by the process of tissue sectioning prior to debris extraction *in situ*. However, a more likely scenario is that the small metal particles are lost at some point during their digestion routine.

The methodology now adopted, almost universally, is tissue digestion followed by ultra-centrifugation, the filtering of the supernatant fluid and examination of the debris using SEM. A wide range of chemicals are used for the digestion of the tissue (Table 2.6) but all result in the liquefaction of the tissue and breakdown of all the long-chain molecules. It is important that the agent used for the digestion of the

tissue does not affect the particles. Margevicius et al.[156] looked at the morphology of titanium and polyethylene particles before and after their isolation procedure and concluded that the particles were identical.

The successful isolation of wear debris has initiated a substantial amount of work into the size distribution of wear debris found in vivo. However, in reviewing the literature currently available one must exercise caution as the published studies may be subject to criticism in many regards. For example the study of Yamac et al.[157] employs a very small dataset within which there are variations in joint type. There is a general trend towards not specifying the origin of the periprosthetic tissue, beit lytic or fibrous, femoral or acetabular[157-159]. This is an important parameter as the migration of debris through the tissue is likely to be related to the size of the particles[48]. The studies of Tipper et al.[160] and Hirakawa et al.[161] represent well designed experiments yet even in these there are discrepancies. Hirakawa uses sequential filtering with pore sizes of $10\mu m$ and then $0.4\mu m$, whilst Tipper uses $10\mu m$ and then $0.1\mu m$. It should therefore come as little surprise that the modal size of debris reported by Hirakawa is $0.8\mu m$ and that of Tipper is within the range 0.1-$0.5\mu m$. Hirakawa's choice of pore size has resulted in the loss of the majority of the wear particles in the filtrate.

It seems likely then that the modal size of the UHMWPE debris is within the range reported by Tipper et al.[160]. However, as the techniques involved are refined and the minimum size of particles retrievable reduces it may be that this figure has to be refined. The size of the metal or PMMA wear particles has been investigated by few authors, many of the retrieval procedures documented are in fact designed only to yield polyethylene particles. It is interesting to note that the studies of Kobayashi et al.[159] and Yamac et al.[157], regarding UHMWPE and metallic particles respectively, yield very similar dimensions for the debris. The work of Soh et al.[162] on wear debris retrieved from metal-on-metal hip joints gave a much smaller modal size lying within the range $0.15-0.25\mu m$. This suggests that the comparable results of Yamac et al. and Kobayashi et al. are quite possibly an artefact of the similar retrieval protocols. A modification of the method of Kobayashi et al. was used by Iwaki et al.[163] to study the size of PMMA particles and again this gives similar results.

Conversely, it is of interest that certain parameters in the study of wear debris become less important to the quality of the results. In the study of wear volume, the femoral head diameter has a great influence on the wear rate. However in the study of wear debris Campbell et al.[158], showed that the femoral head diameter had little effect on the morphology of the wear particles this would only be the case where the different femoral heads were of the same roughness.

The fact that various prosthetic designs all yield similar size distributions of particles has prompted interest in the mass distribution of these particles. Whilst there are few of the larger 10µm sized particles their far greater volume may result in their contributing more substantially to the mass of the debris than their numbers may suggest. Work carried out at Leeds University[160,164] on debris retrieved from tissue taken from a group of 18 Charnley prostheses has shown a considerable variation in the mass distribution. A wide variation was reported with a range of 3% to 82% of the mass of material being greater than 10µm in size. The authors attempt to ascribe this variation to head roughness, oxidative degeneration and "patient factors". However the effect of the multiple sampling errors must contribute heavily to the variation observed. The omission of any of the larger particles as a result of the many sampling stages would act to heavily skew the result.

As the science of debris isolation has advanced, methods of counting particles either electronically or by graphical techniques have evolved. This has enabled authors to produce figures for the load of particles found in the periprosthetic tissue, expressed as particles per gram (Table 2.6)[156,157,159-161,165]. Whilst this is of interest in terms of the cellular reaction (Chapter 2.2.3), these figures must be viewed as approximations. In the words of Kobayashi et al.[159] "The number of particles on the filter face was counted by multiplying the average number of particles seen per unit area of the SEM photographs by the area of the filter face. The number of particles extracted could then be related to the wet weight of the tissue which originally contained them since all the dilutions and the extraction ratio (previously calculated) of the particles were known.". This process compounds a number of errors which will reduce the accuracy of the extrapolation.

If the values of UHMWPE particle density derived are compared between studies we observe a degree of variance (Table 2.6). The studies of Maloney et al.[165] and Tipper

et al.[160], which make no distinction between tissue taken from osteolytic regions or not, produce similar ranges (0.23-6.1 & 0.15-13.0 billion particles per gram of wet tissue respectively). However, Kobayashi *et al.*[166,167] showed that the concentrations of particles in the areas of osteolysis were significantly greater than those in areas without osteolysis. A mean of 34.0×10^9 particles per gram for the osteolytic and 4.32×10^9 for the non-osteolytic regions were found. This agrees with the histological studies that the concentration of particles is a factor in the generation of osteolysis. However whilst these figures may be indicative of a trend, they should not be interpreted as absolute values for the stimulation of osteolysis. It is interesting to note that the concentration of metallic wear debris within the tissue[157] is an order of magnitude less than that of UHMWPE debris as would be anticipated.

In addition to work on the size distribution and particle density, interest is being focused on the shape of the debris as this again may have bearing on the osteolytic potential of the particles. The qualitative description of the various fibrils, beads and platelet-type wear particles is undertaken by most authors. However the quantitative description of the shape is in its infancy. The introduction of computer based graphical analysis packages has enabled the use of many descriptors of shape such as aspect ratio, equivalent circle diameter (ECD) and roundness[157,166,168]. The use of these parameters is gaining popularity possibly in part due to the ease with which these values can be produced. Their value as ways of distinguishing debris produced from different wear mechanisms is yet to be shown. Kobayashi *et al.*[159] failed to show any difference in the ECD, aspect ratio or roundness when comparing THR and TKR wear debris. This contradicts the more qualitative study of Schmalzried *et al.*[24] where TKR debris was shown to be larger than that of THR.

The technique of debris isolation has also been employed to compare the wear debris produced *in vitro* with that found in the periprosthetic tissue. Hailey *et al.*[169] isolated wear debris produced by UHMWPE pins sliding against steel plates using water and bovine serum as lubricant, and compared it to that from a group of Charnley THRs. They observed a number of similarities between the *in vitro* debris produced by a smooth plate and the *in vivo* wear debris, but not for the laboratory tests using rougher counterfaces. Similarly, McKellop *et al.*[170] showed that the wear debris produced by a joint simulator was comparable with that produced *in vivo*.

Author	Technique Employed	Sample Size	Debris Species	Filter Size (μm)	Debris Size Range (μm)	Particle Density (10⁹/g)
Campbell et al., 1996 [158]	NaOH digestion, centrifuge & SEM	10 THR & 15 surface replacement	UHMWPE	0.1	beads 0.35 fibrils 2.3	-
Hailey et al., 1996 [169]	KOH digestion & SEM	8 THR	UHMWPE	0.2	0.3 to 3mm	-
Hirakawa et al., 1996 [161]	nitric acid digestion, SEM, EDAX & counter	88 THRs - various designs	UHMWPE & metal	10, 0.4	mean 0.79	0.08 to 57 dry
Kobayashi et al., 1997 [159]	NaOH digestion, centrifuge, SEM, EDAX	10 TKR, 3 THR & 5 surface replacements	UHMWPE	0.1	0.82 (ECD)	0.52 to 91.7 wet
Lee et al., 1992 [155]	isolation - digestion non-isolation - histology	30 THR	metal UHMWPE	-	0.3 to 0.7 2 to 13	0.23 to 6.1
Maloney et al., 1995 [165]	papain digestion, SEM of digest	35 loose femoral THR	UHMWPE metal	-	0.5 0.7	1.7 wet
Margevicius et al., 1994 [156]	nitric acid digestion, SEM	14 TKR 5 THR	UHMWPE metal	10, 0.4	mode 0.65	0.85 to 141.85 dry
McKellop et al., 1995 [170]	NaOH disgestion, SEM	3 THR & simulator lubricants	UHMWPE	-	beads 0.2-0.8 fibrils 0.5-4.0	-
Schmalzried et al., 1994 [24]	optical of histological slides	24 THR 19 TKR	UHMWPE	-	THR <1 TKR 2 to 20	-
Shanbhag et al., 1994 [171]	KOH digestion, SEM, FTIR spec., EDAX	11 failed THRs	UHMWPE + others	-	0.53	-
Tipper et al., 1997 [160]	KOH digestion, sequential filter, SEM	19 cemented THR	UHMWPE	10, 0.1	mode 0.1-0.5	0.15 to 13.0 wet
Yamac et al., 1996 [157]	NaOH digestion, SEM, EDAX	5 THR, 1 TKR	metal	0.1	0.55 (ECD)	0.005 to 3.1 wet

Table 2.6:   Studies of Particle Size. Particle density describes the number of particles estimated to occupy a gram of tissue.

2.5.3 Surface Roughness Measurement

The texture of any surface can be characterised with three sets of features defined as form, waviness and roughness. Form error can be regarded as inaccuracy in the overall shape of the component. Waviness error features are those which repeat themselves regularly and are often as a result of the machining process. Roughness is the remaining deviation from the ideal surface[172]. The component errors of the actual surface are shown schematically in Figure 2.10.
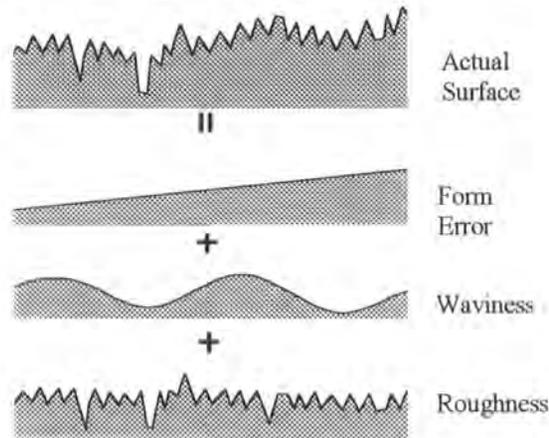
Figure 2.10: Schematic representation of surface texture components.

There are many different methods used to measure surface texture. These may be classified in terms of their data collection mechanism. Measurement systems fall into two categories; contacting or non-contacting. Contacting types involve the use of a mechanical stylus (e.g. Talysurf). Non-contacting systems include optical focus detection, optical interferometry, light scattering, capacitance and electron tunnelling. Contacting methods and optical focus detection only give surface information for the profile over which they travel. To give 3-dimensional information a series of measurements is required. However, techniques such as optical interferometry give immediate 3D information for the surface[173]. Each of the above measurement systems has its limitations. For example the size of the minimum surface defect capable of being resolved by contacting systems is dictated by the shape and size of the tip of the contacting stylus. It is important to be aware of the efficacy of each system and the influence this has on the roughness values measured.

There are many parameters used to describe the surface texture of components. A full description of the measurement technique and parameters used in this study can be found in Chapter 3.2.5 and Appendix 3.

2.6 Summary

John Charnley called for surgeons to have an understanding of elementary engineering. Similarly it has been shown that for the continued optimisation of joint replacement technologies it is increasingly necessary for bioengineers to be equipped with a fundamental knowledge of subjects outwith traditional engineering.

The influence of numbers, size and shape of wear particles has been illustrated. In order to modify the wear characteristics of the present generation of THRs to release less damaging debris we need to have a complete understanding of the wear mechanisms occurring. Only when this is achieved may it be possible to choose the correct strategy to relieve the problem of osteolysis.

The poor survivorship rates of the PCA compared with the Charnley will be considered in light of the information provided by the investigation of the wear parameters of the PCA. The complete characterisation of the tribology of the PCA joint will provide insight into the possible ways to address the challenges in improving the longevity of the THR.

3. Experimental Procedure

3.1 Materials

One hundred and nineteen joints were retrieved at revision by consultant surgeon Mr.
I. M. Pinder, Freeman Hospital, Newcastle-Upon-Tyne. However, due to the
modular nature of the PCA system the numbers of each component received varied
(see Table 3.1). The earliest recorded revision date was in July 1990, with the most
recent being in August 1998.

Femoral		Acetabular	
Stem	Head	Metal backing	Liner
17	6 of 26mm ∅	57 one-piece	57 one-piece
(3 HA coated)	2 of 28mm ∅	50 snaplock	59 snaplock
	73 of 32mm ∅		

Table 3.1:   Summary of received components.

All of the snaplock joints were of the hooded variety. Unfortunately not all the joints
received were identified leading to the inclusion of twenty-four joints of unknown
origin.

The ninety-five joints of known origin were obtained from eighty individuals, forty-
two of whom were men. Fifty-three of these ninety-five joints were from the right
side. The median age at primary surgery was 45.98 years (range 15.8 - 75.5). The
mean mass of the patients was 70.0kg (SD 14.2). The mean implant life was 6.29
years (SD 3.47). The diagnoses at primary and revision operations are given in Table
3.2. A full listing of all patient information can be found in Appendix 1.

Primary		Revision	
Diagnosis	Numbers	Diagnosis	Numbers
Rheumatoid Arthritis	31	Migration	39
Osteoarthritis	36	Pain	15
CDH	11	Lysis	21
Avas. Necrosis	2	Wear	13
Ankyl. Spondy.	4	Dislocation	3
Other	8	Sepsis	2

Table 3.2:   Summary of diagnoses.

3.2   Methods

3.2.1   Initial Examination

Clearly a number of the explanted joints involved in this study were removed prior to the date of commencement. These joints were processed in exactly the same manner as those received during the study.

The joints removed at surgery during the course of the study where promptly collected and transported to the Centre for Biomedical Engineering, University of Durham were they were soaked for at least 8 hours in Gigasept solution (Schulke & Mayr). This is a formaldehyde based fixative and sterilising fluid. The components were then cleaned and any excess bone or tissue was removed. The joints were catalogued and stored individually.

A preliminary study of the joints was undertaken to assess the gross wear features of the components. The presence of specific features such as delamination, dissociation, fracture, rotation and ridges were noted. Definitions of these terms can be seen in Table 3.3.

Feature	Definition	Recorded
Ridges	Ridge between the worn and unworn regions of the liners articulating surface.	Number present
Delamination	Flaking wear of the UHMWPE liner.	Internal - within cup External - on rim
Dissociation	The release of the UHMWPE liner from its metal backing *in vivo* (One-piece only).	yes/no
Rotation	One-piece only, spinning of the liner within its metal backing around the polar peg. Evidenced by gouging of rim by tab of metal backing.	yes/no
Fracture	Snaplock only, gross cracking of the liner through its thickness.	yes/no
Ingression	The infiltration of metal beads from the porous coating into the articulating space.	yes/no
Impingement	Wear of the rim due to contact of the neck of the femoral component at extremes of motion.	yes/no
Oxidation	Physical changes to the UHMWPE evidenced by the discolouration of the liner	yes/no

Table 3.3:   Definitions of gross wear features.

The occurrence of polishing of the stem of the femoral component due to micromotion was quantified using a scoring system. The stem was assessed using the zones of Gruen *et al.*[103] (Figure 3.1). The severity of the polishing was scored according to the percentage of the surface area of the relevant zone which was involved. If no polishing could be observed a score of 0 was recorded, 1-25% scored 1, 26-50% scored 2 and 51-100% scored 3.

The angle of the wear vector was calculated from the angle of the metal backing, the angle of penetration relative to the open face of the liner and the knowledge of the liner type involved. The angle of the metal backing, α, was ascertained using the method of Heekin *et al.*[78] (Figure 3.2). The measurement of the penetration angle, β, is covered in Section 3.2.3. Once these two angles had been established the angle of the wear vector relative to the saggital plane and in the coronal plane was calculated using equations 3.1a and 3.1b. Two versions are necessary due to the presence of the $10°$ hood in the snaplock type socket.

$$\text{wear angle} = 90 - (\alpha + \beta) \qquad (3.1a)$$

$$\text{wear angle} = 90 - (\alpha + \beta + 10) \qquad (3.1b)$$

The calculation of these parameters necessitated the assumptions that the wear vector lay in the coronal plane and that the hood was always positioned superiorly.
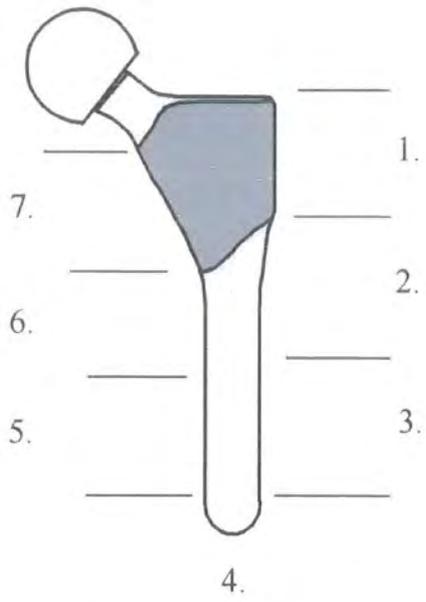
Figure 3.1:   Femoral component zones, modified after Gruen *et al.* 1979.
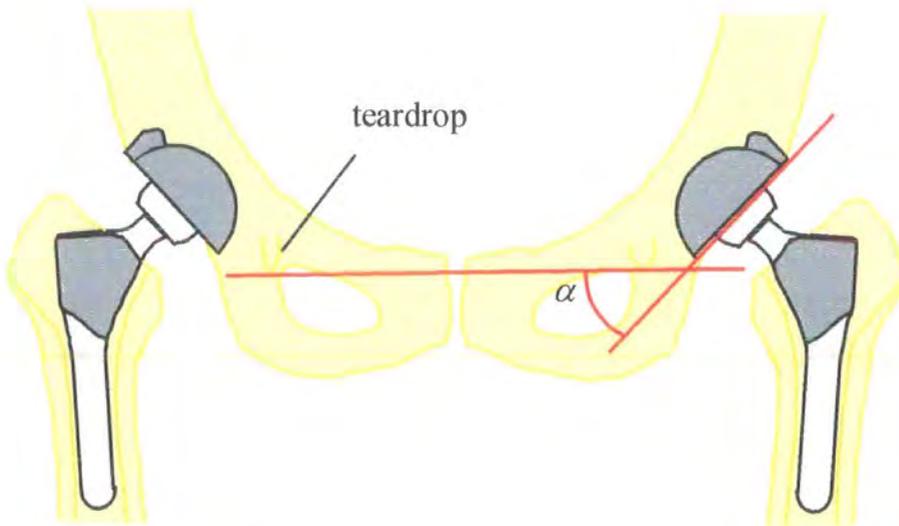
Figure 3.2:   Acetabular component angles after Heekin *et al.* 1993.

3.2.2 Friction Testing

Apparatus

The frictional resistance of each joint was measured using the Durham Hip Function Simulator. The simulator has previously been described in depth[60,174]. In summary, the hip function simulator comprised a PC for data analysis and control, a 68020-based microprocessor for data acquisition and servo-control and the simulator itself.

A schematic diagram of the simulator is given in Figure 3.3. The joints were tested in an inverted position. The acetabular jig (A) was supported in a tray which floated on two sets of externally pressurised bearings, allowing the tray to translate in the x and y directions and rotate about the x-axis. The femoral head was mounted on a taper which was in turn secured to a frame (B). To simulate motion the frame reciprocates about the x-axis through an arc of ±20° and the load (F) was applied by a servo-hydraulic system. Any rotation of the tray about the x-axis was resisted by a Kistler piezo-electric transducer which was calibrated in terms of frictional torque.
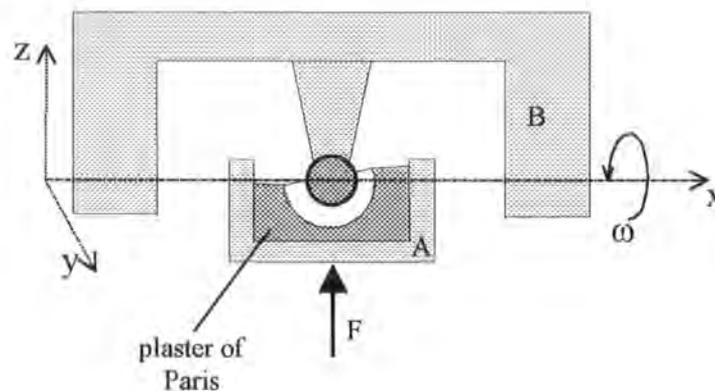
Figure 3.3: Schematic representation of friction simulator.

To ensure that the components of the joint under test were positioned exactly on the x axis when in the simulator, care had to be taken during their mounting. The femoral component was secured onto a taper ensuring that it was properly seated. The height of the head and taper when in the mounting block had to be adjusted in order that the centre of the head would coincide with the centreline of oscillation. The acetabular component (including metal backing) was secured into the tray using plaster of Paris.

Again care had to be taken to ensure that it was mounted at the correct height. A mounting jig held the socket in the correct position, relative to the femoral head, until the plaster had set. The head was abutted to the worn part of the acetabular cup which was orientated at approximately 33° to mimic the correct joint reaction force direction. Any possibility of contamination of the joint with plaster dust during testing was reduced by painting all exposed plaster surfaces with an acrylic varnish.

The loading cycle used was obtained by English & Kilvington[175] from patients with a primary hip replacement (Figure 3.4). The maximum and minimum loads imposed on the components during testing were 2000N and 100N respectively. The frequency of oscillation was 0.83Hz and each test run consisted of 40 cycles with the angular displacement, frictional torque and load being sampled 128 times per cycle. The data sampled for the last cycle was that used in the calculation of the friction factor.
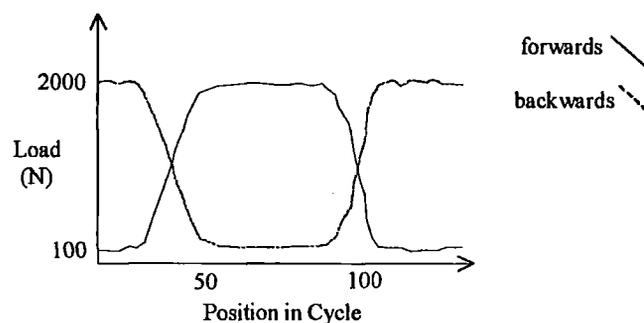
Figure 3.4:   Load curve characteristics.

It was necessary to perform two experimental runs prior to the calculation of the friction factors. Any error in the positioning of the joint about the axis of rotation would produce an error in the torque. This was compensated for by running a forward test in which the load was applied during the forward swing of the cycle and also performing a backward test in which load was applied during the backwards swing of the cycle. The torques produced during the two test runs are seen in Figure 3.5. The true frictional torque could then be calculated using the equation:

$$T = \frac{|T_b - T_f|}{2}$$
(3.2)
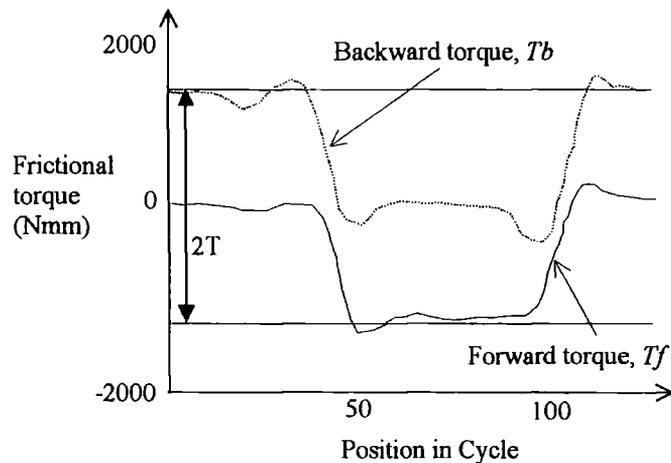
Figure 3.5: Torques produced during two experimental runs.

Testing

Twenty-two explanted joints and two new joints (supplied by Howmedica) were friction tested. Prior to testing, the joints were ultrasonically washed in a detergent solution (Neutracon, Merck). Five different viscosities of lubricant were used in the friction tests: 0.001, 0.003, 0.010, 0.030 and 0.100 Pa s, approximately. The viscosities of 0.003 to 0.100 Pa s were made from aqueous solutions of carboxymethyl cellulose which has been shown to have similar rheological properties to synovial fluid[107]. The 0.001 Pa s lubricant was de-ionised water and to ensure repeatability, the friction was tested twice at this viscosity. The viscosities were measured using a Ferranti-Shirley cone-on-plate viscometer at a shear rate of 3000 s^{-1}.

The order of testing using different viscosities of lubricant was randomised. All six tests on each joint were conducted consecutively. The joints were thoroughly washed with de-ionised water and wiped with acetone between the tests to ensure no cross contamination of the lubricants could occur.

3.2.3 Wear Measurement

The shadowgraph method was the chosen technique for measuring the depth of femoral head penetration into the UHMWPE liner. It was selected because it was inexpensive, and has been shown to perform as well as direct measurement using 3D co-ordinate measuring instruments[133].

59

The penetration was assessed in ninety-seven acetabular components, forty-eight being of the one-piece type. Nineteen joints had to be excluded due to gross wear, or fracture, of the liner. The preparation of the liners involved the removal of any burs and other protrusions from the rim of the cup so as to facilitate the removal of the cast. The cups were positioned using a spirit level so that the open face was horizontal. They were secured in position using a compliant adhesive. A two-part silicone rubber casting agent (Ambersil RV 2039) was then poured into the cup to the level of the open face. This moulding agent has a shrinkage of less than 0.1 percent. The moulds were left for at least 24 hours to set. The compliant mould was then carefully removed.

Shadowgraph tracings at a magnification of ten times were produced using a Societe Genevoise D'Instruments de Physique AP-6 (National Gear Metrology Laboratory, University of Newcastle-Upon-Tyne). The profile of the mould when orientated in the wear plane was traced. The initial position of the femoral head, x, was located by the use of a stencil fitted against the unworn region of the profile. The centre of the femoral head when in its final position, y, was found by placing the stencil against the worn region (Figure 3.6). In some cases there seemed to be two distinct directions of wear as evidenced by the presence of more than one ridge in the liner (Appendix 2). In these cases the orientation which produced the largest displacement was chosen. The penetration depth and angle were calculated from these two points. The experimental error of these two measurement was $\pm\,0.05$mm and $\pm\,0.5°$ respectively.
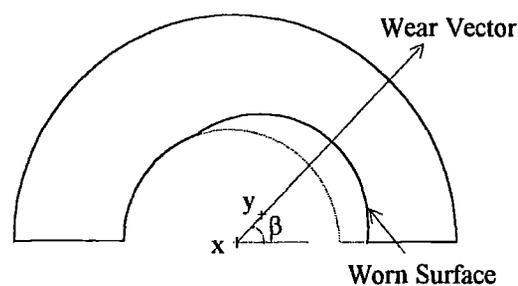
Figure 3.6:   Schematic representation of liner cross-section in the wear plane.

The Kabo formula (see Section 2.5.1) was selected to calculate the wear volume. The criticisms of this formula given by Derbyshire[138] were not considered to be significant for the PCA joint due to its purely hemispherical design. In cases where the

penetration was too small to be reliably measured, a penetration depth of 0.05mm and angle of 90° were assigned to the liners. In the calculation of the mean total wear volume, all the available joints were considered including those without patient notes (85 at 32mm, 5 at 28mm and 5 at 26mm).

3.2.4 Calculation of Wear Parameters

The calculation of all the wear parameters was conducted using Stata 4.0 statistical analysis software (Stata Corp., Texas). Due to the presence of unidentified joints within the study group a maximum of seventy-six joints could be analysed. Only nine of these were of head diameters other than 32mm. Hence, for the calculation of the wear parameters only the 32mm joint size provided a large enough cohort to perform reliable statistics.

In the case of two joints, the periods of implantation were too small for the joint to have undergone many cycles of wear (<1 month), these joints were excluded. Standard linear regression was used on the remaining sixty-nine 32mm joints to calculate the mean rate of penetration and the mean volumetric wear rate. The model used for this analysis had the form:

$$\Delta P = m\Delta T + c \qquad\qquad (3.3)$$

where ΔP is the penetration depth, ΔT is the implant period and m and c are constants. Given that experimental evidence indicates that the creep component is constant after a relatively short period of time[142,145,151], then the gradient, m, of the function is equal to the penetration rate, $\Delta P/\Delta T$. The regression constant, c, may incorporate changes in the internal bore volume or the penetration depth due to creep. Mean volumetric wear rate was calculated in a similar manner.

Clinical wear factor, $k_{clinical}$, is a development of the fundamental wear equation which states that the wear volume is proportional to the load and the sliding distance (see Chapter 2.4.2). To be applicable to the clinical situation the load is the joint reaction force which is a function of the patient weight. The sliding distance becomes a combination of the number of wear cycles and femoral head radius. The clinical wear

factor is the constant of proportionality and may be deduced from the simplification of the wear equation produced by Dowson and Wallbridge[176];

$$\Delta V = k_{clinical}(2.376 N W r) + C \qquad (3.4)$$

where N is an estimate of the number of cycles to which the joint has been subjected during its life, r is the radius of the femoral head and W is the patient weight. The number of cycles is calculated using the following empirical formula derived by Wallbridge and Dowson[177] relating age to activity,

$$N = 0.5 \left(A_r - A_p \right) \left[6.58 - 0.032 \left(A_r + A_p \right) \right] \times 10^6 \qquad (3.5)$$

where A_p is the patient age at primary surgery and A_r age at revision surgery. This formula was based on data gained from normal subjects and therefore it may vary from the level of activity achieved by patients. However, Wallbridge and Dowson[177] warn against the assumption that patients are less active than normal subjects. Recent work published by Schmalzried et al.[178] presents data for a large study of patients who had undergone lower limb joint replacement. In the age range 40-80 years the relationship given by Schmalzried et al. estimates a significantly larger number of cycles than that of equation 3.5. It was decided that the relationship proposed by Wallbridge and Dowson should be used in order to remain comparable to previous work involving the calculation of a clinical wear factor. The mean clinical wear factor was calculated, again using regression analysis, in the manner described by Hall et al.[142]. Clinical wear factors of individual sockets were calculated using equation 3.4 with the assumption that the creep, C, was negligible.

3.2.5 Assessment of Surface Topography

A combination of differential interference contrast (DIC) microscopy (Axiotech, Ziess) and scanning electron (SEM) microscopy (Joel JSM IC848) was used for the qualitative assessment of the surface topography of the components. DIC was conducted at magnifications of x50, x100 and x200 in order to assess the wear features over large areas. The SEM employed a range of magnifications up to x10,000 to ascertain the nature of the nanometre scale surface features.

Prior to their assessment the components were washed ultrasonically in a Neutracon solution and wiped with acetone. The UHMWPE samples for use in the microscope were left overnight in a dessicator and then sputter-coated with gold.

The quantitative measurements of the surface texture of the prostheses were conducted using a NewView 100 optical interferometric profilometer (Zygo Corp., Connecticut). This instrument has a sub-nanometre vertical resolution. The horizontal resolution is dependent on the optical magnification chosen. The number of data points remains constant whatever the area under examination, therefore the greater the magnification the smaller the horizontal resolution.

Two different measurement protocols were used, one for the femoral head surfaces and another for the acetabular liners. In the case of the femoral heads the surfaces remain smooth and little form error was anticipated therefore a x40 objective was used giving a true magnification of x400. This resulted in a measurement area of 180μm by 135μm and a horizontal resolution of 0.56μm per pixel. The liners display a much more macroscopically textured surface due to their machining and granular structure. Therefore, a x10 objective (true magn. x100) was chosen, giving 730μm by 550μm of coverage and a horizontal resolution of 2.28μm per pixel.

The measurement protocols and description of the parameters used can be seen in Appendix 3. In summary, the heads were measured in nine positions, six in the worn area and three peripherally. In the case of the liners this was increased to ten and four, respectively, as the number of modes of wear observed was increased. The surface texture parameters were chosen prior to testing rather than afterwards. This eliminated the possibility of inappropriate parameters being considered.

The surface topography of fifty-five femoral heads and sixty-seven acetabular liners was assessed. In addition, two pairs of unimplanted heads and liners were measured. All components were cleaned ultrasonically in a solution of Neutracon detergent and subsequently wiped with acetone to ensure that no surface contaminants remained. The liners were cut into quarters to facilitate their positioning under the profilometer.

3.2.6 The Relationship of Surface Topography with Wear

Two simple models to predict the influence of counterface roughness on the rate of wear of the UHMWPE were presented in Section 2.4.2. That of Dowson et al.[116]

$$k = 4 \times 10^{-5} (R_a)^{1.2}$$ (2.3)

and that of Wang et al.[118]

$$\frac{\Delta V}{N} \propto L^{1.5} R_a^{1.5} \frac{1}{\sigma_u^{1.5} \varepsilon_u}$$ (2.4)

These models predict that the femoral head roughness will have a strong influence on the wear of the UHMWPE counterface. This being the case it is of considerable importance to establish the effect that femoral head degradation has on the rate of wear of the UHMWPE sockets. There have been a number of reports concerning the roughening of the femoral head *in vivo* [179-183] and it has been shown that this phenomenon is of concern whatever the fixation technique employed by the joint or which metal is used to make the head[183]. It was noted by Wroblewski et al.[184] in a study of four retrieved joints that their low rates of head penetration coincided with the maintenance of the surface finish of the head.

Few authors have attempted to reproduce the relationships shown in laboratory tests using data from *ex vivo* components. Hall et al.[142] demonstrated that the model proposed by Wang et al. was as good as that proposed by Dowson et al. in describing the relationship between R_a and k for a series of *ex vivo* components. However, in either case the association was weaker than that found *in vitro*, a result also observed by Atkinson et al.[136].

The models of Dowson et al.[116] and Wang et al.[118] shown above were considered in order to ascertain if they are applicable to the clinical situation. The area roughness as opposed to profile roughness values were used (S_a not R_a).

3.2.7 Investigation of Crystallinity

It is recognised that the material properties of the polyethylene used for the acetabular liners may vary during the life of the prosthesis (Chapter 2.4.2). In order to assess the

degree of change that the liners experience, a series of investigations into their crystallinity was undertaken.

A preliminary study was conducted using a range of unimplanted 'raw' UHMWPE samples. Specifically, the effect of irradiation was examined by comparing three samples of UHMWPE from different production batches. Once the preliminary study had been completed a study of *in vivo* degradation could be undertaken. Joints which had been explanted for a long time were excluded from this study in order not to bias the results. Six joints were selected, of which only one was of unknown origin. The duration of implantation of all five identified joints was in the range 6 to 9 years. All were stored frozen prior to their assessment. Differential scanning calorimetry was the method chosen to quantify the crystallinity. This was undertaken at the I.R.C. Polymer Chemistry Unit, University of Durham using a Perkin Elmer DSC7 instrument.

Samples weighing approximately 3 grams were removed from the liners from a number of specific sites. These sites were the rim, the worn region and the unworn region. A number of samples were taken across the profile of the liner beneath the worn and unworn regions in order to ascertain if the depth within the bulk of the material had any influence.

3.3   Wear Debris Study

In Section 2.5.2 the importance of the debris retrieval protocol on the quality of the information obtained was examined. The influence of experimental errors due to the source of tissue samples and the compounding of error at each stage of the retrieval protocol cannot be understated. Initial investigations into the efficacy of two methods of debris retrieval are detailed below.

3.3.1   The Tipper Method

The first method which was assessed was that of Tipper *et al.*[160]. A listing of this protocol can be seen in Appendix 5a. This is a refinement of the method published by Hailey *et al.*[169].

A number of weaknesses were identified. The most deleterious was the constant increase in volume of digestate with every step of the protocol. In particular the need to dilute the concentrated KOH solution down to a level where it was no longer harmful to the polycarbonate filter membranes. The filtration rate through the membranes was slow due to the small pore size. Therefore the two-stage filtration utilised took a substantial time to perform.

A typical SEM micrograph can be seen in Figure 3.7. The wear particles were closely interwoven and often appeared to be coated with some contaminant. The presence of unusual spherical particles was frequently noted. This is considered to be some form of contamination.

The weaknesses of the Tipper *et al.* protocol prompted interest in alternative protocols which were more "compact". The method of Campbell *et al.*[185] was identified as one which had been shown to perform well and had been adopted in a modified form by other research groups[159,166].
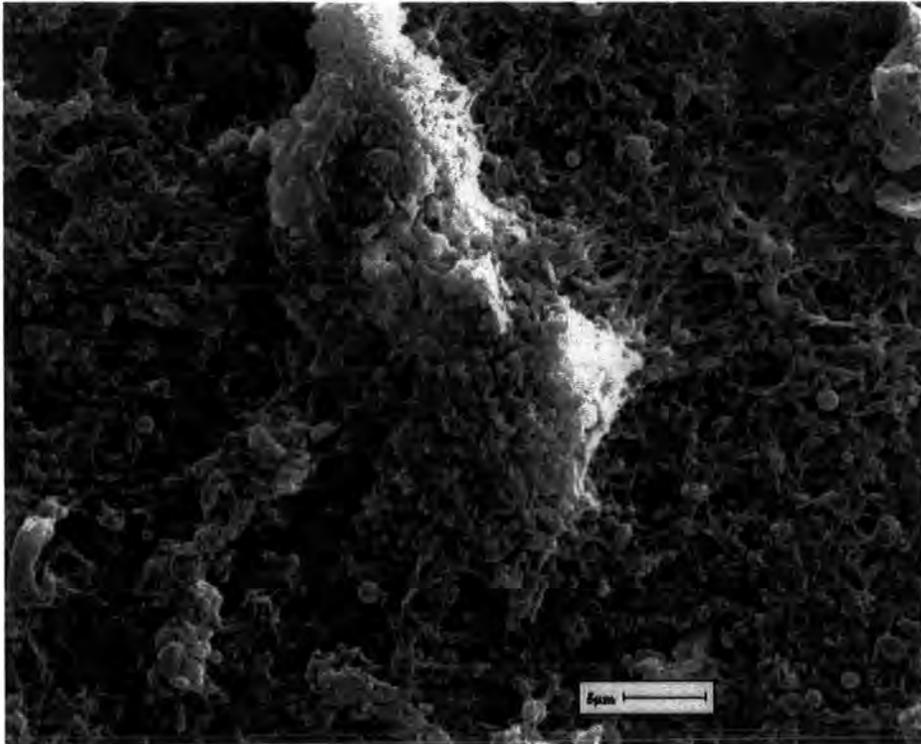
Figure 3.7: SEM image of debris retrieved using the Tipper *et al.* protocol.

3.3.2 The Campbell Method

The second method to be considered was that of Campbell et al.[185,186]. A listing of this protocol can be seen in Appendix 5b. This is in essence similar to the method of Tipper et al. using a strong base to hydrolyse the protein, with chloroform/methanol solution used for extraction of low density lipids, followed by centrifugation and filtration. However, the two methods vary greatly in the detail of how this is achieved.

A substantial difference in terms of the centrifugation stage of these protocols can be observed. The two techniques are so disparate the first impression may be that one is in error. The terminal velocity of the particles can be calculated from Stoke's Law (eqn. 3.6)[187];

$$u_s = \frac{\left(\rho_s - \rho_f\right)d^2 g}{18\eta} \qquad (3.6)$$

where u_s is the terminal velocity of the particle with a diameter, d, and density, ρ_s, in a fluid of density, ρ_f and viscosity, η. Let us examine the sedimentation potential in terms of maximum displacement of the slowest moving, smallest, particles for the two protocols. Assume the diameter of the smallest wear particle to be $0.1\mu m$ and the density of UHMWPE as $930 kgm^{-3}$. For Tipper et al.'s protocol the fluid density is approximately $1.24 kgl^{-1}$ and viscosity can be assumed to be that of water $1.0 \times 10^{-3} Pa$ s. The terminal velocity of the particle can be calculated to be $-3.4 \times 10^{-6} ms^{-1}$, the negative indicating that the particle will travel upwards. For a centrifuge duration of 15 minutes the maximum displacement will be 3.06mm upwards. A similar calculation for the Campbell et al. protocol shows that the particles are capable of terminal velocities of approximately $-37 \times 10^{-6} ms^{-1}$ in the 10% w/w sucrose solution and $-43.6 \times 10^{-6} ms^{-1}$ in the 5% w/w sucrose solution. This means that the particles can move completely through a depth of 0.216m of each solution. Clearly the method of Campbell et al. is more than capable of moving the entire particle population to the surface of the liquid. However the method of Tipper et al. will not achieve this situation. A sizeable proportion of the particles may be expected to still reside within the bulk of the liquid. If only the top portion of the liquid were removed then this may result in a bias towards the larger particle sizes. The protocol of Tipper et al. requires the retention of the supernatant fluid after this first centrifugation step which

must be drawn off to within at least 3mm of the base of the centrifuge tube. This first centrifugation step of the Tipper *et al.* protocol may be regarded as sedimentation of dense waste matter rather than the floatation of the UHMWPE wear debris.
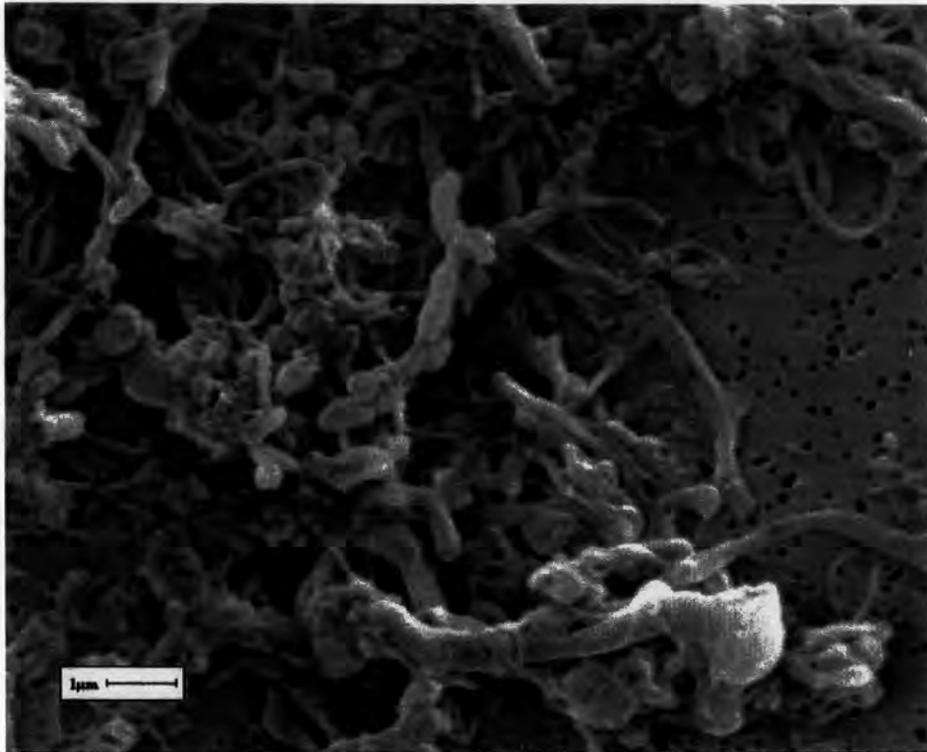
Figure 3.8:   SEM image of debris retrieved using the Campbell *et al.* protocol.

The results produced by the Campbell *et al.* protocol seemed to be superior to those of the Tipper *et al.* method.   Figure 3.8 shows the debris retrieved using the Campbell *et al.* protocol.   The images obtained seemed to be free of foreign matter and in particular the complete absence of the spherical contaminants was noted.

The advantages of the Campbell *et al.* protocol were the production of a pure concentrated solution of the wear debris held within a colourless medium (this advantage will be discussed in Section 3.3.5).   The method is more compact than that of Tipper *et al.* and as such is less time consuming.   Further Campbell *et al.*'s procedure is used by a number of groups world-wide and as such the direct comparison of results is facilitated.

3.3.3 Errors Associated with Drying and Weighing of Retrieved Debris

Once the debris has been isolated by digestion and filtration it is necessary to ascertain the mass of material retrieved. A brief investigation into the errors involved with this stage of the protocol was conducted.

Accurate measurements of the membrane weight before and after the extraction of debris are needed. The polycarbonate membrane used for the filtration has a highly hydrophilic nature, as does the UHMWPE to a lesser degree. Therefore it is necessary to completely dry the membrane prior to weighing. This is achieved in Tipper *et al.*'s protocol by heating the membranes under infrared lamps for 4 to 6 hours.

The effect of moisture absorption after drying was investigated and the results can be seen in Figure 3.9. The filter membrane rapidly absorbed moisture up to a period of 5 minutes becoming constant at a rate of approximately $2\mu g/min$. after 20 minutes. To achieve a reasonable level of accuracy and repeatability measurements would require a period of rest after drying of approximately 10 minutes in a temperature and humidity controlled environment.
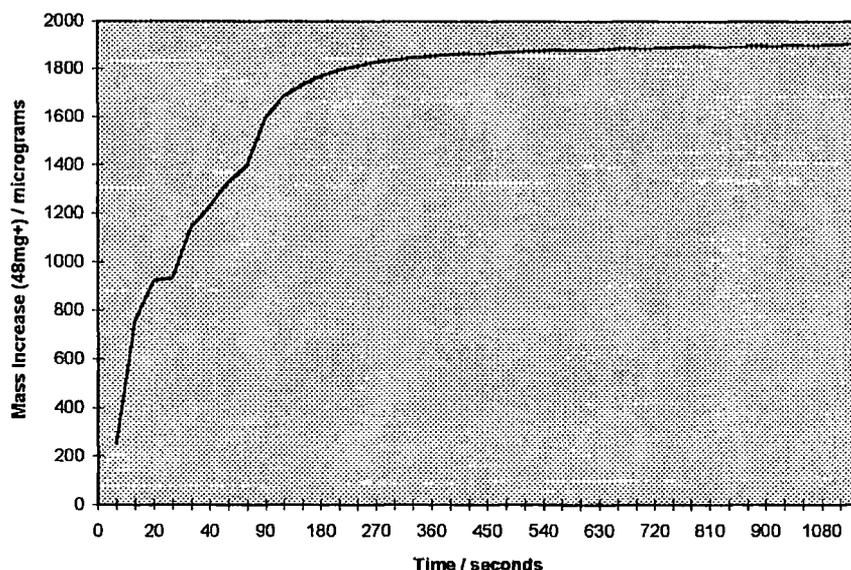
Figure 3.9:   Mass increase with time after drying for 2 hours under an infrared lamp. Note the x-axis scale is non-linear.

The accumulation of static charge in the membrane must also be considered. The removal of moisture from the membrane will increase its potential for gathering charge. The adoption of de-ionising fans by the Leeds group attests to this fact. Sufficient equipment was not available to allow an assessment of this phenomenon.

The drying and weighing of the membrane introduces a number of handling steps where there may be contamination of the membrane with dust and so on.

This drying and weighing stage of the procedure has the potential to introduce considerable error into the assessment of debris mass. In Tipper *et al.*'s[160] paper they measured a range of debris masses from 27μg to many hundreds of micrograms. Clearly the effect of any weighing errors on this minimum figure may be significant.

3.3.4 Errors Associated with the SEM Analysis of Particle Size

The universal method of ascertaining the range of particle sizes retrieved is by SEM of the filter membrane. This can provide the high magnifications necessary to resolve the particles and gives information on the morphology of the particles.

Unfortunately this method may be criticised due to the opportunity for the introduction of sampling errors from a number of sources. The majority of workers take a small series of micrographs across the membrane and extrapolate the data obtained for the whole membrane[158,159,188]. It is unlikely that these sample areas will have the same distribution of particles as the whole. There may well be gradient of particle sizes across the membrane due to meniscus and surface tension effects during the filtration.

The assessment of the particles within each micrograph is also prone to observer error. There is the possibility that the observer may be biased towards a certain size of particle. This may be overcome by the use of graphical analysis packages. However graphical analysis packages rely on being able resolve individual particles. If the SEM images were similar to those shown in Figures 3.7 and 3.8 with large numbers of particles conglomerated together the use of this technique would become inappropriate.

The most fundamental concern about the use of 2-dimensional SEM analysis to infer a 3-dimensional size population is the risk of unrepresentative sampling of the particles. Only a small number of particles were assessed by most workers even with the assistance of graphical analysis packages see Table 3.4. The likelihood of a 2000 particle sample accurately representing a particle population of 2000 million particles is small.

Author	Graphical Analysis Used	No. of Particles Assessed
Besong et al. [188]	Image-pro Plus, Datacell Ltd.	2000
Campbell et al. [158]	yes	100
Kobayashi et al. [159]	Quantimet 570, Lieca Ltd.	100
Lee et al. [155]	Model 3000, Image Tech Corp.	250
Maloney et al. [165]	no	100
Shanbhag et al. [171]	no	not specified

Table 3.4:   Summary of number of polyethylene particles analysed in various studies.

3.3.5   Laser Diffraction Particle Analyser

The use of automated particle counters has been investigated by some workers[156,165]. These papers detail the use of Coulter counters to ascertain the size distribution of the particles. These devices were designed to measure the size distribution of red blood cells suspended in a dilute electrolyte. The change in electrical capacitance of blood was measured as the cells passed through an orifice. The inherent disadvantage of these devices is the use of the aperture orifice which is designed to ensure that particles/cells pass the electrodes one at a time. The size of the orifice will dictate the range of particles that the device can measure. If a 19μm orifice was used for example, this would allow the detection of particles within the size range 0.4 to 13μm[165].

The limitations of Coulter counters described in the above studies has diverted attention away from the usefulness of alternative devices such as Low Angle Laser Light Scattering (LALLS) particle analysers. This method relies on the fact that

diffraction angle of laser light is inversely proportional to particle size it passes. Modern machines use Mei theory which completely solves the equations for the interaction of light and matter. The particles can be recirculated through the laser beam in suspension allowing the assessment of millions of particles[189].

The use of LALLS particle analysers is widespread especially in the food, pharmaceutical and paint industries. It has a long track record and has been shown to be highly accurate.

The advantages that LALLS particle analysers offer for the assessment of wear debris particulates are twofold. Firstly, the sizing can be done in suspension making filtering unnecessary. Secondly, the numbers of particles assessed is increased by a factor of 10^5 greatly reducing the possibility of introducing sampling errors. The measurement of laser light scatter is conducted over a given time period as the solution is recirculated. The volume of the suspension used is small and therefore it is likely that each particle may be measured multiple times. This instrument cannot then be used to give an absolute number of particles within the suspension.

A review of literature relating to wear debris studies was conducted in Section 2.5.2. It was related that the absolute size of the particles was an important parameter in terms of the resultant macrophage reaction. Similarly the importance of the mass distribution and its relationship to the wear of the socket was also elucidated. The data obtained from the particle analyser may be presented either in terms of a number distribution or a volume distribution. Clearly the volume distribution is directly related to the mass distribution. The ability of the particle analyser to report these two results simultaneously further adds to its versatility.

To assess the application of this instrument to the quantification of wear debris a number of trial experiments were performed. Two sources of representative debris were chosen, PMMA powder and *ex vitro* wear debris produced on the Mk. 1 Durham Hip Wear Simulator. The simulator debris was obtained in the bovine serum lubricating medium. The PMMA powder was also suspended in bovine serum. The two samples were digested using the method of Tipper *et al.* together with a sample of bovine serum without particles to act as a background. A background sample was necessary so that the refractive effect of the solution could be compensated for by the particle analyser. The results of the trial runs are contained in Appendix 5c. The

particle analyser was shown to be capable of giving highly accurate and repeatable results even at the very low particle concentrations which this application requires.

After establishing that LALLS as a technique was suitable for this application *ex vivo* tissue samples were considered. However a number of shortcomings were identified with respect to the use of the Tipper *et al.* protocol for quantifying debris retrieved from tissue samples. It was noted that the resultant solution bearing the debris after digestion varied in intensity of colour. This variation is attributed to the variation in the constituents of each tissue sample. This causes difficulties in removing background scattering information. Further the particles were held within a considerable volume of solution resulting in the assessment of fewer particles during the measurement period.

It was decided to adopt the method of Campbell *et al.* as this yields the debris in a form readily usable by the particle analyser. The debris is held within a solution of colourless isopropanol and is highly concentrated in comparison with the product of the Tipper *et al.* method. Further as detailed in Sections 3.3.1 and 3.3.2 the protocol of Campbell *et al.* seems to yield a purer sample with less experimental effort.

3.3.6   Methodology Adopted for Tissue Retrieval Study

A preliminary study was conducted using a modified version of Campbell *et al.*'s original protocol (detailed in Appendix 5b) was used to retrieve the UHMWPE debris particles from five tissue samples. The tissue samples were harvested by Mr. I. M. Pinder at revision surgery from three patients (three from one patient and one each from two).

The resulting debris solutions were analysed by Malvern Instruments, Malvern, England using a Mastersizer S LALLS particle analyser using a small volume dispersal unit. This instrument is capable of sizing particles within the range 0.5 to 1000μm.

4. Results

4.1 Preliminary Descriptive Examination

The acetabular liners were assessed for the presence of a number of specific wear features. These were impingement, delamination - both internal and external to the socket, a ridge at the boundary of the worn region, discolouration due to oxidation, ingression of metal beads, dissociation, rotation of the one-piece liners and liner fracture. Table 3.3 contains descriptions of these wear phenomena and Appendix 2 contains a full listing of the occurrence of these features.

Evidence of impingement of the neck of the femoral component was observed in thirty-five of the one hundred and sixteen sockets. Twenty-one of these were of the one-piece design. This equates to 36.8% of the one-piece cohort experiencing impingement as opposed to only 23.7% of the snaplock group. The influence of the skirted femoral head could not be deduced as there were few heads in the study that were of the offset design.

Delamination within the liner's inner surface occurred in twenty-three cases. An example of this form of wear can be seen in Figure 4.1. The one-piece liners were more prone to this form of wear accounting for twenty-one of the twenty-three cases, or 36.8% of the one-piece cohort. External delamination on the rim of the liner was observed in twenty-seven liners. The relationship between the liner type and this phenomenon was again strong (twenty-three were one-piece, 40.3% of cohort). A degree of association was found between the two locations of delamination with fifteen joints having both forms of this phenomenon.

The presence of a ridge bordering the worn region was noted in forty-one liners. Six of these liners had more than one ridge present (two ridges in five and three ridges in one) with five of them displaying evidence of impingement. The association of the presence of an established ridge region and the amount of penetration recorded was tested. The mean penetration for the liners with and without ridges was 2.49mm and 0.76mm respectively which was shown to be statistically different (t-test, t=-8.08, p<0.0001).

Figure 4.1:   Sectioned liner showing internal delamination. The pole is positioned at the base of the photo with the open face of the cup uppermost.
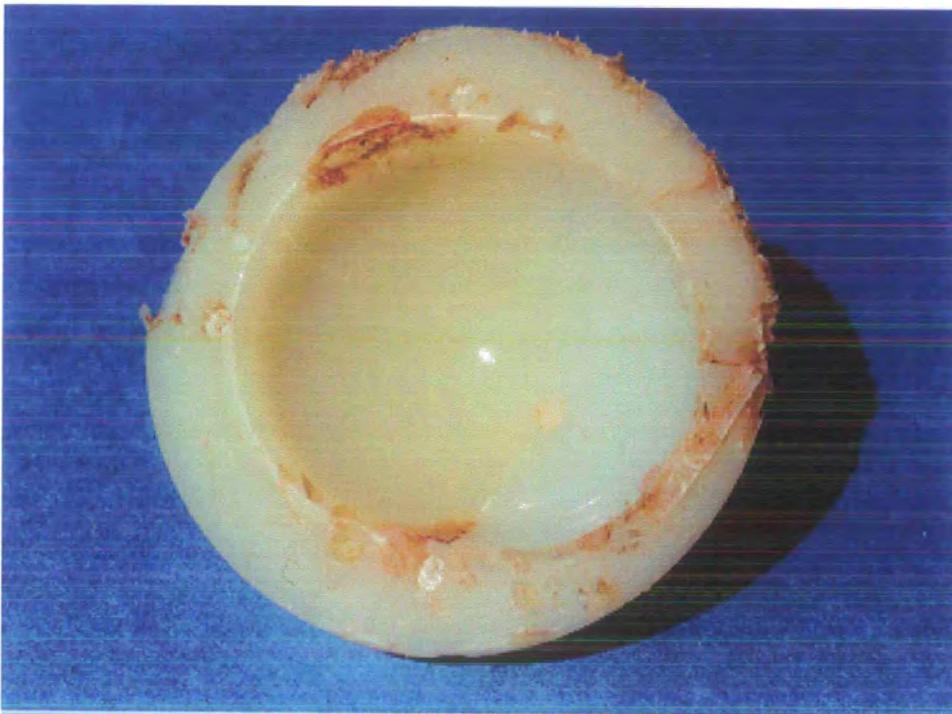
Figure 4.2:   Discolouration of the liner. Note the white colour in the worn right side of the liner.

Oxidation was evidenced by the discolouration of the UHMWPE. A yellowing, or slight greenish cast, to the liner was observed in forty-four cases (Figure 4.2). Thirty-two of these were of the one-piece design. The mean service life of the joints displaying oxidation was 8.2 years compared with those with no signs of oxidation of 5.2 years. These were shown to be statistically different using a t-test (t=-4.28, p<0.0001).

There were seven joints where ingression of metal beads had taken place. No relationship could be found between the cause of revision and the presence of beads.

Dissociation of the UHMWPE liner from its metal-backing was observed in three joints all of which were the one-piece design. The effect of the liner detaching from its backing was dramatic, the action of the head tended to displace the liner. Once the liner had slipped the head began articulating directly onto the metal backing. This resulted in the wear of both components as evidenced by the polishing of the metal-backing. The liner, now out of position, was subjected to frequent impingement with the neck of the femoral component causing large quantities of wear. These features can all be seen in Figure 4.3.

The occurrence of rotation in the sockets of the one-piece design was high. Twenty of the sockets of this type (35.1%) showed evidence of rotation. The influence of the duration of implantation and the estimated number of cycles imposed on the joint was investigated. Neither of these parameters was shown to have a relationship with the occurrence of rotation using Student's t-test (see Table 4.1). The propensity of the alternative forms of rim damage, delamination and oxidation, in combination to rotation was also examined. Nine of the twenty liners with rotation had delamination on the rim. Fourteen liners had combined evidence of rotation of the liner and oxidation of the polyethylene. Only one of the liners with multiple wear ridges suffered from rotation.

	No Rotation	Rotation	t, (p value)
Observations (n)	20	37	-
Implant Duration (yrs) mean (SD)	8.05 (2.22)	9.38 (3.66)	-1.47 (0.1494)
Est. No. Cycles (x10^6) mean (SD)	13.1 (3.7)	14.2 (5.5)	-0.77 (0.4464)

Table 4.1:   Summary statistics for rotation investigation.

The fracture of the liner occurred in sixteen liners all but one of which were the snaplock design (see Figure 4.4). Nine of the fractured snaplock liners were from joints with 32mm heads with 46/49mm backings. A further five came from joints with 26mm heads and a backing of 40/43mm outer diameter. The remaining snaplock joint had a 32mm head with a 52/55mm backing. Fourteen of these liners had a polyethylene thickness adjacent to the snaplock mechanism of less than 2mm at implantation.

The occurrence of fracture was heavily associated with gender, all but two of these joints came from female patients. Also the sample contained an atypical cross-section of diagnoses for primary surgery (6 for CDH and two each for avascular necrosis, RA and OA). Similarly this group had an unusually high incidence of oxidation compared with the general snaplock population (37.5% compared to 20.3%). Wear potential may be expressed in terms of the parameter NWr,

$$NWr = 2.376(N \times 9.81\{\text{patient mass}\} \times \{\text{socket radius}\}) \qquad (4.1)$$

where N is the number of cycles to which the joint has been subject as calculated by equation 3.5. The wear potential of this group of patients was not different from that of the remainder of the cohort (t-test, t=-0.63, p=0.5290).

Polishing of the stem was observed in all but two of the seventeen components. The highest score of 10 out of a possible 24 was achieved by two stems. The mean scores and their distribution over the components are shown in Figure 4.5. No association between reasons for primary or revision surgery and the presence of stem polishing

could be ascertained. However, it was noted that this group contained a disproportionate number of males with only three of the components being from female patients. Further the group had a high mean mass of 77.0 (SD10.6)kg which was shown to approach significance (t-test, t=-1.95, p=0.054) when tested against the remainder of the cohort.

A summary of the angles found for the thirty-five joints investigated are seen in Table 4.2. All the joints were of 32mm femoral head diameter. The wear angle for the snaplock joints was calculated with the assumption that the 10° hood was positioned superiorly. The wear angle of the two socket designs was not found to be statistically different (t-test, t=0.77, p=0.4511). Therefore the two socket types were combined to generate an overall wear vector angle of 17.1 (SD 14.7)°. The association between penetration depth and wear angle was investigated (Figure 4.6). The absence of any observations with large medially directed penetrations was noted.

	Angle of metal backing, α	Angle of penetration, β	Wear Angle
One-piece	52.1 (10.0)	19.3 (11.6)	18.9 (10.7)
Snaplock	51.8 (11.6)	34.0 (18.6)	14.6 (19.1)

Table 4.2:   Table of acetabular angles (mean and standard deviations in parentheses) for the two component types.
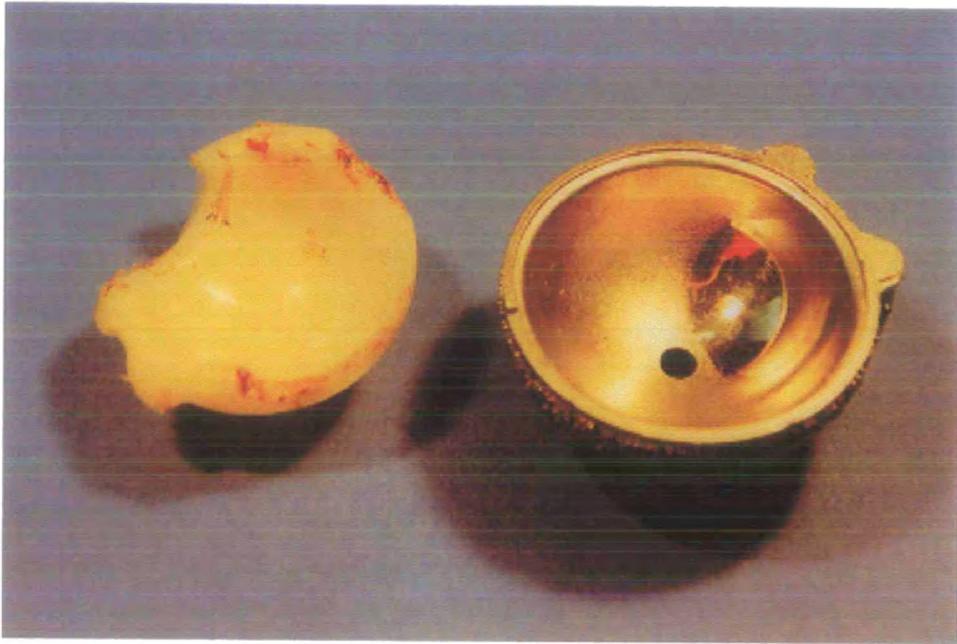
Figure 4.3:   Dissociation of the liner from its backing.
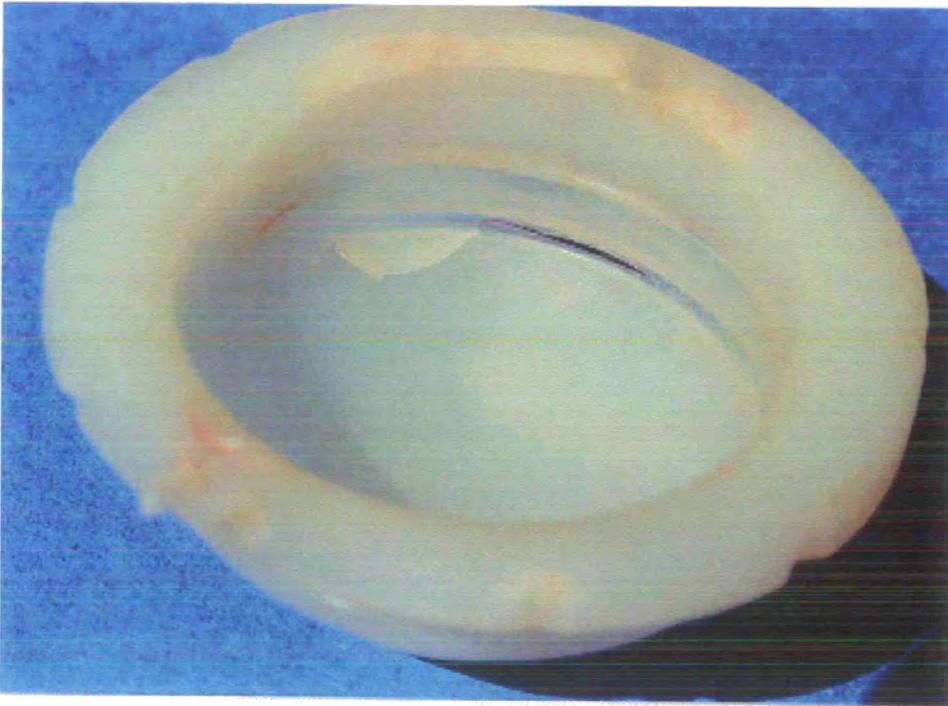
Figure 4.4:   Fracture of the UHMWPE snaplock type liner.

Figure 4.5: Distribution of stem polishing. Mean score, percentage of components showing polishing in that zone in parentheses.

Figure 4.6: Variation of penetration direction with depth. Medial penetrations are recorded with negative angles and lateral with positive.

4.2 Friction Results

The results of the friction tests are presented as Stribeck plots. A typical one of these is seen in Figure 4.7. All the joints tested displayed a downwards trend in friction factor as the viscosity of the lubricant increased. At each individual viscosity of lubricant tested, the median and mean friction factor values obtained from the explanted joints were statistically compared with those from the unused joints using the Wilcoxon rank-sum test and the t-test, respectively (values shown in Table 4.3). No statistically significant difference could be found between these two cohorts of data.
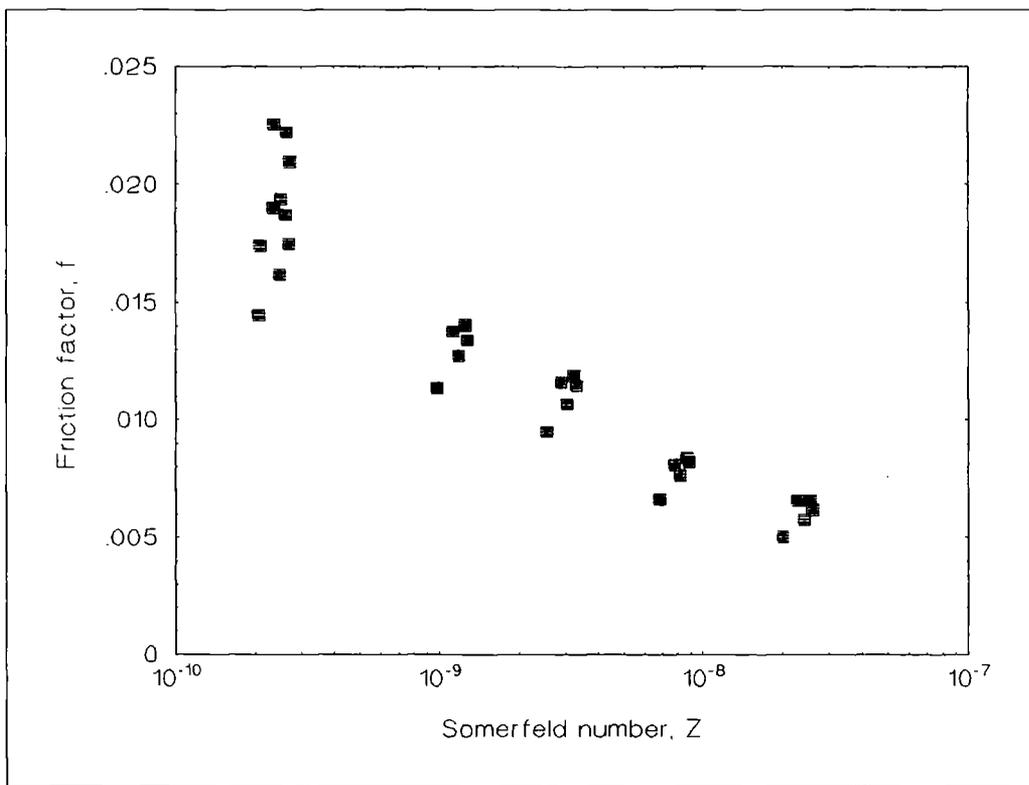
Figure 4.7:   A typical Stribeck plot for an explanted joint.

		Friction Factor at viscosities below:				
	n	1 Pa s	3 Pa s	10 Pa s	30 Pa s	100 Pa s
New	2	0.041	0.025	0.025	0.022	0.016
Explanted	22	0.024	0.032	0.029	0.024	0.014

Table 4.3:   Median friction factor values at each viscosity tested.

4.3   Wear Volume Results

The median penetration depth for all ninety-seven joints shadowgraphed was found to be 1.00 (IQR 0.55-2.40)mm.   The median total wear volume for these joints was calculated to be 419 (IQR 224-1021)mm^3.   The histogram describing the distribution of the wear volumes can be seen in Figure 4.8.   The mean penetration and wear volumes for each socket diameter can be seen in Table 4.4.
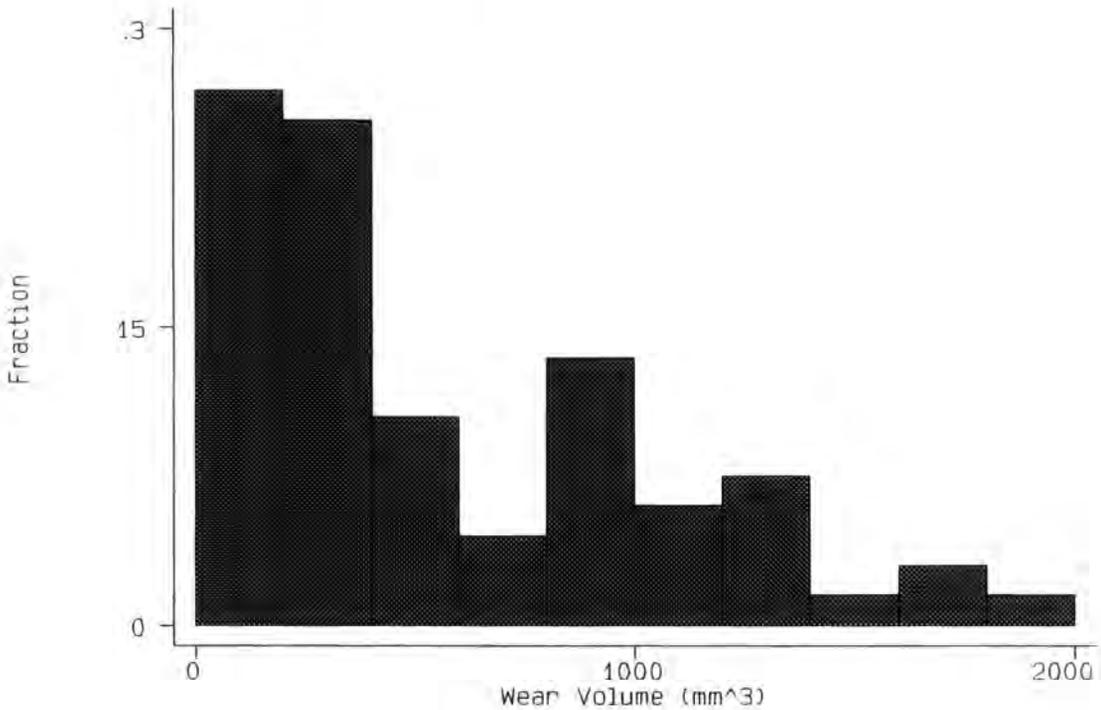
Figure 4.8:   Histogram of total wear volumes.

Sixty-five joints of a 32mm head diameter were suitable for use in the calculation of the wear parameters.   Simple linear regression was found to be insufficient to calculate the mean rate of penetration.   The residuals of the regression were found to have a heteroscadastic distribution[190] (see Figure 4.9).   The values of the residuals at long service lives were much larger than those for the shorter service lives.   The residuals of the datapoints with long service lives would therefore have an undue influence over the position of the best fit line.   In order to compensate for this phenomenon a weighting had to be introduced to the regression to keep the variance at a constant value[191] (see Figure 4.10).   The weighting, w, is a dimensionless statistical parameter and was of the form:

$$w = \frac{1}{\{\text{resolution of shadowgraph}\}^2 + k\{\text{service life}\}^2} \qquad (4.2)$$

where k is a constant. The value of k was determined by an iterative process performed within Stata. The resolution of the shadowgraph machine in terms of penetration was 0.05mm. The weighted regression gave a penetration rate of 0.22 (SE 0.02)mm/year with a coefficient of determination, R^2, of 0.528. The "hat" statistics were calculated for the weighted regression. These give a measure of the leverage of an observation on the resulting regression line. It can be seen that the outlier in Figures 4.9 and 4.10 does not exert an undue influence on the gradient of the regression line. It should be noted that the intercept of the regression line is approximately zero (Figure 4.11).
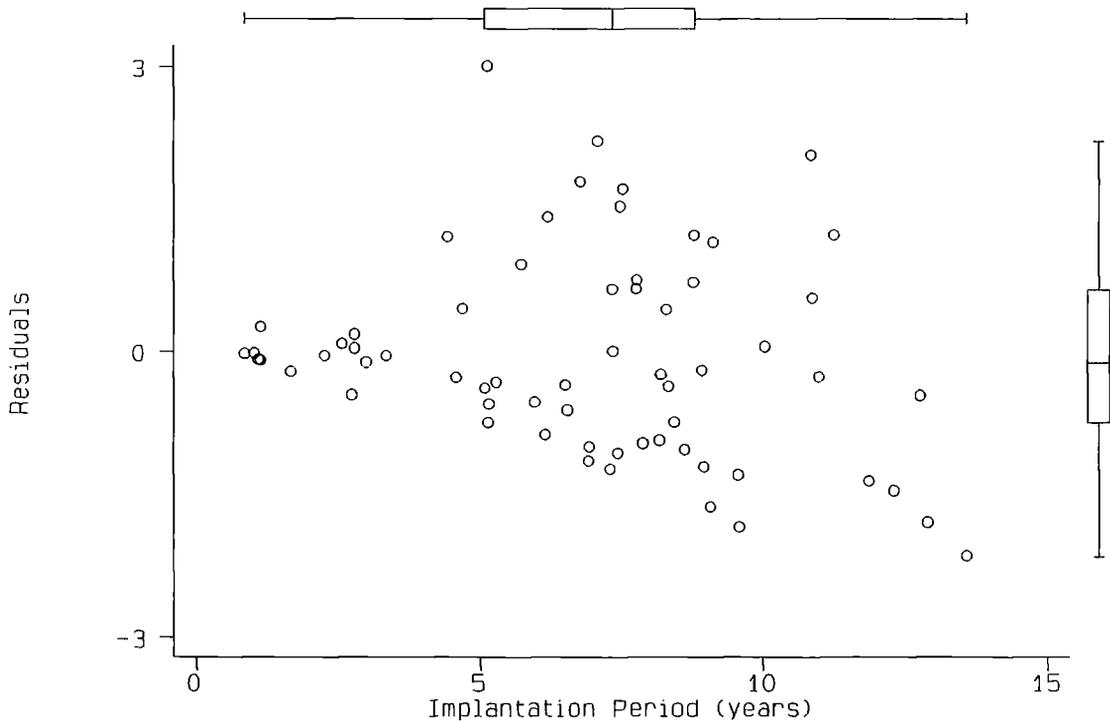
Figure 4.9:   Plot of residuals of linear regression against implant period.
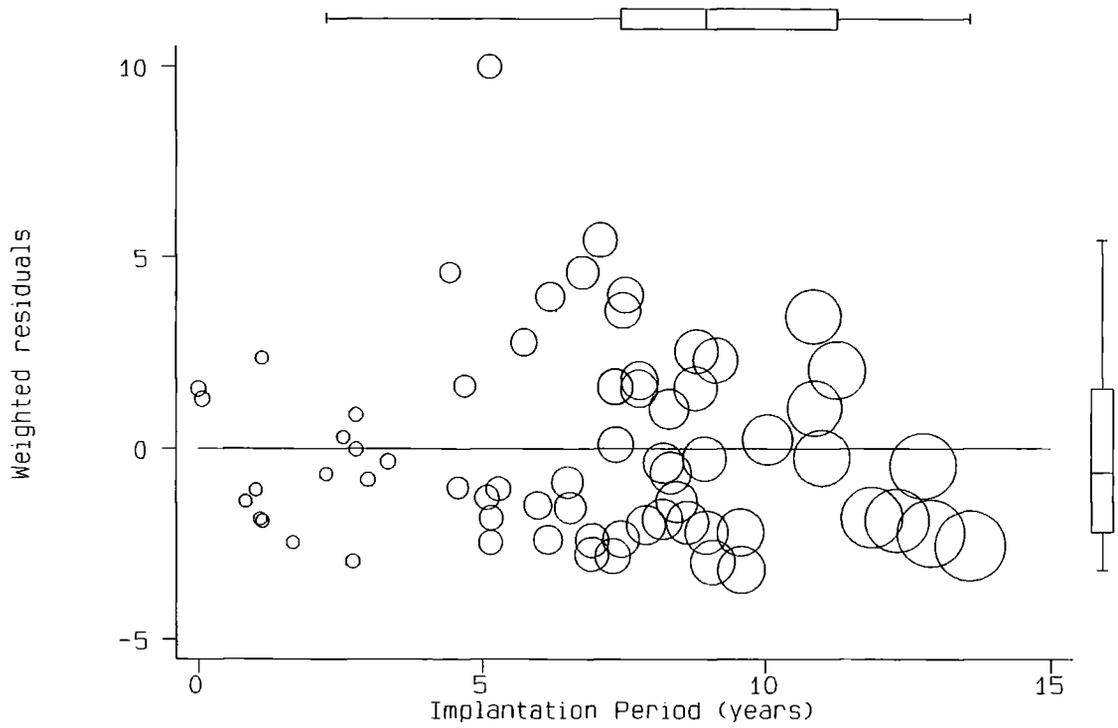
Figure 4.10: Plot of residuals of weighted linear regression. The diameter of the circle denotes the value of the hat statistic, a measure of influence. Hat has the range (0.0149-0.4089).
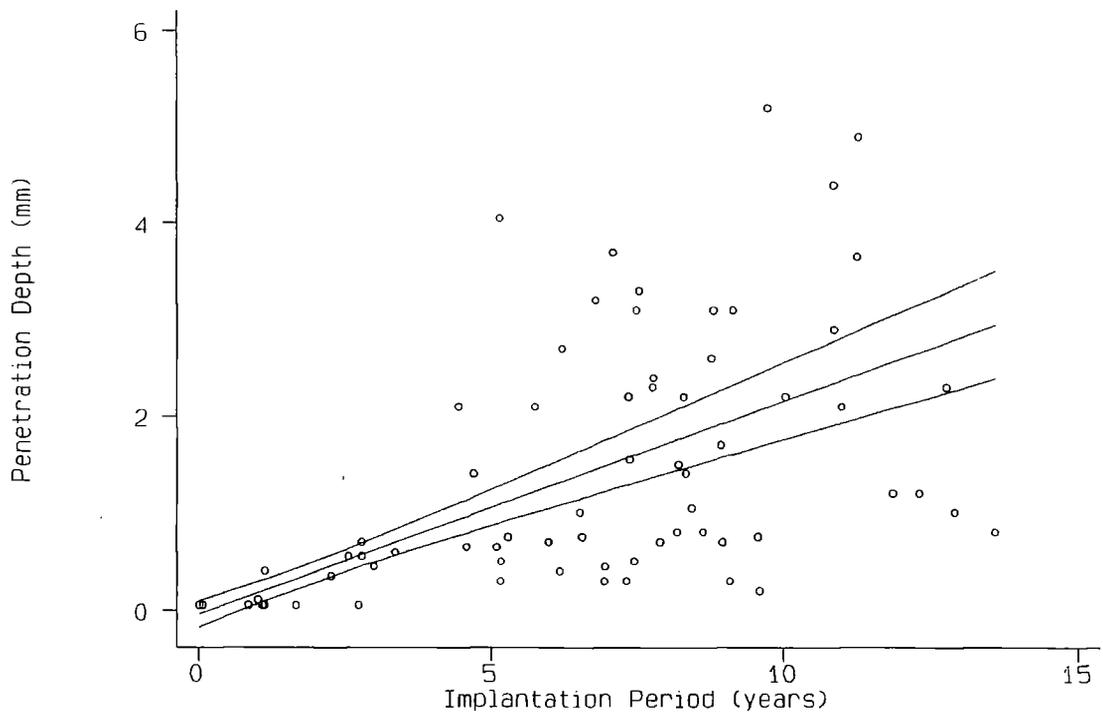
Figure 4.11: Fit of regression line for penetration rate, including 95% confidence intervals. Note that the intercept is approximately zero.

Diameter	Observations	Age at Primary (years)	Implant period (years)	Patient Mass (kg)	Penetration (mm)	Wear Volume (mm^3)	Penetration Rate (mm/yr)	Volumetric Wear Rate (mm^3/yr)	Clinical Wear Factor (mm^3/Nm)
	n	median (range)	mean (SD)	mean (SE)	mean (SE)	mean (SE)	mean (SE)	mean (SE)	mean (SE)
All	97	45.98 (-)	6.28 (3.47)	69.97 (14.2)	1.41 (0.14)	626 (77)	-	-	1.82 (0.23)
26	5	28.22 (25.1-65.6)	3.53 (2.64)	66.6 (15.2)	0.10 (0.06)	34.8 (8.2)	-	-	-
28	5	41.8 (24.9-68.6)	3.58 (2.21)	68.1 (13.8)	0.61 (0.09)	191 (13)	-	-	-
32	87	48.0 (15.8-75.5)	6.85 (3.40)	70.5 (14.3)	1.53 (1.27)	692 (83)	0.22 (0.02)	88 (10)	2.00 (0.28)

Table 4.4:   Summary of liner wear performance by socket diameter. In the case of the 26 & 28mm liners insufficient numbers were available to perform reliable regressions.

The mean volumetric wear rate was calculated in the same manner as the mean penetration rate. The resolution of the shadowgraph machine in this situation was 40.2mm^3 as calculated from the error in penetration using the cylindrical wear formula (see Chapter 2.4.3). A mean volumetric wear rate of 88 (SE 10)mm^3/year was deduced (R^2=0.486) (see Figure 4.12). Again an intercept of approximately zero was observed.

In order to maintain a constant variance the mean clinical wear factor was calculated, as previously, using weighted linear regression. In this case however, the model of the weighting changed slightly with "service life" in the denominator of Equation 4.2 being replaced with NWr as defined in Equation 4.1.

The mean clinical wear factor for all sockets of a 32mm diameter was calculated to be 2.00 (SE 0.28)x10^{-6} mm^3/Nm (R^2=0.443) (see Figure 4.13). Once more the intercept of the regression line is approximately zero.
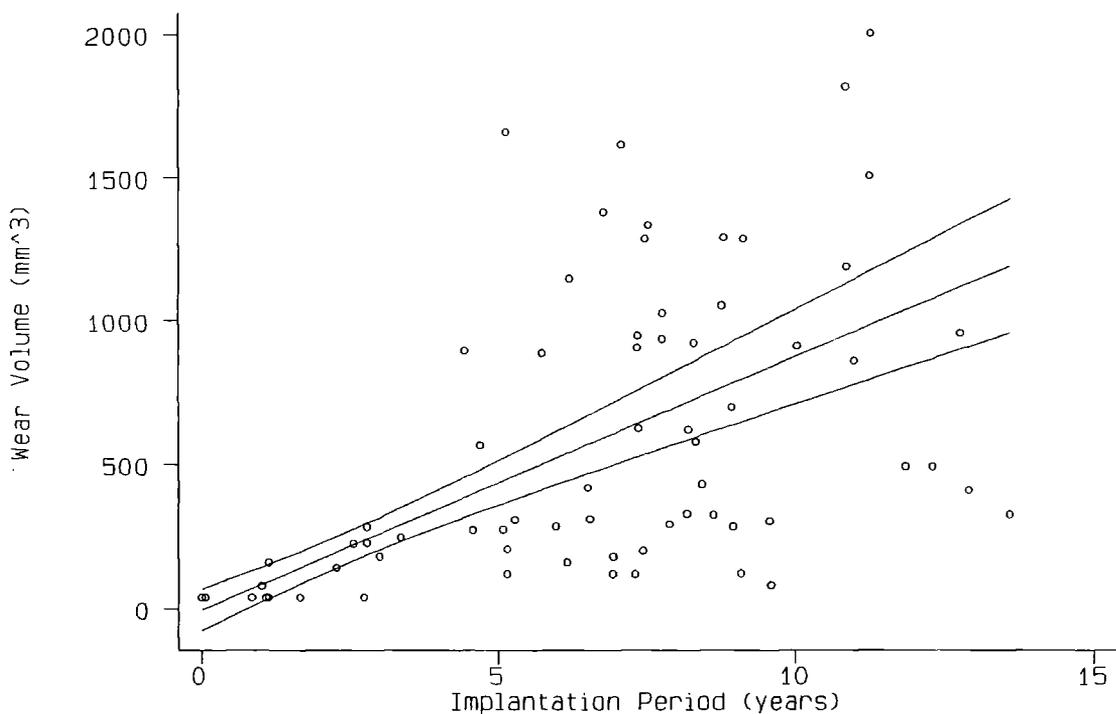
Figure 4.12:   Fit of regression line for volumetric wear rate, including 95% confidence intervals. Again note that the intercept is approximately zero.
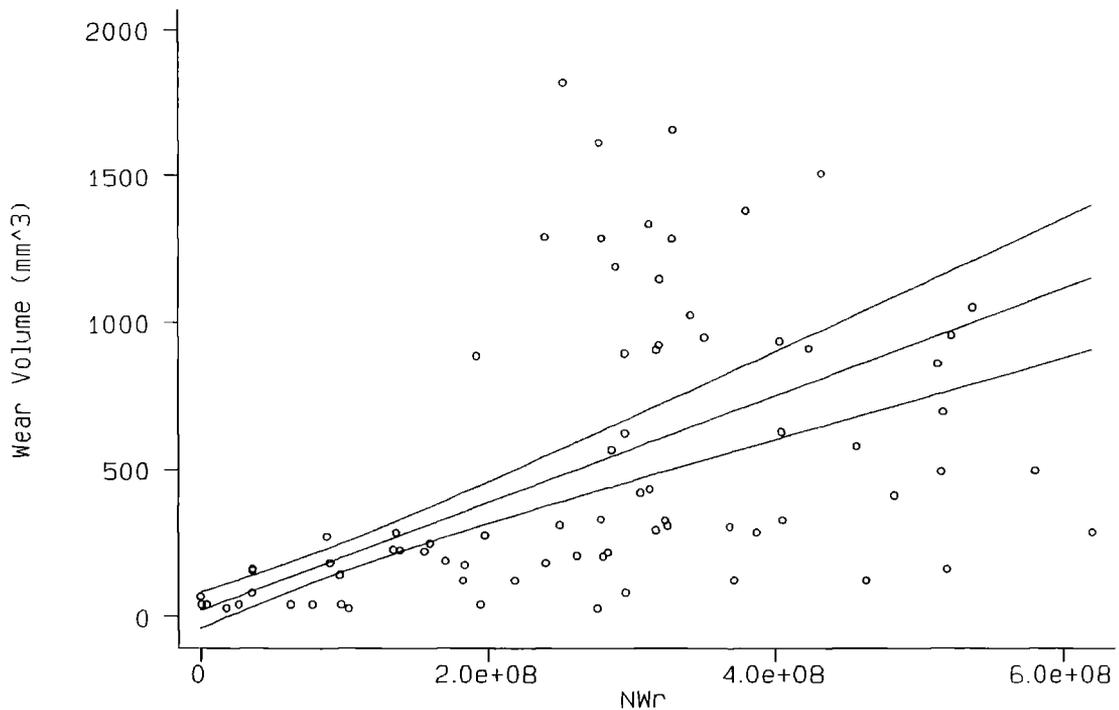
Figure 4.13:   Fit of regression line for clinical wear factor, including 95% confidence intervals.

The effect of the different socket types on the clinical wear factor was also investigated. A new model was developed for use with multiple regression analysis. This model took the form shown in Equation 4.3. This model utilises a dummy slope variable by incorporating the categorical parameter "*snap*" (*snap*=0 for one-piece sockets, and *snap*=1 for snaplock sockets).

$$\Delta V = C + b_1 (NWr) + b_2 (snap)$$

(4.3)

This regression was performed with the iterative weighting procedure described previously. The results of this can be seen in Figure 4.14 and Equation 4.4. The residuals of the regression are shown in Figure 4.15.

$$\Delta V = 48.9 + 2.39 \times 10^{-6} (NWr) - 1.40 \times 10^{-6} (snap) \qquad (4.4)$$

The adjusted co-efficient of determination, R_a^2, for this regression was 0.567. This is preferred in more complex models. A summary of the values obtained can be seen in Table 4.5.
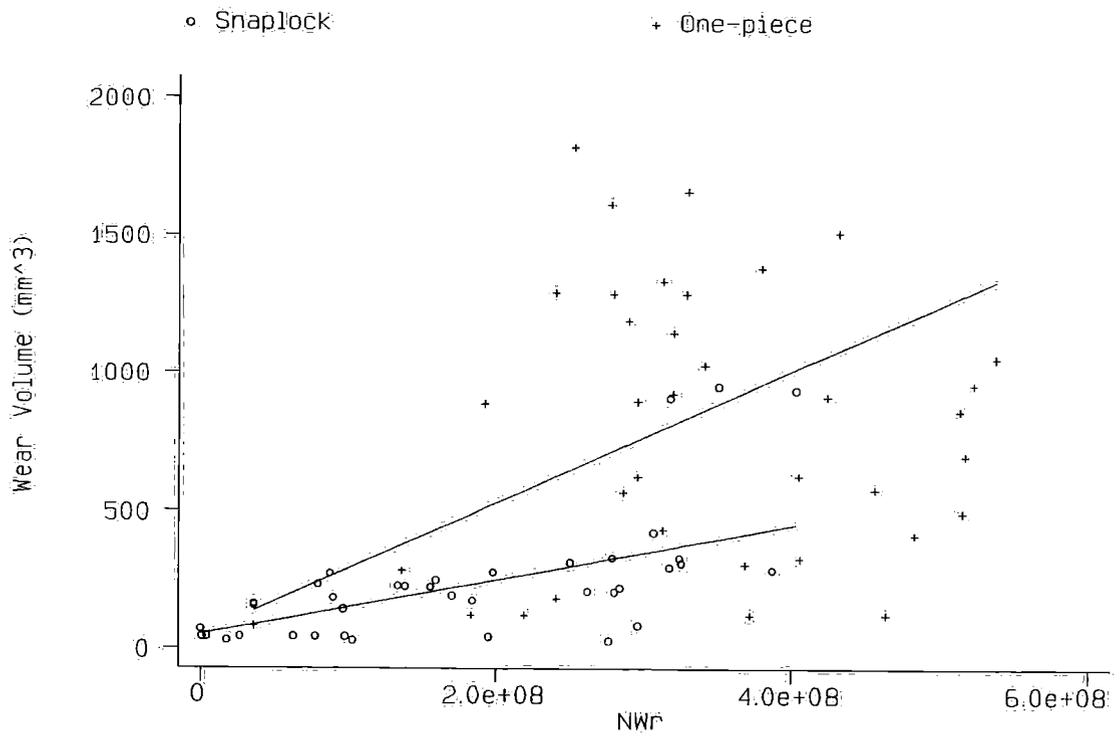
Figure 4.14: Lines predicted by multiple regression for 32mm sockets of two types.
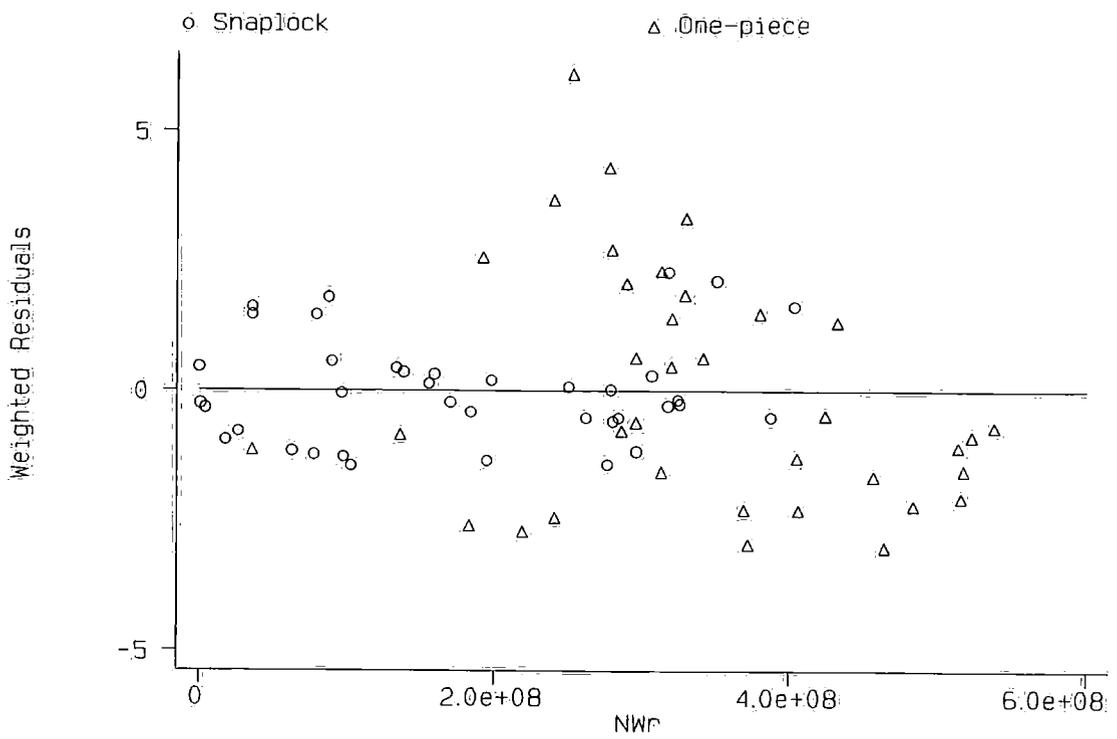
Figure 4.15: Plot of residuals for weighted multiple regression.

Type	Observations (n)	Implant Period mean,SD(yrs)	Wear Volume mean,SE(mm^3)	Clinical Wear Factor mean,SE(mm^3/Nm)
One-piece	36	8.49 (0.47)	800 (90)	2.39 (0.44)x10^{-6}
Snaplock	28	4.81 (0.48)	267 (45)	0.99 (0.25)x10^{-6}

Table 4.5:   Summary table of data for 32mm sockets by type.

The influence of liner thickness on the wear performance of the sockets was investigated using non-parametric trend analysis. The liners were ranked in terms of their minimum thickness, for the snaplock liners this occurred beneath the snaplock mechanism. The rankings are defined in Appendix 4a. Figure 4.16 shows the lack of any association between the liner rank and the clinical wear factor. Analysis of the two liner types independently again revealed no relationship.
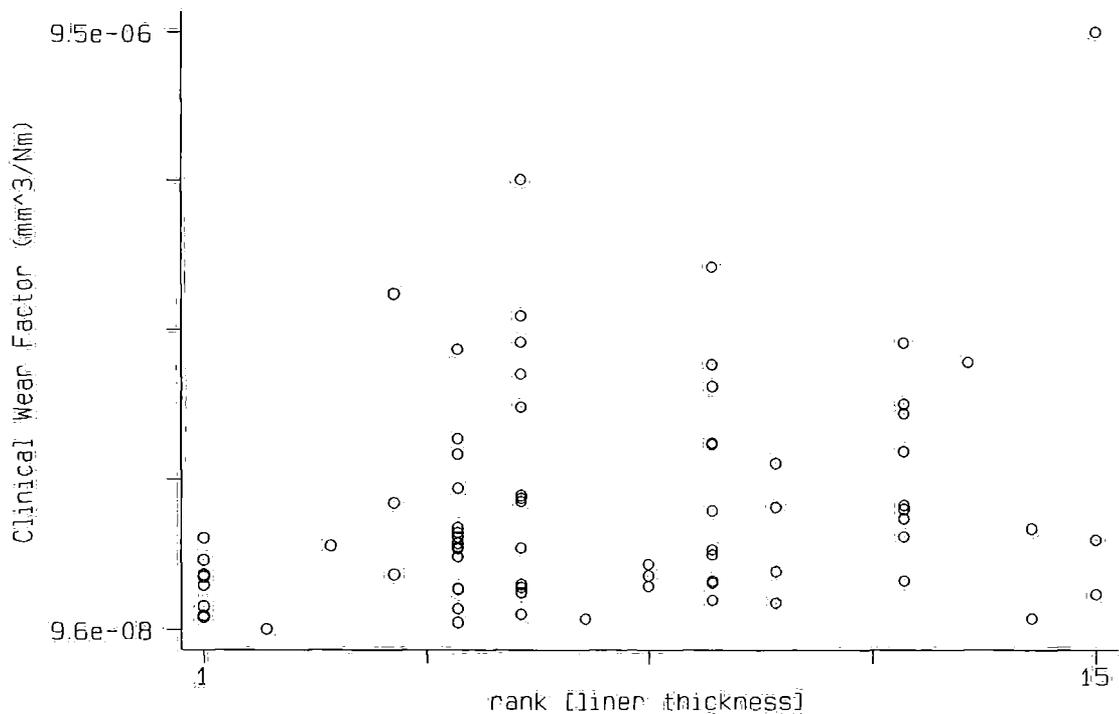
Figure 4.16:   Variation of clinical wear factor with liner thickness rank for both liner types.

4.4 Surface Topography Investigations

4.4.1 Qualitative - DIC Microscopy & SEM

Heads

It was possible to identify the worn region of the femoral head with the naked eye. A diffuse matting could be observed covering about one quarter of the head, centred around a position of approximately 30° to the pole. DIC microscopy showed that the scratching was multidirectional with no one direction having a greater degree of scratching. Occasionally the base of the head was badly damaged, this was due to the instrument used to remove it from its taper during surgery.

SEM proved poor at providing good quality images of the metallic surface.

Sockets

The surface of the UHMWPE acetabular liners exhibited a more complex picture. Three typical sets of surface features were observed which could be loosely grouped with respect to their location; articular regional features, ridge features and unworn regional features (see Figure 4.17).
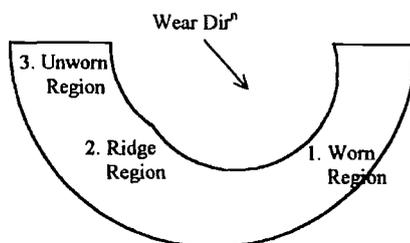
Figure 4.17: Cross-section of liner in wear plane showing typical wear feature locations.

1. Worn Region - Prior to microscopic assessment of the UHMWPE liners it was noted that the worn region exhibited a highly polished nature. The microscopy provided valuable information on the nature of the UHMWPE surface. The grain structure of the UHMWPE was easily distinguishable using the DIC microscope (Figure 4.18), however the SEM seemed less capable in this regard (Figure 4.19). SEM proved to be valuable for surface features where the rate of change of the slope was great. The width of the grains ranged from under 50μm to

approximately 250μm. No variation in the distribution of grain sizes was observed between the two liner varieties.

Light scratching was observed in the worn region with no dominant orientation. Occasional deep scratches in the worn region were thought to be attributable to damage sustained during surgery.

Subsequent SEM at high magnification allowed images to be obtained at the grain boundary regions (Figure 4.20). Deep cracks running along the boundary for hundreds of microns were frequently observed. The polyethylene exhibited a rippled texture on the nanometre scale as can be seen in Figures 4.20 and 4.21.

Figure 4.18: DIC micrograph showing the granular structure of the worn surface (Magn. x 200).

2. Ridge Region - In the region immediately adjacent to the ridge (within 2mm on the worn side) there existed an area in which two typical features dominated. Small, raised prominences were interspersed with lower regions of roughened material (Figure 4.22). The raised regions under high-powered SEM were shown to very smooth with an extruded texture (Figure 4.23). The lower regions had a much rougher microscopic appearance, characterised by a more open structure to the texture (Figure 4.22 & 4.24).
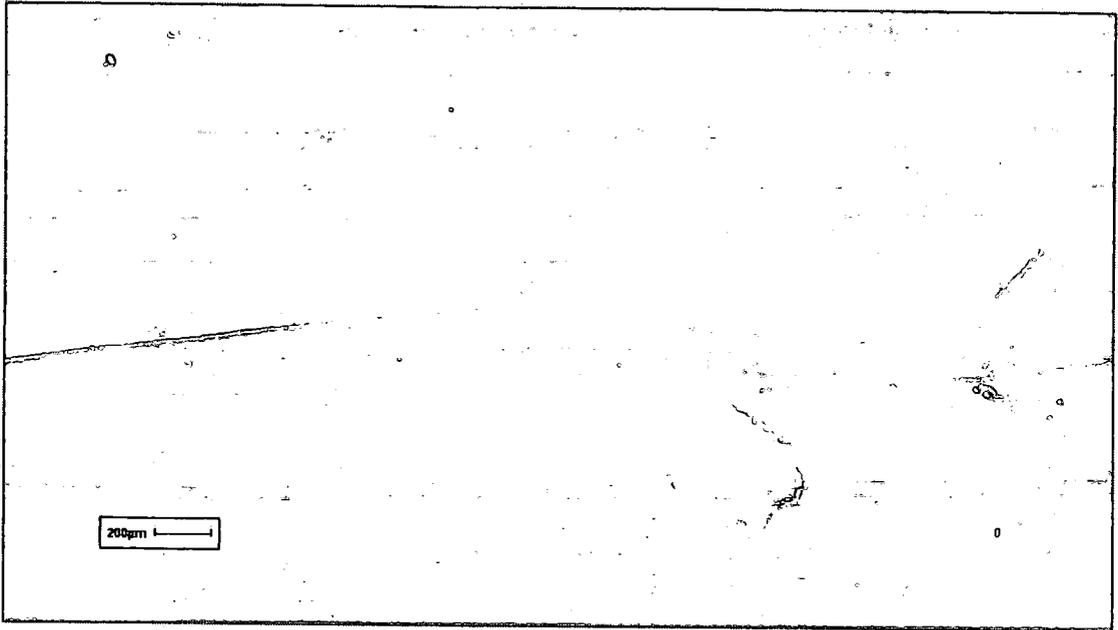
Figure 4.19: SEM micrograph of worn region. Note good resolution of scratching but poor image of grain boundary detail (Magn. x170).
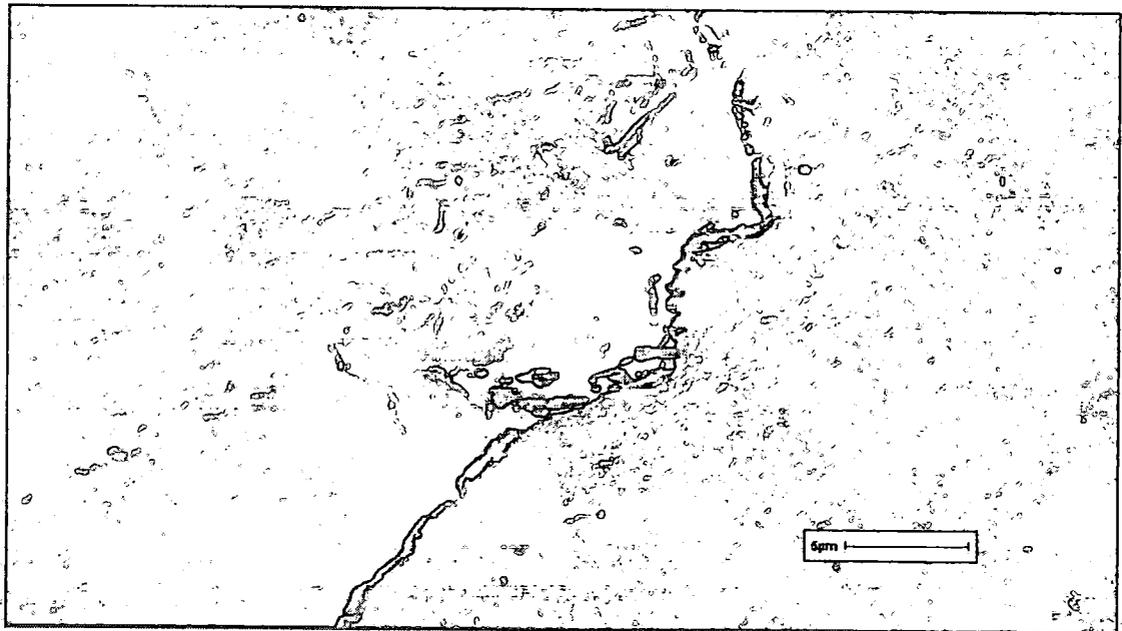
Figure 4.20: SEM image of the cracking at the grain boundaries (Magn. x2000).
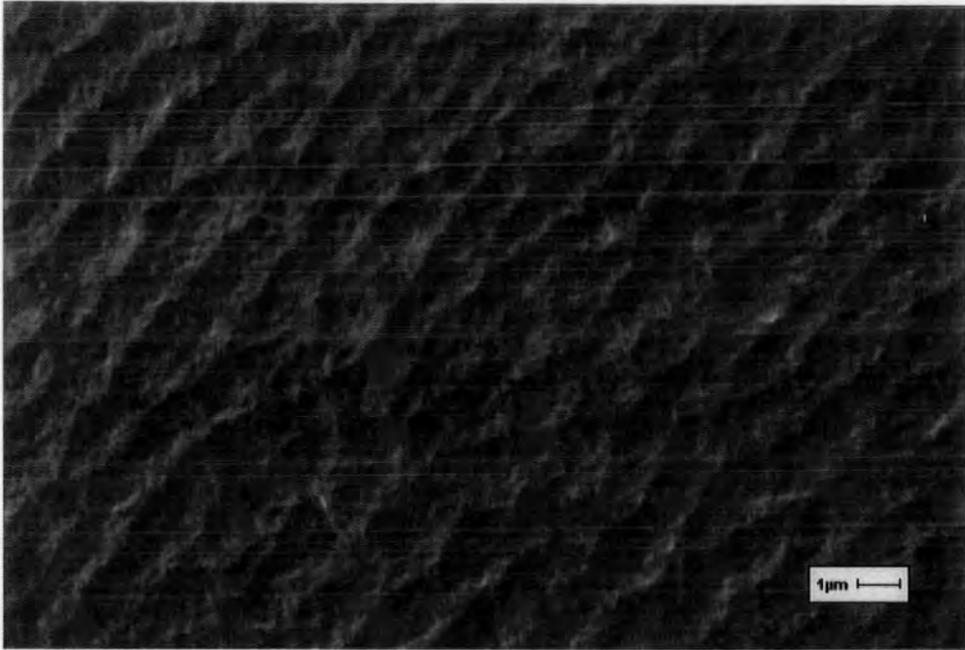
Figure 4.21:   SEM image of rippling of UHMWPE surface (Magn. x5000).
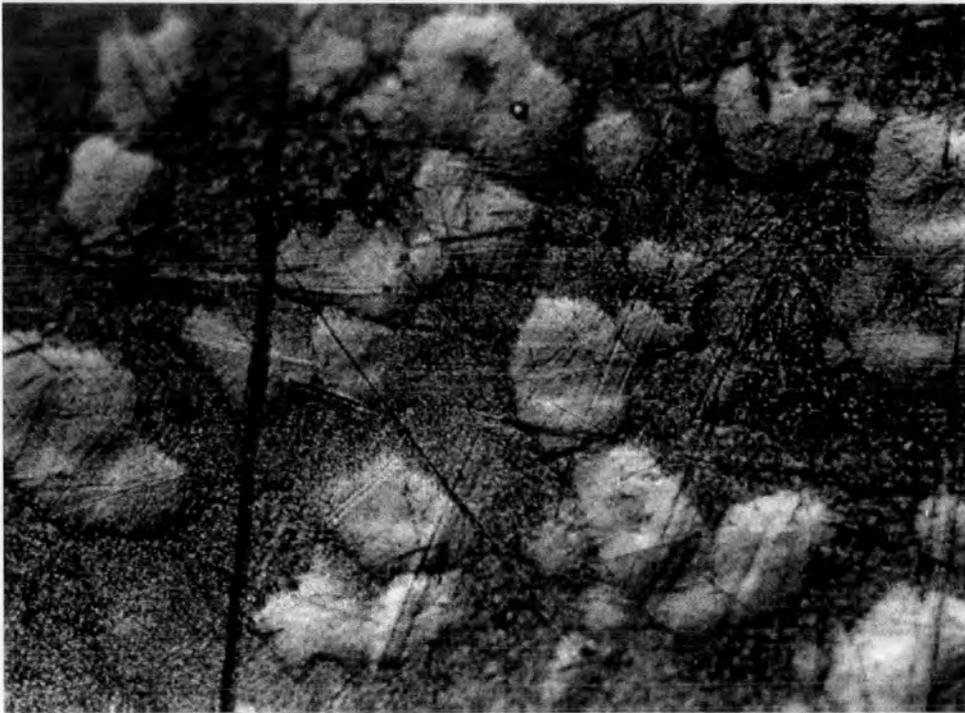
Figure 4.22:   DIC micrograph showing two wear features in boundary region (Magn. x200).

3. Unworn Region - The unworn region was characterised by the presence of the original machining marks in the majority of the sockets in this study. This region

often displayed evidence of deep scratching superimposed on the machining marks (Figure 4.25). It was within this region that the ingression of beads from the porous coating was occasionally observed.
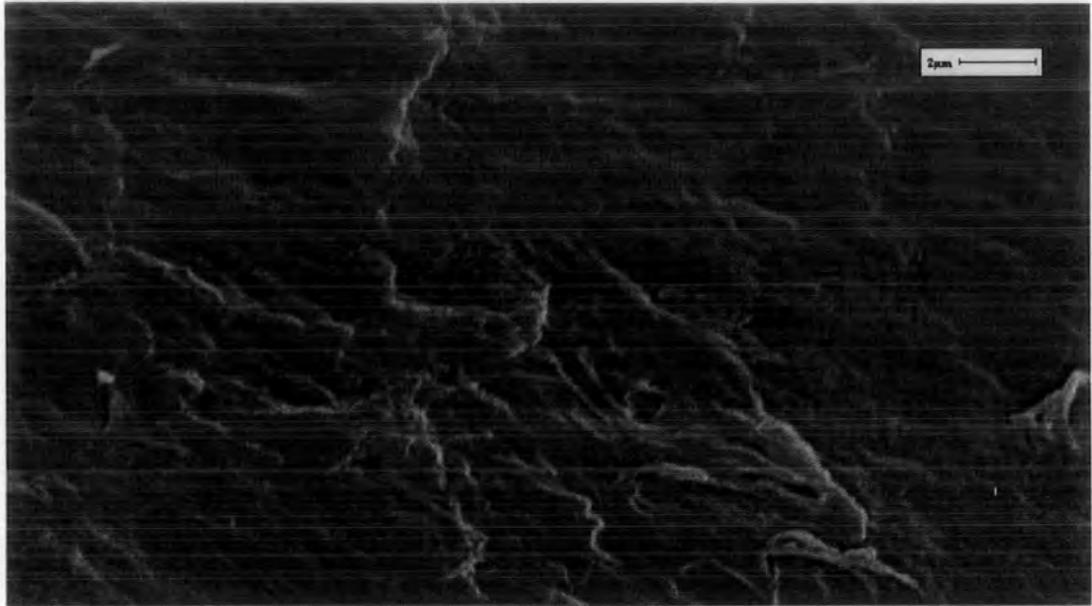
Figure 4.23: SEM image of raised dominant asperities (Magn. x4000).
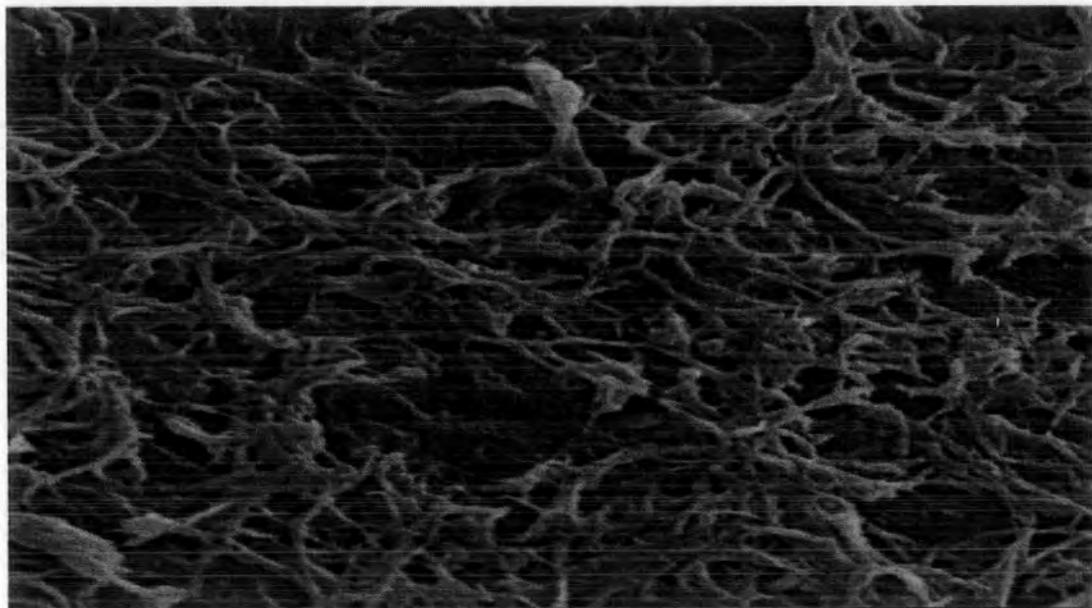
Figure 4.24: SEM image of lower lying inter-asperity area (Magn. x4000, micron marker as above).

Figure 4.25:   SEM image of unworn region showing machining marks and scratching (Magn. x15).

4.4.2   Quantitative - Optical Interference Profilometry

Heads

The surface roughnesses of fifty-seven explanted femoral heads and two unused heads were assessed. The features observed were in agreement with those seen using the DIC microscopy. The magnitude of the measured roughness parameters can be seen in Table 4.6.

The Wilcoxon rank-sum test was used to assess the equality of the medians between the worn, unworn and new heads. The values for all the roughness parameters were significantly larger for the worn areas of the explanted heads (see Table 4.6).

If we consider the skewness and kurtosis values for the explanted heads, we have observed a fall in S_{sk} from a median of -0.19 to -1.95. This negative skew is indicative of a large number of scratches below the mean plane. The very large values of kurtosis are due to the presence of outliers some distance from the mean plane. The typical worn surface may then by characterised as having a high proportion of valleys below the mean plane some extending to substantial depth. This is also testified to by the proportion of the S_{PV} height which the S_{Peak} height represents: S_{PV} is 447.6nm whilst S_{Peak} is 99.8nm.

| | Worn | Wilcoxon worn/unworn | Unworn | Wilcoxon unworn/unused | Unused |
	Median (IQ Range)	z (p-value)	Median (IQ Range)	z (p-value)	Median (IQ Range)
S_{PV}	447.6 (921.8)	-13.08 (0.0001)	59.6 (300.2)	0.28 (0.78)	61.4 (49.2)
S_{Peak}	99.8 (342.8)	-10.68 (0.0001)	25.6 (45.9)	-0.08 (0.94)	20.7 (19.9)
S_a	10.35 (8.74)	-16.57 (0.0001)	3.05 (1.80)	5.36 (0.0001)	5.06 (6.20)
S_q	16.4 (18.35)	-16.45 (0.0001)	3.99 (3.09)	4.68 (0.0001)	6.44 (8.34)
S_{sk}	-1.95 (6.1)	11.96 (0.0001)	-0.19 (0.72)	-1.98 (0.0001)	-0.37 (0.67)
S_{ku}	27.5 (101.4)	-6.38 (0.0001)	4.45 (55.8)	-2.40 (0.0165)	3.57 (1.50)
S_k	27.6 (20.9)	-11.86 (0.0001)	9.35 (5.50)	.	.
S_{pk}	9.7 (10.4)	-14.25 (0.0001)	3.57 (3.15)	.	.

Table 4.6: Surface roughness values for femoral heads. The values in italics and the parameters S_{sk} and S_{ku} are dimensionless, all others are in nanometres.

The multidirectional nature of the scratching is clearly seen in Figure 4.26 with regions of raised material adjacent to the scratches. Whilst the damage seen in Figure 4.26 looks severe the S_{PV} and S_a values for this surface are only 146.56nm and 9.81nm respectively.
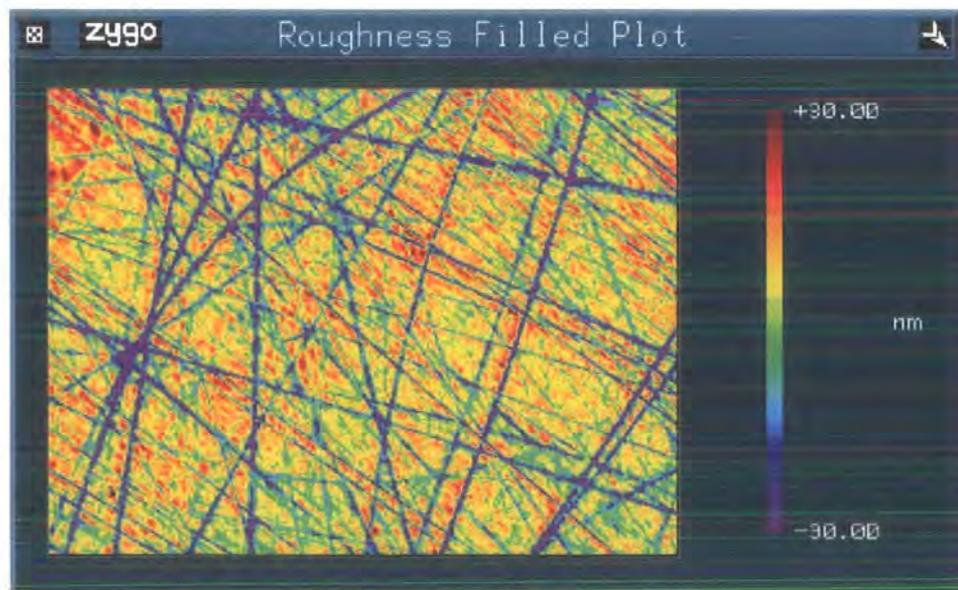
Figure 4.26: Contour plot of explanted head, worn region.

The unused heads showed no evidence of scratching, however there was a lay evident which is thought to correspond to the direction of polishing. In Figure 4.27

this can be seen from top to bottom. The skewness and kurtosis values for the new heads (-0.37 & 3.57) show that this surface deviates little from the mean plane. There are few outlying spikes, or pits, with a greater proportion of the S_{PV} height being above the mean plane than in the explant.
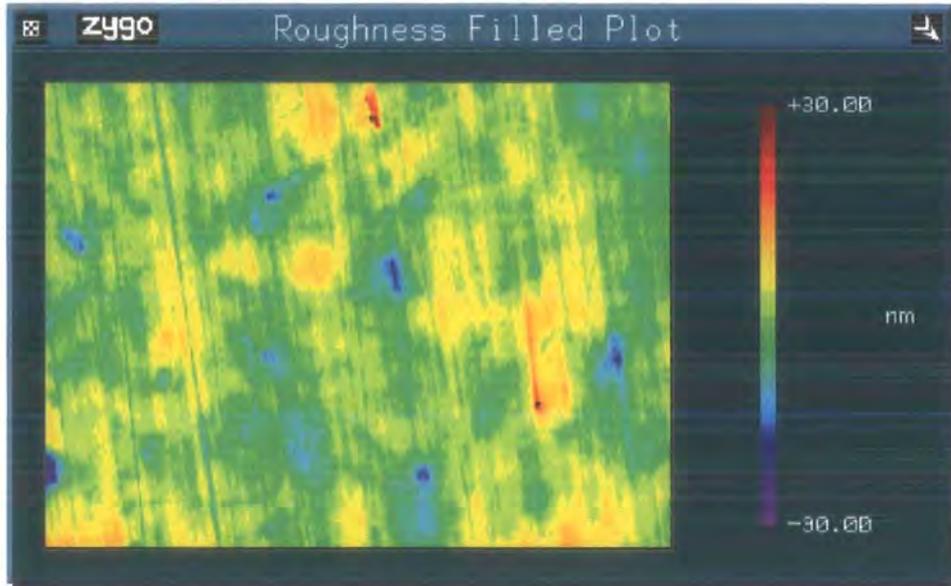
Figure 4.27: Contour plot of new head.

The relationship of head roughness and implant period was investigated using the Spearman rank correlation test (see Table 4.7). No roughness parameter was found to have a significant relationship to implant period.

	S_{PV}	S_{Peak}	S_a	S_q	S_{sk}	S_{ku}	S_k	S_{pk}	Implant Period
S_{PV}	1.00								
S_{Peak}	0.83	1.00							
S_a	0.69	0.67	1.00						
S_q	0.82	0.73	0.91	1.00					
S_{sk}	-0.47	-0.14*	-0.14*	-0.37	1.00				
S_{ku}	0.64	0.33	0.06*	0.31	-0.75	1.00			
S_k	0.58	0.58	0.92	0.75	-0.02*	-0.07*	1.00		
S_{pk}	0.67	0.71	0.82	0.76	0.04*	0.04*	0.81	1.00	
Implant Period	-0.03*	0.001*	0.02*	-0.07*	0.14	-0.10*	0.01*	-0.01*	1.00

Table 4.7: Relationship between head topography and implant period for explanted components. Spearman's rank correlation coefficient is shown. * denotes t>0.0001.

Sockets

The topographical features of sixty-seven explanted liners were assessed. Fifteen of these had been previously friction tested. Statistical testing showed that the roughness values for the joints friction tested were significantly different from those that had not been tested. The damage to the liner caused by the friction testing necessitated that these joints were excluded from the study into surface topography. In addition two unused liners were assessed.

Again the assessment of the explanted liner's topographical features could be subdivided into the three regions observed in the qualitative study. For the purpose of the statistical analysis of the changes in surface topography of the worn region, (1), and unworn region, (3) were considered. These are shown in Table 4.8. A separate study of the ridge region was performed.

Again statistical analysis showed that there were no differences between the liner types in terms of their surface roughness parameters. Hence both types of liner are included in Table 4.8.

Topographical Parameter	Median, IQ Range (Micrometres)		Equality of Medians Worn-unworn	
Roughness	Worn	Unworn	z	p
S_{peak}	2.22, 3.25	19.45, 11.44	15.30,	0.0001
S_a	0.041, 0.047	0.212, 0.247	14.37,	0.0001
S_q	0.07, 0.08	0.39, 0.50	14.91,	0.0001
S_{sk}	1.01, 1.41	-1.38, 3.58	-9.70,	0.0001
S_{ku}	32.5, 27.6	79.2 89.8	10.72,	0.0001
Waviness				
W_{peak}	0.44, 0.69	3.16, 2.92	14.41,	0.0001
W_a	0.081, 0.101	0.76, 0.76	15.10,	0.0001
W_q	0.104, 0.206	0.971, 0.947	15.18,	0.0001
W_{sk}	-0.132, 0.694	-0.236, 0.928	-2.44,	0.0146
W_{ku}	3.79, 2.20	3.52, 2.90	-3.06,	0.0022

Table 4.8:   Surface roughness and waviness values for the worn liners. All values, bar skewness, kurtosis and the statistical parameters z & p-value are in micrometres.

The previously reported quantitative studies of the liners has illustrated the complete difference in the topography of the worn and unworn regions of the liners. This is reflected by the substantial differences in all the topographical parameters presented.

Let us focus attention on the worn region. The skewness and kurtosis of the waviness for this area shows that the distribution of height is approximately symmetrical, approximating to a Gaussian distribution about the mean plane. The peaks of the waviness are small and will be equal in magnitude to the troughs. The degree of roughness which is superimposed upon the waviness is low with a root mean square deviation of only 70nm. Again as in the qualitative DIC images the granular nature of the UHMWPE was clearly distinguishable using profilometry (Figure 4.28).

In Figure 4.28 a depression of the order of 100μm wide and 1μm deep is seen. Depressions similar to this were frequently observed in the worn region. Their presence was restricted to the more polished of the liners and usually away from the peripheries of the worn region.

In region 2, adjacent to the ridge, DIC microscopy revealed curious dominant asperities. These were quantified using the profilometer. Typically the dominant asperities were approximately 5μm high and 100μm in width (see Figure 4.29). These dominant asperities usually displayed no regular spacing or orientation, however in a few cases the dominant asperities could be seen to be projections of the nearly completely worn machining marks (see Figure 4.30).
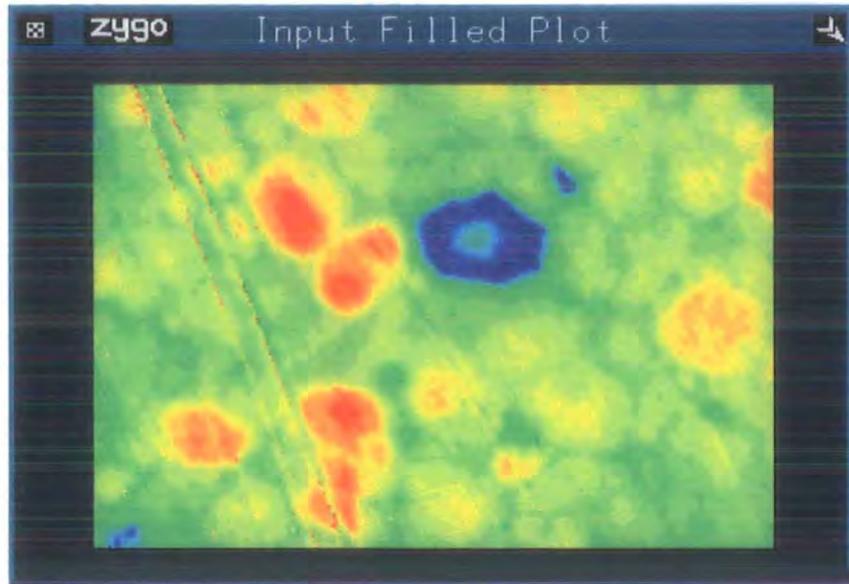
Figure 4.28:   Contour plot of liner (550μm x 730μm) with PV height of 2.3μm.
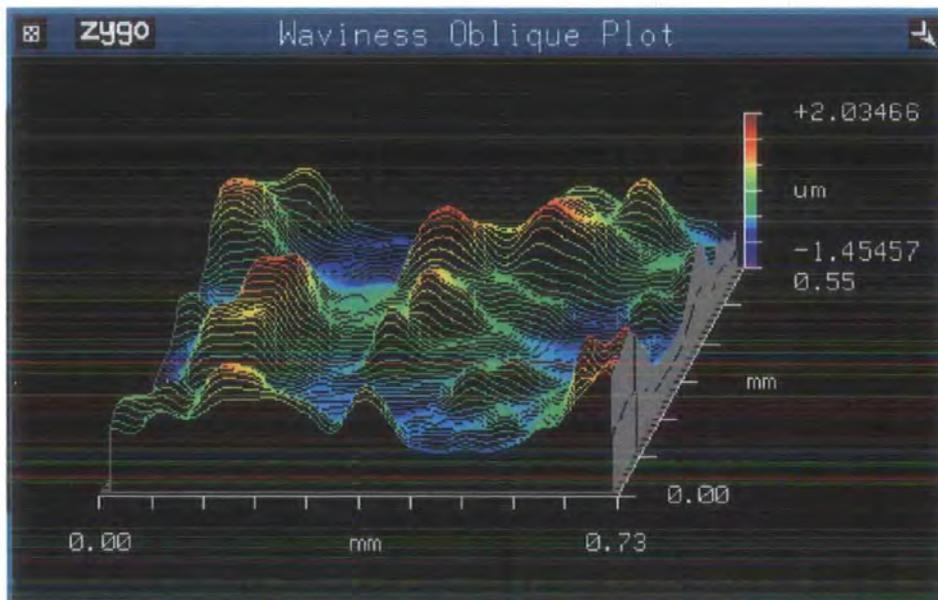
Figure 4.29:   Oblique plot of dominant asperities.

The machining marks observed in the unworn region can be seen in Figures 4.30 and 4.31. They were clearly similar to those of the unused liners but the sharpness of the peaks had been smoothed. This phenomenon was especially marked as the image approached the border with the worn region (See Figure 4.31).
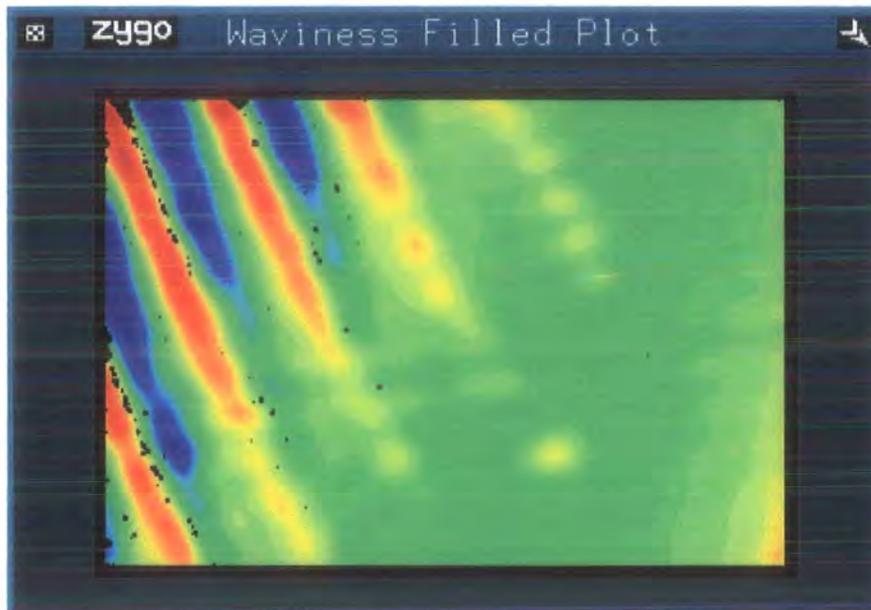
Figure 4.30: Contour plot of boundary between wear regions. 550μm x 730μm with W_{PV} height of 4μm. This image has been filtered to remove roughness as described in Liner Protocol Appendix 3.
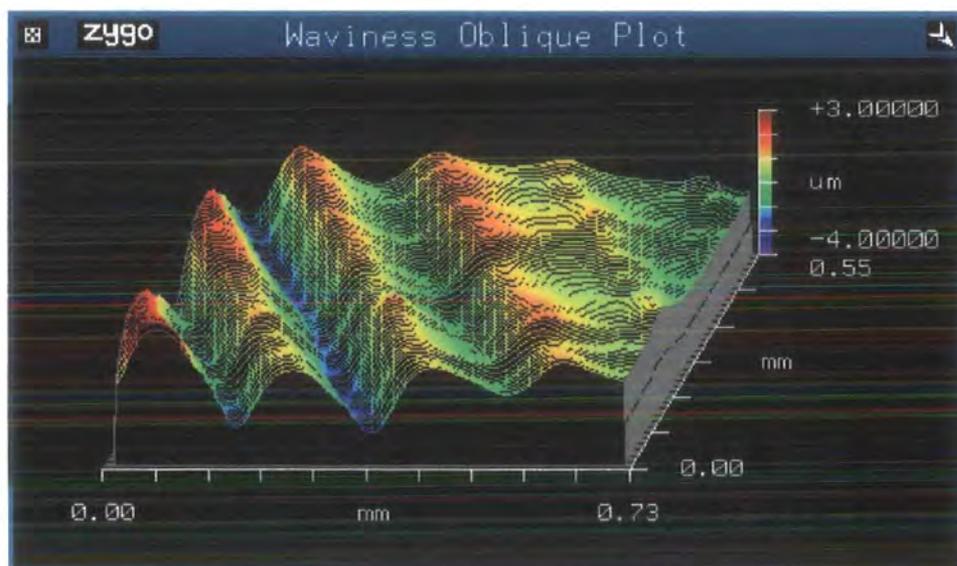
Figure 4.31: Oblique plot of ridge region (550μm x 730μm). Shows decaying waviness as machining marks are removed through wear. This image has been filtered to remove roughness as described in Liner Protocol Appendix 3.

Any correlation between the roughness values for the femoral heads and those of the acetabular liners was tested using Spearman's rank correlation test. The values obtained by this analysis can be seen in Table 4.9. No significant relationships between the surfaces of the two components were observed.

Head	Liner - contact region					
	S_a	S_q	S_{sk}	W_a	W_q	W_{sk}
S_a	-0.0712	-0.0650	0.2041	0.1182	0.1061	0.1338
	(0.6053)	(0.6374)	(0.1350)	(0.3899)	(0.4407)	(0.3302)
S_q	-0.0801	-0.0844	0.2441	0.0843	0.0814	0.1012
	(0.5610)	(0.5209)	(0.0725)	(0.5407)	(0.5545)	(0.4621)
S_{sk}	-0.0190	-0.0111	0.0761	0.0172	0.0095	0.1343
	(0.8904)	(0.9360)	(0.5809)	(0.9008)	(0.9450)	(0.2381)
S_{ku}	0.0137	-0.0047	0.0202	-0.0186	-0.0201	-0.0698
	(0.9211)	(0.9728)	(0.8838)	(0.8927)	(0.8842)	(0.6124)
S_{pk}	-0.0358	-0.0527	0.2997	0.0505	0.0383	0.1040
	(0.8152)	(0.7308)	(0.0455)	(0.7416)	(0.8025)	(0.4968)
S_k	0.0724	0.0717	0.1580	0.1331	0.1084	0.1406
	(0.6364)	(0.6398)	(0.3000)	(0.3834)	(0.4783)	(0.3570)

Table 4.9: Relationship between head and liner topographies for explanted components. Spearman's rank correlation coefficient is shown with the associated p-value in parentheses.

4.4.3 Investigating the Relationship Between Head Roughness and Wear

Linear regression was used to yield the values of the constants a and b in equation (2.3) proposed by Dowson et al.[116]. The relationship can be seen in Figure 4.32. The values of the constants a and b were found to be 4.1 (SE 4.2)x10^{-6} and -0.30 (SE 0.31) respectively with a R^2 of 0.027.

The effect of using the alternative roughness parameters S_a, S_{pk} and S_k in Dowson's relationship was investigated but produced equally weak associations. No significant association could be found for Wang et al.'s[118] theoretical relationship between $\Delta V/N$ and $L^{1.5}R_a^{1.5}$ for this dataset (Spearman's $\rho=0.0440$, $p=0.7988$, Figure 4.33).
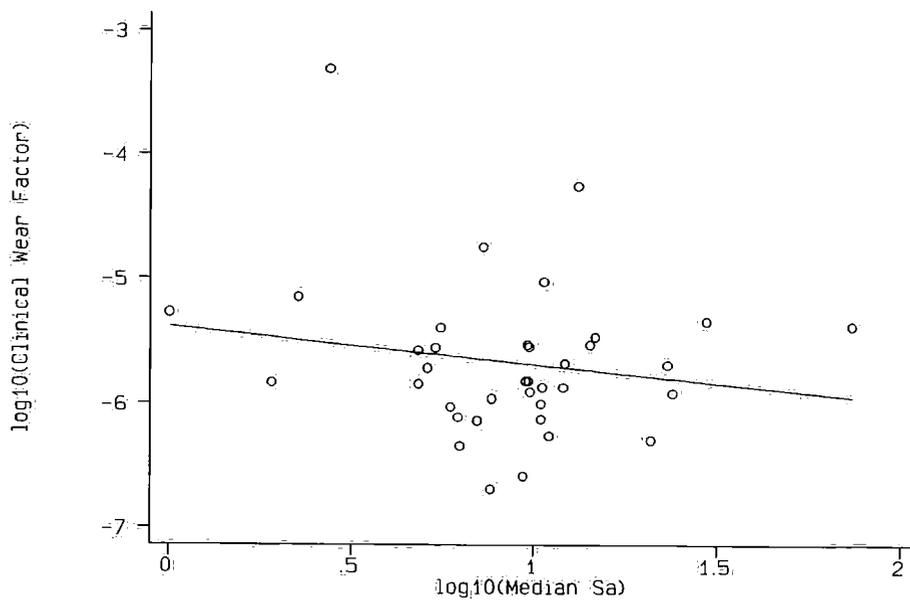
Figure 4.32: Variation of clinical wear factor with respect to arithmetic mean roughness, S_a.
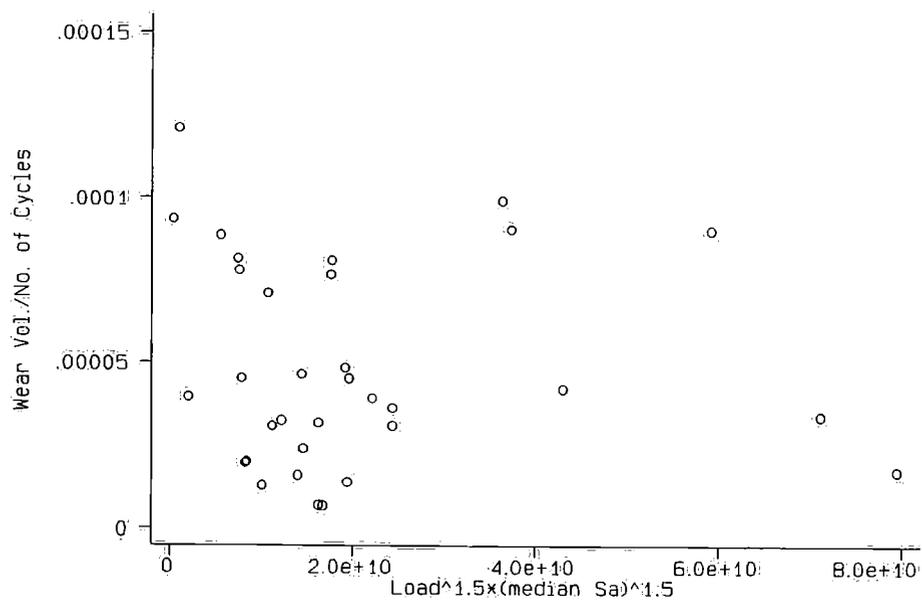
Figure 4.33: Plot of $\Delta V/N$ by $L^{1.5}S_a^{1.5}$.

4.5 Crystallinity Investigations

The preliminary investigation showed higher values of crystallinity for the irradiated samples (see Table 4.10). Unfortunately the numbers of samples tested were insufficient to make statistical analysis of variance possible. The values found for the study of *ex vivo* samples are presented in Table 4.11. Once again numbers were too low to facilitate meaningful statistics.

Polyethylene	Crystallinity, %	
	Non Irradiated	Irradiated
0642	51.1	54.3
1020	52.8	56.9
1150	50.3	51.0

Table 4.10: Median crystallinity values for raw polyethylene.

Region	Crystallinity, %	
	Median	Range
Rim	61.5	55.7 - 75.5
Worn - surface	59.3	56.4 - 60.6
Worn - bulk	57.6	55.1 - 58.1
Unworn - surface	62.5	58.1 - 67.6
Unworn - bulk	58.5	58.3 - 62.2

Table 4.11: Crystallinity values for explanted liners.

4.6 Debris Retrieval Study

A typical plot of size distribution by number and volume can be seen in Figure 4.34 and 4.35, respectively. Table 4.12 shows the minimum size of particle reported was 0.49μm, this represents the limit of detection of this instrument not the smallest particle size present. The notation $D(n,0.5)$ represents the number median diameter. The notation $D(4,3)$ is the equivalent volume mean diameter, also known as the De Broucker mean[192].
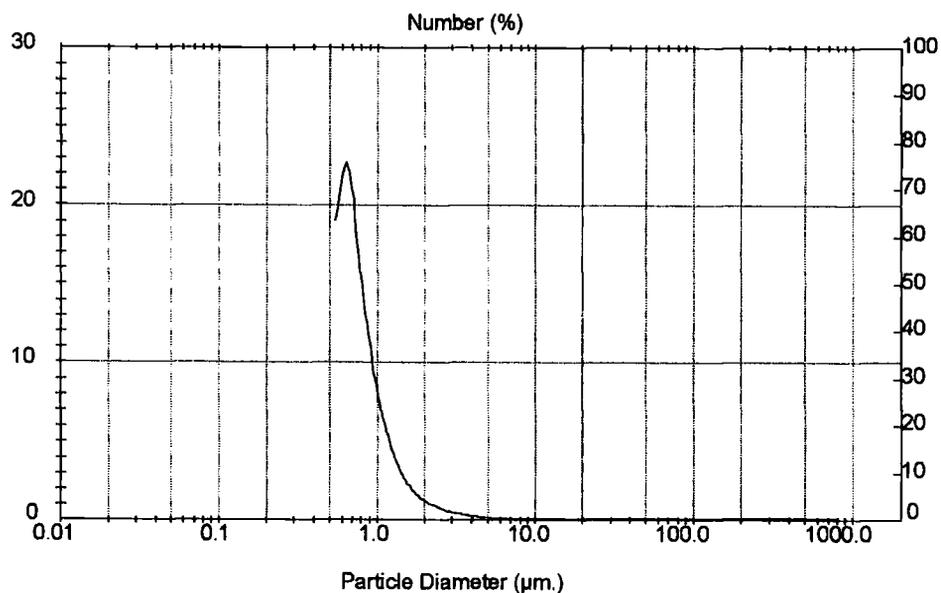
Figure 4.34: Size distribution of particles by number.
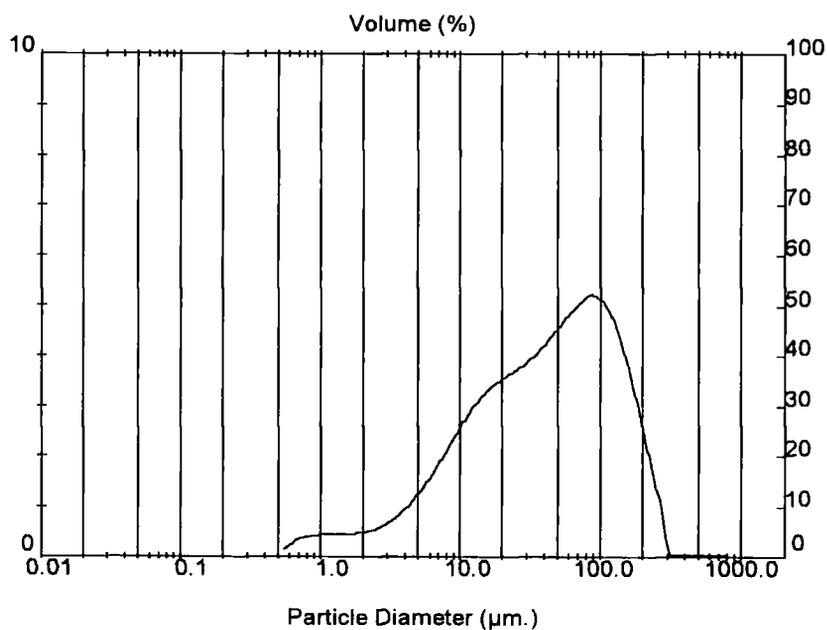
Figure 4.35: Size distribution of particles by volume.

Sample	Retrieval Site	Particle Size (μm)			
		Smallest	D(n,0.5)	D(4,3)	Largest
A	Greater Trochanter	0.49	4.53	37.9	140.58
A	Neck of Femur	0.49	0.74	10.12	41.43
A	Acetabulum	0.49	0.76	17.09	222.28
B	-	0.49	0.71	249.69	878.67
C	-	0.49	0.72	64.54	409.45

Table 4.12: Summary of particle sizes given by LALLS analyser.

5.0 Discussion

The layout adopted throughout the Discussion section of this thesis attempts to reflect that of the results section. Each successive finding, as presented in the results section, will be addressed in turn under the same sub-heading.

Additionally, a certain number of interesting points can be deduced purely from an initial overview of the patient profiles and component distribution given in Section 3.1. Consider the median age of the patients at primary operation in comparison to that of the typical patient involved in a Charnley retrieval study. The recipients of PCA THRs have a mean age of 45.98 years and as such are considerably younger than those of Charnley joints at 56 years[142]. Indeed the general perception within the medical profession is that cementless designs are more suitable than cemented joints for younger patients.

As a result of this, the range of indications for primary surgery also differ between the PCA joint and the Charnley. The distribution of indications for primary implants in the present study are; 33% for osteoarthritis, 38% rheumatoid arthritis, 12% CDH, 4% ankylosing spondylitis and 13% for other conditions. A direct comparison of this profile with that of the patients in Hall *et al.*'s[142] study of Charnley joints where 74% are for osteoarthritis, 8% CDH, 7% rheumatoid arthritis and 11% for other conditions reveals that there is a substantial difference in patient profiles between the two studies.

The variation of age and diagnosis for primary cases between the two joint types may affect the performance of the joint in a number of ways. For example, the possible coexistence of osteoporosis with osteoarthritis effects bone density and hence prosthesis fixation. Alternatively, reduced activity levels may be expected in patients suffering from rheumatoid arthritis due to pain from joints other than the hips. However, it is not feasible to assess the effects of such relationships fully due to their inter-reliance. Instead we must ensure that the database on which we draw our conclusions is sufficiently large to compensate for any bias introduced.

Considering the distribution of the components retrieved it becomes immediately evident that the femoral component seems much more successful than the acetabular component. The number of acetabular components (metal-backings) that need revision exceeds that of the stem by a ratio of 6.3:1. This concurs with the study of

Owen et al.[84] in which osteolysis of the acetabular side was identified as the dominant reason for long-term failure. Indeed a lack of any evidence of bony ingrowth at the time of revision was noted in this study testifying to the possibility of osteolysis behind the acetabular component.

Why then should the acetabular component be more affected by lack, or loss, of bony ingrowth. Firstly the quality of ingrowth into the metal-backing must be questioned. Fractures of the acetabulum are characterised by non-union and the formation of fibrous membranes[193]. The response to the trauma of surgery must be similar. There is doubt as to whether bony ingrowth to the acetabular component ever occurs, fixation is likely to be through a stable fibrous membrane. However, Bloebaum et al.[194] reported that for seven autopsy specimens a mean of 84% of the porous coating had direct apposition of bone. Conversely, the porous coating of the femoral component will lie adjacent to the cancellous bone of the intertrochanteric region. This bone is characterised by its rapid and complete union of fractures even with the simplest of treatment. The natural response of this bone is osseointegration[193] and as such effective bone ingrowth can be expected provided the initial interference fixation of the component is effective.

The loss of bone surrounding a joint through osteolysis affects the acetabular component of the PCA system to a much greater degree than the femoral component[84]. This phenomenon is likely to be due to the ease of migration of the wear debris. During the course of walking, micromotion between the component and bone causes the fluid in these regions to become pressurised. The resultant pumping action forces the debris laden fluid to flow[19], leaving behind its load of wear debris. In the case of the acetabular component the fluid may be forced between the fibrous membrane and component at the rim, and also through the hole in the metal-backing at the pole (see Figure 2.7a). However, the circumferential porous-coating of the femur and the ingrowth of bone will act to limit the available routes for debris migration into the femur.

5.1 Preliminary Descriptive Study

The preliminary study of the components revealed a number of interesting findings. The majority of these related to aspects of the design of the components rather than their tribological performance.

The occurrence of evidence of impingement was found in 36.8% of one-piece and 23.7% of the snaplock design. This compares favourably with the Charnley joint in which Wroblewski[131] found impingement in 64% of the explanted joints he studied whilst Isaac et al.[144] reported 48%. Impingement of the neck of the femoral component against the rim of the acetabular socket is most likely to occur when the joint is fully flexed in situations such as rising from a seat or getting out of a car. Many parameters are capable of influencing whether a joint will be subjected to this mode of wear. The high rate of impingement in Charnley joints is due, to a great extent, to the small head to neck diameter ratio. The work of Hall et al.[195] showed that the standard Charnley stem ratio (22:12.5mm) had a probability of impingement of 50% but the later reduced neck diameter (22:10mm) Charnley stems only achieved this probability of impingement when penetration reached 2mm. The head to neck ratio for the PCA is considerably larger (32/28/26:12.5mm) and as such this joint has a considerably lower incidence of this phenomenon. There were too few observations to establish if the joints using 26mm or 28mm femoral heads were more prone to impingement than those using 32mm heads. Wroblewski[131] and Isaac et al.[144] both observed that as penetration increased the joint became more likely to impinge. Similarly Hall et al.[195] reported a strong association between these two parameters. This is because with the head in its new position it will require a smaller ROM to cause impingement. This mechanism will also affect the PCA but the total penetration depths in the PCA are much lower than those of the Charnley prosthesis. Similarly it has been shown that a high degree of encapsulation of the head by the socket will increase the likelihood of impingement[195], but this is not relevant to the PCA design.

This explains the Charnley joint's predisposition to this wear mode, however these mechanisms cannot explain the variation between the two different PCA liner varieties. The answer may lie in the varying angles of the open face of the acetabular cup. The metal-backing of the two designs both have a mean implantation angle of approximately 52° to the horizontal. However the 10° hood of the snaplock liners

will reduce this angle to a minimum of 42°. We can assume that the hood would never be positioned anteriorly but it may have been placed posteriorly to combat dislocation. If we consider the case where the neck of the femoral component is at 45° to the vertical and the joint is moving in flexion/extension only, then it can be seen in Figure 5.1 that the more steeply angled acetabular component will impinge first.

ROM > ROM
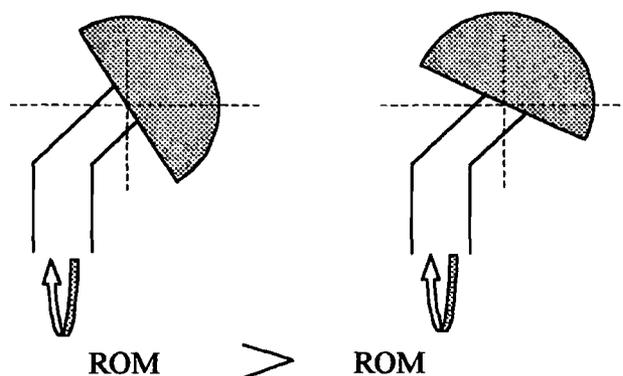
Figure 5.1:   Schematic diagram showing how acetabular angle may affect impingement.

Alternatively, or more probably additionally, the higher average total penetration depth of the one-piece cohort as compared to the snaplock will increase the former's tendency to impinge. As in the Charnley, joint penetration of the head into the liner will increase the chance of impingement. The difference in the occurrence of impingement between the two types of PCA acetabular component may also be due to variations in the range of motion (ROM) achievable by the patient groups. However this is unlikely as there is no evidence in terms of age or diagnosis to suggest that either patient group is more flexible.

Delamination of the UHMWPE was observed both within the articulating region of the joint and on the rim of the liner. The observation that delamination, both internal and external, occurred almost exclusively in the one-piece population indicates that this phenomenon is likely to be attributable to a material parameter. The tribological and loading regimes of the two joint types will be very similar therefore such a strong disposition towards delamination in the one-piece cohort must be due to the quality of the UHMWPE. The attention of the orthopaedic manufacturers has been focused on UHMWPE quality by the problem of delamination in TKR. It has been shown that sterilisation by irradiation causes extensive oxidation of the UHMWPE just below the

surface[196-199]. The presence of defects within the granular structure of the bulk material also compromises its strength[200,201]. Substantial improvements in the quality of the UHMWPE and sterilisation techniques have been made and it is likely that the low occurrence of delamination in the snaplock type liner is due to these improvements.

The presence of a ridge between the worn and unworn regions of the liner may be regarded as an indicator of the level of penetration and the variation in the wear vector during the life of the prosthesis. Clearly a moderate penetration must be reached before a ridge region may become established, as testified to by the widely varying mean penetrations for the liners with and without a ridge. Multiple ridges are thought to be due to the migration of the acetabular component. The association of multiple ridges and impingement suggests that the migration may be caused by impingement. This concurs with the work of Yamaguchi *et al.*[202]. The socket may migrate and become restrained in a new position where the wear will continue. Alternatively there may be a change in the position of the wear vector through a change in the location of the axis of rotation of the joint or in that of the joint reaction force. It is uncertain whether this alternative mechanism would be capable of producing three discrete wear directions such as have been observed in this study.

The effect of oxidation in terms of delamination has been discussed previously and it was hypothesised that the UHMWPE quality of the one-piece liners was inferior to that of the snaplock type. This is attested to by the observation of oxidation as evidenced by discolouration of the liners. Thirty-two of the forty-four observed cases came from one-piece sockets. The correlation between the implantation durations and oxidation observed was deemed to be spurious. Oxidation is part of the ageing process of UHMWPE and as such it should be related to implant duration. However the rate at which oxidation takes place *in vivo* will be low in comparison to that imposed by the irradiation and ageing prior to implantation[197]. Unfortunately it was not possible to acquire the necessary information to study the influence of shelf-life on the presence of oxidative discolouration.

Clearly being a cementless design there is no opportunity for PMMA ingression into the articulating region. However the presence of imbedded metallic beads from the porous coating was observed in the liners of seven joints. This very low frequency is

contrary to the findings of Owen et al.[84], all 26 of their retrieved PCA acetabular components exhibited bead ingression. The findings of this study suggest that metal bead ingression is not of primary concern. It was observed that when bead ingression took place the beads were imbedded almost exclusively in the non-articulating region of the liners and hence their potential to cause damage was limited. Further, the majority of the components assessed in this study were failed primary prostheses. It was observed on the post-revision radiographs that a substantial number of beads could be released into the joint environment during revision surgery. It is possible that the ingression of beads may become a more significant problem for the implant inserted at revision surgery. However, consideration of radiographs up to 5 years post-revision revealed that the beads had little potential for migration through the soft tissue.

The phenomenon of liner dissociation from the metal-backing is one that has been observed previously in case studies by Brien et al.[89] and Ries et al.[90]. In this study 5.26% of the failures experienced in one-piece joints were due to dissociation. This catastrophic failure causes the rapid production of vast amounts of both metallic and UHMWPE wear debris (Figure 4.3). In the three examples included in this study the duration of implantation could be ascertained for two, these were 11.4 and 11.7 years. These are particularly long durations when considering this joint type. However, the three case studies presented by Ries et al. had durations of 2, 4 and 2 years and the four cases studied by Brien et al. had durations of 0.5, 2, 4 and 5 years. It seems that this form of failure is not reserved to elderly implants. Yet one may hypothesise that as the age of the implants of this type increases the embrittlement of the polyethylene combined with the fatiguing cyclical load imposed on the peg will increase the tendency towards of this type of failure. Additionally the quality of the UHMWPE of the peg may be questionable due to the use of ultrasonic welding as the method of attachment.

Another phenomenon which was observed solely in the one-piece group of liners is the rotation of the liner within the metal-backing. This was seen in a large proportion of the sockets (35.1%). An association between the occurrence of rotation and oxidation was also noted. As mentioned previously the oxidation would act to embrittle the UHMWPE and when combined with the cyclical nature of the forces

would lead to the failure of the material immediately around the single anti-rotation tab.

The fracture of the polyethylene next to the snaplock mechanism occurred in 29% of the liners of this type. A groove in the liner (see Figure 2.7b) locates into a circumferential ring in the metal-backing to secure the liner into position. This creates a point of minimum polyethylene thickness which lies at approximately 40° to the centre of rotation. Coincidentally the angle of the wear vector relative to the open face of the cup has a mean value of 34°. This design has created a situation where the direction of maximum penetration is towards the thinnest portion of the liner. The fact that all the liners to fracture involved a combination of 26mm heads with 40/43mm backings or 32mm heads with 46/49mm backings leaves no doubt as to the folly of creating a joint with a working polyethylene thickness of less than 2mm (Appendix 4a). Indeed of the twenty-three liners of these size combinations involved in this study sixty-one percent were observed to have evidence of liner fracture. To compound the problem the notch in the liner also acts as a stress raiser which when located into a convenient metallic indentor of the backing creates a scissor action that will rapidly lead to fracture of the polyethylene. It is almost certain that this will be through the yielding of the material rather than through a fatiguing action.

The association of liner fracture with gender was considered to be an artefact of the trend for women to have smaller pelvises than men. Hence their smaller acetabulae have necessitated the use of the small metal backing diameters. However the use of 32mm femoral heads was a parameter over which the surgeon had control. In patients with acetabulae which are very small, less than say 46mm diameter, small head sizes are indicated. However, if the patient is predisposed to dislocation a large head may be required. The use of an acetabular component which does not utilise a metal-backing may be prudent. The atypical primary diagnosis profile for the patient group experiencing liner fracture is also considered to be a spurious relationship.

The unusually high incidence of oxidation for the fractured snaplock liners may contribute to the fracture failure of these liners. The propensity for oxidative changes to these sizes of liners could be attributable to either of two effects. The small sizes would be infrequently employed and as a result their shelf-lives may be longer than the more regularly used sizes. This would allow a greater time for the rapid oxidative

change in the presence of air. Alternatively the thin UHMWPE liners may be more susceptible to damage by irradiation during sterilisation. The thickness of the liner with ranks of 1 & 2 (Appendix 4a) lies in the range 2mm to 3mm depending on the position. If oxidative damage due to irradiation reaches a peak at approximately 1mm below the surface then the effects of irradiation from each side may compound to form a single area of high degradation (see Figure 5.2).
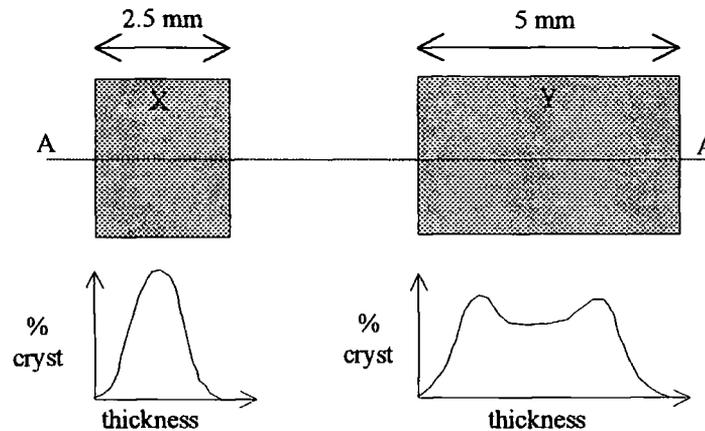
Figure 5.2:   Irradiation damage of thin UHMWPE components. Consider two pieces of UHMWPE one 2.5mm thick (X) and the other 5mm thick (Y). During irradiation the source is moved around the component, or vice versa[197]. The amount of oxidation caused will be a function of the depth. It is possible that the degradation is compounded at the centre of the thinner piece. This is shown as % crystallinity along the axis A-A.

Fifteen of the seventeen femoral stems received showed evidence of polishing. The distribution of polishing around the stem was similar to that reported by Shardlow *et al.*[203] for Charnley prostheses. Polishing is caused by the micromotion of the stem against the fibrous membrane or bone. As such it is not surprising that such a high proportion of the explanted stems exhibited polishing. All of the stems would have been loose (as evidenced by migration or pain) to be recommended for revision and so all will have been subject to polishing micromotion. The two which showed no evidence of polishing were only implanted for short durations. Similarly the agreement between the PCA and Charnley stems on the distribution of polishing is attributable to the two joints performing under similar load conditions. The only difference between the two joints would be that the Charnley would be polished against cement.

The atypically heavy patient group that the revised stems come from is due to the greater demands placed upon the fixation regime that these patients exert. The

surgeon will be able to achieve a certain level of interference fit between the PCA stem and the bone. This level of fit will be approximately constant regardless of the patient's size. It may be that the loading imposed by the heavier patients causes a level of micromotion from implantation that will inhibit the ability of the bone to create osseointegration. This will then make these joints more liable to fixation failure. A similar observation is made for cemented stems when early migration can be used as a predictor of fixation failure at a later date[93].

The angle of insertion of the acetabular metal-backing was shown to be approximately 52° whichever type of liner was being used. In Table 5.1 the insertion angles of a number of hip designs are compared. The angle of insertion suggested in the manufacturers literature is 45° for the PCA and also 45° for the Charnley joint.

The actual values for the Charnley tend to lie more closely to the desired values than those for the PCA. There is the perception in the clinical community that the anti-rotation lugs on the PCA must be inserted superiorly. In order to do so it may be necessary to implant the joint more open (vertical) to achieve sufficient anchorage.

Author	Prosthesis	Metal-backed	Number	Acetabular angle	Head diameter
Devane et al. 1995 [97]	PCA	y	141	50.9	32
Devane et al. 1997 [141]	Mallory-Head	y	139	43.4	28
Hall et al. 1998 [205]	Charnley	n	84	46	22
Kabo et al. 1993 [132]	various	y/n	60	36.9	various
Kennedy et al. 1998 [204]	Mallory-Head	y	38	61.9	28
			37	49.7	28
Knight et al. 1998 [206]	PCA	y	70	45	32 / 28
Learmonth et al. 1996 [207]	PCA	y	24	42.9	32
Perez et al. 1998 [208]	Biomet St-cup	y	27	41.7	28
Sychterz et al. 1996 [149]	various	y/n	26	47.5	32
Wroblewski et al. 1985 [131]	Charnley	n	22	48	22

Table 5.1:   Summary of acetabular component insertion angles.

It is not just the PCA that suffers from this practice. The Mallory-Head prosthesis has peripheral fins which the manufacturers specify should be oriented such that they are all fully imbedded into the bone. A study by Kennedy et al.[204] showed that when the

insertion directions were followed the insertion angle averaged 61.9°. In their study they implanted a second group of joints at an average angle of 49.7°. This second group seemed to perform well but their follow-up was too short (4 years) to draw firm conclusions.

In order to discuss the angle of the wear vector found in this study we must first have an appreciation of the motion and load found in a healthy natural hip joint. The classic paper of Paul[209] is widely cited when joint forces are discussed. In his study Paul used gait analysis and force plate data to deduce the joint reaction force (JRF) during the walking cycle. This peaked at approximately four times body weight at the heel-strike and toe-off phases of gait. It can be seen from his data that the direction of the JRF lies medial to the sagittal plane through the centre of rotation of the hip. The study of Bergmann et al.[210] in which they use a telemetred hip prosthesis explicitly states that the JRF varies on average between 25° and 40° medially during a single gait cycle (see Figure 5.3). The magnitude of the JRF measured returned to the pre-operative values.
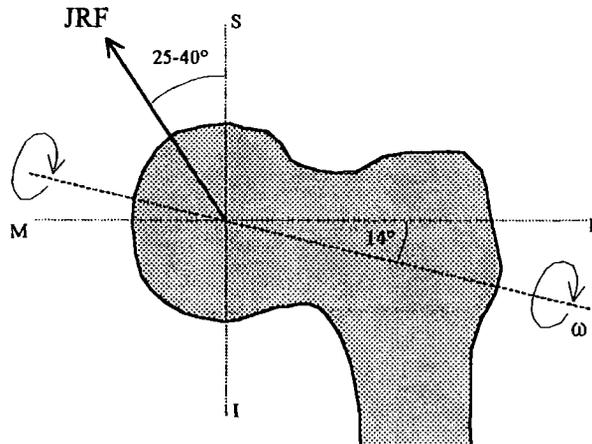
Figure 5.3: The force and rotational axis alignment in the natural hip joint. JRF as given by Bergmann[210], axis of rotation as given by Murray & O'Connor[212].

Bergmann et al. also give data on the axis of rotation during gait. Their work concurs with that of Johnston & Smidt[211] on natural joints. Johnston & Smidt gave a range of motion of 52° in flexion/extension, 12° abduction/adduction and 13° internal/external rotation. Murray & O'Connor[212] used Bergmann et al.'s raw data to calculate the instantaneous angle of the axis of rotation. The axis of rotation is widely regarded as being horizontal, lying in the coronal plane. The instantaneous axis calculated by

Murray & O'Connor may lie as much as 50° off the horizontal. The average angle of the axis was given as approximately 14°. The position of the force vector and axis of rotation for the physiological situation is given in Figure 5.3.

Now let us examine the penetration angles found from clinical and retrieval studies. A summary of these studies is given in Table 5.2. Unfortunately the subject of penetration direction has not been widely studied and there is little similar work for comparison. Further the studies which have been published, and the results presented in this study, are open to criticism. The deduction of penetration vector angles from radiographs introduces two sources of error. Firstly, there is a lack of a reliable reference axes, the angles of the pelvis and the acetabular component must be deduced from anatomical features as described in Section 3.1. Secondly the use of anterior-posterior radiographs assumes that the penetration vector lies in the coronal plane. This is not the case, it has been shown to lie just posterior to the coronal plane. The direct measurement of penetration angle relative to the open face of the acetabular component in the shadowgraph technique removes the doubt as to the location of the wear vector relative to the coronal plane. However it introduces an alternative source of error as shown by Cunningham et al.[137]. Despite this the values obtained in this study agree closely with the post-mortem study of Sychterz et al.[149] which may be considered to be the optimal data source.

Author	Number	Head diameter	Cup material	Median penetration vector angle
this study	35	32	UHMWPE	17° laterally
Elson & Charnley 1968 [213]	37	22	PTFE	8° medially
Hall et al. 1998 [205]	84	22	UHMWPE	6° laterally
Sychterz et al. 1996 [149]	26	32	UHMWPE	17° laterally
Wroblewski 1985 [131]	22	22	UHMWPE	range 34.5° med. to ~30° lat.

Table 5.2:   Summary of penetration vector positions reported in literature.

The value of 17° laterally for Sychterz et al. and the present study both refer to 32mm diameter femoral heads. This appears systematically different from those for smaller

head sizes (Table 5.2). Yet all the penetration vector angles are very different from the angle of the JRF we expect.

That the penetration vector and force vectors are not co-incident is attributable to the fact that wear is proportional to sliding distance. If we assume that the hip axis of rotation is horizontal (ie. in flexion/extension only) then the maximum sliding distance will occur at the very top of the femoral head. If the force direction lies at 30° medially then the penetration vector will lie medial to the vertical. The angle between the force and wear vectors can be predicted using the data from McLeish & Skorecki's[214] analytical study. This calculation neglects the contribution of creep to the penetration. If we now introduce Murray & O'Connor's average angle of the axis of rotation of 14° laterally then by McLeish & Skorecki's relationship the predicted angle of penetration is 12° medially. This still lies a substantial distance from that observed clinically.

At this point we must introduce another variable. The penetration vector is a combination of wear and creep. If the penetration vector angles are plotted against penetration depths we observe a trend (Figure 4.6). This trend is also observed in the work of Hall et al.[205]. This phenomenon is caused by the effects of creep. The direction of creep will be coincident with the JRF as it is independent of sliding. It is known that creep occurs rapidly shortly after implantation but slows considerably with time[151,215-217]. If we assume the effects of creep are constant between joints and stablise after one year, then the joints that are revised shortly after one year will have a medial penetration direction. Equally joints from inactive patients will not have worn a great deal and the penetration direction will again be dominated by the creep component. However in joints that have undergone a reasonable amount of wear the creep component will be overwhelmed by the effect of the wear and the penetration vector will tend towards the wear direction as predicted by McLeish & Skorecki.

Unfortunately the effects of creep will only draw the direction of penetration towards that of the force. For the situation assumed previously this will be medial. As penetration direction can be influenced only by the positions of the axis of rotation or the line of action of the JRF, then to create the 17° lateral angle observed in this study, both of these parameters must lie laterally. This is contrary to the work of

Bergmann *et al.* and Johnston & Smidt where in most cases a normal gait pattern and force direction was restored after THR.

5.2   *Friction*

This study has shown that for the PCA system there was no significant difference between the frictional characteristics of the new and the explanted joints. This is in contrast to the Charnley joint in which the friction factor in 34% of the explanted joints was greater than the unused joints by at least twice the standard deviation[61].

The rise in friction factor for the Charnley joints can be attributed to the effect of the ingression of cement debris into the articulating interface. The presence of the cement debris may act to increase the friction in two ways. The cement debris will become lodged in the softer UHMWPE and will itself become part of the bearing surface. The cement will act to increase the effective hardness of the surface, thereby increasing the friction between the two surfaces. Alternatively, or possibly additionally, the cement will act to damage the metallic femoral head. The roughening of the Charnley head is more pronounced than that which was observed in the PCA study. This increased roughness will increase the friction between the two surfaces. This concurs with the work of Smith *et al.*[218] where friction was found to be higher with femoral heads roughened after hip simulator wear testing. We shall return to the roughening of the heads in Section 5.4.1.

If we consider the mean friction factors of the explanted joints for both designs when lubricated by fluid of viscosity 0.010 Pa s the value for the Charnley[61] is 0.040 and for the PCA is 0.025. However, when the effect of the different femoral head sizes is accounted for the Charnley frictional torque will only be 10% higher than that of the PCA.

Whilst the value of friction factor, and hence frictional torque, found both in this, and previous, studies are too small to cause failure of the prosthesis fixation, they may contribute to the progression of the loosening process in joints already effected by osteolysis.

5.3 Wear

The statistical analysis used in the presentation of the Wear Results (Section 4.3) illustrates that basic routines are incompatible with the complex distribution of the data complied in retrieval studies. This may serve to detract from any comparisons with other studies where the statistical practises have not been extensively reported.

Initial univariate analysis revealed that the penetration and also total wear volume had a positive skew. This dictates the reporting of the median values as opposed to the mean. The only directly comparable study is that of Hall et al.[142] in which a median total wear volume of 508 mm^3 is reported. A review of Table 2.5 can show that Atkinson et al.[136], Devane et al.[97] and Hashimoto et al.[139] also gained similar values. Direct comparison of these values is inadvisable due to the varying methods used in the data acquisition, calculation and reporting of the results. However there seems to be a degree of consensus with an approximate range of 400-600mm^3 of socket wear at revision for failure. This applies for any type of UHMWPE against hard counterface articulation. The lack of variation in total wear volume is an interesting observation that shall be returned to later in this section.

Penetration rate is a parameter which has been reported widely, again using various techniques. Far from becoming a well categorised and understood parameter the wealth of studies has detracted from its value. If we review the data presented in Table 2.5 it is possible to observe a spread in penetration rates from 0.07mm/yr to 0.26mm/yr. This variation comes from differences not only in the joint designs but also from errors introduced by the experimental methods used.

Let us be more objective in our selection of comparative studies. If we compare values derived solely from studies using the shadowgraph method then we obtain the data shown in Table 5.3. This shows that the penetration rates appear to be approximately 0.20mm/yr whatever the diameter of the femoral head or the fixation technique employed. The presence of two reports which differ substantially is noted. The work of Sychterz et al.[149] uses post-mortem specimens these are not directly comparable to revision specimens for reasons which will be discussed in Section 5.4.3. Hashimoto et al.'s[139] study produces a very large penetration rate, this may be an artefact of the small implant durations of the prostheses involved in this study. The

contribution of creep to the penetration early in the joint's life has been discussed and in Section 5.4.3 the existence of a wear-in period will be investigated.

The finding that femoral head diameter has little influence on penetration rates appears to be contradictory to conventional wisdom which suggests that larger diameter heads penetrate more slowly. This was also the finding of a study by Hall *et al.*[219] in which no correlation was found between the penetration and femoral head diameter across a range of sizes (22-39.8mm).

Author	Head Diameter (mm)	Penetration Rate (mm/yr)	Volumetric Wear Rate (mm³/yr)
Atkinson *et al.* 1985 [136]	22	0.20	65
Hall *et al.* 1996 [142]	22	0.20	55
Hall *et al.* 1995 [219]	32	0.20	89
	39.6	0.21	137
Hashimoto *et al.* 1995 [139]	32	1.05	544
Isaac *et al.* 1992 [144]	22	0.21	-
Kabo *et al.* 1993 [132]	22	0.13	26
	28	0.23	76
Kusaba *et al.* 1997 [147]	32	0.21	-
Sychterz *et al.* 1996 [149]	32	0.07	39.8
Wroblewski *et al.* 1985 [131]	22	0.21	-

Table 5.3: Selected references relating to penetration rate and volumetric wear rate as calculated using the shadowgraph technique.

To gain a greater appreciation of the differences between the effect of the various head sizes it is necessary to consider the corresponding volumetric wear rates calculated. It is plain to see that the larger head sizes create more rapid volumetric wear (see Table 5.3). This is in accordance with the simple wear theory stated in equation 2.2. The volume of wear is proportional to the sliding distance. The larger the head diameter then the greater the sliding distance to which the joint is subjected for each walking cycle. The sliding distance of a 32mm head is 45% greater than that of a 22mm head and as such it can be expected to produce 45% more wear than a 22mm head for a given number of wear cycles. The volumetric wear rate for 32mm

heads obtained in this study is however 60% greater than the 22mm heads reported by Hall *et al.*[142].

The relationship between femoral head diameter and volumetric wear rate can also be investigated by reviewing the results published for hip simulator studies. The work of a number of groups is summarised in Table 5.4. This again illustrates the influence that head diameter has over the volumetric wear of the UHMWPE. The increases in wear rate for the various heads tend to lie close to those predicted by equation 2.2. However the results of Saikko *et al.*[220] show a much greater increase in wear rates. This is likely to be attributable to the use of water as a lubricant and the deleterious effects of excessive adhesive wear and possible transfer-film formation.

Author	Wear Rates for Various Femoral Head Diameters			
	22	26	28	32
Besong *et al.* 1998 [221]	.	.	30.03	32.09
Bragdon *et al.* 1998 [222]	20.8	25.2	.	33.7
Clarke *et al.* 1996 [223]	23.2	31.9	32.8	.
McKellop *et al.* 1995 [224]	41	.	.	55
Saikko *et al.* 1993 [220]	49	.	.	165*

Table 5.4: Summary of hip simulator studies employing various femoral head diameters. All values are in $mm^3/10^6$. *Saikko *et al.* study conducted using water as lubricant, whilst the other studies used bovine serum.

In our attempts to deduce the relative merit of various joints we must now turn to yet another parameter with which to compare joints. The clinical wear factor attempts to compensate for variations in the patient groups of the different joints. There are few studies which have utilised this parameter. Atkinson *et al.*[136] and Hall *et al.*[142] obtained figures of 2.10×10^{-6} mm^3/Nm and 1.96×10^{-6} mm^3/Nm both for Charnley 22mm heads. These compare very well with the 2.00×10^{-6} mm^3/Nm found for the whole 32mm head cohort in this study. This shows that any variation in the volumetric wear rates between the Charnley and PCA cohorts may be explained by the effects of the head size in conjunction with those of the younger, more active patient group for the PCA joint. There is no advantage, or disadvantage, in terms of wear to the cemented fixation of the Charnley joint or the metal-backing of the PCA

prosthesis. This is in agreement with the work of Manley et al.[225] and Önsten et al.[226] who found no correlation between wear rate and the presence of a metal-backing.

Unfortunately this is an oversimplification of the situation. A profound difference was found between the one-piece and the snaplock variety of acetabular liner in terms of clinical wear factor (Figure 4.16 and Table 4.4). The value for the one-piece liner, 2.39×10^{-6} mm^3/Nm, remains comparable to those of the Charnley studies but the snaplock seems to be much more resistant to wear. If we accept that we have accounted for variations in the patient groupings by considering the clinical wear factor then an alternative explanation for this result must be found. Consider once more the fundamental wear equation 2.4, wear can also be seen to be inversely proportional to the hardness of the material. It may be that a variation in the material parameters of the UHMWPE of the two liner varieties is responsible for the difference in wear performance.

Hardness is related to the crystallinity of the polymer, the more crystalline phase which is present, the harder the plastic. Irradiation in air is known to cause scission of the polymer chains of UHMWPE allowing them to become more aligned. This increases the crystallinity, density and hardness of the UHMWPE[198,227,228]. However concurrent with these changes there is also a decrease in the ultimate tensile strength and fatigue strength[199,227,229]. The irradiation and subsequent oxidation of the UHWMPE will act to enhance the hardness of the material, by equation 2.4 this may be expected to reduce the rate of wear. However there are a number of reports linking irradiation damage with increased wear rates[188,230]. This apparent contradiction is due to the inability of the simple wear/hardness relationship (equation 2.4) to apply to all material combinations. Evans & Lancaster[231] devised an alternative relationship for the abrasive wear of polymers, their empirical model is given below.

$$\Delta V \propto \frac{1}{\sigma_u \varepsilon_u} \tag{5.1}$$

The parameters σ_u and ε_u are ultimate tensile strength and elongation at rupture, respectively. This equation predicts that for a given material, a fall in ultimate tensile strength will increase the wear. This is the situation that is observed in irradiated UHMWPE.

How does this relate to the variation in clinical wear factor between the two joints which was found in this study? The potential for degradation of the UHMWPE by gamma-irradiation sterilisation has been identified for some time. Attempts to limit the damage have led to modifications of the sterilisation protocols utilised. It is quite possible that the snaplock components received a lower dose of gamma-radiation than the earlier one-piece design. Further variation in the degree of oxidation of the UHMWPE may be attributable to the differences in the length of time since the irradiation of the sockets. Increased awareness of ageing has led to the minimisation of shelf-life prior to implantation in contemporary joints.

An alternative that may figure in the high wear rate of the older liners is the evolution of production methods for UHMWPE. The bulk polymer is formed by the sintering of beads of UHMWPE under high temperatures and pressures. The incomplete consolidation of the beads leaves intergranular voids in the bulk polymer[200,201,232,233]. The occurrence of these voids has been reduced by using increased pressures and alternative techniques during the sintering of the bulk polymer. It is therefore also possible that the UHMWPE used in the more recent snaplock liners is of a higher quality than that used in the earlier one-piece sockets.

It has been suggested that the thickness of the UHMWPE employed in the liner may have some influence on the wear of the polymer. In the case of TKR, where the bearings are incongruent and the Hertzian contact stresses are high, the thickness of the tibial insert is indeed important. However it has been shown using finite element analysis of both stress[234,235] and wear[236,237] that in the hip, where congruency is high, liner thickness has no influence on wear. This concurs with the findings of this study (Figure 4.15). Unfortunately there are still proponents of this outmoded theory. Oonishi et al.[238,239] in retrieval studies published recently concluded that "When polyethylene thickness was more than 11mm, the volumetric wear rate for the three kinds of prosthetic cup seemed to become similar, that is 32mm^3/yr on average.". The three joints in question had 22mm, 28mm and 32mm diameter femoral heads. As we know from the wealth of clinical, retrieval and simulator studies detailed above, the wear that occurs with these different head sizes for a given number of wear cycles can never be similar regardless of the thickness of the socket.

Returning to the observation that there is a degree of equivalence in the median total wear volume between the studies of various joint types. We learnt during in Section 2.2 that there is a dose of particles above which the cellular response to their presence intensifies. It is reasonable to suppose that this dose will be reflected by there being a corresponding critical wear volume at which this dose will be approached. This was eluded to by Bos et al.[18] who reported a correlation between the number of particles observed in periprosthetic tissue and the wear volume of the joint. Clearly there are many variables which will influence this figure including patient debris sensitivity, efficacy of debris transport, the size distribution of the particles and so on. The accordance between the wear volumes at explant lends weight to the hypothesis of a critical wear volume.

If we accept that there may be certain volume of wear at which an osteolytic response becomes likely then it is of paramount importance to reduce the rate at which this volume is reached thereby prolonging joint life. The most immediate step that can be taken to achieve this goal is the disuse of the larger head sizes commonly employed. A head size of 22mm has been shown to offer the optimum solution using current materials[240].

Alternatively the modification of the tribological regimes of the joints may result in the production of debris which is small enough to be pinocytosed. This may result in a greatly reduced osteolytic promotion potential for a given wear volume. The surface roughness of the articulating components has a profound influence over the amount and size of wear debris produced. This that we shall be discussed in Section 5.4.3.

5.4   Surface Topography

5.4.1   Femoral Head Topography

In this section we will discuss the changes observed in the femoral head roughness. An attempt to compare these values with those of other researchers will be undertaken, but only after examining the difficulties that such a comparison experiences. Finally the mode of roughening of the heads will be discussed in the light of various joint parameters.

The unused femoral heads which were assessed for this study possess the supersmooth surfaces which will limit the potential for wear. Their S_{sk} value of -0.37, and their low initial roughness (median S_a 5.06nm) is much better than the standards set by British Standard BS 7251:Part 4 which requires an R_a of not greater then 50nm[241].

The joints assessed in this study retain very low values of roughness throughout their operational life with a median S_a value at revision of 10.35nm which is substantially less than the approved value (BS 7251) and only twice the value of unused PCA heads. To assess how the quality of the head as a bearing surface degrades, it is necessary to consider alternative roughness parameters (see Appendix 3). In terms of wear, the most damaging features will be those substantially above the mean plane. As such the parameter S_{peak} merits some attention. Whilst median S_a only increases two-fold over the unused heads, the median value of S_{peak} can be seen to increase five-fold. Clearly an asperity 100nm in height has considerable potential to cause wear, but this is an over-simplification of the situation. If the asperity is a single peak it will have less effect than if it is a scratch. A thorough investigation of the relationship of surface roughness parameters and the wear of the acetabular components is undertaken in Section 5.4.3.

The roughening of the PCA's CoCrMo femoral head is clearly discernible (Table 4.4) but how does it compare with other prostheses and head materials? In order to answer this question we must first have an appreciation of the difficulties involved with comparing the various published studies.

There are a number of different measurement techniques used to characterise surfaces. These where summarised in Section 2.5.3. Unfortunately due to the differing methods employed to obtain surface data, the results produced will vary subtlely. This produces a situation were the data from 2D contacting, 2D non-contacting and 3D non-contacting studies on exactly the same surface would be different[242]. To add further uncertainty the effects of observer bias must be considered. The selection of an area of the head to assess and the possibility of bias for, or against, specific features introduced by the operator is an additional source of error. With these limitations in mind, we may now compare the relevant literature.

A summary of the quantitative studies regarding the roughening of explanted femoral heads is given in Table 5.5. This highlights yet another source of ambiguity in the comparison of these studies. The duration of implantation may have an influence on the amount of surface degradation[147].

The study which bears the greatest resemblance to ours is that of Bauer *et al.*[183]. They used 3D non-contacting interference profilometer on CoCrMo femoral heads including a cohort from porous-coated cementless joints. They reported a median S_a value of 47nm, which is clearly much greater than the S_a value of 10.35nm obtained in this study in spite of a considerably shorter implant duration for their cohort.

The only other paper reporting 3D measurement is that of McGovern *et al.*[243] giving the mean S_a as 155nm. The implant durations in McGovern *et al.*'s paper are more in line with this study but the Ti-6Al-4V femoral head material behaves in a substantially different manner to the CoCrMo. The studies of Kusaba *et al.*[147] and Minakawa *et al.*[244] also highlight the influence that head material has on the degradation of the surface. Clearly the if head is made from a hard material then it will be more resistant to scratching. However the ductility of the material will effect the morphology of the scratch. A more ductile material will be capable of being "ploughed" leaving lips of material above the mean plane and hence dramatically increasing the wear potential of the surface. Conversely this does not happen with hard materials such as ceramics, material will be removed to form a scratch rather than be displaced. The influence of the parameters of lip height and aspect ratio have been the subject of work by McNie *et al.*[245].

Hall *et al.*[180], in their work concerning the 37 explanted Charnley joints, found that the median R_a and R_q values were three times greater in the *ex vivo* group. Wroblewski *et al.*[184] using a third measurement technique also report a rise in roughness for Charnley joints from an R_a of 19nm when new to 34nm when explanted. Why then is the damage caused to the Charnley so much more severe than the PCA femoral head?

The damage caused to the femoral head is almost certainly due to the presence of third body particles within the articulating region. In the case of the Charnley joint this will be cement debris. Isaac *et al.*[246] showed that the presence of hard radiopaque markers in the PMMA were capable of scratching stainless steel. Jasty *et al.*[182] in a qualitative study of CoCrMo femoral heads from both cemented and cementless

126

joints, attributed the scratching in both joint types to the presence of metallic third bodies. He cites the similar topography of the scratches between the two joint types as proof that the third body must be the same. This may not be the case, as discussed above the morphology of the scratch will be more dependent on the material properties of the metal rather than the third body.

PMMA debris is not present in the PCA system so an alternative source of hard third bodies must be identified. Possible candidates for the role of third bodies in the PCA system, in order of likelihood, are bone fragments, metallic wear debris, porous-coating beads and impurities within the UHMWPE. Bone fragments will be present around the joint both immediately after surgery and possibly in the longer term due to micromotion between the prosthesis and bone, especially once loosening is initiated. This micromotion would also be a source of metallic wear debris along with that released due to fretting corrosion at the femoral head taper[247,248]. The potential for damage to the head by bead ingression was treated in Section 5.1. Finally, hard bodies within the UHMWPE may exist due to the introduction of calcium stearate in the manufacturing process. This is included to help the polyethylene maintain its whiteness during processing. The amount which may be present will be very small and as such this is the least likely source of third body damage.

All of these alternative third bodies will reside in the joint environment of the PCA prosthesis in much lower numbers than the PMMA debris within a cemented joint. Therefore the cemented joints will possess a far greater potential for degradation of the articulating surfaces as revealed by the comparison of the various topographical studies.

Author	Head Material	Fixation Method	Implant Duration (months)	Cohort Size	Head Diameter (mm)	Measurement Instrument	Parameter Reported	Value (nm)
Bauer et al. 1994 [183]	CoCr	HA Porous Cemented	1-22 1-32 1-32	15 15 15	. . .	Zygo Laser 3D Interferometry	S_a	median 6.9, range (2-18) 47.0, (7.4-123) 35, (8.1-47) #
Drabu et al. 1994 [181]	Ti-6Al-4V	hybrid	36-96	18	.	2D contacting	R_a	median 32, range (23-84)
Hall et al. 1997 [180]	Stainless Steel	cemented	36-252	37	22	Rodenstock Laser 2D Interferometry	R_a R_q	median 62, iqrange (41-80) 95, (75-143)
Isaac et al. 1992 [144]	Stainless Steel	cemented	10-210	71	22	2D contacting	R_a	mean 53, range (13-400)
Kusaba et al. 1997 [147]	CoCr CoCr Alumina Alumina	cemented cemented cemented cemented	56-188 7-128 18-198 7-125	36 40 54 19	32 22 32 22	2D contacting	R_a	mean 23, SD 15 33, 102 11, 3 10, 2
McGovern et al. 1996 [243]	Ti-6Al-4V	cemented	64-155	16	28	Wyko 3D Interferometry	S_a	mean 155, SD 64
Minakawa et al. 1998 [244]	Stainless steel CoCr Ti Alumina Zirconia	cemented cemented cem. & uncem. cem. & uncem. cem. & uncem.	mean 174 173 - 57 41	10 10 7 10 8	22	2D contacting	R_p	mean 68 56 241 18 35
Wroblewski et al. 1992 [184]	Stainless Steel	cemented	204-276	4	22	2D contacting	R_a	median 31, range (8-102)

Table 5.5:   Summary table of quantitative femoral surface roughness studies. # - not as quoted in study, modified due to assumed typographical error.

5.4.2 Liner Topography

The most immediately discernible change in the topography of the 'mature' retrieved liner was the formation of a very polished, smooth region where the head had worn into the UHMWPE. The principal wear mechanism in operation in this region of the mature liner is believed to be microscopic adhesion (microadhesion) between the asperities of the femoral head and the polyethylene. The rippled appearance of the surface at very high magnification (Figures 4.20 & 4.21) is similar to that described by Schallamach[112] in his studies investigating the interaction between single asperities and elastomers. When using blunt indentors, or low loads, a raised lip is formed ahead of the asperity as it traverses the surface, no material is removed but the residual plastic strains from the lip remain as short wavelength ripples in the surface. In the situation in which we are interested the cyclical nature of the articulation produces incremental plastic strains resulting in fatigue failure, and detachment of a portion of the ripple[114].

The creation of a smooth polymer surface may itself influence the tribological conditions in which the joint operates and the friction, and wear, of the polyethylene may be reduced. The clinical studies of Jasty et al.[145] and Önsten et al.[226] showed a biphasal wear rate with a higher wearing-in period followed by a steady-state situation in which the rate of wear did not change. This phenomenon has also been observed in simulator studies[217,249]. Similarly, the friction measured in a series of joints after 5 million cycles in a wear simulator was lower than when new[218]. This may be due to the more rapid recruitment of asperities to share the load which is possible when those asperities are of a more uniform height. The higher asperities therefore become less highly loaded and hence less prone to adhesion of the contacts.

In the ridge region (2) the peaks display a very different surface morphology to those of the surrounding low lying areas. The extruded texture of the peaks (Figure 4.23) suggests that this is due to the adhesion of these asperities to the metallic counterface, resulting in the drawing out of material until fracture releases it from its attachment. The texture of the low lying areas seems to be the result of a more intermittent, and lower stress, contact where the material does not become adherent to the counterface. Instead it is rubbed and this creates the roughened appearance of this surface under high-powered microscopy (Figure 4.24).

What is the reason behind the two contrasting wear modes of the worn and border regions? If we consider the biphasal nature of the tribology of the hip prosthesis, which the work of Wroblewski et al.[217] and Smith et al.[216] suggests, we may find a possible answer. The initial wear of the prosthesis, or the wearing-in period, may be characterised by the removal of the machining marks concurrent with a degree of material modification due to strain hardening of the UHMWPE. These very high peaks will be subject to substantial deformations in order to support the load. The ridges will be rapidly eroded through a combination of adhesion and fatigue. The inter-ridge areas will not contribute substantially to supporting the load and may only be subjected to intermittent, low stress, abrasion. This scenario, just described, bears many similarities to the ridge region, the ridge region may then be a snapshot of the wear processes involved during the wearing-in period.

Alternatively, the different wear modes may be due to the varied distribution of loads across the head. At the centre of the worn region the pressure under the head will be greater than that at the peripheries of its contact area. Thus the contact stress imposed upon the polymer asperities will vary. During normal articulation the contact stresses will not be sufficient to flatten the asperities at the ridge region. Therefore the low-lying areas will only contact occasionally creating the rubbed texture which is observed. The tops of the dominant asperities will wear adhesively as before. As the socket is worn the ridge region will migrate away from the wear vector, thus creating fresh dominant asperities from the machining marks on which it is encroaching (Figure 4.31).

Macroscopic and Microscopic Wear

If we consider the hypothesis for macroscopic and microscopic mechanisms for the wear of UHMWPE proposed by Cooper et al.[250] we find that it fails to withstand rigorous scrutiny.

The analysis of *in vivo* wear debris has shown that the majority of wear particles are sub-micron in size[170,171], with a mode in the range 0.1-0.5μm[160]. However, the presence of large smooth platelets of 10-100μm in diameter has been observed in the case of wear of UHMWPE by supersmooth counterfaces[169]. It has been shown previously that the femoral head of the PCA prosthesis remains remarkably smooth

during its life. It may then be hypothesised that these particles would be produced by the *in vivo* articulation of the currently studied prostheses.

Cooper *et al.*[250] suggested that the large particles might be caused by the fatigue and detachment of long wavelength asperities from the surface. This theory relies on the stress levels in the asperity being large enough to fatigue the polyethylene before it is abraded. The topographical studies on which this theory is based state that "peaks with an amplitude of up to 10µm" are observed having a wavelength of approximately 200µm. Our studies show that the maximum peak height of the waviness has a median amplitude of 0.44µm and a range of wavelengths of the order of 100-300µm. The strains achieved in the undulations revealed by our studies would be lower in magnitude, hence a very large number of cycles would be needed to achieve the fatigue limit of the UHMWPE[227,229,251]. It is doubtful whether the fatigue limit would be approached prior to the removal of this material by microadhesion or abrasion. Cooper *et al.*'s wear model would also be self-limiting in that once the asperities have detached the surface would be devoid of any long wavelength asperities. Therefore the mechanism by which this mode of wear is created has been removed.

The treatment of UHMWPE as a homogenous continuum by Cooper *et al.*'s model may not be justified. As discussed previously the presence of intergranular defects in both finished components and the bulk UHMWPE prior to manufacture has been reported by many authors[200,201,232]. The microscopic investigation reported in Section 4.4.1 clearly shows the grain structure at the surface of the UHMWPE and thus the fatigue model of Cooper *et al.*, which does not exploit the intergranular weaknesses of the UHMWPE, must be limited.

The large particle dimensions are strikingly similar to those of the depressions seen in the topographical studies presented in this study (Figure 4.28). This suggests that the depressions observed are caused by the release of a platelet wear particle from the surface. The mechanism by which this would happen is illustrated in Figure 5.4. The bulk of the UHMWPE is removed by microadhesion or abrasion, creating the submicron sized wear particles. However, when only a portion of an individual grain remains it is vulnerable to fatiguing of the grain boundary region by a combination of Hertzian and shear stresses. The contribution of the Hertzian component of the fatiguing stress and the depth of the maximum stress are calculated in Appendix 6. As

can be seen this calculation assumes that the grain asperities have a truncated spherical shape that gives a maximum Hertzian stress of 9.21MPa approximately 10μm beneath the surface. The contribution of the shear stress from the motion of the joint will amplify the fatiguing effect of these stresses. This may result in the failure of the mechanical interlock between the grains. This amorphous region of the UHWMPE is known to be of a considerably lower strength than the ordered material within the grains. The fatiguing of the UHMWPE would facilitate the removal of the remaining portion of the grain by a plucking, or rolling, motion.

2. Weakened at the grain boundaries, the remanants of a grain are plucked from surface as a platelet.

1. Very smooth. Material removed through abrasion/adhesion. Fatiguing of material close to surface especially at grain boundaries.

3. Process of abrasion & platelet plucking leaves a polished surface with grain boundary cracks & occasional shallow depressions
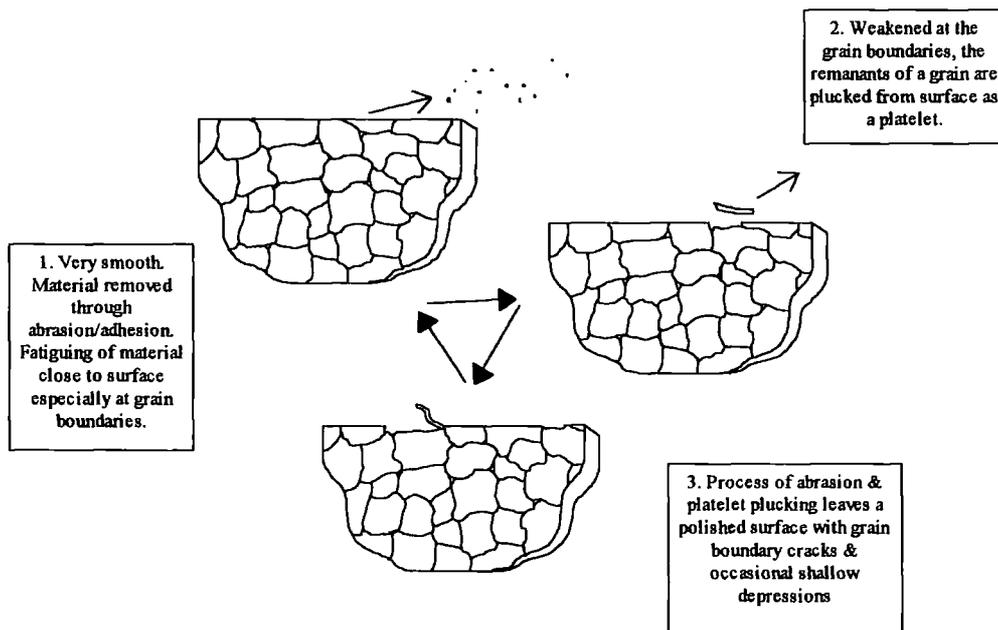
Figure 5.4:   Proposed wear mechanism. Diagram represents section through liner perpendicular to the articular surface. Not to scale.

The failure to observe the depressions in all the liners may reflect the random nature of the selection of sites assessed. This mode of wear may be restricted to a certain set of tribological conditions or region of the liner. Alternatively, the variation in the quality and granular integration of the UHMWPE could explain this phenomenon.

This model exploits the granular structure of the UHMWPE. By fatiguing the bulk material at its weakest point, it is capable of producing the surface topography observed and the wear debris predicted. This wear model whilst devised from observations on the wear features of THR may also be applicable to TKR. The level of agreement between the wear features presented in this thesis and the work published by Cornwall et al.[252] suggests that similar wear mechanisms may be

occurring in modern TKR tibial components. The level of shear and Hertzian stresses imposed on these components will exceed that of THR due to the incongruity of the bearing surfaces, this may result in a bias towards grain removal wear.

Correlation of Topographical Features

The lack of correlation between the surface topography of the femoral head and that of the liner may be attributable to sampling errors. An inherent source of error in all assessments of roughness is the assumption that the entire surface has the same topography as the small sample area that is selected. This is very unlikely to be the case but by using a reasonable number of sample sites across the worn region the effect of this error will be minimised. The failure of the *ex vivo* data to reveal any relationship between the surface topography of the femoral heads and that of the liners may then be an artefact of the small sample areas used when assessing the topography.

5.4.3 The Influence of Femoral Head Roughness on UHMWPE Wear

Turning to the relationship between the roughness of the femoral head and the wear of the acetabular component, the investigation into Dowson *et al.*'s[116] relationship yielded similar values to those obtained when re-analysing the data of Atkinson *et al.*[136] (see Table 5.6). The values of the exponent found using Atkinson's data and those of this study do not vary significantly from zero, suggesting that no relationship between S_a and $k_{clinical}$ exists.

	$a \times 10^{-6}$	b	R^2
Atkinson *et al.* [136]	1.5 (SE 1.9)	-0.23 (SE 0.36)	0.050
Hall *et al.* [142]	9.7 (SE 6.0)	0.54 (SE 0.23)	0.140
this study	4.1 (SE 4.2)	-0.30 (SE 0.31)	0.027

Table 5.6: Constants of the Dowson model (Equation 2.3).

This result may be an anomaly as a result of the inability of the parameter S_a to distinguish between damaging peaks and harmless valleys. It is known that the further the surface deviates from a Gaussian distribution then averaging parameters such as S_a and S_q become increasingly poor predictors of wear performance. The alternative

roughness parameters S_k and S_{pk} were used in equation (2.3) to establish if these could better predict the wear performance but the results were not improved. Similarly the lack of correlation could be attributable to the effect of the sampling errors discussed previously in Section 5.4.2.

An alternative explanation for the lack of any correlation could be that we are comparing two temporally variant parameters. The calculated clinical wear factor is necessarily a mean for the entire life of the prosthesis. It has been shown that the rate of wear varies over the life of the prosthesis[216,217]. The mean value of clinical wear factor for the life of the prosthesis may not equate to the value just prior to revision. In contrast, the roughness data recorded were all end-term values. Kusaba et al.[147] reported a linear relationship between the roughness of the femoral head and the duration of implantation, albeit weak ($R^2=0.20$). This would imply that the roughening of the prosthesis is a gradual process. No such relationship could be found for this dataset and as such it is likely that the heads roughened in a discrete event. However, there is no way to establish when the degradation in surface roughness occurred. It may have been on implantation when there was the possibility of bone debris entering the articulating capsule due to the preparation of the bone surfaces for the implant. However, it may equally have been as an end event due to the release of third bodies produced by the loosening of the prosthesis just prior to failure, creating bone or metal debris.

These problems also apply to Wang et al.'s model. Further, in Wang et al.'s[118] theoretical relationship, the inclusion of material parameters for the UHMWPE introduces a further variable. It is known that the material properties of the UHMWPE vary during time in vivo. This was not compensated for in the testing of Wang et al.'s model as the contribution of this phenomenon to any error was considered to be small.

Laboratory evidence of a relationship between roughness and wear is strong[116,118-120]. However, this relationship is not found to hold for explanted joints. The inability to substantiate any of the models may be due to a combination of the above reasons. Also other patient factors such as lifestyle, medical history etc. will contribute another source of error in the prediction of the parameters N and $k_{clinical}$. However the models themselves may be subject to criticism. Consider Dowson et al.'s[116] model. The

134

values for the constants in equation 2.3 were found experimentally using reciprocating pin-on-plate testing with water lubricant. Clearly neither of these conditions reproduce those found in the clinical joint environment. Further the range of counterface roughness values used in the laboratory tests were considerably greater than those of the explanted heads. Similarly Wang *et al.*'s[118] theoretical relationship is based upon the supposition that the motion is of a reciprocating nature. The experimental work presented to support the model, in addition to that of Weightman & Light[119], shows that the model is indeed applicable to a unidirectional wear regime.

The data presented in this study, and that of Atkinson *et al.*[136] suggests that simple unidirectional models are not applicable to the complex tribological environment of the artificial hip joint. A number of studies have elucidated the vastly greater wear factors produced by hip simulators configured to run with physiological motion when compared to reciprocation[114,122,124].

As mentioned in Section 2.4.2 Wang *et al.*[253] have themselves acknowledged the limitations of their early theoretical roughness/wear model. They have superseded their model by using a MTS hip simulator to create motion more akin to that of the physiological joint. Their paper presents the empirical relationship

$$k_{wear} = 7.21 \times 10^{-6} \left(R_a \right)^{0.42} \qquad (5.2)$$

where k_{wear} is the wear factor expressed in mm^3/Nm. Whilst this work attempts to reflect the true nature of the relationship between the roughness and the wear *in vivo* it may be criticised on a number of levels. The motion of the MTS simulator is indeed multi-directional but it is not truly physiological. The importance of this subtle distinction is the subject of some debate in the research community. Similarly the twelve femoral heads used in the simulator were artificially roughened. Whilst Wang *et al.* ensured that these scratches were multidirectional it would not be possible to replicate the complex scratching found on explanted heads perfectly. The final criticism of Wang *et al.*'s study may be the most damning. The decision to terminate their wear test at 1 million cycles is misguided. As mentioned previously there is a definite wearing-in period associated with these joints. Smith *et al.*[216] have shown this to be relevant for the first two million cycles of a simulator test. Consequently Wang *et al.*'s results do not represent the mature joint *in vivo*. Notwithstanding this Wang

et al.'s study shows with no uncertainty the importance of multidirectionality on the rate of wear.

A similar study to that of Wang *et al.* was conducted at Durham albeit on a smaller scale. Three explanted femoral heads were tested in the Mk.1 Durham Hip Wear Simulator to 5 million cycles. Detailed descriptions of the experimental procedure and results are given in Smith *et al.*[216] and Elfick *et al.*[254]. The summarised results can be seen in Table 5.7 and Figure 5.5. The three explanted heads showed no sign of a wearing-in period, or rather the wearing-in period was far shorter than that of the smooth heads. This suggests that Wang *et al.*'s results for the rougher heads may be considered to be representative of the mature case. However the results for the smoother heads will be greater than those for the mature situation. It can be speculated then that the exponential of Wang *et al.*'s empirical model may be an underestimate of the relationship for the mature joint situation.

Returning to the results of the Durham wear simulation, it can be seen from Table 5.7 that the *in vitro* wear greatly exceeds the mean wear rate for the *in vivo* period. If the explanted head roughness is capable of wearing the UHMWPE at this accelerated rate then it is certain that this roughness did not exist for the majority of the joint's life. Further from Figure 5.5 it can be seen there seems to be a relationship between the roughness and the simulator wear rate.

The results provide strong evidence to support the earlier hypothesis that the roughness at revision is not representative of that responsible for the wear of the joint for the majority of its life. A regression was performed in order to create a best fit curve for this data (Figure 5.5). It was found to have the equation

$$\frac{\Delta V}{\Delta N} = 13.46 \times \left(S_q\right)^{0.552} \qquad (5.3)$$

where $\Delta V/\Delta N$ is the wear volume per cycle. The coefficient of determination of the regression was $R^2 = 0.951$.

Parameter	A	B	C
Ex vivo Details			
Gender	f	f	m
Weight (kg)	55	51	59
Age at Primary (yrs)	30.7	32.8	73.9
Implant Duration (days)	1546	1869	475
Primary Diagnosis	CDH	CDH	RA
Joint Type	PCA	PCA	Ultima, J & J
Wear Volume (mm^3)	189.3	173	30.8
Est. No. of Cycles (10^6)	7.35	11.0	1.13
Ex vivo wear rate (mm^3/10^6)	25.8	15.7	27.3
In vitro Results			
Median S_q Before Test Worn / Periphery (nm)	47.14 / 2.98	88.16 / 5.19	57.28 / 9.02
Median S_q After Test Worn / Periphery (nm)	48.46 / 3.65	96.11 / 5.38	45.46 / 6.81
Sim. Wear Rate (mm^3/10^6)	103.7	149.5	120.4

Table 5.7: Summarised results of *ex vivo* and simulator testing of wear/roughness relationship.
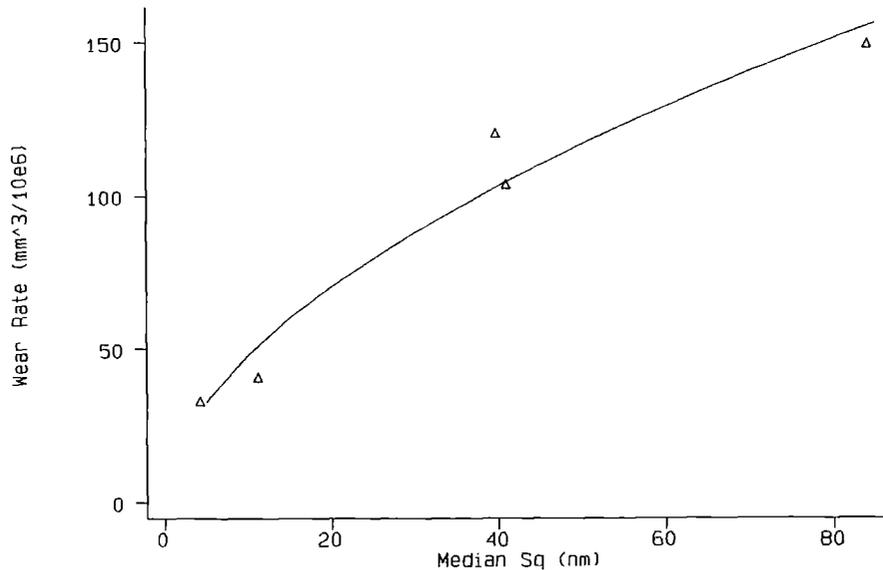
Figure 5.5: Plot of wear rate by head roughness for simulator study. This includes data points from a previous simulator study using new CoCrMo and zirconia heads[216].

Caution must be exercised in the interpretation of this result. There are too few points to be able to present this as an absolute model of polymer wear. However the value of the exponent is strikingly similar to that deduced by Hall *et al.*[142] using a large Charnley cohort (see equation 5.4).

$$k_{clinical} = 9.7 \times 10^{-6} (R_a)^{0.54}$$ (5.4)

However as reported in Section 4.4.3 no relationship between roughness and clinical wear factor for the PCA prosthesis. The lack of agreement between this study and Hall *et al.*'s[142] work on Charnley joints may be explained if the roughening of the heads occurred at different times during the two different joints' lives. Consider the fixation techniques used, suppose the cemented Charnley releases cement debris shortly after implantation, roughening the head in a discrete event early during the joint's life. The joint will thereafter wear at the rate predicted by equation 5.3, making it possible for Hall *et al.*[142] to derive the relationship in equation 5.4. Conversely the cementless PCA prosthesis may not release significant quantities of third bodies until the joint becomes loose at the end of its life. The roughness when explanted would then have little relationship with the mean wear for the joint's life as found for the present cohort. In both these cases the roughness of the femoral head will not possess any association with implantation period. This was the case for the Charnley retrievals of Hall *et al.*[179], the titanium heads of McGovern *et al.*[243] and the present study (see Section 4.4.2). However Kusaba *et al.*[147] did report a weak relationship between roughness and implantation time for a mixed group of joints with CoCrMo femoral heads.

We have now substantiated that the head roughens during its use and this is an end weighted effect. As discussed earlier there is simulator and clinical data to support the claim that there is a wearing-in period during which rapid removal of UHWMPE takes place. However the clinical data comes from radiographic studies that are known to be error prone. An alternative source of information on clinically well functioning joints are post-mortem studies. A re-analysis of the data presented by Jasty *et al.*[145] and Sychterz *et al.*[149] to yield clinical wear factors gives the result shown in Figure 5.6. There is a clear trend towards reduction in clinical wear factor with time for both of these studies.
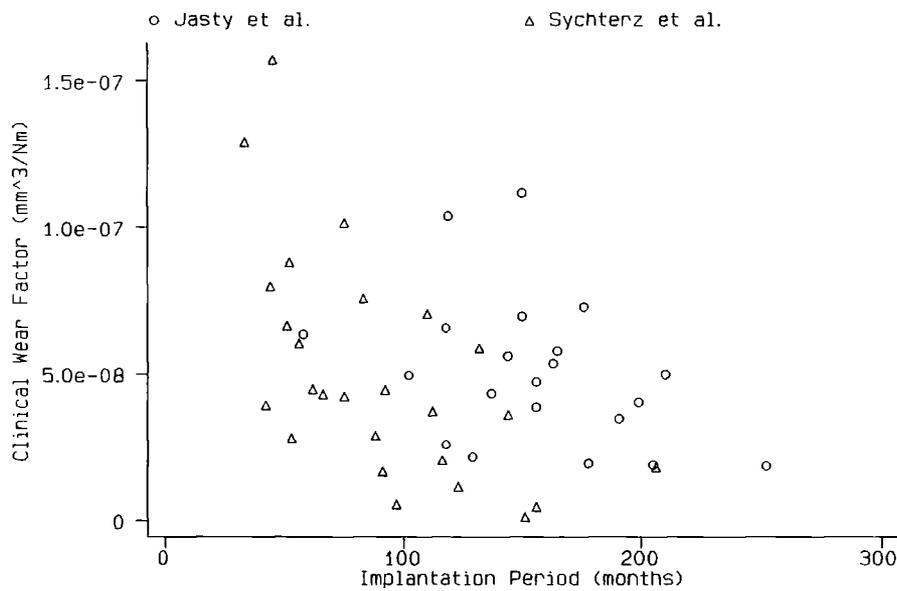
Figure 5.6:   Clinical wear factors calculated from the data of Jasty *et al.*[145] and Sychterz *et al.*[149]. Note low values in comparison to those reported for explant studies[136,142]. Also there is a decreasing trend with implantation period.

There is then considerable variation in the wear rate of the UHMWPE liner during the lifetime of a THR. After a early period of wear, topographical and material changes create a gradual reduction in the wear rate. As the joint matures the wear rate will stabilise and may start to increase as the surface finish of the head slowly degrades. Wear will continue at this pace until a loosening event takes place. In the long-term this loosening event is likely to coincide with the onset of osteolysis due to the critical volume of wear debris being achieved. As discussed previously this volume will vary from patient to patient depending on their tolerance to, and transport of, the wear debris. The loosening event will release third bodies that will act to greatly increase the roughness of the femoral head. This occurrence of a single late roughening event serves to explain the lack of any correlation between the explant roughness and the *in vivo* wear rate. A summary of the changes in wear behaviour of a typical joint may be summarised as seen in Figure 5.7.

139
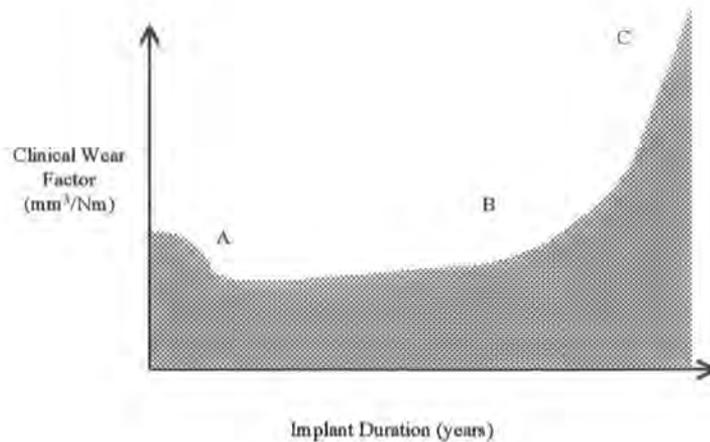
Figure 5.7:   Hypothetical variations in the wear behaviour of a THR. After an initial wearing-in period (A), the joint wears stably until (B) were a roughening event takes places. The wear rate at (C) bears little resemblance to that of the majority of the joint's life.

5.5   *Crystallinity Study*

The small series of experiments conducted concerning the change in crystallinity of the UHWMPE may best be regarded as a pilot study. It is known that irradiation, and oxidation, affects the crystallinity of the UHWMPE[196,227,232]. What is yet to be established is the effect that the tribological environment in which the prostheses operate has on the crystallinity.

The investigation of both irradiated, and non-irradiated, raw polyethylene from the same production batches shows that the process of irradiation increases crystallinity. This is widely reported in literature[198,229]. This rise is due to the scission of the polymer chains which occurs, allowing greater alignment. It is believed that the environment in which the UHMWPE is irradiated has influence. The absence of oxygen during irradiation has been shown to promote cross-linking of the polymer chains as opposed to their scission[197,228].

As discussed in Section 5.3, changes in crystallinity are accompanied by changes in the material properties of the UHMWPE. These result in the more rapid wear of the polyethylene. Similarly changes in hardness may be due to alternative mechanisms such as strain hardening. The action of the cyclic strains imposed upon the socket at the articular surface may act to harden a shallow layer of the UHMWPE. It may be that this material change will influence the wear behaviour, such as contributing to the wearing-in phenomenon. The investigation of this phenomenon using DSC of wear

debris and microhardness testing of the immediate subsurface region is proposed as future work.

5.6   *Wear Debris - Case Studies*

The use of the LALLS particle analyser offers a considerable improvement in the quality of information which wear debris retrieval studies may provide. The case studies presented in this thesis show the advantages offered by this method.

The minimum particle size reported by the instrument was $0.49\mu m$ for all the tissue samples. This is an artefact of the lower cut-off of the machine and testifies to the presence of particles below this limit. An instrument capable of detecting particles within the size range $0.02\text{-}2000\mu m$ has superseded the machine used for this case study. This promises the detection of particles currently lost to all wear debris studies.

The number median diameter of the particles was constant at approximately $0.7\mu m$ with the exception of one sample. This value is similar to those predicted by analysis of SEM micrographs of retrieved debris. Similarly the value is comparable to those reported by other groups (see Table 2.6). However the mean equivalent volume diameter varied between $10.12\mu m$ and $249.69\mu m$. This is as a result of the small contribution to the total wear debris volume made by the millions of submicron sized particles in comparison to the tens of particles greater than $10\mu m$ is size.

The variation in particle size distribution between the three samples taken at various sites around a single prosthesis (case A) suggests that there may be a variation in the mobility of particles. Alternatively this could be a non-systematic variation. The use of the particle analyser eliminates the possibility that this is due to sampling error during the assessment of the particles.

Clearly it is not possible to draw any firm conclusions about the size distribution, mobility or osteolytic potential of the wear debris from this brief study. However the development and validation of a highly profitable procedure has been illustrated. Further development of this method will allow the retrieval and characterisation of metallic and PMMA wear debris.

6. Conclusion

Production of the PCA THR as described in this study has recently been discontinued and, as such, any recommendations for its use are no longer pertinent. This does not however detract from the lessons that can be learnt from the study of its tribology. Here the conclusions are distilled from the Discussion Section and presented in order of merit.

- There is a level of agreement between various prosthesis types in the total wear volume at explant. This invites the hypothesis that there is a threshold wear volume of approximately 400-600mm^3 above which loosening due to osteolysis becomes likely (assuming a similar distribution of particle sizes from joint to joint).

- Large femoral head diameters create greater volumetric wear rates. The optimisation of prosthesis life expectancy requires the reduction of wear rates to delay the realisation of the threshold wear volume. Consequently femoral head diameters must be minimised to optimise joint life.

- Cemented fixation and metal-backing of acetabular components have no effect on the wear performance of THRs. Two qualifications to this statement are required. Firstly, an exception to this is where liner thickness is reduced to a point where total penetration, or fracture, becomes likely. A second exclusion is circumstances where the femoral head surface becomes damaged by cement ingression.

- The PCA THR system has been shown to perform well in terms of femoral head roughening. This is due to a combination of the lack of PMMA third bodies and the hardness of the CoCrMo head material.

- An alternative wear mechanism has been proposed. This mechanism is capable of creating the observed liner surface topography and of producing the expected wear debris.

- The application of unidirectional wear models, empirical and theoretical, to the multi-directional motion experienced by THRs has been shown to be fallacious. The influence of femoral head roughness on the rate of wear was investigated

using the Durham Hip Wear Simulator and a preliminary empirical model derived (seen below).

$$\frac{\Delta V}{\Delta N} = 13.46 \times \left(S_q\right)^{0.552}$$

(5.3)

This model requires further study before it may be presented as an absolute relationship. The simulator study undertaken, in conjunction with previous work, also provided evidence of the variation of wear during the life of the prosthesis. Three phases of wear were identified for cementless joints; a wearing-in period, a steady state period and an acceleration of wear as the consequence of a roughening event late in the joint's life. It is likely that the wear history of a cemented joint will show similar trends but with the super-imposition of an implant roughening event.

- A novel method of assessing wear particle size has been devised and validated. This method offers great improvements over existing techniques in terms of number of particles measured and the ease, cleanliness and hence accuracy with which the data can be obtained. This technique promises detailed, accurate and repeatable measurements over a range of sizes currently unachievable. Applications of this new process include the complete characterisation of *in vivo* and *in vitro* wear debris hence allowing direct comparison and validation of simulator machines for any joint type, be it hip, knee, finger etc. Further the understanding of the role of wear debris, the influence of particle size and debris concentration, on the pathogenesis of osteolysis may be advanced.

- The friction factors of explanted joints were found to be similar to those of unused joints. Frictional torque remained low and as such was not responsible for loosening. However, frictional torque may act to accelerate the failure of joints in which the fixation has been compromised for other reasons.

- The tendency for the original one-piece liners to dissociate from their metal backings or rotate about their pole within the backing suggests that the effects of the rotational torque were underestimated. The response to these problems was the introduction of the snaplock system. Whilst addressing the above difficulties and providing true modularity, these acetabular components introduced other

weaknesses. Patients requiring small acetabular components received joints where the UHMWPE thickness had been reduced to less than 2mm. This situation has been shown to be unacceptable. In future surgeons should be encouraged to employ smaller femoral head sizes, or use non-metal-backed components, whenever acetabular size limits polyethylene thickness.

- The direction of the penetration wear vector was found to lie lateral to the sagittal plane. The observed lateral angle of 17° in the coronal plane was substantially greater than that reported for the Charnley. Indeed there seemed to be a systematic variation between the penetration vector position depending on head size. The position of the penetration vector may be influenced by that of the JRF and the axis of rotation of the joint. However consideration of these two factors failed to account for the observed penetration vector. The influence of head size requires further investigation so that insight into the cause of the vector's lateral position may be gained.

7. References

1. Newman, K.J.H. (1993): Total Hip and Knee Replacements: a survey of 261 hospitals in England. Journal of the Royal Society of Medicine 86, 527-529.

2. Ries, M.D., Philbin, E.F., Graff, G.D., et al. (1997): Effect of Total Hip Arthroplasty on Cardiovascular Fitness. Journal of Arthroplasty 12, 84.

3. Barrack, R.L. (1995): Economics of Revision Total Hip Arthroplasty. Clin. Orthop. Rel. Res. 319, 209-214.

4. Wroblewski, B.M. (1990): Revision Surgery in Total Hip Arthroplasty. Springer-Verlag, London. 236 pages.

5. Charnley, J. (1960): Surgery of the Hip Joint, Present and Future Developments. Br. Med. J. i, 821-826.

6. Charnley, J., Follacci, F.M. and Hammond, B.T. (1968): The Long-Term Reaction of Bone to Self-Curing Acrylic Cement. J Bone Joint Surg 50B, 822-829.

7. Jasty, M.J., Floyd, W.E., Schiller, A.L., et al. (1986): Localised Osteolysis in Stable, Non-Septic Total Hip Replacement. J Bone Joint Surg 68A, 912-919.

8. Maloney, W.J., Jasty, M., Rosenberg, A., et al. (1990): Bone Lysis in Well-Fixed Cemented Femoral Components. J Bone Joint Surg 72B, 966-970.

9. Anthony, P.P., Gie, G.A., Howie, C.R., et al. (1990): Localised Endosteal Bone Lysis in Relation to the Femoral Components of Cemented Total Hip Arthroplasties. J Bone Joint Surg 72B, 971-979.

10. Santavirta, S., Hoikka, V., Eskola, A., et al. (1990): Aggressive Granulomatous Lesions in Cementless Total Hip Arthroplasty. J Bone Joint Surg 72B, 980-984.

11. Santavirta, S., Konttinen, Y.T., Bergroth, V., et al. (1990): Aggressive Granulomatous Lesions Associated with Total Hip Arthroplasty. J Bone Joint Surg 72A, 252-258.

12. Harris, W.H. (1995): The Problem Is Osteolysis. Clin. Orthop. Rel. Res. 311, 46-53.

13. Zicat, B., Engh, C.A. and Goken, E. (1995): Patterns of Osteolysis Around Total Hip Components Inserted With and Without Cement. J Bone Joint Surg 77A, 432-439.

14. Jones, L.C. and Hungerford, D.S. (1987): Cement Disease. Clin. Orthop. Rel. Res. 225, 192-206.

15. Lawrence, E. (1989): A Guide to Modern Biology: Genetics, Cells and Systems. Longman Scientific and Technical.

16. Gaudin, A.J. and Jones, K.C. (1989): Polyethylene Wear of Metal-Backed Tibial Components in Total and Unicompartmental Knee Prostheses. Harcourt Brace Jonanovich, Orlando. 868 pages.

17. Agins, H.J., Alcock, N.W., Sansal, M., et al. (1988): Metallic Wear in Failed Titanium-Alloy Total Hip Replacement. J Bone Joint Surg 70A, 347-356.

18. Bos, I., Fredebold, D., Diebold, J., et al. (1995): Tissue Reactions to Cemented Hip Sockets - Histologic and Morphometric Autopsy Study of 25 Acetabula. Acta. Orthop. Scand. 66, 1-8.

19. Schmalzried, T.P., Jasty, M. and Harris, W.H. (1992): Periprosthetic Bone Loss in Total Hip Arthroplasty: Polyethylene Wear Debris and the Concept of Effective Joint Space. J Bone Joint Surg 74A, 849-863.

20. Wang, J.Y., Tsukayama, D.T., Wicklund, B.H., et al. (1996): Metal Ions Interfere with Functions of Osteoblasts. Fifth World Biomaterials Congress,Toronto, Canada.

21. Voronov, I., Hinek, A., Callaghan, J.W., et al. (1996): Phagocytosis of Polyethylene Particulate by Macrophages In Vitro. Fifth World Biomaterials Congress, Toronto, Canada.

22. Howie, D.W., Manthey, B., Hay, S., et al. (1993): The Synovial Response to Intra-articular Injection in Rats of Polyethylene Wear Particles. Clin. Orthop. Rel. Res. 292, 352-357.

23. Chambers, T.J. (1978): Multinucleate Giant Cells. J. Pathol. 126, 125-148.

24. Schmalzried, T.P., Jasty, M., Rosenberg, A., et al. (1994): Polyethylene Wear Debris and Tissue Reactions in Knee As Compared to Hip Replacement Prostheses. J. App. Biomat. 5, 185-190.

25. Santavirta, S., Nordstrom, D., Metsarinne, K., et al. (1993): Biocompatibility of Polyethylene and Host Response to Loosening of Cementless Total Hip Replacement. Clin. Orthop. Rel. Res. 297, 100-110.

26. Jasty, M.J., Jiranek, W. and Harris, W.H. (1992): Acrylic Fragmentation in Total Hip Replacements and its Biological Consequences. Clin. Orthop. Rel. Res. 285, 116-128.

27. Murray, D.W. and Rushton, N. (1990): Macrophages Stimulate Bone Resorption When They Phagocytose Particles. J Bone Joint Surg 72B, 988-992.

28. Shanbhag, A.S., Jacobs, J.J., Black, J., et al. (1994): Macrophage/particle Interaction: Effect of size, composition and Surface Area. Journal of Biomedical Materials Research 28, 81-90.

29. Revell, P.A., Al-Saffar, N. and Kobayashi, A. (1997): Biological Reaction to Debris in Relation to Joint Prostheses. Proc. Instn. Mech. Engrs. 211, 187-197.

30. Athanasou, N.A. (1996): Cellular Biology of Bone-Resorbing Cells. J Bone Joint Surg 78A, 1096-1112.

31. Vaes, G. (1989): Cellular Biology and Biomechanical Mechanism of Bone Resorption: A Review of recent developments on the formation, activation, and mode of action of osteoclasts. Clin. Orthop. Rel. Res. 231, 239.

32. Green, T.R., Matthews, J.B., Stone, M., et al. (1998): Clinically Relevant UHMWPE Particles and Bone Resorption by Primary Macrophages. J Bone Joint Surg 79B:S4, 464.

33. Gelb, H., Schumacher, H.R., Cuckler, J., et al. (1994): In Vivo Inflammatory Response to Polymethylmethacrylate Particulate Debris: Effect of Size, Morphology and Surface Area. J. Orthop. Res. 12, 83-92.

34. Tabata, Y. and Ikada, Y. (1988): Effect of Size and Surface Charge of Polymer Microspheres on Their Phagocytosis by Macrophage. Biomaterials 9, 356-362.

35. Haynes, D.R., Rogers, S.D., Hay, S., et al. (1993): The Differences in Toxicity and Release of Bone-Resorbing Mediators Induced by Titanium and Cobalt-Chromium-Alloy Wear Particles. J Bone Joint Surg 75A, 825-834.

36. Maloney, W.J., Castro, F., Schurman, D.J., et al. (1991): Orthopaedic Implant Metallic Debris: Effects on Fibroblasts and Cartillage Cells. Trans. Orth. Res. Soc., 190.

37. Maloney, W.J., Smith, R.L., Castro, F., et al. (1993): Fibroblast Response to Metallic Debris In Vitro: Enzyme Induction, Cell Proliferation and Toxicity. J Bone Joint Surg 75A, 835-844.

38. Peters, P.C., Engh, A.C. and Merritt, K. (1991): Evaluation of Serum and Urine Cobalt, Chromium and Nickel Levels Eight Years Post Implantation of Extensively Porous Coated, Cementless Cobalt Chrome Total Hip Femoral Implants. Trans. Orth. Res. Soc., 224.

39. Dorr, L.D., Bloebaum, R., Emmanual, J., et al. (1990): Histologic, Biochemical and Ion Analysis of Tissue and Fluids Retrieved During Total Hip Arthroplasty. Clin. Orthop. Rel. Res. 261, 82-95.

40. Bendall, S.P., Radfar, A.J., Frondoza, C., et al. (1996): Metallic Wear Debris from Periprosthetic Tissue of Failed Arthroplasty Induces TNFa and IL-1a Release from Synoviocytes. Fifth World Biomaterials Congress.

41. Wang, W., Ferguson, D.J.P., Quinn, J.M.W., et al. (1997): Biomaterial Particle Phagocytosis by Bone-Resorbing Osteoclasts. J Bone Joint Surg 79B, 849-856.

42. Morrow, P.E. (1988): Possible Mechanisms to Explain Dust Overload of the Lungs. Fundamental Applied Toxicology 10, 369.

43. Amstutz, H.C., Campbell, P., Kossovsky, N., et al. (1992): Mechanism and Clinical Significance of Wear Debris-Induced Osteolysis. Clin. Orthop. Rel. Res. 276, 7-18.

44. Athanasou, N.A., Quinn, J. and Bulstrode, C.J.K. (1992): Resorption of Bone by Inflammatory Cells Derived From the Joint Capsule of Hip Arthroplasties. J Bone Joint Surg 74B, 57-62.

45. Pandey, R., Quinn, J. and Joyner, C. (1996): Arthroplasty Implant Biomaterial Particle Associated Macrophages Differentiate into Lacunar Bone Resorbing Cells. Ann. Rheum. Dis. 55, 388-395.

46. Willert, H.-G., Buchorn, G., Luederwald, I., et al. (1982): Influences of Special Features of Polymer Wear Particles on the Reacting Features Near Joint Replacements. Proceedings International Conference on Biomaterial Polymers, University of Durham.

47. NIH Consensus Statement.

48. Noble, J., Jones, A.G., Davies, M.A., et al. (1983): Leakage of Radioactive Particle Systems from a Synovial Joint Studied with a Gammma Camera. Its Approach to Radiation Synovectomy. J Bone Joint Surg 65A, 381-389.

49. Case, C.P., Langkamer, V.G., James, C., et al. (1994): Widespread Dissemination of Metal Debris from Implants. J Bone Joint Surg 76B, 701-712.

50. Goodfellow, J. (1992): Malignancy and Joint Replacement. J Bone Joint Surg 74B, 645.

51. Gillespie, W.J., Frampton, C.M.A., Henderson, R.J., et al. (1988): The Incidence of Cancer Following Total Hip Replacement. J Bone Joint Surg 70B, 539-542.

52. Langkamer, V.G., Case, C.P., Heap, P., et al. (1992): Systemic Distribution of Wear Debris After Hip Replacement. J Bone Joint Surg 74B, 831-839.

53.   Benz, E.B., Sherburne, B., Hayek, J.E., et al. (1996): Lymphodenopathy Associated with Total Joint Prostheses. J Bone Joint Surg 78A, 588-593.

54.   Willert, H.-G., Bertram, H. and Buchorn, G.H. (1990): Osteolysis in Alloarthroplasty of the Hip: The Role of Ultra-High Molecular Weight Polyethylene Wear Particles. Clin. Orthop. Rel. Res. 258, 95-107.

55.   Wroblewski, B.M. (1997): Wear of the High-Density Polyethylene Socket in Total Hip Arthroplasty and its Role in Endosteal Cavitation. Proc. Instn. Mech. Engrs., 211, 109-118.

56.   Aspenberg, P. and Van Der Vis, H. (1998): Fluid Pressure May Cause Periprosthetic Osteolysis. Acta. Orthop. Scand. 69, 1-4.

57.   Aspenberg, P. and Herbertsson, P. (1996): Periprosthetic Bone Resorption: Particles versus Movement. J Bone Joint Surg 78B, 641-646.

58.   Howie, D., Vernon-Roberts, B., Oakeshott, R., et al. (1988): A Rat Model of Resorption of Bone at the Cemented Bone Interface in the Presence of Polyethylene Wear Particles. J Bone Joint Surg 70A, 257-263.

59.   Anderson, G.B.J., Freeman, M.A.R. and Swanson, S.A.V. (1972): Loosening of the Cemented Acetabular Cup in Total Hip Replacement. J Bone Joint Surg 54B, 590-599.

60.   Hall, R.M., Unsworth, A., Wroblewski, B.M., et al. (1994): Frictional Characterisation of Explanted Charnley Hip Prostheses. Wear 175, 159-166.

61.   Hall, R.M., Unsworth, A., Wroblewski, B.M., et al. (1997): The Friction of Explanted Hip Prostheses. Brit. J. Rheum. 36, 20-26.

62.   Mai, M.T., Schmalzried, T.P., Dorey, F.J., et al. (1996): The Contribution of Frictional Torque to Loosening at the Cement-Bone Interface in Tharies Hip Replacements. J Bone Joint Surg 78A, 505-511.

63.   Hall, R.M., Siney, P., Unsworth, A., et al. (1998): Prevalence of Impingement in Explanted Charnley Acetabular Components. J. Orthop. Sci. 3, 204-208.

64.   Charnley, J. (1961): Arthroplasty of the Hip - A New Operation. Lancet 1, 1129-1132.

65.   Waugh, W. (1990): John Charnley: The Man and The Hip. Springer-Verlag, London.

66.   Charnley, J. (1979): Low Friction Arthroplasty of the Hip. Theory and Practice. Springer, Berlin Heidelberg New York.

67.   English, T.A. and Dowson, D. (1981): Total Hip Replacement. In: Introduction to the Biomechanics of Joints and Joint Replacements. (: Dowson, D. and Wright, V.) Mechanical Engineering Publications, London, 188-198.

68.   D'Aubigne, R.M. and Postel, M. (1954): Functional Results of Hip Arthroplasty with Acrylic Cement. J Bone Joint Surg 36A, 451.

69.   Wroblewski, B.M. and Siney, P.D. (1993): Charnley Low-Friction Arthroplasty of the Hip. Clin. Orthop. Rel. Res. 292, 191-201.

70.   Wroblewski, B.M. and Siney, P.D. (1992): Charnley Low-Friction Arthroplasty in the Young Patient. Clin. Orthop. Rel. Res. 285, 45-47.

71.   Shelley, P. and Wroblewski, B.M. (1980): Socket Design and Pressurisation in the Charnley Low-Friction Arthroplasty. J Bone Joint Surg 70B, 358.

72.   Wroblewski, B.M. (1993): Cementless Versus Cemented Total Hip Arthroplasty.
        Orthopaedic Clinics of North America 24, 591-597.

73.   Wroblewski, B.M., Fleming, P.A., Hall, R.M., et al. (1998): Stem Fixation in the Charnley
        Low-Friction Arthroplasty in Young Patients Using an Intramedullary Bone Block. J Bone
        Joint Surg 80B, 273-278.

74.   Howmedica (1982): Manufacturers Information Literature.

75.   Sletgaard, J. : The PCA Total Hip System. Acta. Orthop. Scand., 325-326.

76.   Sorbie, C., Duncan, C., Bourne, R., et al. : Canadian Experience with the PCA Porous
        Coated Cementless Hip Arthroplasty. J Bone Joint Surg S, 336.

77.   Malchau, H., Herberts, P., Lucht, U., et al. : Two Years' Experience of PCA Total Hip
        Replacement In Younger Patients. Acta. Orthop. Scand., 325.

78.   Heekin, R.D., Callaghan, J.J., Hopkinson, W.J., et al. (1993): The Porous-Coated Anatomic
        Total Hip Prosthesis, Inserted without Cement. J Bone Joint Surg 75A, 77-91.

79.   Callaghan, J.J., Dysart, S.H. and Savory, C.G. (1988): The Uncemented Porous-Coated
        Anatomic Hip Prosthesis. J Bone Joint Surg 70A, 337-346.

80.   Buckart, B.C., Bourne, R.B., Rorabeck, C.H., et al. (1993): Thigh Pain in Cementless Total
        Hip Arthroplasty. Orthopaedic Clinics of North America 24, 645-653.

81.   Campbell, A.C.L., Rorabeck, C.H., Bourne, R.B., et al. (1992): Thigh Pain After
        Cementless Hip Arthroplasty. J Bone Joint Surg 74B, 63-66.

82.   Weidenhielm, L.R.A., Kikhail, W.E.M., Nelissen, R.G.H.H., et al. (1995): Cemented
        Collarless (Exeter-CPT) versus Cementless Collarless (PCA) Femoral Components. Journal
        of Arthroplasty 10, 592-597.

83.   Maric, Z. and Karpman, R.R. (1992): Early Failure of Noncemented Porous Coated
        Anatomic Total Hip Arthroplasty. Clin. Orthop. Rel. Res. 278, 116-120.

84.   Owen, T.D., Moran, C.G., Smith, S.R., et al. (1994): Results of Uncemented Porous-Coated
        Anatomic Total Hip Replacement. J Bone Joint Surg 76B, 258-262.

85.   Kim, Y.-H. and Kim, V.E.M. (1993): Uncemented Porous-Coated Anatomic Total Hip
        Replacement. J Bone Joint Surg 75B, 6-13.

86.   Astion, D.J., Saluan, P., Stulberg, B.N., et al. (1996): The Porous Coated Anatomic Total
        Hip Prosthesis: Failure of the Metal-Backed Acetabular Component. J Bone Joint Surg 78-
        A, 755-766.

87.   Berry, D.J., Harmsen, W.S., Ilstrup, D., et al. (1995): Survivorship of Uncemented
        Proximally Porous Coated Femoral Components. Clin. Orthop. Rel. Res. 319, 168-177.

88.   Krismer, K., Stockl, B., Fischer, M., et al. (1996): Early Migration Predicts Late Aseptic
        Failure of Hip Sockets. J Bone Joint Surg 78B, 422-426.

89.   Brien, W.W., Salvati, E.A., Wright, T.M., et al. (1990): Dissociation of Acetabular
        Components After Total Hip Arthroplasty. J Bone Joint Surg 72A, 1548-1550.

90.   Ries, M.D., Collis, D.K. and Lynch, F. (1992): Separation of the Polyethylene Liner From
        Acetabular Cup Metal Backing. Clin. Orthop. Rel. Res. 282, 164-169.

91. Barrack, R.L., Burke, D.W., Cook, S.D., et al. (1993): Complications Related to Modularity of Total Hip Components. J Bone Joint Surg 75B, 688-692.

92. Engh, C.A., Massin, P., Suther, K.E. (1990): Roentgenographic Assessment of the Biologic Fixation of Porous Surfaced Femoral Components. Clin. Orthop. Rel. Res., 257, 107-128.

93. Karrholm, J., Boessen, B., Lowenhielm, G., et al. (1994): Does Early Micromotion of Femoral Stem Prostheses Matter? 4-7-year Stereoradiographic Follow-Up of 84 Cemented Prostheses. J Bone Joint Surg 76B, 912-917.

94. Krismer, K., Stockl, B., Sischer, M., et al. (1996): Early Migration Predicts Late Failure of Hip Sockets. J Bone Joint Surg 78B, 422-426.

95. Kim, Y.-H. and Kim, V.E.M. (1993): Early Migration of Uncemented Porous Coated Anatomic Femoral Component Related to Aseptic Loosening. Clin. Orthop. Rel. Res. 295, 146-155.

96. Learmonth, I.D., Smith, E.J. and Cunningham, J.L. (1997): The Pathogenesis of Osteolysis in Two Different Cementless Hip Replacements. Proc. Instn. Mech. Engrs. 211, 59-63.

97. Devane, P.A., Bourne, R.B., Rorabeck, C.H., et al. (1995): Measurement of Polyethylene Wear in Metal-Backed Acetabular Cups: II. Clinical Application. Clin. Orthop. Rel. Res. 319, 317-326.

98. Kim, Y.S., Brown, T.D., Pedersen, D.R., et al. (1995): Reamed Surface Topography and Component Seating in Press-fit Cementless Acetabular Fixation. Journal of Arthroplasty 10 Supp, S14-S21.

99. Ahmed, M., Bergstrom, J., Lundblad, H., et al. (1998): Sensory Nerves in the Interface Membrane of Aseptic Loose Hip Prostheses. J Bone Joint Surg 80B, 151-155.

100. Wolff, J. (1892): Das Gesetz der Transformation der Knochen. Quarto, Berlin.

101. Minuesa, A., Garcia-Cimbrelo, E. and Munuera, L. (1997): Bone Remodelling Changes in Two Cementless Femoral Stems: A Comparative Study with a Minimum Follow Up of 8 Years. J Bone Joint Surg 79(S2), 229.

102. Turan, S., Oken, O.F. and Oken, O.A. (1997): Bone Remodelling in the Proximal Femur After Cementless Total Hip Arthroplasty. J Bone Joint Surg 79B(S2), 229.

103. Gruen, T.A., McNeice, G.M. and Amstutz, H.C. (1979): "Modes of Failure" of Cemented Stem-Type Femoral Components. A Radiographic Analysis of Looseneing. Clin. Orthop. Rel. Res. 141, 17-27.

104. Gruen, T.A., Hedley, A.K., Borden, L.S., et al. (1991): Adaptive Remodelling Associated with Cementless Porous Coated Femoral Total Hip Replacement Components - Five Year Minimum Follow-Up Radiographic Analysis. 58th Annual Meeting Ammerican Academy of Orthopaedic Surgeons, Anaheim.

105. Bugbee, W.D., Culpepper, W.J., Engh, C.A., et al. (1997): Long-Term Clinical Consequences of Stress-Shielding After Total Hip Arthroplasty Without Cement. J Bone Joint Surg 79A, 1007-1012.

106. Rabinowicz, E. (1965): Friction and Wear of Materials. John Wiley & Sons Ltd, New York.

107. Arnell, P.D., Davies, P.B., Halling, J., et al. (1991): Tribology - Principles and Design Applications. Macmillan, London.

108. Davidson, J.A., Gir, S. and Paul, J.P. (1988): Heat Transfer Analysis of Frictional Heat Dissipation During Articulation of Femoral Implants. Journal of Biomedical Materials Research 22, 281-309.

109. Bergmann, G., Graichen, F. and Rohlmann, A. (1991): In Vivo Measurement of Temperature Rise in a Hip Implant. 37th Orth.Res.Soc., Anaheim, Calif.

110. Lancaster, J.K. (1990): Material-Specific Wear Mechanisms: Relevance to Wear Modelling. Wear 141, 159-183.

111. Brown, K.J., Atkinson, J.R., Dowson, D., et al. (1976): The Wear of Ultra-high Molecular Weight Polyethylene and a Preliminary Study of its Relation to the in vivo Behaviour of Replacement Hip Joints. Wear 40, 255-264.

112. Schallamach, A. (1952): Abrasion of Rubber by a Needle. J. Polymer Sci. 9, 385-404.

113. Briscoe, B. (1981): Wear of Polymers: An Essay on Fundamental Aspects. Tribology International, 231-243.

114. Wang, A., Stark, C. and Dumbleton, J.H. (1996): Mechanistic and Morphological Origins of Ultra-High Molecular Weight Polyethylene Wear Debris in Total Joint Replacement Prostheses. Proc. Instn. Mech. Engrs. 210, 141-154.

115. Archard, J.F. (1953): Contact and Rubbing of Flat Surfaces. J. Appl. Phys. 24, 981-988.

116. Dowson, D., Diab, M., Gillis, B., et al. (1985): Influence of Counterface Topography on the Wear of UHMWPE Under Wet or Dry Conditions. American Chemical Society, pp171-187.

117. Lancaster, J.G., Dowson, D., Isaac, G.H., et al. (1997): The Wear of Ultra-High Molecular Weight Polyethylene Sliding on Metallic and Ceramic Counterfaces Representative of Current Femoral Surfaces in Joint Replacement. Proc. Instn. Mech. Engrs. 211, 17-24.

118. Wang, A., Sun, D.C., Stark, C., et al. (1995): Wear Mechanisms of UHMWPE in Total Hip Replacements. Wear 181-183, 241-249.

119. Weightman, B. and Light, D. (1986): The Effect of the Surface Finish of Alumina and Stainless Steel on the Wear Rate of UHMWPE. Biomaterials 7, 20-24.

120. Rose, R.M., Cimino, W.R., Ellis, E., et al. (1982): Exploratory Investigations on the Structure Dependence of the Wear Resistance of Polyethylene. Wear 77, 89-104.

121. Elloy, M. (1993): Simulator Testing of Joint Prostheses: The Need for Realistic Simulator Testing. In: Proceedings SERC/IMechE Annual Expert Meeting on the Failure of Joint Prostheses. Mechanical Engineering Publications, London, 79.

122. Bragdon, C.R., O'Connor, D.O., Lowenstein, J.D., et al. (1996): The Importance of Multi-Directional Motion on the Wear of Polyethylene. Proc. Inst. Mech. Eng. 210, 157-165.

123. Fisher, J., Barbour, P.S.M., Besong, A.A., et al. (1997): Advanced Simple Configuration Tests. Technical Report Task 2.1 DTI CAM1 Project.

124. Smith, S.L. (1998): Unidirectional Hip Simulator Wear Testing. Personal Communication.

125. Unsworth, A., Pearcy, M.J., White, E.F.T., et al. (1987): Soft Layer Lubrication of Artificial Hip Joints. Proceedings International Conference on Tribology-Friction. Fifty Years On. Mechanical Engineering Publications.

126.   Unsworth, A. (1978): The Effects of Lubrication in Hip Prostheses. Phys. Med. Biol. 23, 253-268.

127.   Cooke, A.F., Dowson, D. and Wright, V. (1978): The Rheology of Synovial Fluid and Some Potential Synthetic Lubricants for Degenerate Synovial Joints. Proc. Instn. Mech. Engrs. 7, 66-72.

128.   Charnley, J. and Cupic, Z. (1973): The Nine and Ten Year Results of the Low-Friction Arthroplasty of the Hip. Clin. Orthop. Rel. Res. 95, 9-25.

129.   Charnley, J. and Halley, D.K. (1975): Rate of Wear in Total Hip Replacement. Clin. Orthop. Rel. Res. 112, 170-179.

130.   Clarke, I.C., Black, K., Rennie, C., et al. (1976): Can Wear in Total Hip Arthroplasties be Assessed From Radiographs. Clin. Orthop. Rel. Res. 121, 126-142.

131.   Wroblewski, B.M. (1985): Direction and Rate of Socket Wear in Charnley Low-Friction Arthroplasty. J Bone Joint Surg 67B, 757-761.

132.   Kabo, J.M., Gebhard, J.S., Loren, G., et al. (1993): In Vivo Wear of Polyethylene Acetabular Components. J Bone Joint Surg 75B, 254-258.

131.   Hall, R.M., Unsworth, A., Hardaker, C., et al. (1995): Measurement of Wear in Retrieved Acetabular Sockets. Proc. Instn. Mech. Engrs. 209, 233-242.

134.   Hall, R.M., Siney, P., Craig, P.S., et al. (1998): Discrepancy Between Penetration Depths Derived From Radiographic and Direct Measurement of Acetabular Components. Proc. Instn. Mech. Engrs. 212, 57-64.

135.   Hall, R.M. (1998): Radiographic Measurement of Wear in Total Hip Arthroplasty. Current Orthopaedics 12, 202-208.

136.   Atkinson, J.R., Dowson, D., Isaac, J.H., et al. (1985): Laboratory Wear Tests and Clinical Observations of the Penetration of Femoral Heads into Acetabular Cups in Total Replacement Hip Joints III: The measurement of internal volume changes in explanted Charnley sockets after 2-16 years in vivo and the determination of wear factors. Wear 104, 225-244.

137.   Cunningham, J.L., Bisbinas, I. and Learmonth, I.D. (1998): Factors Influencing the Repeatibilty and Reproducibility of Wear Measurement Using the Shadowgraph Technique. presented at B.O.R.S. Conference, Autumn 98, Dublin.

138.   Derbyshire, B. (1998): The Estimation of Acetabular Cup Wear Volume from Two-Dimensional Measurements: A Comprehensive Analysis. Proc. Instn. Mech. Engrs. 212, 281-291.

139.   Hashimoto, Y., Bauer, T.W., Jiang, M., et al. (1995): Polyethylene Wear in Total Hip Arthroplasty: Volumetric Wear Measurement of Retrieved Acetabular Components. Trans. Orth. Res. Soc. 20, 116.

140.   Cates, H.E., Faris, P.M., Keating, E.M., et al. (1993): Polyethylene Wear in Cemented Metal-Backed Cups. J Bone Joint Surg 75B, 249-253.

141.   Devane, P.A., Robinson, E.J., Rorabeck, C.H., et al. (1997): Measurement of Polyethylene Wear in Acetabular Components Inserted With and Without Cement: A Randomised Trial. J Bone Joint Surg 79A, 682-689.

142. Hall, R.M., Unsworth, A., Wroblewski, B.M., et al. (1996): Wear in Retrieved Charnley Acetabular Sockets. Proc. Instn. Mech. Engrs. 210, 197-207.

143. Hernandez, J.R., Keating, E.M., Faris, P.M., et al. (1994): Polyethylene Wear in Uncemented Acetabular Components. J Bone Joint Surg 76B, 263-266.

144. Isaac, G.H., Wroblewski, B.M., Atkinson, J.R., et al. (1992): A Tribological Study of Retrieved Hip Prostheses. Clin. Orthop. Rel. Res. 276, 115-125.

145. Jasty, M., Goetz, D.D., Bragdon, C.R., et al. (1997): Wear of Polyethylene Acetabular Components in Total Hip Arthroplasty: An Analysis of 128 Components Retrieved at Autopsy or Revision Operations. J Bone Joint Surg 79A, 349-358.

146. Kesteris, U., Ilchmann, T., Wingstrand, H., et al. (1996): Polyethylene Wear in Scanhip Arthroplasty With a 22mm or 32mm Head. Acta. Orthop. Scand. 67, 125-127.

147. Kusaba, A. and Kuroki, Y. (1997): Femoral Component Wear in Retrieved Hip Prostheses. J Bone Joint Surg 79B, 331-336.

148. Pedersen, D.R., Callaghan, J.J., Olejniczak, J.P., et al. (1995): Polyethylene Wear Rates for Five different In Vivo Acetabular Components Used Over a Five to Twenty-Two Year Period. 41st Annual Meeting, Orthopaedic Research Society, February 1995, Orlando Florida.

149. Sychterz, C.J., Moon, K.H., Hashimoto, Y., et al. (1996): Wear of Polyethylene Cups in Total Hip Arthroplasty. J Bone Joint Surg 78A, 1193-1200.

150. Woolson, S.T. and Murphy, M. (1995): Wear of the Polyethylene of Harris-Galante Acetabular Components Inserted without Cement. J Bone Joint Surg 77A, 1311-1314.

151. Derbyshire, B., Hardaker, C.S., Fisher, J., et al. (1994): Assessment of the Change in Volume of Acetabular Cups Using a Co-ordinate Measuring Machine. Proc. Instn. Mech. Engrs. 208, 151-158.

152. Clarke, I.C., Starkebaum, W., Hosseinian, A., et al. (1985): Fluid-sorption Phenomena in Sterilised Polyethylene Acetabular Prostheses. Biomaterials 6, 184-188.

153. McDonald, M.D. and Bloebaum, R.D. (1995): Distinguishing Wear and Creep in Clinically Retrieved Polyethylene Inserts. Journal of Biomedical Materials Research 29, 1-7.

154. Derbyshire, B., Fisher, J., Dowson, D., et al. (1994): Comparative Study of the Wear of UHMWPE with Zirconia Ceramic and Stainless Steel Femoral Heads in Artificial Hip Joints. Medical Engineering and Physics 16, 229-236.

155. Lee, J.-M., Salvati, E.A., Betts, F., et al. (1992): Size of Metallic and Polyethylene Debris Particles in Failed Cemented Total Hip Replacements. J Bone Joint Surg 74B, 380-384.

156. Margevicius, K.J., Bauer, T.W., McMahon, J.T., et al. (1994): Isolation and Characterisation of Debris in Membranes Around Total Joint Prostheses. J Bone Joint Surg 76A, 1664-1675.

157. Yamac, T., Kobayashi, A., Bonfield, W., et al. (1996): Extraction and Characterization of Metallic Wear Particles in Total Joint Replacements. Fifth World Biomaterials Congress.

158. Campbell, P., Doorn, P., Dorey, F., et al. (1996): Wear and Morphology of Ultra-High Molecular Weight Polyethylene Wear Particles from Total Hip Replacements. Proc. Instn. Mech. Engrs. 210, 167-174.

159. Kobayashi, A., Bonfield, W., Kadoya, Y., et al. (1997): The Size and Shape of Particulate Polyethylene Wear Debris in Total Joint Replacement. Proc. Instn. Mech. Engrs. 211, 11-15.

160. Tipper, J.L., Ingham, E., Hailey, J.L., et al. (1997): Quantitative Comparison of Polyethylene Wear Debris, Wear Rate and Head Damage in Retrieved Hip Prostheses. Trans. Orth. Res. Soc. 22, 355.

161. Hirakawa, K., Bauer, T.W., Stulberg, B.N., et al. (1996): Characterisation and Comparison of Wear Debris from Failed Total Hip Implants of Different Types. J Bone Joint Surg 78A, 1235-1243.

162. Soh (1996): Trans. Orth. Res. Soc. 21, 462.

163. Iwaki, H., Kobayashi, A., Kadoya, Y., et al. (1998): The Size, Shape and Number of PMMA Bone Cement Particles in Failed Total Joint Replacement. presented at B.O.R.S. Conference, Autumn 98, Dublin.

164. Fisher, J., Barbour, P.S.M., King, M.J., et al. (1997): Wear of Ultrahigh Molecular Weight Polyethylene in Artificial Joints: A New Approach to the Quantification of Wear Debris. 5th European Conference on Advanced Materials and Processes and Applications, 21st-23rd April, Maastricht.

165. Maloney, W.J., Smith, L., Schmalzried, T.P., et al. (1995): Isolation and Characterisation of Wear Particles Generated in Patients Who Have Had Failure of a Hip Arthroplasty without Cement. J Bone Joint Surg 77A, 1301-1310.

166. Kobayashi, A., Freeman, M.A.R., Bonfield, W., et al. (1997): Number of Polyethylene Particles and Osteolysis in Total Joint Replacements. J Bone Joint Surg 79B, 844-848.

167. Kadoya, Y., Kobayashi, A., Ohashi, H. (1998): Wear and Osteolysis in Total Joint Replacement. Acta. Orthop. Scand. 69(S278).

168. Stachowiak, G.W., Stachowiak, G.B. and Campbell, P. (1997): Application of Numerical Descriptors to the Characterisation of Wear Particles Obtained from Joint Replacements. Proc. Instn. Mech. Engrs. 211, 1-10.

169. Hailey, J.L., Ingham, E., Stone, M., et al. (1996): Ultra-high Molecular Weight Polyethylene Wear Debris Generated in vivo and in Laboratory Tests; The Influence of Counterface Roughness. Proc. Instn. Mech. Engrs. 210, 3-10.

170. McKellop, H.A., Campbell, P., Park, S.-H., et al. (1995): The Origin of Submicron Polyethylene Wear Debris in Total Hip Arthroplasty. Clin. Orthop. Rel. Res. 311, 3-20.

171. Shanbhag, A.S., Jacobs, J.J., Glant, T.T., et al. (1994): Composition and Morphology of Wear Debris in Failed Uncemented Total Hip Replacement. J Bone Joint Surg 76B, 60-67.

172. Sander, M. (1989): A Practical Guide to the Assessment of Surface Texture. Feinpruf GmbH, Gottingen. 118 pages.

173. Stout, K.J. and Blunt, L.A. (1995): Application of 3D Topography to Bio-Engineering. Int. J. Mach. Manufact. 35, 219-229.

174. Unsworth, A., Pearcy, M.J., White, E.F.T., et al. (1988): Frictional Properties of Artificial Hip Joints. Engineering in Medicine 17, 101-104.

175. English, T.A. and Kilvington, M. (1979): In Vivo Records of Hip Loads Using a Femoral Implant With Telemetric Output (A Preliminary Report). J. Biomed. Eng. 1, 111-115.

176. Dowson, D. and Wallbridge, N.C. (1985): Laboratory Wear tests and Clinical Observations of the Penetration of Femoral Heads into Acetabular Cups in Total Hip Joints I: Charnely Prostheses with Polytetrafluoroethylene Acetabular Cups. Wear 104, 203-215.

177. Wallbridge, N.C. and Dowson, D. (1982): The Walking Activity of Patients with Artificial Joints. Engineering in Medicine 11, 95-96.

178. Schmalzried, T.P., Szuszczewicz, E.S., Northfield, M.R., et al. (1998): Quantitative Assessment of Walking Activity after Total Hip or Knee Replacement. J Bone Joint Surg 80A, 54-59.

179. Hall, R.M., Unsworth, A., Siney, P., et al. (1996): The Surface Topography of Retrieved Femoral Heads. Journal of Material Science: Materials in Medicine 7, 739-744.

180. Hall, R.M., Siney, P., Unsworth, A., et al. (1997): The Effect of Surface Topography of Retrieved Femoral Heads on the Wear of UHMWPE Sockets. Medical Engineering and Physics 19, 711-719.

181. Drabu, K.J., Michaud, R.J., McCullagh, P.J.J., et al. (1994): Assessment of Titanium Alloy on Polyethylene Bearing Surfaces in Retrieved Uncemented Total Hip Replacements. Proc. Instn. Mech. Engrs. 208, 91-95.

182. Jasty, M., Bragdon, C.R., Lee, K., et al. (1994): Surface Damage to Cobalt-Chrome Femoral Head Prostheses. J Bone Joint Surg 76B, 73-77.

183. Bauer, T.W., Taylor, S.K., Jiang, M., et al. (1994): An Indirect Comparison of Third-Body Wear in Retrieved Hydroxyapatite-Coated, Porous and Cemented femoral Components. Clin. Orthop. Rel. Res. 298, 11-18.

184. Wroblewski, B.M., McCullagh, P.J. and Siney, P.D. (1992): Quality of the Surface Finish of the Head of the Femoral Component and the Wear Rate of the Socket in Long-Term Results of the Charnley Low-Friction Arthroplasty. Proc. Instn. Mech. Engrs. 206, 181-183.

185. Campbell, P., Ma, S., Schmalzried, T., et al. (1994): Tissue Digestion for Wear Debris Particle Isolation. Journal of Biomedical Materials Research 28, 523-526.

186. Campbell, P., Ma, S., Yeom, B., et al. (1995): Isolation of Predominantly Submicron-Sized UHMWPE Wear Particles From Periprosthetic Tissues. Journal of Biomedical Materials Research 29, 127-131.

187. Ford, T.C., Graham, J.M. (1991): An Introduction to Centrifugation. BIOS Scientific publishers Ltd. London.

188. Besong, A.A., Tipper, J.L., Ingham, E., et al. (1998): Quantitative Comparison of Wear Debris from UHMWPE That Has and Has Not Been Sterilised by Gamma Irradiation. J Bone Joint Surg 80B, 340-344.

189. Malvern (1998): Manufacturers Information Literature.

190. Hamilton, L.C. (1992): Regression With Graphics : A Second Course in Applied Statistics. Wadsworth Inc., Belmont, California. 363 pages.

191. Chatterjee, S. and Price, B. (1977): Regression Analysis by Example. John Wiley & Sons, Inc., New York. 228 pages.

192. Rawle, A. : The Principles of Particle Size Analysis. Malvern Instruments.

193. Malcolm, A.J. (1990): Pathology of Cemented Low-Friction Arthroplasties in Autopsy Specimens. In: Implant Bone Interface. (: Older, J.) Spring Verlag, London, 77-81. (N)

194. Bloebaum, RD., Milhaloulus, NL., Jensen, JW., et al. (1997): Postmortem Analysis of Bone Ingrowth into Porous Coated Acetabular Components. J Bone Joint Surg 79A, 1013-1022.

195. Hall, R.M., Siney, P., Unsworth, A., et al. (1998): Prevalence of Impingement in Three Types of Prostheses. J Bone Joint Surg 80B:S3, 273.

196. Sutula, L.C., Collier, J.P., Saum, K.A., et al. (1995): Impact of Gamma Sterilization on Clinical Performance of Polyethylene in the Hip. Clin. Orthop. Rel. Res. 319, 28-40.

197. Premnath, V., Harris, W.H., Jasty, M., et al. (1996): Gamma Sterilisation of UHMWPE Articular Implants: An Analysis of the Oxidation Problem. Biomaterials 17, 1741-1753.

198. Ries, M.D., Rose, R.M., Greer, J., et al. (1995): Sterilization-Induced Effects on UHMWPE Performance Properties. 62nd Meeting AAOS, Feb. 16-21, Orlando.

199. Collier, J.P., Sutula, L.C., Currier, B.H., et al. (1996): Overview of Polyethylene as a Bearing Material. Clin. Orthop. Rel. Res. 333, 76-86.

200. Li, S., Chang, J.D., Barrena, E.G., et al. (1995): Nonconsolidated Polyethylene Particles and Oxidation in Charnley Acetabular Cups. Clin. Orthop. Rel. Res. 319, 54-63.

201. Collier, J.P., Mayor, M.B., Surprenant, B.A., et al. (1990): The Biomechanical Consequences of Polyethylene as a Bearing Surface. Clin. Orthop. Rel. Res. 261, 107-113.

202. Yamaguchi, M., Bauer, T.W. and Hashimoto, Y. (1997): Three-Dimensional Analysis of Multiple Wear Vectors in Retrieved Acetabular Cups. J Bone Joint Surg 79A, 1539-1544.

203. Shardlow, D.L., Hailey, J.L., Ingham, E., et al. (1997): Fretting Wear of Charnley LFA Stems: Patterns of Wear and Clinical Significance. J Bone Joint Surg 79B S4, 458.

204. Kennedy, J.G., Rogers, W.B., Soffe, K.E., et al. (1998): Effect of Acetabular Component Orientation on Recurrent Dislocation, Pelvic Osteolysis, Polyethylene Wear and Component Migration. Journal of Arthroplasty 13, 530-534.

205. Hall, R.M., Siney, P., Unsworth, A., et al. (1998): Observations on the Direction of Wear in Charnley Sockets Retrieved at Revision Surgery. J Bone Joint Surg 80B, 1067-1072.

206. Knight, J.L., Atwater, R.D. and Guo, J. (1998): Clinical Results of the Midstem Porous-Coated Anatomic Uncemented Femoral Stem in Primary Total Hip Arthroplasty. Journal of Arthroplasty 13, 535-545.

207. Learmonth, I.D., Hussell, J.G. and Grobler, G.P. (1996): Unpredictable Progression of Osteolysis Following Cementless Hip Arthroplasty. Acta. Orthop. Scand. 67, 245-248.

208. Perez, R.E., Rodriguez, J.A., Deshmukh, R.G., et al. (1998): Polyethylene Wear and Periprosthetic Osteolysis in Metal-Backed Acetabular Components with Cylindrical Liners. Journal of Arthroplasty 13, 1-7.

209. Paul, J.P. (1967): Forces Transmitted by Joints in the Human Body. Proc. Instn. Mech. Engrs. 181, 8-15.

210. Bergmann, G., Graichen, F. and Rohlmann, A. (1993): Hip Joint Loading During Walking and Running, Measured in Two Patients. J. Biomech. 26, 969-990.

211. Johnston, R.C. and Smidt, G.L. (1969): Measurement of Hip-Joint Motion During Walking: Evaluation of a Electrogoniometric Method. J Bone Joint Surg 51A, 1083-1094.

212. Murray, D.W. and O'Connor, J.J. (1998): Superolateral Wear of the Acetabulum. J Bone Joint Surg 80B, 197-200.

213. Elson, R.A. and Charnley, J. (1968): The Direction of the Resultant Force in Total Prosthetic Replacement of the Hip Joint. Med. Biol. Engng. 6, 19-27.

214. McLeish, R.D. and Skorecki, J. (1968): Analysis of Wear in a Spherical Joint. Proc. Instn. Mech. Engrs., 1-4.

215. Bigsby, R.J.A., Hardaker, C.S. and Fisher, J. (1997): Wear of Ultra-High Molecular Weight Polyethylene Acetabular Cups in a Physiological Hip Joint Simulator in the Anatomical Position Using Bovine Serum Lubricant. Proc. Instn. Mech. Engrs. 211, 265-269.

216. Smith, S.L. and Unsworth, A. (1998): A Comparison Between Gravimetric and Volumetric Techniques of Wear Measurement of UHMWPE Acetabular Cups Against Zirconia and CoCrMo Femoral Heads in a Hip Joint Simulator. submitted to Proc. Inst. Mech. Eng., .

217. Wroblewski, B.M., Siney, P.D., Dowson, D., et al. (1996): Prospective Clinical and Joint Simulator Studies of a New Total Hip Arthroplasty Using Alumina Ceramic Heads and Cross-Linked Polyethylene Cups. J Bone Joint Surg 78B, 280-285.

218. Smith, S.L., Pifferi, S. and Unsworth, A. (1998): Friction Tests for Hips with Physiological Loading. Technical Report DTI CAM1 Project Task 3.4.

219. Hall, R.M., Siney, P., Unsworth, A., et al. (1998): The Association Between Rates of Wear in Retrieved Acetabular Components and the Radius of the Femoral Head. Proc. Instn. Mech. Engrs. 212, 321-326.

220. Saikko, V.S., Paavolainen, P.O. and Slatis, P. (1993): Wear of the Polyethylene Acetabular Cup - Metallic and Ceramic Heads Compared in a Hip Simulator. Acta. Orthop. Scand. 64, 391-402.

221. Besong, A.A., Bigsby, R.J.A., Barbour, P.S.M., et al. (1998): Effect of Head Size and Loading Regime on the Wear of UHMWPE Acetabular Cups in a Hip Joint Simulator. Abs. World Trib. Conf., 732.

222. Bragdon, C.R., O'Connor, D.O., Lowenstein, J.D., et al. (1998): Quantitative Comparison of Volumetric Wear Using 22mm, 26mm and 32mm Femoral Heads: A Hip Simulator Study. J. Biomech. 31 S1, 167.

223. Clarke, I.C., Gustafson, A., Jung, H., et al. (1996): Hip Simulator Ranking of Polyethylene Wear: Comparisons Between Ceramic Heads of Different Sizes. Acta. Orthop. Scand. 67, 128-132.

224. McKellop, H., Ebramazadeh, E., Lu, B., et al. (1995): Effect of Ball Material Diameter and Surface Roughness on the Wear of Polyethylene Acetabular Cups. Transcripts of the 21st Annual Meeting of the Society of Biomaterials, 45.

225. Manley, M.T. and Serekian, P. (1994): Wear Debris - An Environmental Issue in Total Joint Replacement. Clin. Orthop. Rel. Res. 298, 137-146.

226. Önsten, I., Carlsson, A.S. and Besjakov, J. (1998): Wear in Uncemented Porous and Cemented Polyethylene Sockets. J Bone Joint Surg 80B, 345-350.

227. Sauer, W.L., Weaver, K.D. and Beals, N.B. (1996): Fatigue Performance of Ultra-High Weight Polyethylene: Effect of Gamma Radiation Sterilization. Biomaterials 17, 1929-1935.

228. Goldman, M., Gronsky, R., Pruitt, L. (1998): The Influence of Sterilization Technique and Ageing on the Surface and Morphology of Medical Grade Ultra-High Molecular Weight Polyethylene. J. Mat. Sci.: Mat. in Med. 9, 207-212.

229. Ries, M.D., Weaver, K., Rose, R.M., et al. (1996): Fatigue Strength of Polyethylene After Sterilization by Gamma Irradiation or Ethylene Oxide. Clin. Orthop. Rel. Res. 333, 87-95.

230. Rose, R.M., Goldfarb, E.V., Ellis, E., et al. (1984): Radiation Sterilisation and Wear Rate of Polyethylene. J. Orthop. Res. 2, 393.

231. Evans, D.C. and Lancaster, J.K. (1973): . Wear 25, 155-170.

232. Li, S. and Burstein, A.H. (1994): Current Concepts Review: Ultra-High Molecular Weight Polyethylene. J Bone Joint Surg 76A, 1080-1090.

233. Parasnis, N.C., Ramani, K. (1998): Analysis of the Effect of Pressure on Compression Moulding of UHMWPE. J. Mat. Sci.: Mat. in Med. 9, 165-172.

234. Bartel, D.L., Burstein, A.H., Toda, M.D., et al. (1985): The Effect of Conformity and Plastic Thickness on Contact Stresses in Metal-Backed Plastic Implants. J. Biomed. Eng. 107, 193-199.

235. Bartel, D.L., Bicknell, V.L. and Wright, T.M. (1986): The Effect of Conformity, Thickness, and Materials on Stresses in Ultra-High Molecular Weight Components for Total Joint Replacement. J Bone Joint Surg 68A, 1041-1051.

236. Maxian, T.A., Brown, T.D., Pedersen, D.R., et al. (1996): 3-Dimensional Sliding/Contact Computational Simulation of Total Hip Wear. Clin. Orthop. Rel. Res. 333, 41-50.

237. Maxain, T.A., Brown, T.D., Pedersen, D.R., et al. (1997): Finite Element Analysis of Acetabular Wear. Clin. Orthop. Rel. Res. 344, 111-117.

238. Oonishi, H., Iwaki, H., Kin, H., et al. (1998): The Effects of Polyethylene Cup Thickness on Wear of Total Hip Prostheses. Journal of Material Science: Materials in Medicine 9, 475-478.

239. Oonishi, H., Tsuji, E. and Kim, Y.Y. (1998): Retrieved Total Hip Prostheses Part 1 The Effects of Cup Thickness, Head Size and Fusion Defects on Wear. Journal of Material Science: Materials in Medicine 9, 393-401.

240. Hall, R.M., Siney, P., Unsworth, A., et al. (1997): Optimum Femoral Head Size and Socket Loosening in Total Hip Arthroplasty. J Bone Joint Surg 79B S4, 464-465.

241. BSI (1990): British Standard - Orthopaedic Joint Prostheses. Part 2 & 4.

242. Hall, R.M., Elfick, A.P., Siney, P., et al. (1998): Levels of Agreement Between the Surface Roughness Values of Femoral Heads measured Using Two Different Optical Techniques presented at B.O.R.S. Conference, Autumn 98, Dublin.

243. McGovern, T.E., Black, J., Jacobs, J.J., et al. (1996): In Vivo Wear of Ti6Al4V Femoral Heads: A Retrieval Study. Journal of Biomedical Materials Research 32, 447-457.

244. Minakawa, H., Stone, M.H., Wroblewski, B.M., et al. (1998): Quantification of Third-Body Damage and Its Effect on UHMWPE Wear With Different Types of Femoral Head. J Bone Joint Surg 80B, 894-899.

245. McNie, C. et al. (1997): Technical Report 3.6: Stress analysis and prediction of UHMWPE caused by third body damage. DTI CAM 1 Project, Accelerated test methods to predict the durability of materials and surface treatments employed for total hip replacements.

246. Isaac, G.H., Atkinson, J.R., Dowson, D., et al. (1987): The Causes of Femoral Head Roughening in Explanted Charnley Hip Prostheses. Engineering in Medicine 16, 167-173.

247. Jacobs, J.J., Gilbert, J.L. and Urban, R.M. (1998): Corrosion of Metal Orthopaedic Implants. J Bone Joint Surg 80A, 268-282.

248. Collier, J.P., Surprenant, V.A., Jensen, R.E., et al. (1992): Corrosion Between the Components of Modular Femoral Hip Prostheses. J Bone Joint Surg 74B, 511-517.

249. Smith, S.L. and Unsworth, A. (1998): Surface Topography and Wear Rates of Zirconia and CoCrMo Femoral Heads Compared In Vitro. J Bone Joint Surg 80B:S3, 262.

250. Cooper, J.R., Dowson, D. and Fisher, J. (1993): Macroscopic and Microscopic Wear Mechanism in Ultra-High Molecular Weight Polyethylene. Wear 162-164, 378-384.

251. Huang, D.D. and Li, S. (1992): Cyclic Fatigue Behaviours of UHMWPE and Enhanced UHMWPE. Trans. Orth. Res. Soc., 403.

252. Cornwall, G.B., Hansson, C.M., Bowe, A.J., et al. (1997): Surface Degradation Features and Microstructural Properties of Ultra-High Molecular Weight Polyethylene. Journal of Material Science: Materials in Medicine 8, 303-309.

253. Wang, A., Polineni, V.K., Stark, C., et al. (1998): Effect of Femoral Head Surface Roughness on the Wear of Ultrahigh Molecular Weight Polyethylene Acetabular Cups. Journal of Arthroplasty 13, 615-620.

254. Elfick, A.P., Smith, S.L., Unsworth, A. : Variation in the Wear Rate During the Life of a Total Hip Replacement. submitted to J. Arth.

255. Dong, W.P., Sullivan, P.J., Stout, K.J. (1994): Comprehensive Study of Parameters for Characterising Surface Topography III: Parameters for Characterising Amplitude and Some Functional Properties. Wear 178, 29-43.

256. Timoshenko, S.P. (1970): Theory of Elasticity. McGraw Hill, Singapore.

Appendix 1- Patient Details

Patient Number	Sex	Side	Weight (kg)	Age at Primary	Age at Revision	Service Life (days)	Reason Primary	Reason Revision
0005193T	0	l	65	26.26	32.22	2177	cdh	p
0006761W	1	l	60	53.25	59.00	2099	ra	m
0007598X	1	l	57.7	58.70	69.56	3969	oa	m
0018244G	1	l	58	39.11	46.65	2753	ra	l
0018267L	0	l	90	38.21	39.35	414	ra	s
0020382T	1	l	76	22.01	30.97	3273	cdh	p
0023121X	0	l	87.7	33.45	36.19	1001	fnf	m
0027715R	0	r	73	55.74	62.29	2395	ra	m
0031985L	0	r	119	57.61	66.55	3263	oa	p
0044805E	1	r	51	32.79	37.91	1869	cdh	l
0047591U	0	l	76	54.84	66.09	4110	oa	l
0048208H.l2	1	l	49	48.12	49.26	414	ra	m
0048208H.l3	1	l	49	49.26	50.10	308	ra	m
0048208H.l4	1	l	49	50.10	53.10	1096	ra	m
0051035B	0	r	70	37.15	46.23	3317	oa	p
0055569R.r	1	r	81.8	60.00	68.63	3150	oa	p
0055569R.r2	1	r	81.8	68.63	69.88	457	oa	m
0061576W.l	1	l	54	25.95	28.74	1021	ra	m
0061576W.l2	1	l	53	25.95	28.74	1021	ra	m
0061576W.r	1	r	54	19.83	26.04	2269	ra	m
0061576W.r2	1	r	53	26.04	29.40	1226	ra	m
0063335L	1	r	65	52.28	60.49	2998	as	p
0065745H	1	l	58.8	27.79	33.88	2226	cdh	p
0066364W	0	l	80.7	49.62	56.98	2688	ra	m
0070268J	1	l	55	49.00	50.02	372	ra	p
0087617L	0	r	74.7	55.36	62.45	2590	oa	l
0090136A	1	l	59	53.62	67.21	4963	oa	w
0091161Y	0	l	71	44.05	50.57	2380	ra	m
0094223D	0	r	84.5	48.27	48.35	28	oa	m
0097018G	0	r	71	53.25	61.56	3032	oa	l
0104541E	0	r	75	43.94	56.25	4495	t	m
0104577B	0	l	60	38.80	48.84	3666	ra	l
0105366P.r	0	r	68	55.57	61.72	2247	ra	m
0105366P.r2	0	r	68	61.72	66.96	1913	ra	p
0106995J.l	0	l	69	51.18	60.75	3494	oa	m
0106995J.r	0	r	69	50.88	63.78	4712	oa	l
0108145W	1	r	45	54.03	64.88	3963	oa	m
0108824P	0	r	68	30.40	37.18	2477	as	p
0111698W	1	l	56.6	48.09	55.03	2536	ra	m
0112223M	1	r	76	57.71	66.15	3083	oa	w
0113827X	1	r	67.3	37.10	42.27	1887	oa	d
0114412R	0	r	80.8	54.00	67.77	4662	oa	l
0114903N.l	0	l	72	48.01	55.50	2736	oa	m
0114903N.r	0	r	72	55.09	60.18	1860	oa	.
0114903N.l2	0	l	72	47.87	55.66	2843	oa	m
0118153P	0	l	103	26.45	37.72	4117	oa	l
0121147E	1	r	55	30.69	34.92	1546	cdh	.
0122783H.r	0	r	73.1	47.07	58.93	4331	other	w

Patient Number	Sex	Side	Weight (kg)	Age at Primary	Age at Revision	Service Life (days)	Reason Primary	Reason Revision
0122783H.l	0	l	73.1	46.46	57.87	4166	other	w
0123170Q	0	r	106	60.38	71.37	4013	ra	l
0125831R.r2	0	r	83	42.70	44.37	609	.	m
0125831R.r3	0	r	83	44.37	45.46	399	.	s
0127109Y.l	0	l	73.7	63.10	74.77	4262	ra	w
0127109Y.l2	0	l	73.7	74.77	75.03	92	ra	d
0128086K	0	l	75	42.33	49.64	2671	cdh	m
0129768X	1	r	63.6	57.31	66.90	3501	oa	l
0134785Y	0	r	70	36.89	39.45	936	as	l
0135149D	0	l	84	15.81	21.98	2254	cancer	m
0137791E	1	r	61.5	32.15	32.17	5	ra	.
0142810J	0	l	67	30.14	38.48	3044	ra	p
0151185D	0	r	74.8	59.53	69.27	3556	oa	w
0152000P	1	r	44	63.24	74.31	4040	oa	l
0152602R	0	r	92	45.00	49.71	1717	oa	w
0153658H	1	r	67	59.91	66.85	2533	ra	m
0158318N	1	l	46.5	49.28	58.08	3214	ra	p
0163765G	0	r	73.2	49.66	57.02	2686	oa	l
0166280P	0	r	59	24.98	31.14	2251	ra	l
0166369H	0	l	97	45.50	54.28	3205	oa	m
0172585H	0	l	58.6	28.57	37.77	3360	av nec	w
0186485A	0	r	75	28.58	33.72	1877	ra	w
0188306N	1	l	64.2	75.51	80.09	1673	oa	p
0188366A	0	r	62.7	45.14	53.03	2883	av nec	w
0189957T	1	r	70.64	65.59	70.89	1939	cdh	m
0193742Y	1	r	67	19.58	24.72	1877	t	m
0196702T	1	l	88.6	25.11	37.20	2590	cdh	w
0200609K	1	l	91.3	43.73	49.02	1933	cdh	m
0208695Y	1	r	62	52.68	60.86	2989	oa	l
0210421U	1	r	57.6	28.13	30.89	1008	cdh	l
0219157P	1	r	75	63.67	69.13	1994	oa	w
0221458R	0	l	80	30.86	35.30	1622	t	l
0222386N	1	r	73	30.77	32.54	645	cdh	m
0222703S	1	r	40	38.15	38.15	2	dcp	d
0233254N	1	l	100	53.54	54.78	453	av nec	s
0244498J	0	r	87	41.82	42.36	198	oa	m
0264829K	0	r	98.6	22.64	23.48	306	oa	m
1334642J	1	r	52.3	49.27	58.40	3336	oa	l
1414968A	1	l	67.8	53.22	55.54	848	ra	p
1421193Q.l	1	l	57	17.89	23.89	2192	ra	m
1421193Q.r	1	r	57	17.91	24.52	2414	ra	l
1445098U	1	l	78	40.08	47.45	2691	oa	m
1479141N	1	r	59.4	28.22	30.65	888	oa	m
1492068X	0	r	87	37.44	43.42	2184	as	m
2007588N	1	r	70	36.80	44.56	2839	oa	w
2013560W	1	l	82	60.63	68.08	2720	oa	l
2083785X	0	r	86.6	43.44	43.79	130	av nec	m
B107423	0	r	83	58.54	60.80	827	oa	p
UA	.	.	.	.	.	.	.	.
UB	.	.	.	.	.	.	.	.
UC	.	.	.	.	.	.	.	.

Patient Number	Sex	Side	Weight (kg)	Age at Primary	Age at Revision	Service Life (days)	Reason Primary	Reason Revision
UD	.	.	.	.	.	.	.	.
UE	.	.	.	.	.	.	.	.
UF	.	.	.	.	.	.	.	.
UG	.	.	.	.	.	.	.	.
UH	.	.	.	.	.	.	.	.
UI	.	.	.	.	.	.	.	.
UJ	.	.	.	.	.	.	.	.
UK	.	.	.	.	.	.	.	.
UL	.	.	.	.	.	.	.	.
UM	.	.	.	.	.	.	.	.
UN	.	.	.	.	.	.	.	.
UO	.	.	.	.	.	.	.	.
UP	.	.	.	.	.	.	.	.
UQ	.	.	.	.	.	.	.	.
UR	.	.	.	.	.	.	.	.
US	.	.	.	.	.	.	.	.
UT	.	.	.	.	.	.	.	.
UV	.	.	.	.	.	.	.	.
UW	.	.	.	.	.	.	.	.
UX	.	.	.	.	.	.	.	.

Abbreviations:

oa	osteoarthritis
ra	rhuematoid arthritis
t	trauma
as	ankylosing spondylitis
av nec	avascular necrosis
cdh	congenital dysplasia of the hip
dcp	dyschondroplasia
other	other then causes listed above

Patient Number	Femoral Head Diameter	Joint Type	Fracture	Impingement	Internal Delamination	Internal Delamination	Ridge	Oxidation	Ingression	Dissociation	Rotation
0005193T	26	Snap	0	0	0	0	0	1	0	0	.
0006761W	32	One	0	1	1	1	1	1	0	0	0
0007598X	32	One	0	0	0	0	0	0	0	0	0
0018244G	32	One	0	0	1	1	1	1	1	0	0
0018267L	32	Snap	0	0	0	0	0	0	0	0	.
0020382T	32	Snap	1	0	0	0	0	0	0	0	.
0023121X	32	Snap	0	0	0	0	0	0	0	0	.
0027715R	32	Snap	0	0	0	0	0	1	0	0	.
0031985L	32	One	0	0	0	0	1	1	0	0	0
0044805E	28	Snap	0	0	0	0	0	0	0	0	.
0047591U	32	One	0	0	1	1	1	1	0	0	1
0048208H.l2	32	Snap	0	0	0	0	0	0	0	0	.
0048208H.l3	32	Snap	0	0	0	0	0	0	0	0	.
0048208H.l4	32	Snap	0	0	0	0	0	0	0	0	.
0051035B	32	One	0	0	0	0	1	1	0	0	0
0055569R.r	32	Snap	0	0	0	0	0	0	0	0	.
0055569R.r2	28	Snap	0	1	0	0	0	0	0	0	0
0061576W.l	32	One	0	1	1	1	0	0	0	0	.
0061576W.l2	32	Snap	0	1	0	0	0	0	0	0	1
0061576W.r	32	One	0	0	0	0	2	0	0	0	.
0061576W.r2	32	Snap	0	0	1	1	0	1	0	0	0
0063335L	32	One	1	1	0	1	2	1	0	0	0
0065745H	26	Snap	0	1	0	0	0	1	0	0	.
0066364W	32	Snap	0	0	0	0	0	0	0	0	1
0070268J	32	One	0	0	0	0	0	0	0	0	.
0087617L	32	One	0	0	1	1	1	1	0	0	1
0090136A	32	One	0	0	1	1	0	1	0	0	1
0091161Y	32	Snap	0	0	0	0	0	0	0	0	.
0094223D	32	Snap	0	0	0	0	0	0	0	0	.
0097018G	32	One	0	0	0	0	1	1	0	0	0

Patient Number	Femoral Head Diameter	Joint Type	Fracture	Impingement	Internal Delamination	Internal Delamination	Delamination	Ridge	Oxidation	Ingression	Dissociation	Rotation
0104541E	32	One	0	0	0	0	0	0	0	0	0	0
0104577B	32	One	0	0	0	0	0	0	1	0	0	0
0105366P.r	32	One	0	0	0	0	0	1	0		0	0
0105366P.r2	32	.	.	.	.	.	.	.	.	.	.	.
0106995J.l	32	One	0	0	0	0	0	0	1	0	0	0
0106995J.r	32	One	0	0	1	1	1	0	1	1	0	1
0108145W	32	One	0	0	1	1	1	1	1	0	0	1
0108824P	32	One	0	0	0	0	0	3	0	0	0	0
0111698W	32	One	0	1	0	0	0	1	1	0	0	0
0112223M	32	One	1	0	0	0	0	1	1	0	0	.
0113827X	32	Snap	0	1	0	0	0	0	0	0	0	1
0114412R	32	One	0	1	1	1	1	1	1	0	0	0
0114903N.l	32	One	0	1	1	1	1	2	1	0	0	0
0114903N.r	32	One	0	1	1	1	1	2	1	0	0	.
0114903n.l2	32	Snap	0	1	0	0	0	0	1	0	0	1
0118153P	32	One	0	0	1	0	0	1	0	0	0	1
0121147E	28	Snap	0	0	0	0	0	0	0	0	1	0
0122783H.r	32	One	0	0	0	0	0	0	0	0	0	0
0122783H.l	32	One	0	0	0	0	0	0	0	0	0	0
0123170Q	32	One	0	0	0	0	0	1	0	0	0	.
0125831R.r2	32	Snap	0	0	1	0	0	0	1	1	0	1
0125831R.r3	32	Snap	0	0	0	0	0	0	0	0	0	0
0127109Y.l	32	One	0	1	0	0	0	1	0	0	0	1
0127109Y.l2	32	Snap	0	1	0	0	0	0	0	0	1	.
0128086K	32	One	0	1	0	0	0	1	0	0	0	0
0129768X	32	Snap	0	1	0	0	0	0	0	0	0	.
0134785Y	32	Snap	0	0	0	0	0	1	0	0	0	.
0135149D	32	Snap	0	0	0	0	0	0	0	0	0	.

Patient Number	Femoral Head Diameter	Joint Type	Fracture	Impingement	Internal Delamination	Internal Delamination	Ridge	Oxidation	Ingression	Dissociation	Rotation
0137791E	32	Snap	0	0	0	0	0	0	0	0	.
0142810J	32	One	0	0	0	0	1	0	0	0	0
0151185D	32	One	0	0	0	0	0	1	0	0	1
0152000P	32	One	0	0	0	1	1	0	0	0	1
0152602R	32	One	0	1	0	1	0	1	0	0	1
0153658H	32	One	0	1	0	1	1	0	0	0	0
0158318N	32	One	0	0	0	1	1	0	0	0	0
0163765G	32	Snap	0	1	0	0	0	1	1	0	.
0166280P	32	Snap	0	0	0	0	0	0	0	0	.
0166369H	32	One	0	0	0	0	0	1	0	0	0
0172585H	32	Snap	1	0	1	0	1	1	0	0	1
0186485A	32	One	0	0	0	0	0	1	0	0	.
0188306N	32	Snap	0	0	0	0	0	0	0	0	.
0188366A	32	Snap	1	0	0	0	0	1	0	0	.
0189957T	26	Snap	1	0	0	0	0	1	0	0	.
0193742Y	32	Snap	1	0	0	0	.	0	0	0	.
0196702T	26	Snap	1	1	1	1	0	1	1	0	.
0200609K	32	Snap	0	0	0	0	0	0	0	0	.
0208695Y	32	Snap	1	1	0	0	1	1	0	0	.
0210421U	26	Snap	1	0	0	0	0	0	1	0	.
0219157P	28	Snap	0	1	1	1	1	1	0	0	.
0221458R	32	One	0	1	0	0	0	0	0	0	0
0222386N	32	Snap	1	0	0	0	0	0	0	0	.
0222703S	26	Snap	0	0	0	0	0	0	0	0	.
0233254N	26		.	.	.	.	.	.	.	.	.
0244498J	28		.	.	.	.	.	.	.	.	.
0264829K	26		.	.	.	.	.	.	.	.	.
1334642J	32	One	0	0	1	1	1	1	0	0	0
1414968A	28	Snap	0	1	0	0	0	1	0	0	.
1421193Q.l	32	Snap	1	0	0	1	0	1	0	0	0
1421193Q.r	32	Snap	1	0	0	0	1	0	0	0	.

165

Patient Number	Femoral Head Diameter	Joint Type	Fracture	Impingement	Internal Delamination	Internal Delamination	Ridge	Oxidation	Ingression	Dissociation	Rotation
1445098U	32	One	0	1	1	0	0	0	0	0	0
1479141N	26	Snap	0	0	0	0	0	0	0	0	.
1492068X	32	Snap	0	0	0	0	0	0	0	0	.
2007588N	32	Snap	0	0	0	0	1	0	0	0	.
2013560W	32	Snap	0	0	0	0	0	0	0	0	.
2083785X	26	Snap	0	1	0	0	0	0	0	0	.
B107423	32	Snap	0	0	0	0	0	0	0	0	.
UA	32	One	0	1	1	1	0	0	0	0	0
UB	32	One	0	1	1	1	1	1	0	0	1
UC	32	One	0	1	1	1	2	0	0	0	0
UD	32	One	0	0	0	0	0	0	0	0	1
UE	32	Snap	0	0	0	0	0	0	0	0	.
UF	32	One	0	0	1	1	0	0	0	0	0
UG	32	One	0	1	1	1	1	1	0	0	0
UH	32	One	0	1	1	1	1	1	0	0	1
UI	26	Snap	0	0	0	0	0	0	0	0	.
UJ	32	One	1	0	0	0	0	1	0	1	1
UK	32	One	0	0	1	1	1	1	1	0	1
UL	26	Snap	1	0	0	0	0	0	0	0	.
UM	32	One	0	0	1	1	1	1	0	0	0
UN	32	One	0	0	0	0	0	0	0	0	0
UO	32	One	0	0	1	1	1	0	0	0	0
UP	32	One	0	0	0	0	1	1	0	0	1
UQ	32	Snap	0	0	0	0	0	0	0	0	.
UR	32	Snap	0	1	0	0	1	1	0	0	.
US	32	One	0	1	0	0	1	1	0	0	0
UT	32	One	0	0	0	0	1	1	0	0	0
UV	32	Snap	0	0	0	0	0	0	0	0	.
UW	32	Snap	1	0	0	1	1	1	0	0	.
UX	32	One	0	0	0	1	1	0	0	0	0

Appendix 3 - Surface Roughness Parameters

Parameter	Definition	Selection Criteria
Peak to Valley height, S_{PV}	Height from the highest peak to the lowest valley.	Gives information on the total range of height deviation on the surface.
Peak height, S_{peak}	Height from mean plane to highest peak in sample area.	Gives information on most damaging feature on the surface.
Arithmetic mean roughness, S_a	$S_a = \dfrac{1}{l_x l_y} \displaystyle\int_0^{l_x} \int_0^{l_y} \lvert \eta \rvert dxdy$	Widely used and specified in BS 7251 Part 4 for the maximum line roughness of the metallic component.
Root mean square roughness, S_q	$S_q = \sqrt{\dfrac{1}{l_x l_y} \displaystyle\int_0^{l_y} \int_0^{l_y} \eta^2(x,y) dxdy}$	Alternative to S_a. Gives a greater significance to features further from the mean plane.
Skewness, S_{sk}	$S_{sk} = \dfrac{1}{S_q^3} \displaystyle\int_{-\infty}^{\infty} \int_{-\infty}^{\infty} \eta^3(x,y) p(\eta) dxdy$	Statistical term describing the shape of the amplitude distribution. Indicates the presence of a disproportionate number of peaks or valleys.
Kurtosis, S_{ku}	$S_{ku} = \dfrac{1}{S_q^4} \displaystyle\int_{-\infty}^{\infty} \int_{-\infty}^{\infty} \eta^4(x,y) p(\eta) dxdy$	Statistical term describing the sharpness, or peakedness, of the amplitude distribution.
Reduced peak height, S_{pk}	Derived from AFC.	Gives information on the damaging top portion of the surface.
Core roughness depth, S_k	Derived from AFC.	The working part of the surface influencing tribological performance.

Description of topopgraphical parameters selected. Definitions as given by Dong et al.[255], Sander[172] and Stout & Blunt[173].

*Note - The convention referring to parameter notations as recommended by the 1st and 2nd EC Workshops on Surface Measurement and Characterisation in Three Dimensions, September 1991 and April 1993, has been followed throughout this thesis. That is to say in order to distinguish between 2D and 3D parameters a capital R and capital S are used respectively ie. arithmetic mean roughness would be denoted R_a in 2D and S_a in 3D.
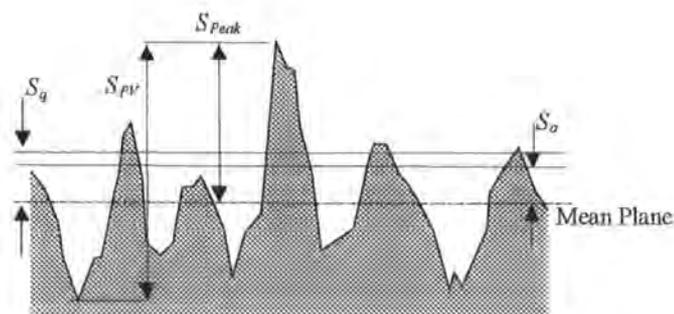
Graphical representation of the parameters described above.
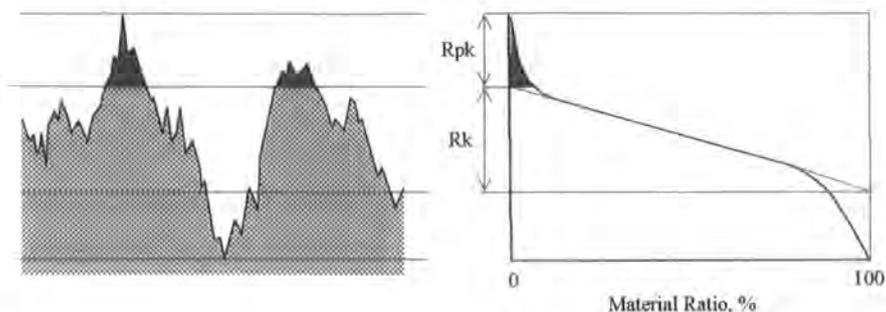
Graphical representation of the parameters derived from the Abbott-Firestone curve.

Head Measurement Protocol

General
x40 objective, no zoom
10 worn images, 4 peripheral images

Advanced Texture Application
Filter: OFF
       remove spikes: ON   (spike height 7.5xRMS)
       remove form: sphere

Parameters:

PV	Ra	Rq	Rsk	Rku	R3z
H	Rk	Rpk	V1	Peak	

Liner Measurement Protocol

General
x10 objective, no zoom
6 images in worn, 3 images in unworn

Advanced Texture Application
Filter: wavelength $50\mu m$
       frequency 20 mm^{-1}
       remove spikes   ON   (spike height 7.5xRMS)
       remove form   Cylinder

Parameters:

Peak	Rq	Rsk	Rku	Ra
Rk	Rpk	Wmax	Wa	Wq

Appendix 4a: Liner Thickness Rank

Description (Type, Inner ∅, Outer ∅)	Approximate Minimum UHMWPE Thickness (mm)	Rank
snap, 32, 46/49	1.8	1
snap, 26, 40/43	2.0	2
snap, 28, 46/49	3.3	3
one-piece, 32, 46	4.5	4
snap, 32, 52/55	5.0	5
one-piece, 32, 49	5.5	6
snap, 26, 46/49	6.0	7
snap, 28, 52/55	6.5	8
one-piece, 32, 52	7.0	9
snap, 32, 58/61	8.0	10
snap, 26, 52/55	8.2	11
one-piece, 32, 55	8.5	12
snap, 28, 58/61	9.0	13
one-piece, 32, 58	10.0	14
snap, 26, 58/61	11.0	15
snap, 32, 64/67	11.0	15

Patient Number	Penetration (mm)	Wear Angle (degrees)	Penetration Rate (mm/yr)	Wear Rate (mm^3/yr)	Est. No. of Cycles	Wear Volume (mm^3)	Clinical Wear Factor (mm^3/Nm)	Thickness Rank
0005193T	0.1	25	0.016778	4.464051	1.40E+07	26.60709	9.44E-08	2
0006761W	2.1	31	0.365424	154.3194	8585214	886.8348	4.53E-06	6
0007598X	2.9	10	0.266875	109.4998	1.34E+07	1189.883	4.03E-06	6
0018244G	3.3	3	0.437822	177.2697	1.45E+07	1336.136	4.19E-06	9
0018267L	0.05		0.044112	35.47723	2322470	40.21239	5.06E-07	10
0020382T	0.7	20	0.078116	31.73091	2.19E+07	284.3402	4.50E-07	1
0023121X	0.05		0.018244	14.6729	5962746	40.21239	2.02E-07	
0027715R	0.75	45	0.114379	47.36679	9189823	310.5913	1.22E-06	5
0031985L	1.7	18	0.190293	78.2028	1.16E+07	698.6331	1.33E-06	9
0044805E	0.55	42	0.107484	33.8369	1.10E+07	173.1447	9.42E-07	8
0047591U	3.65	11	0.32437	134.1186	1.52E+07	1509.178	3.43E-06	12
0048208H.l2	0.4	21	0.352899	142.776	1963079	161.8324	4.43E-06	5
0048208H.l3	0.05		0.059294	47.68693	1433787	40.21239	1.51E-06	1
0048208H.l4	0.45	4	0.149966	60.38032	4917499	181.1823	1.98E-06	10
0051035B	0.3	44	0.033034	13.43703	1.78E+07	122.0277	2.58E-07	13
0055569R.r	0.8	25	0.092762	37.85544	1.06E+07	326.474	9.88E-07	10
0055569R.r2	0.5	8	0.399617	123.425	1.34E+06	154.4291	4.31E-06	
0061576W.l	0.7	11	0.250416	101.2436	6750466	283.0109	2.04E-06	4
0061576W.l2	0.55	50	0.196756	81.1833	6750466	226.9354	1.67E-06	5
0061576W.r	2.7	28	0.43463	184.7517	1.59E+07	1147.712	3.52E-06	6
0061576W.r2	0.6	44	0.178752	73.53738	8065710	246.836	1.52E-06	5
0063335L	1.5	29	0.182747	75.91747	1.22E+07	623.1364	2.07E-06	6
0065745H					1.40E+07			2
0066364W	2.2	40	0.29894	129.0306	1.17E+07	949.5803	2.65E-06	10
0070268J	0.1	90	0.098186	78.96568	1737073	80.425	8.06E-07	6
0087617L	3.7	30	0.521786	227.6301	9963839	1614.132	5.82E-06	9
0090136A	0.8	27	0.058876	24.0593	1.84E+07	326.9162	8.06E-07	6
0091161Y	1	48	0.153466	64.43849	1.16E+07	419.8867	1.34E-06	5
0094223D	0.05		0.652232	524.5562	133703	40.21239	9.36E-06	14
0097018G	2.2	27	0.265023	111.3234	1.21E+07	924.1136	2.84E-06	12
0104541E	1.2	28	0.097508	40.20573	2.08E+07	494.7974	8.36E-07	12
0104577B	2.2	20	0.21919	90.94911	1.89E+07	912.8527	2.11E-06	6
0105366P.r	0.3	32	0.048765	19.75588	8694159	121.5372	5.41E-07	6
0105366P.r2								

Patient Number	Penetration (mm)	Wear Angle (degrees)	Penetration Rate (mm/yr)	Wear Rate (mm^3/yr)	Est. No. of Cycles	Wear Volume (mm^3)	Clinical Wear Factor (mm^3/Nm)	Thickness Rank
0106995J.l	0.75	12	0.078402	31.72735	1.43E+07	303.5054	8.07E-07	9
0106995J.r	1	31	0.077515	31.91569	1.88E+07	411.7365	8.36E-07	9
0108145W	4.4	9	0.405526	167.5928	1.51E+07	1818.4	7.06E-06	6
0108824P	3.2	30	0.471861	203.6794	1.50E+07	1381.284	3.57E-06	12
0111698W	0.45	3	0.064812	26.08664	1.14E+07	181.1245	7.39E-07	6
0112223M	1.05	28	0.124396	51.13366	1.10E+07	431.6086	1.35E-06	6
0113827X	0.5	53	0.096781	39.9451	1.04E+07	206.3693	7.73E-07	1
0114412R	2.3	21	0.180196	75.006	1.73E+07	957.366	1.83E-06	
0114903N.l	3.1	15	0.413843	171.9152	1.22E+07	1287.775	3.84E-06	9
0114903N.r	0.65	63.5	0.127641	53.98855	7362514	274.9314	1.36E-06	5
0114903N.l2	2.4	34	0.308336	131.9688	1.27E+07	1027.207	2.95E-06	9
0118153P	4.9	5	0.434716	177.7911	2.55E+07	2004.014	2.01E-06	12
0121147E	0.6	42	0.141753	44.71436	9481946	189.2632	1.09E-06	8
0122783H.l					1.85E+07			4
0122783H.r	1.2	25	0.101201	41.6011	1.89E+07	493.2907	9.57E-07	4
0123170Q	2.1	14	0.191135	78.461	1.30E+07	862.051	1.68E-06	
0125831R.r2	0.05		0.029988	24.11753	3162715	40.21239	4.03E-07	5
0125831R.r3	0.05		0.045771	36.81096	2023889	40.21239	6.30E-07	14
0127109Y.l					1.26E+07			9
0127109Y.l2					224981.4			13
0128086K	0.3	27.5	0.041024	16.59926	1.33E+07	121.3871	3.20E-07	6
0129768X	0.2	58	0.208655	8.497347	1.25E+07	81.44891	2.75E-07	1
0134785Y	0.55	32	0.214623	87.48538	5301087	224.1925	1.59E-06	5
0135149D	0.4	23	0.064818	26.24105	1.66E+07	161.9366	3.06E-07	1
0137791E	0.05		3.6525	2937.515	30944.89	40.21239	5.56E-05	1
0142810J	1.4	26.5	0.167986	69.42709	1.83E+07	578.6066	1.24E-06	9
0151185D	5.2	-11	0.534111	627.0552	1.20E+07	6104.883	1.79E-05	9
0152000P					1.20E+07			9
0152602R	1.4	7	0.297816	120.5779	8342351	566.8234	1.94E-06	12
0153658H	0.3	23	0.043259	17.4836	8750861	121.2484	5.44E-07	9
0158318N	3.1	16.5	0.352295	146.8406	1.38E+07	1292.117	5.28E-06	4
0163765G	2.2	16	0.299162	123.3194	1.16E+07	906.8748	2.80E-06	5
0166280P	0.7	24	0.113583	35.46504	1.47E+07	218.5676	7.70E-07	8
0166369H	2.6	4	0.296303	120.0123	1.49E+07	1053.086	1.92E-06	9

Patient Number	Penetration (mm)	Wear Angle (degrees)	Penetration Rate (mm/yr)	Wear Rate (mm^3/yr)	Est. No. of Cycles	Wear Volume (mm^3)	Clinical Wear Factor (mm^3/Nm)	Thickness Rank
0172585H	.	.	.	.	2.05E+07	.	.	1
0186485A	4.05	7	0.788099	323.1832	1.18E+07	1660.821	4.94E-06	6
0188306N	0.65	56	0.141908	59.25205	3665748	271.3995	3.03E-06	5
0188366A	0.7	55	0.886837	37.07988	1.36E+07	292.6798	9.22E-07	1
0189957T	.	.	.	.	5873188	.	.	2
0193742Y	.	.	.	.	1.33E+07	.	.	1
0196702T	.	.	.	.	1.68E+07	.	.	1
0200609K	0.75	40	0.141716	58.41428	9557812	309.1439	9.32E-07	1
0208695Y	0.8	37.5	0.097758	40.27105	1.21E+07	329.5556	1.18E-06	1
0210421U	.	.	.	.	6473628	.	.	2
0219157P	0.7	36	0.128222	40.38942	6360951	220.4969	1.39E-06	3
0221458R	2.1	36	0.472888	201.695	9909937	895.6861	2.97E-06	9
0222386N	.	.	.	.	4021130	.	.	2
0227703S	0.2	88	36.525	12370.65	11327.13	67.73798	0.000484	2
0233254N	.	.	.	.	1930531	.	.	.
0244498J	.	.	.	.	1053326	.	.	.
0264829K	.	.	.	.	2143747	.	.	.
1334642J	3.1	15	0.339411	140.9952	1.43E+07	1287.775	4.52E-06	12
1414968A	0.5	24	215369	99.66885	3598325	231.4	2.91E-06	5
1421193Q.l	.	.	.	.	1.57E+07	.	.	1
1421193Q.r	.	.	.	.	1.73E+07	.	.	1
1445098U	1.55	5	0.210382	85.05576	1.39E+07	626.6531	1.52E-06	12
1479141N	0.1	5	0.041132	10.92392	5708282	26.55836	2.54E-07	7
1492068X	0.7	22	0.117067	47.60527	1.19E+07	284.6541	7.21E-07	5
2007588N	2.3	8	0.295905	120.5208	1.55E+07	936.779	2.32E-06	5
2013560W	0.5	21	0.067141	27.20543	9.16E+06	202.5975	7.23E-07	5
2083785X	0.05	.	0.140481	74.58533	674236.1	26.54646	1.47E-06	14
B107423	0.35	7	0.15458	62.26618	3126059	140.9832	1.43E-06	5
UA	2.3	25	.	.	.	964.338	.	12
UB	0.9	67	.	.	.	392.3986	.	4
UC	2.5	9	.	.	.	1021.148	.	9
UD	0.95	23	.	.	.	388.1475	.	9
UE	0.05	.	.	.	.	26.54646	.	11
UF	1.1	27	.	.	.	452.1993	.	13

Patient Number	Penetration (mm)	Wear Angle (degrees)	Penetration Rate (mm/yr)	Wear Rate (mm^3/yr)	Est. No. of Cycles	Wear Volume (mm^3)	Clinical Wear Factor (mm^3/Nm)	Thickness Rank
UG	3.2	15	.	.	.	1330.687	.	9
UH	3.2	11	.	.	.	1318.64	.	6
UI	.	.	.	.	.		.	11
UJ	.	.	.	.	.		.	4
UK	3.35	36	.	.	.	1477.321	.	12
UL	.	.	.	.	.		.	2
UM	0.65	29	.	.	.	265.1272	.	6
UN	3.1	23	.	.	.	1311.815	.	12
UO	0.6	25	.	.	.	243.9605	.	6
UP	3	30	.	.	.	1289.428	.	9
UQ	0.35	17	.	.	.	141.3424	.	10
UR	0.6	36	.	.	.	245.459	.	1
US	2.3	17	.	.	.	950.7573	.	6
UT	1.25	31	.	.	.	517.6733	.	9
UV	0.8	28	.	.	.	327.1436	.	1
UW	3	19.5	.	.	.	1257.345	.	5
UX	.	.	.	.	.		.	4

Appendix 5: Debris Retrieval Study

Appendix 5a: Debris retrieval protocol after Tipper et al.[160]

1. Day One

Hydrolysis of proteins using 12M KOH solution:

  For tissue samples prepare solution then add to sample.
  For serum etc add correct weight of solid KOH direct to liquid.

* Note: $\text{Molarity} = \dfrac{\text{weight of KOH}}{\text{molecular weight} \times \text{volume}}$

Leave for 24 hours.

2. Day Two

i. Add equal volume of ethanol to KOH solution to achieve *at least* a 50/50 mix.
ii. The resulting mix should be decanted in a glass screw-top jar (with top screwed on lightly).
iii. Place onto magnetic stirrer at a moderate speed and leave for 24 hours.

3. Day Three

i. Pour liquor into glass beaker.
ii. Wash out stirrer jar with ethanol.
iii. Decant into centrifuge tubes (as UHMWPE particles float on top of liquid).
iv. Balance centrifuge tubes in pairs.
v. Place tubes in opposing centrifuge buckets.
vi. Centrifuge for 2 hours at 3000 rpm (Mistral 3000e centrifuge).
vii. Decant supernatant fluid into glass beaker.
viii. Resuspend pellet
    - add 5ml filtered water.
    - using pipette suck up pellet & fluid to break it up.
ix. Centrifuge resuspended fluid for a further 2 hours at 3000 rpm.
x. Decant supernatant fluid into beaker with that from first centrifuge run
    - label & retain any residual pellet for possible future use.
xi. Filtration Procedure
    a. Dilute spun liquor with filtered water to <0.5M KOH soln.
    b. Pass through filtration rig
      - ensure adequate washing of beaker and reservoir sides.
xii. Store filter in petri dish.

General
1. Triple wash all glassware with filtered water prior to use.

Appendix 5b: Debris Retrieval Protocol After Campbell *et al.* [185,186]

Day One

i.   Weigh petri dish, tare. Remove tissue from container, shake off excess water, place in petri dish and weigh wet tissue.

ii.   Empty liquid from glass vial, replace tissue in vial. Add 2:1 chloroform/methanol solution to fill vile. Leave for 24 hours.

Day Two

1.

i.   Remove tissue from chloroform/methanol solution.

ii.   Use dissecting scissors to cut tissue into small lumps.

iii.   Add 10ml filtered water and necessary weight of NaOH to create 5M solution.

iv.   Place in water bath at 65°C for 1 to 5 hrs until tissue digested.

v.   Aggitate digested tissue sample for 1 hr in ultrasonic bath at 60°C.

2.

i.   Set up sucrose density gradient. Using 50ml centrifuge tubes add 5ml 10% solution to centrifuge tube. Using Pasteur pipette add 5ml 20% to bottom of centrifuge tube. Follow same protocol with 50% solution. Add 5% solution to on top of 10% layer using U-pipette.

ii.   Add 5ml of the digestion product to the top of the sucrose gradient using pipette.

iii.   Centrifuge for 3 hours at 40,000rpm (Beckman L70 ultracentrifuge, SW41 Ti rotor).

Day Three

1.

i.   Remove top layer of sucrose density gradient containing milky band of particulates using 50ml pipette and pipette-pump.

ii.   Add to 50ml centrifuge tube and fill with filtered water to dilute the sucrose. Wash out pipette with filtered water into centrifuge tube. Leave for 1 hour in 37°C water bath.

iii.   Add 10ml of product into 15ml centrifuge tubes. Top with 2ml each of first 0.96g/ml and then 0.90g/ml isopropanol.

iv.   Centrifuge for 1 hours at 40,000rpm.

v.   Remove particles from the interface of the two isopropanol densities.

# Appendix 5c: Preliminary Results using LALLS Particle Analyser

Result: Analysis Report

Sample Details

Sample ID: PMMA in water
Sample File: DURUNI
Sample Path: C:\SIZERS\DATA\
Sample Notes: Background Measured against wate
10 sec

Run Number: 2
Record Number: 24

Measured: 23 Jun 1998 12:19
Analysed: 23 Jun 1998 12:19
Result Source: Analysed

System Details

Range Lens: 300RF mm
Presentation: 3OHD
Analysis Model: Polydisperse
Modifications: None

Beam Length: 2.40 mm
[Particle R.I. = (1.5295, 0.1000); Dispersant R.I. = 1.3300]

Sampler: MS1

Obscuration: 9.0 %

Residual: 0.289 %

Result Statistics

Distribution Type: Volume
Mean Diameters:
D [4, 3] = 61.79 um

Concentration = 0.0272 %Vol
D (v, 0.1) = 23.88 um
D [3, 2] = 18.20 um

Density = 1.000 g / cub. cm
D (v, 0.5) = 54.47 um
Span = 1.593E+00

Specific S.A. = 0.3298 sq. m / g
D (v, 0.9) = 110.67 um
Uniformity = 5.009E-01

Size Low (um)	In %	Size High (um)	Under%	Size Low (um)	In %	Size High (um)	Under%
0.05	0.00	0.06	0.00	6.63	0.23	7.72	3.86
0.06	0.00	0.07	0.00	7.72	0.24	9.00	4.10
0.07	0.00	0.08	0.00	9.00	0.26	10.48	4.36
0.08	0.00	0.09	0.00	10.48	0.31	12.21	4.67
0.09	0.00	0.11	0.00	12.21	0.46	14.22	5.12
0.11	0.00	0.13	0.00	14.22	0.74	16.57	5.87
0.13	0.00	0.15	0.00	16.57	1.21	19.31	7.07
0.15	0.00	0.17	0.00	19.31	1.91	22.49	8.98
0.17	0.00	0.20	0.00	22.49	2.96	26.20	11.94
0.20	0.00	0.23	0.00	26.20	4.46	30.53	16.39
0.23	0.00	0.27	0.00	30.53	6.39	35.56	22.79
0.27	0.01	0.31	0.01	35.56	8.46	41.43	31.24
0.31	0.03	0.36	0.05	41.43	10.11	48.27	41.36
0.36	0.07	0.42	0.11	48.27	10.97	56.23	52.33
0.42	0.12	0.49	0.23	56.23	11.17	65.51	63.49
0.49	0.18	0.58	0.41	65.51	9.77	76.32	73.26
0.58	0.23	0.67	0.64	76.32	8.08	88.91	81.35
0.67	0.29	0.78	0.93	88.91	6.39	103.58	87.74
0.78	0.31	0.91	1.24	103.58	4.78	120.67	92.52
0.91	0.32	1.06	1.56	120.67	3.32	140.58	95.84
1.06	0.32	1.24	1.88	140.58	2.13	163.77	97.97
1.24	0.30	1.44	2.18	163.77	1.22	190.80	99.19
1.44	0.26	1.68	2.44	190.80	0.60	222.28	99.79
1.68	0.20	1.95	2.64	222.28	0.21	258.95	100.00
1.95	0.14	2.28	2.78	258.95	0.00	301.68	100.00
2.28	0.10	2.65	2.88	301.68	0.00	351.46	100.00
2.65	0.08	3.09	2.96	351.46	0.00	409.45	100.00
3.09	0.08	3.60	3.04	409.45	0.00	477.01	100.00
3.60	0.09	4.19	3.13	477.01	0.00	555.71	100.00
4.19	0.12	4.88	3.25	555.71	0.00	647.41	100.00
4.88	0.17	5.69	3.42	647.41	0.00	754.23	100.00
5.69	0.20	6.63	3.62	754.23	0.00	878.67	100.00
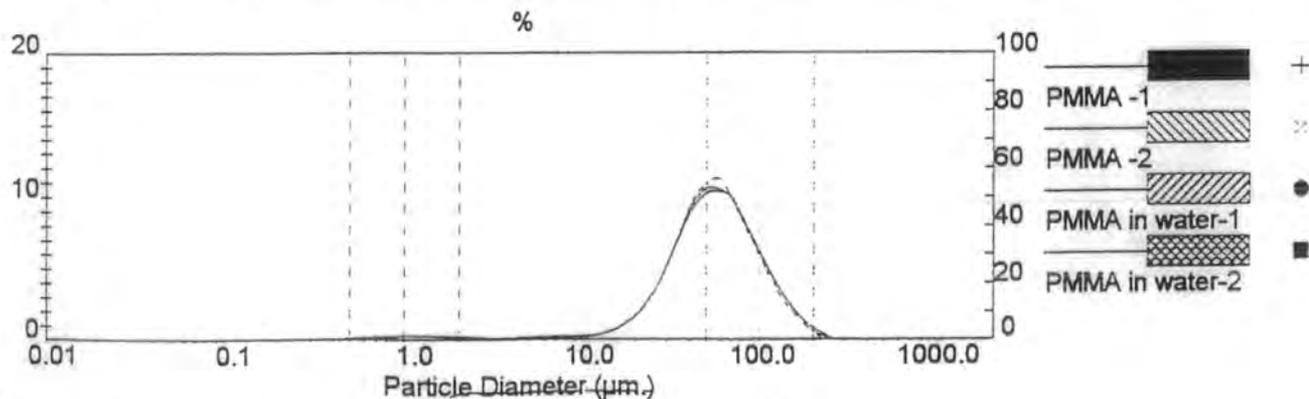
Particle Diameter (µm.)

- PMMA -1 +
- PMMA -2 ×
- PMMA in water-1 ●
- PMMA in water-2 ■

Result: Analysis Table

Range: 300RF mm Beam: 2.40 mm Sampler: MS1　　　Obs': 8.4 %
Presentation: 3PHD　　Analysis: Polydisperse　　Residual: 0.489 %
Modifications: −

Conc. = 0.0105 %Vol Density = 1.000 g/cm^3 S.S.A.= 0.5977 m^2/g
Distribution: Number　D[4, 3] = 62.90 um　　D[3, 2] = 10.04 um
D(n, 0.1) = 0.89 um　D(n, 0.5) = 1.33 um　D(n, 0.9) = 2.47 um
Span = 1.185E+00　　Uniformity = 3.987E-01

Size (um)	Number In %	Size (um)	Number In %	Size (um)	Number In %	Size (um)	Number In %
0.05	0.00	0.58	0.00	6.63	0.14	76.32	0.00
0.06	0.00	0.67	2.39	7.72	0.08	88.91	0.00
0.07	0.00	0.78	8.99	9.00	0.05	103.58	0.00
0.08	0.00	0.91	14.60	10.48	0.04	120.67	0.00
0.09	0.00	1.06	16.78	12.21	0.02	140.58	0.00
0.11	0.00	1.24	15.04	14.22	0.02	163.77	0.00
0.13	0.00	1.44	12.49	16.57	0.01	190.80	0.00
0.15	0.00	1.68	9.94	19.31	0.01	222.28	0.00
0.17	0.00	1.95	6.99	22.49	0.01	258.95	0.00
0.20	0.00	2.28	4.84	26.20	0.00	301.68	0.00
0.23	0.00	2.65	3.12	30.53	0.00	351.46	0.00
0.27	0.00	3.09	1.95	35.56	0.00	409.45	0.00
0.31	0.00	3.60	1.17	41.43	0.00	477.01	0.00
0.36	0.00	4.19	0.68	48.27	0.00	555.71	0.00
0.42	0.00	4.88	0.40	56.23	0.00	647.41	0.00
0.49	0.00	5.69	0.23	65.51	0.00	754.23	0.00
0.58		6.63		76.32		878.67	

Volume Distribution +
Number Distribution ×
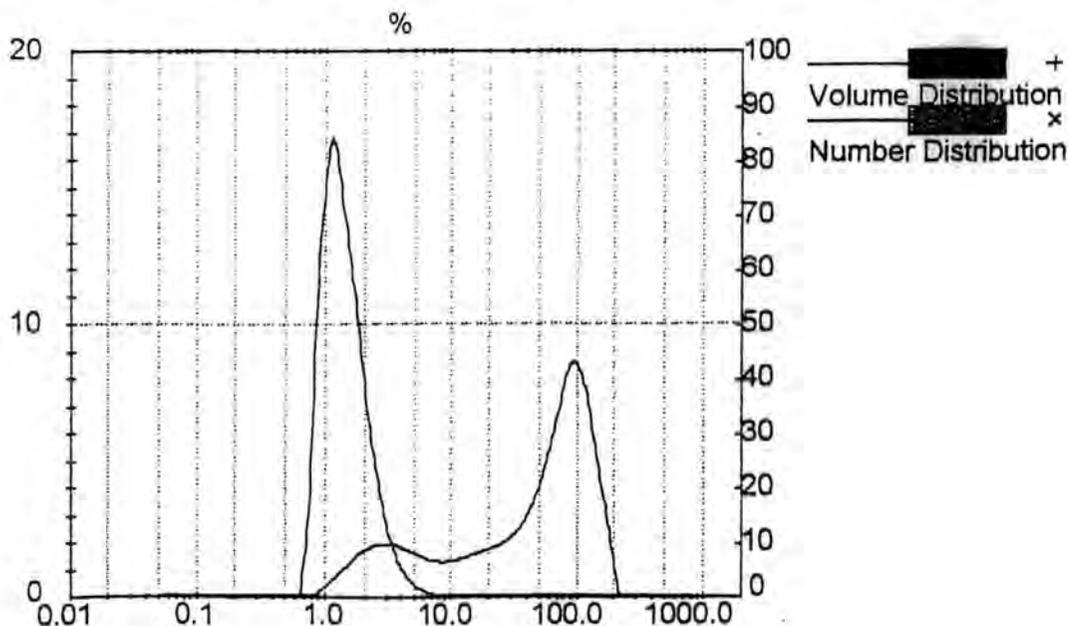
Appendix 6: Hertzian Stress Calculation
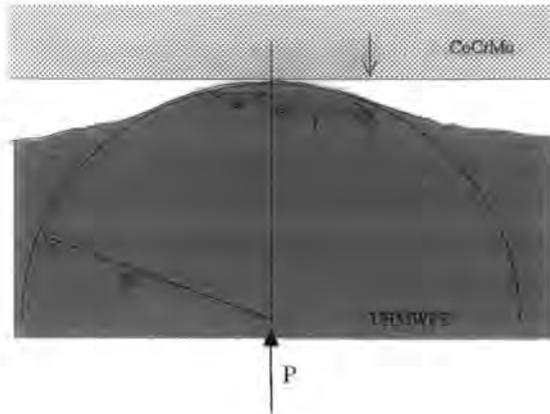
Material Properties:

CoCrMo	$E_c = 2.1 \times 10^5$ MPa	
	$v_c = 0.3$	
UHMWPE	$E_p = 2.0 \times 10^3$ MPa	
	$v_p = 0.4$	

Assume the typical asperity has the form of a truncated sphere 1.2μm high with a radius of 50μm.

$$R = \frac{r^2}{2\alpha} = \frac{\left(50 \times 10^{-6}\right)^2}{2\left(1.2 \times 10^{-6}\right)} = 1.04 \text{mm}$$

From Zygo plots it can be seen that there are approximately 20 asperities of this nature per image with an area of 7.68×10^{-8} m² area. Total joint area of contact, assume that of a circle.

$$\text{Joint contact area} = \pi r^2 = \pi (0.0016)^2 = 804 \text{ mm}^2$$

The total number of asperities supporting the load must therefore be,

$$\text{No. of apserities} = \frac{804 \times 10^{-6}}{7.68 \times 10^{-8}} \times 20 = 210000 \text{ approx.}$$

If average body mass is 70kg and peak load is 4 times body weight[209], then the load per asperity P is,

$$P = \frac{4(70 \times 9.81)}{210000} = 0.013 \text{ N}$$

From Timoshenko[256],

$$a = \sqrt[3]{\frac{3\pi P}{4}\left(k_p + k_c\right)R}$$

where

$$k_p = \frac{1 - v_p}{\pi E_p} = 1.34 \times 10^{-10} \qquad \text{and} \qquad kc = \frac{1 - v_c}{\pi E_c} = 1.38 \times 10^{-12}$$

$$a = \sqrt[3]{\frac{3\pi \times 0.01}{4}\left(1.34 \times 10^{-10} + 1.38 \times 10^{-12}\right) \times 1.04 \times 10^{-3}} = 14.5 \times 10^{-6} \text{ m}$$

Further from Timoshenko[256],

$$q_0 = \frac{3P}{2\pi a^2} = \frac{3 \times 0.013}{2\pi \left(14.5 \times 10^{-6}\right)^2} = 29.7 \times 10^6 \text{ Nm}^{-2}$$

If we assume the load produces a uniform pressure across the area of contact, then Timoshenko shows,

$$\tau_{max} = \frac{q_0}{2}\left[\frac{1-2\nu}{2} + \frac{2}{9}(1+\nu)\sqrt{2(1+\nu)}\right]$$

$$Z_{max} = a\sqrt{\frac{2(1+\nu)}{7-2\nu}}$$

Substituting for q_0 and $\nu=0.4$ for UHMWPE,

$$\tau_{max} = 0.31q_0 = 9.21 \text{ MPa}$$

$$z_{max} = 0.672a = 9.74 \mu m$$

Appendix 7: Publications

1. Elfick AP, Hall RM, Pinder IM, Unsworth A (1997): A Tribological Study of Explanted PCA Total Hip Replacements. (Abstract). Journal of Bone & Joint Surgery 79B S(3), 368.

2. Elfick AP, Hall RM, Pinder IM, Unsworth A (1997): Surface Topography of PCA UHMWPE Acetabular Liners: Its Relevance to Debris Production. (Abstract). Journal of Bone & Joint Surgery 79B S(4), 466.

3. Elfick AP, Hall RM, Pinder IM, Unsworth A (1998): Wear in Retrieved Acetabular Components - Effect of Head Radius and Patient Parameters. Journal of Arthroplasty 13, 291-295.

4. Elfick AP, Hall RM, Pinder IM, Unsworth A (1998): Surface Topography of Retrieved PCA Acetabular Liners: Proposal of a Novel Wear Mechanism. Journal of Materials Science Letters 17, 1085-1088.

5. Elfick AP, Hall RM, Pinder IM, Unsworth A (1998): The Frictional Behaviour of Explanted PCA Hip Prostheses. Proc. Inst. Mech. Eng.: Part H 212, 395-397.

6. Elfick AP, Hall RM, Pinder IM, Unsworth A (1998): Tribological Performance of the PCA Total Hip Replacement. (Abstract). Journal of Bone & Joint Surgery 80B S(3), 273-274.

7. Elfick AP, Hall RM, Pinder IM, Unsworth A
   The Influence of Femoral Head Surface Roughness on the Wear of Ultra-High Molecular Weight Polyethylene Sockets in Cementless Total Hip Replacement.
   accepted for Journal of Biomedical Materials Research: Applied Biomaterials.

8. Hall RM, Elfick AP, Siney P, Unsworth A, Wroblewski BM
   Levels of Agreement Between the Surface Roughness Values of Femoral Heads Measured Using Two Different Optical Techniques. (Abstract)
   presented at Autumn '98 B.O.R.S. Conference, Dublin.

9. Elfick AP, Hall RM, Pinder IM, Unsworth A
   The Relationship of Femoral Head Roughness with Wear in THR. (Abstract)
   presented at Autumn '98 B.O.R.S. Conference, Dublin.

10. Hall RM, Elfick AP, Siney P, Unsworth A, Wroblewski BM
    The Apparent Differences Observed in the Wear-Roughness Relationship When Using Two Different Techniques For Measuring Surface Topography. (Abstract)
    presented at O.R.S. Anaheim, California, Feb. 1999.

11. Elfick AP, Smith SL, Unsworth A
    Variation in the Wear Rate During the Life of a THR - A Simulator and Retrieval Study
    submitted to Journal of Arthroplasty

12. Smith SL, Elfick AP, Pinder IM, Unsworth A
    An Evaluation of the Performance of Zirconia and CoCrMo Femoral Heads
    accepted for Journal of Materials Science: Materials in Medicine

13. Elfick AP, Green SM, Pinder IM, Unsworth A
    A Novel Technique for the Characterisation of Wear Debris
    submitted to Journal of Materials Science: Materials in Medicine

Study Group, mean loss 12.31, median 10, Std Dev 5.33, SE of mean 1
Control Group, mean loss 12.69, median 10, Std Dev 7.10, SE of mean 1.4
Dorsi Flexion No Stat Significance Study Group, mean loss 8.65, median 7.5, Std Dev 6.57, SE of mean 1.3
Control Group; mean loss 9.04, median 10, Std Dev 4.69, SE of mean 0.92
3. Gait Study Group, Symmetrical 20, Asymmetrical 6 Control Group, Symmetrical 6, Asymmetrical 20. (p<0.00001).

Discussion: This is an original study and no similar study has been found in literature. They only near similar study has been performed by Hedstrom et al for lateral malleolar fractures, they showed there was no difference at 1 year and 18 months. Thus we decided to assess if there was any benefit what so ever even at 3 months. This has been an unsolved debate since the AO philosophy was introduced. Though the number in the study is small, we think it is adequate to draw the conclusion without any doubt that there is no significant statistical difference in pain or range of motion of the ankle. However, we made an interesting observation the patients in the mobilisation group had a symmetrical gait; we would not like to draw any conclusions about this but it definitely merits further study. We would propose that the symmetrical gait most probably is due to development of better proprioception sense.

THE ABILITY OF ULTRASOUND VELOCITY TO PREDICT THE STIFFNESS OF CANCELLOUS BONE IN-VITRO

R. Hodgskinson, C. F. Njeh, J. D. Currey, and C. M. Langton
Academic Department of Medical Physics, University of Hull and Royal Hull Hospitals, Hull, UK.

Introduction: The mechanical status of bones is an important consideration in skeletal pathological conditions such as osteoporosis, which results in fracture at predominantly cancellous bone sites. Density is a good predictor of the stiffness and strength of cancellous bone. However, these mechanical properties are also dependent on cancellous bone architecture.
Objective: The objective of this work was to investigate the ability of ultrasound velocity to predict the mechanical properties of cancellous bone.
Methods: The cancellous bone specimens were 20 mm cubes from bovine femur and 21 mm diameter medio-lateral cylinders cored from human calcaneus. Ultrasound velocity (V) and Young's modulus (E) were determined in three orthogonal directions for the bovine cubes, and medio-laterally in the calcaneus. Apparent density (r) was determined after the other tests.
Result: Density alone explains 87.6% of the variance of Young's modulus in human calcaneal and bovine femora bone tested in the PD direction only. Velocity however explains 95% and a combination of density and velocity 97%.
Friedman's anova for ranks test shows that velocity and stiffness are not random with respect to the three directions in the bovine cubes (E: $X^2 = 35.0$, p<0.0001, and V: $X^2 = 8.7$, p = 0.013). Further, for each cube we obtained the mean value of E and of V, and characterised each value of E and V by their deviation from their mean. There is an extremely strong positive correlation (r = 0.80) showing that the degree of deviation is consistent for E and V, and of the same sign.
Conclusions: We have demonstrated that the velocity of ultrasound in cancellous bone can give direction-specific information. In particular, knowledge of both density and velocity allows better predictions of mechanical properties than does density, or ultrasound, on their own. Since there are non-invasive methods of measuring density, apart from the velocity of ultrasound, the combination of these two measurements promises, eventually, to give improved predictions of bone that is weak, and liable to fracture.

A TRIBOLOGICAL STUDY OF EXPLANTED PCA TOTAL HIP REPLACEMENTS

A. P. Elfick, R. M. Hall, I. M. Pinder and A. Unsworth:
Centre for Biomedical Engineering, University of Durham, Durham, DH1 3LE.

The PCA cementless total hip replacement is known to perform well in the short term, but its survivorship beyond 6 years is poor.[1] Loosening of the acetabular component is the dominant reason for revision surgery. The loosening appears to be related to the penetration of the head into the socket. However, the exact causal relationship remains elusive, despite the existence of osteolysis. The aim of this study was to investigate both the penetration and wear of these components. An investigation of surface topography and its relationship to the wear of the liner was also undertaken.
Method: Thirty-nine sockets, all of which were coupled with 32 mm heads, were removed at the time of revision surgery. The penetration depth and angle were measured using the shadowgraph technique and the change in the bore volume calculated using the formula presented by Kabo et al.[2,3] Subsequently, the penetration and wear rates and the clinical wear factor[4] were obtained from the slope of a line using weighted regression analysis. Any significant intercept on the ordinate axis may be attributable to short term creep. The weighting in the analysis took into consideration both the heteroscedastic variance and the resolution of the measurement technique. Topographical analysis was undertaken using the Micromap 512 interference profilometer and included measurements of new, as well as explanted sockets.
Results: The mean penetration depth and rate, at the time of revision surgery, were found to be 1.3 (SE: 0.2) mm and 0.24 (SE: 0.04) mm yr[1]. The average wear volume was calculated to be 530 (SE 80) mm[3]. A mean volumetric wear rate of 102 (SE 16) mm[3] yr[1] was observed. The clinical wear factor was deduced as 2.08 (SE 0.3) x 10^{-6} mm[3] N[1] m[1]. In none of the regression analyses was a significant intercept observed. The average root mean square roughness (Rq) of two new PCA CoCr 32 mm heads was equal to 13.8 (SE 2.4) nm. The mean Rq within the most heavily scratched zone of the explanted head was 43.2 (SE 10.4) nm, whilst the relatively undamaged periphery yielded a Rq value of 10.4 (SE 1.3) nm. No correlation was observed between Rq and the clinical wear factor for any of the sockets.
Discussion: There was no evidence in any of the regression analyses that a significant creep contribution attributed to the total change in the bore volume. This is not to suggest that creep does not occur in these or any other series of sockets, only that it cannot be detected in explanted prostheses using this analysis. Thus it seems prudent to suggest that most, if not all, of the change in bore volume may be attributed to wear. The penetration rate of 0.21 (SE 0.03) mm yr[1] determined is comparable with that observed in a radiographic study of PCA hip replacements.[5] The volumetric wear rate is greater than that observed in explanted Charnley prostheses and cannot be accounted for by the greater sliding distance of the larger head size alone. This may indicate a detrimental influence of the metal backing.[6] However, if account is taken of patient activity,[4] and weight, the clinical wear factor was found not to be significantly different from that observed in non-metal backed sockets.[7] The mean surface roughness results show no statistical difference between the new and unworn areas but, as expected, a substantial increase in roughness was observed in the worn articulating region. The lack of correlation between Rq and the wear factor may reflect both the unsuitability of Rq as a measurement of those surface fractures which are important to the wear of the counterface, i.e. the build up of material adjacent to scratches, and the non-uniformity in the damage imparted on the head in vivo.

References:
1. Owen et al. J. Bone Jt. Surg; 76B (1994) 258.
2. Kabo et al. J. Bone Jt. Surg; 75B (1993) 254.
3. Hall et al. Proc. Inst. Mech. Eng. 209 (1995) 233.
4. Atkinson et al. Wear. 104 (1985) 225.
5. Devane et al. Clin. Orthop. 319 (1995) 317.
6. Cates et al. J. Bone Jt. Surg. 75B (1993) 249.
7. Hall et al. Accepted for publication in Proc. Inst. Mech. Eng.

OSTEOBLASTS SECRETE VASCULAR ENDOTHELIAL GROWTH FACTOR (VEGF) IN HUMAN FRACTURE HEALING

J. G. Warner and J. G. Andrew
Dept of Orthopaedic Surgery, University of Manchester, Hope Hospital, Salford.

Vascular endothelial growth factor (VEGF), also known as Vascular Permeability Factor (VPF) and Vasculotropin, is a multifunctional cytokine that exerts several important and possibly independent actions on vascular endothelium. A secreted endothelial cell-specific mitogen, VEGF has been shown to stimulate angiogenesis both in vitro and in vivo.
Angiogenesis is a key feature in the fracture healing process, particularly during the early granulation tissue stage of repair. It has been postulated that inadequate angiogenesis may be associated with delayed fracture healing. Although there is some work on blood flow in fracture healing, the literature is sparse with regard to angiogenesis and fracture healing.
VEGF has previously been investigated in the rat model of fracture healing, where hypertrophic chondrocytes have been shown to produce mRNA for VEGF. It was postulated that VEGF may participate in the signal mechanisms that initiate vascularisation of cartilage during endochondral ossification. Human osteoblast-like cells in culture have also been shown to produce VEGF.
We investigated the expression of VEGF in vivo in human fracture healing, using the techniques of in situ hybridisation and immunohistochemistry to detect the expression of mRNA and protein respectively. Biopsies were collected at the time of open reduction and internal fixation of 20 normally healing fractures treated surgically for loss of position up to 3 week from injury. The study was designed to investigate angiogenesis in the early stages of fracture healing when granulation tissue is a prominent feature. All fractures subsequently healed normally.
VEGF expression was identified in early fracture healing in both macrophages and spindle shaped mesenchymal cells predominant at the granulation tissue stage of repair. Chondrocytes also appeared to express VEGF, but the strongest expression was seen in plump osteoblasts aggregating around the matrix of early trabecular woven bone.
We present, to our knowledge the first report of VEGF expression in human fracture healing and the first confirmation that osteoblasts express VEGF in vivo as well as in vitro. Further research is ongoing to study the expression of the two high affinity receptors for VEGF in human fracture healing. We suggest that VEGF has an important role in angiogenesis in early fracture healing, and postulate that abnormalities of this process could be involved in delayed fracture healing even at this early stage of the repair.

PROLIFERATION OF HUMAN PERIOSTEAL CELLS IS MODULATED BY FLUID SHEAR STRESS

M. Kitano, J-H. Kuiper, Z. V. Hazlehurst, J. B. Richardson, B. A. Ashton
Institute of Orthopaedics, Robert Jones & Agnes Hunt Orthopaedic Hospital, Oswestry, Shropshire, SY10 7AG

Introduction: Cells involved in fracture repair respond to local mechanical stimuli which may include compressive stress, hydrostatic pressure and fluid shear stress. Finite element modelling revealed that fluid shear stress experienced by cells in the developing callus is likely to be in the range (0.1 to 5 Pa, (Kuiper et al., 1996, Proc. B.O.R.S., Dundee meeting). In this communication we describe the effects of fluid shear stress on the proliferation of human periosteal cells in vitro.
Methods: Periosteum was harvested during surgery, and transported to the lab in tissue culture medium. Cells were released by treatment with collagenase and grown as monolayers in Hams/F-12 culture medium supplement with 10% FRC and antibiotics. The cultures were incubated at 37°C in 5% CO2 /air, with the medium changed on a 3/4 day cycle and passaged at confluence.
For the strain experiments, cells were plated in 6-well dishes at 1 x 10^3 cells/cm^2, and grown for 4 days. Uniform fluid shear stresses (1 Pa) were applied using a rotating disc apparatus for 0 (control), 1, 5, 15, 30 & 60 minutes per day for 3 days.

wear debris, its size and mass distributions were determined; and compared to femoral head damage and linear wear rate of the acetabular cups.

Methods: Nineteen explanted Charnley prostheses with a mean implant life of 13 years (range 10-20 yr) were retrieved at revision, with acetabular tissue samples. Femoral heads and cups were examined macroscopically and photographed. Total linear wear rates of the acetabular cups were measured with a co-ordinate measuring machine. Damage to the femoral heads was measured (expressed as surface topography parameters R^a, R^p, R^{pm}, R^t, R^v) and compared with a new Charnley femoral head. Total UHMWPE wear debris was isolated from 1g of randomly selected acetabular tissue by digestion with potassium hydroxide and nitric acid. Lipid and protein was removed by extraction with chloroform/ methanol, ethanol precipitation and centrifugation. UHMWPE wear debris was collected by sequential filtration through $10\mu m$ and $0.1\mu m$ filter membranes. The filters were dried and weighed to determine the mass of wear debris in both size ranges. The particle size distribution was determined using SEM images by 2-D particle sizing. The distribution of the mass of wear debris as a function of particle size was determined for all samples in two size ranges, $0.1-10\mu m$ and $>10\mu m$. The total number of particles was estimated using the mass and frequency distributions as a function of size.

Results: The femoral heads were separated into two groups, high damage ($R^{pm} >0.2\mu m$ (n=9)) and low damage ($R^{pm} <0.2\mu m$ (n=10)). The R^{pm} of the high damage group was $1.5 \pm 0.45\ \mu m$ and the R^{pm} of the low damage group was $0.07 \pm 0.01\ \mu m$, compared to the R^{pm} value for the new Charnley head which was $0.05\ \mu m$. The mean $\pm$ SE linear wear rate for the high damage group was 0.23 ± 0.03 mm/ yr: while the mean linear wear rate for the low damage group was 0.11 ± 0.03 mm/yr (p < 0.05 Students t-test). There was no correlation between the total mass of wear debris isolated and the linear wear rate. The estimated total number of particles varied from patient to patient (range 1.5×108 to 1.3×1010). The mode of the frequency distribution of the particle sizes was in the range $0.1-0.5$ (m for all patients. The mass distributions varied considerably with 18-97% of the UHMWPE wear debris $<10\ \mu m$. There was an association between the proportion of wear debris that was $<10\ \mu m$ and the penetration rate and head damage R^{pm}. At high penetration rates and head damage a large proportion ($>60\%$) of the wear debris was $<10\ \mu m$.

Previous studies have found limited differences in particle size distributions for UHMWPE wear debris. Analysis of the mass distribution as a function of size has allowed differentiation of UHMWPE wear debris from different patients. There is an indication that femoral head damage R^{pm} and increased linear wear rate affect the size of the wear debris. The lack of correlation between wear and mass of debris retrieved may be due to variations in material properties such as oxidative degradation, patient factors such as activity and tissue response or the random nature of the tissue sampling technique.

SYNOVIOCYTES MODULATE OSTEOCALCIN PRODUCTION BY OSTEOBLAST-LIKE CELLS

V.R. Patel, V. Yeh, C.G. Frondoza, R.H. Jinnah and D.S. Hungerford
The Johns Hopkins University Department of Orthopaedic Surgery, Baltimore, USA.

Introduction: Aseptic loosening and osteolysis are major concerns following total joint arthroplasty. Loose prosthetic implants are often associated with formation of a synovial-like membrane at the bone-implant interface infiltrated by macrophages, fibroblasts and particulate wear debris. Macrophages and fibroblasts have been implicated in secreting bone resorbing factors in response to wear debris, leading to osteolysis. Although osteolysis primarily results from osteoclastic bone resorption, it is probably coupled with a failure of reparative bone formation. The interaction between the cells in the synovial-like membrane at the interface and bone-forming osteoblastic cells is unknown. The aim of this study was to analyse the interaction between synovial fibroblasts and osteoblastic cells. An in vitro model simulating conditions prevailing at the interface of a loose prosthetic implant was used.

Material and Methods: Osteoblast-like MG63 cells and synoviocytes isolated from osteoarthritic patients undergoing primary TKR were used in four separate experiments. Duplicate wells of aFLEX-1 flexible bottomed, collagen coated plates (Flexcell Int. Corp., McKeesport, PA) were seeded with MG63 cells (0.5×10^5/well), synoviocytes (1×10^5/well) or a combination of the two and incubated overnight in Hy medium at 37°C, 5% CO_2. The next day, polymethylmethacrylate (PMMA) spheres (0.17 μm, Polysciences Inc., Warrington, PA) or buffer alone were added to the wells. The plates were then incubated in the presence or absence of cyclic strain using a Flexercell Strain Unit (-20 kPa vacuum; 30 cycles per minute: 1 second on, 1 second off). The cells were pulsed with 30μCi of [^{3}H]-thymidine 6 hours later. The supernatants were obtained 24 hours after adding PMMA or buffer and subsequently assayed for osteocalcin (Metra Biosystems, Mountain View, CA). The cells were fixed, processed for autoradiography, counterstained with toluidine blue and enumerated. Results were analysed using ANOVA and student's t tests.

Results: Osteoblastic MG63 cells cultured in the presence of synoviocytes produced lower concentrations of osteocalcin (mean : 55.1 ng/ml; sd : 10.4) than cells cultured in medium alone (mean: 38.4 ng/ml; sd: 9.1) (P < 0.05; fig.). The addition of PMMA particles attenuated this inhibitory effect of synoviocytes on osteocalcin production by osteoblastic cells without significantly affecting their proliferative index (range: 28-57% and 69-80% respectively) as measured by [^{3}H]-thymidine uptake. Synoviocyte inhibition of osteocalcin production by osteoblastic cells and attenuation of this effect by exposure to PMMA were not altered by application of cyclic strain. However, on light microscopy, cells subjected to strain appeared more fusiform and aligned themselves perpendicular to the direction of maximum strain.

Discussion: The principal observation of this study was that synoviocytes can regulate the function of MG63 osteoblast-like cells as measured by osteocalcin production. Abrogation of this effect by exposure to PMMA particles suggests that PMMA particles interrupt the pathway through which synoviocytes modulate osteocalcin production by osteoblastic cells. The precise nature of the interaction between synoviocytes and osteoblastic cells is unclear and requires further elucidation. The present study succeeded in providing an in vitro model to study cellular interaction under conditions of cyclic strain. Further studies using this model may provide insights into the mechanism of osteolysis seen around prosthetic implants.

References:
1. W.A. Jiranek, M. Machado, M. Jasty et al. J. Bone Joint Surg; 75-A: 863-879 (1993)
2. A. Banes. Biochem. Cell Biol; 73: 349 (1995).

SURFACE TOPOGRAPHY OF RETRIEVED PCA ACETABULAR LINERS: PROPOSAL OF A NOVEL WEAR MECHANISM

A.P. Elfick, R.M. Hall, L.M. Pinder and A. Unsworth
Centre for Biomedical Engineering, University of Durham, DH1 3LE

It is commonly accepted that the long term loosening, and subsequent failure, of total hip replacement is due an osteolytic response to particulate wear debris.[1] Moreover the immunological response seems to be dependent on the morphology of the debris produced.[2] Studies on wear debris have indicated that distribution of particle size may be bimodal with particles of tens of microns in size in addition to sub micron particles.[3] The influence of femoral head roughness on the wear of the socket is widely recognised.[4] However, the effect of the socket surface topography on debris production has had little investigation.

The topography of twenty PCA acetabular liners was assessed qualitatively at low magnifications using differential interference contrast microscopy. Selected cups were studied using SEM at magnifications of up to x10,000. Quantitative measurements were made using a non-contacting interference profilometer to assess the surface (NewView 100). A filtering wavelength of $50\ \mu m$ was used to separate the waviness and roughness information. Four topographical parameters were then selected to describe the surface; root mean square and maximum peak height for both the waviness and roughness. The explanted liners were measured at six positions in the articulating region and three times in the periphery.

The microscopy provided valuable information on the nature of the UHMWPE surface. The grain structure of the UHMWPE was easily distinguishable using the DIC microscope, however the SEM seemed less capable in this regard. Light scratching was observed in the worn region with no dominant orientation. The unworn region often displayed evidence of deep scratching superimposed on the machining marks. SEM at high magnification allowed images to be obtained at the grain boundary regions. Deep cracks running for hundreds of microns were observed. The surface features were quantified by the surface profilometry which revealed significant differences between the worn and unworn regions for all the topographical parameters measured. Very low values of root mean square roughness and waviness (0.07 & 0.10 (m, respectively) were observed for the worn region. The surface profilometry revealed the presence of a number of depressions in the surface. These depressions were approximately circular in shape, of the order of 150 μm in diameter and up to 1 μm in depth. These features were only observed in the worn zone and away from the boundary with the unworn region.

The analysis of wear debris from in vivo has show that the majority of wear particles are sub-micron in size.[5,6] However, the presence of large smooth platelets of 10-100μm in diameter has been observed associated with the wear of UHMWPE by supersmooth counterfaces.[3] It has been reported in a previous retrieval study that the femoral head of the PCA prosthesis remains remarkably smooth.[7] It may then be hypothesised that these particles would be produced by the in vivo articulation of the presently studied prostheses. These particle sizes are strikingly similar to the dimensions of the depressions seen in the topographical studies presented in this study.

Cooper et al. suggests that the large particles are created by the fatigue and release of long wavelength asperities.[8] This theory relies on the stress levels in the asperities being large enough to fatigue the polyethylene before it is abraded. The topographical studies on which this theory are based state that peaks with an amplitude of up to 10 μm are observed. Our studies show evidence which contradicts Cooper's theory. Firstly, the peaks of the waviness for the worn region have a median maximum height of 0.47μm. The strain in the asperities would be of a low magnitude, hence a large number of cycles would be needed to achieve the fatigue limit of the UHMWPE. It is doubtful whether this would happen prior to the removal of this material by microadhesion or abrasion. Secondly, Cooper's wear model would be self-limiting; once the asperities are detached the mechanism by which this mode of wear is created has been removed. Finally, the treatment of the UHMWPE as a homogenous continuum by Cooper's model may not be justified. The presence of intergranular defects has been reported by many authors.[9] The microscope investigation reported in this study clearly shows the grain structure at the surface of the UHMWPE.

We hypothesise that the depressions seen are caused by the release of a platelet wear particle from the surface. The bulk of the UHMWPE is removed by microadhesion or abrasion creating submicron sized wear particles. However, when only a portion of an individual grain remains it is vulnerable to fatiguing of the grain boundary region by shear stresses. This may quickly result in the failure of the mechanical interlock between the grains. This would facilitate the removal of the remaining portion of the grain by in a plucking or rolling motion.

Our model exploits the granular structure of the UHMWPE by fatiguing the bulk material at its weakest point, it is capable of producing the surface topography observed and the wear debris expected. Further work including wear debris analysis and finite element analysis of the stresses imposed on the UHMWPE asperities is needed to substantiate this hypothesis.

References:
1. Schmalzried et al. J. App. Biomat. 5 (1994) 185
2. Howie et al. Orth. Clin. N. Am. 24 (1993) 571.
3. Hailey et al. Proc. Inst. Mech. Eng: H210 (1996) 3
4. Dowson et al. Wear 119 (1987) 277
5. McKellop et al. Clin. Orthop. Rel. Res. 311 (1995) 3
6. Shanbhag et al. JBJS 76B (1994) 60
7. Elfick et al. JBJS (199)
8. Cooper et al. Wear 162 (1993) 378.
9. Li et al. JBJS 76A (1994). 1080

Wear in Retrieved Acetabular Components

Effect of Femoral Head Radius and Patient Parameters

Alistair P. D. Elfick, MSc, Richard M. Hall, PhD, Ian M. Pinder, FRCS,
and Anthony Unsworth, FEng

Abstract: Forty-seven explanted Porous Coated Anatomic (PCA, Howmedica, Rutherford, NJ) cementless acetabular components were acquired at revision surgery. All the components articulated against CoCrMo femoral heads of 32-mm diameter. The penetration depth and angle were measured using the shadowgraph technique. The wear volume was then calculated using Kabo's formula. Using weighted linear regression analysis, the mean penetration rate and mean volumetric wear rate were calculated to be 0.23 (SE, 0.03) mm^3/y and 96 (SE, 13) mm^3/y, respectively. The creep component was not found to be significantly different from zero. The clinical wear factor, $k_{clinical}$, for this cohort was also calculated using linear regression analysis but with the assumption that creep was zero. The value found, $k_{clinical} = 1.93$ (SE, 0.29) $\times 10^{-6}$ $mm^3/N\text{-}m$, was similar to those in previous studies involving cemented joints with a 22-mm femoral head diameter. The similar $k_{clinical}$ values of these substantially different joint types suggest that the high volumetric wear rate for the PCA joint can be attributed entirely to its larger head size and the younger, more active, patient profile. Fixation technique and metal backing seem not to influence the rate of wear. **Key words:** total hip arthroplasty, explanted, wear, cementless.

The dominant cause of long-term failure of the Porous Coated Anatomic (PCA, Howmedica, Rutherford, NJ) hip arthroplasty is the loosening, or migration, of the acetabular component. The results achieved with the PCA design were encouraging in the short term, with survivorship rates of 93% at 6 years [1] and 94% of hips attaining a good or excellent Harris rating at 2 years [2]. Survivorship rates of 57% at 8 years, and evidence of acetabular

osteolysis in 36% of hips at 5 years [3], however, demonstrate its poor longevity.

It is generally accepted that the production of particulate debris promotes a foreign-body reaction resulting in resorption of bone and, hence, loosening of the components [4]. The greatest contributor to the amount of debris in the periprosthetic region is wear of the ultrahigh-molecular-weight polyethylene (UHMWPE) socket at the articulating interface. Additional debris may be produced at other interfaces in this modular design, for example, between the liner and backing; however, the volume of debris released from these alternative sources is small in comparison with that from the articulating interface.

The aim of this study was to assess the wear of 47 retrieved acetabular components and to evaluate the effect of the femoral head radius, the polyethylene thickness, and patient parameters.

Materials and Methods

The PCA system is a cementless design relying on the ingrowth of bone into a porous coating for long-term fixation. In early examples of this prosthesis, the liner and backing were supplied as 1 piece and had a simple locking method comprising a single peg at the pole and a tab at the rim to stop rotation about this pole. Later versions incorporated a snaplock mechanism located at the rim and became truly modular. Forty-seven acetabular components were retrieved at revision; 27 were of the 1-piece design and the rest were of the snaplock type. All were coupled with 32-mm-diameter CoCrMo femoral heads. The explanted components were cleaned in a formaldehyde-based solution, and excess bone ingrowth was removed.

The thickness of the UHMWPE has been cited as an important parameter in the performance of the acetabular component [5]; however, the liners of snaplock design were not of constant polyethylene cross-section, and subsequently no single value of wall thickness could be ascribed to each. A ranking for both designs in terms of minimum wall thickness at implantation could be achieved and is detailed in Table 1.

The penetration depth, ΔP, and angle, β, of the wear track into the acetabular liners were measured using a shadowgraph technique [6]. The changes in the internal volume of the bore, ΔV, were calculated using the formula previously presented by Kabo et al. [7]. Those liners that had visual evidence of wear and/or creep but volume changes of insufficient

magnitude to be measured on the shadowgraph instrument were assigned a penetration depth of 0.05 mm, which was equal to the resolution of the apparatus. The change in bore volume of these liners was calculated using a simple linear formula [6].

Mean penetration rates were calculated using regression analysis with a model of the form

$$(1) \qquad \Delta P = m\Delta T + c$$

where ΔP is the penetration depth, ΔT is the implant period, and m and c are constants. Given that experimental evidence indicates that the creep component is constant after a relatively short period [8], then the gradient, m, of the function is equal to the penetration wear rate, $\Delta P/\Delta T$. The regression constant, c, may incorporate changes in the internal bore volume or the penetration depth resulting from creep. Mean volumetric wear rate was calculated in a similar manner.

The clinical wear factor, $k_{clinical}$, is a development of the fundamental wear equation, which states that wear volume is proportional to load and sliding distance. To be applicable to the clinical situation the load is the joint reaction force, a function of patient weight, and the sliding distance becomes a combination of the number of wear cycles and femoral head radius. The clinical wear factor is the constant of proportionality and may be deduced from simplification of the wear equation produced by Dowson and Wallbridge [9]:

$$(2) \qquad \Delta V = k_{clinical} (2.376NWr) + C$$

where N is an estimate of the number of cycles to which the joint has been subjected during its life, r is the radius of the femoral head, and W is patient weight. The number of cycles is calculated using an empirical formula derived by Wallbridge and Dowson [10] relating age to activity:

$$(3) \qquad \begin{aligned} N = 0.5 \, (A_r - A_p) \times \\ [6.58 - 0.032(A_r + A_p)] \times 10^6. \end{aligned}$$

Here, A_p is the patient age at primary surgery, and A_r, the age at revision surgery. This formula was based on data gained from normal subjects and therefore it may vary from the level of activity achieved by patients; however, Wallbridge and Dowson [10] warn against the assumption that patients are less active than normal subjects. The mean clinical wear factor was calculated, using regression analysis, in the manner described by Hall et al. [11]. Clinical wear factors of individual sockets were

Table 1. Ranking in Terms of Minimum Ultrahigh-molecular-weight Polyethylene (UHMWPE) Thickness*

Description	Approximate Minimum UHMWPE Thickness (mm)	Rank
Snaplock, 46/49-mm backing	1.8	1
	—	2
One-piece, 46-mm backing	4.5	3
Snaplock, 52/55-mm backing	5.0	4
One-piece, 49-mm backing	5.5	5
	—	6
	—	7
One-piece, 52-mm backing	7.0	8
Snaplock, 58/61-mm backing	8.0	9
	—	10
One-piece, 55-mm backing	8.5	11
One-piece, 58-mm backing	10.0	12
Snaplock, 64/67-mm backing	11.0	13

*Note that the ranks 2, 6, 7, and 10 are reserved for other head/backing combinations not applicable to this study.

calculated with the assumption that the creep, C, was negligible.

Analysis was undertaken, for the most part, using the STATA 4.0 statistical software package (Stata Corporation, Texas). In determining $k_{clinical}$ and the rates of penetration and volumetric wear, a suitable weighting had to be applied in the regression analysis to maintain a constant variance. The weighting also incorporated a factor to take into account the resolution of the shadowgraph instrument. Trends between the liner thickness, locking mechanism, and individual clinical wear factors were analyzed using nonparametric trend analysis. Nonparametric trend analysis is reasonably robust to changes in value of the ranking values and, hence, is unaffected by the absence of cups of certain ranks.

Clinical Data

Clinical records were available for all the retrieved joints. The primary procedure was undertaken in 17 cases for rheumatoid arthritis. A further 16 were due to osteoarthritis and 3 to posttraumatic osteoarthritis. Ankylosing spondylitis was diagnosed in 4 cases and congenital dislocation of the hip in 3 others. The remaining cases included fractured neck of the femur and benign tumor of the femoral head.

Revision was undertaken in 31 cases for loosening evidenced by migration of components and/or lytic lesions on the radiograph. A further 9 revisions were done because of pain, and 3, because of gross wear of the liner. The other cases were revised for sepsis or instability.

Twenty-two of the patients were male. The average weight of the patients, W, was 705 (SD, 155) N. The median age at primary surgery was 44 (range, 15–76) years and the median implant period, ΔT, was 6.2 (range, 0.1–12.3) years.

Results

The mean penetration depth was found to be 1.3 (SE, 0.2) mm, which gave a mean penetration rate of 0.23 (SE, 0.03) mm/y (Fig. 1). The intercept was not found to be significantly different from zero. The mean wear volume was calculated to be 551 (SE, 77) mm^3 and a corresponding mean volumetric wear rate of 96 (SE, 13) mm^3/y was deduced. The mean total number of cycles to revision was 10.4 (range, 0.03–25.5) $\times$ 10^6. The mean clinical wear factor was found to be 1.93 (SE, 0.29) $\times$ 10^{-6} mm^3/N·m.

The nonparametric trend analysis showed no correlation between the thickness rank or locking mechanism and the clinical wear factor (Fig. 2).

Discussion

The penetration rates found in this study compare well with those found in other studies on 32-mm-diameter heads [7,12]. These values do not support the notion that there is a reduction in penetration
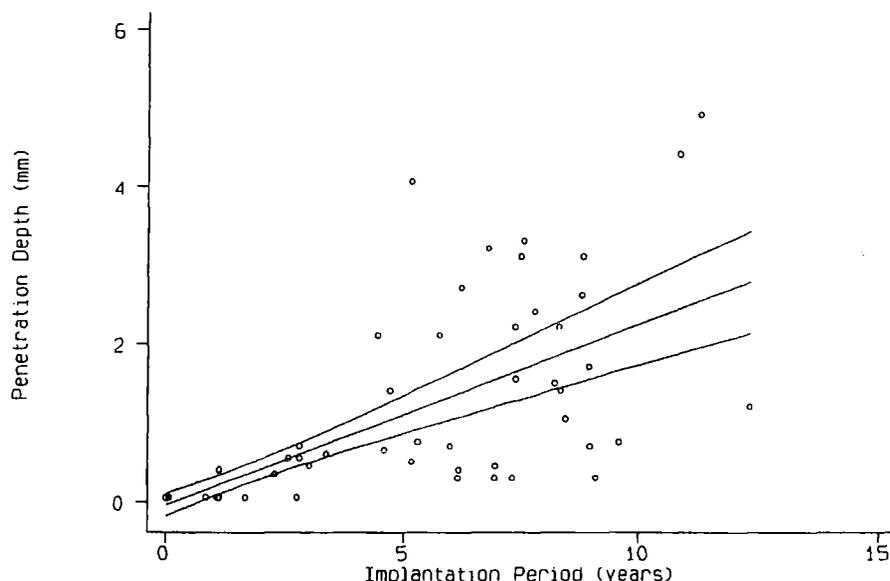

Fig. 1. Determination of the penetration rate using regression analysis. The outer curves are the 95% confidence limits of the prediction. Note that the intercept is approximately equal to zero.
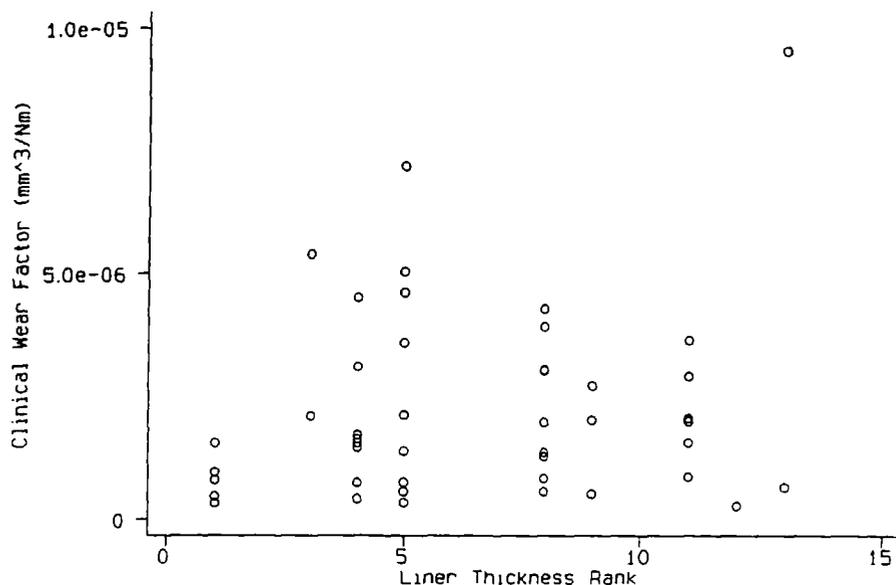
Fig. 2. Variation of the clinical wear factor with liner thickness rank.

with large heads. Indeed, studies involving other head sizes show similar penetration rates; Hernandez et al. reported a penetration rate of 0.22 mm/y with cementless femoral components [13] and Kabo et al. observed a value of 0.23 mm/y [7]; both were for 28-mm-diameter heads. Similarly, for Charnley prostheses (22-mm-diameter heads), Hall et al. [11] and Atkinson et al. [14] both reported linear wear rates of 0.20 mm/y for explant studies.

The similarity in penetration rates may be regarded as coincidental; attention should be focused on the corresponding volumetric wear rates. From Figure 1, it can be seen that the creep component of the penetration is minimal, as evidenced by the zero intercept. Thus, the penetration into the liner is caused mainly by wear. This is reflected in the high mean volumetric wear rate of the PCA, 96 mm^3/y. Similarly high volumetric wear rates for 32-mm-diameter heads are reported by Kabo et al. [7]: 88 mm^3/y; however, smaller heads show lower rates of wear: 75 mm^3/y for 28 mm [7] and 55 mm^3/y for 22 mm [11].

The variation in wear rate is in part attributable to the greater sliding distance associated with the larger femoral head sizes. A 32-mm-diameter head has a 45% greater sliding distance than a 22-mm head per cycle; hence, as wear is proportional to sliding distance, the wear should be 45% larger per cycle. The volumetric wear rate we obtained, however, is approximately twice that of studies on 22-mm heads. This further increase may be attributable to the many differences in the prostheses and the patient groups.

At this point, it is advantageous to consider the clinical wear factor. The great benefit of this parameter is the ability to compare the wear performance of prosthetic designs directly despite different patient groupings. Hence, for a given prosthesis design, a heavy, sedentary patient should achieve the same $k_{clinical}$ as a light, active patient. Conversely, if two joint types, say a cemented and an uncemented design both with 32-mm-diameter heads, have the same $k_{clinical}$, then any difference in the wear rate is attributable to variations in patient activity and weight between the two groups and not the fixation method.

The mean clinical wear factor found in this study of 1.93×10^{-6} mm^3/N-m and those for Charnley joints reported by Hall et al. [11] and Atkinson et al. [14] of 2.1×10^{-6} and 1.96×10^{-6} mm^3/N-m, respectively, are very similar. We have already established that approximately half the increase in wear rate is attributable to the 32-mm head size over the 22-mm size of the Charnley. The equivalence in clinical wear factor indicates that the remaining increase in wear rate found in our study is attributable to the younger, more active, patient group.

Further, the similarity in clinical wear factors between the PCA and Charnley designs suggests that the wear performance of these two joints is similar; the metal backing and cementless system of the PCA have little effect on the wear, nor does the possibility of cement ingression in the Charnley. Hence, if the PCA was to adopt a 22-mm head and have the same patient profile as the Charnley, then their volumetric wear rates would be comparable.

This is in agreement with the findings of Manley and Serekian [15], who observed that the effect of a metal backing is to increase the rate of wear only marginally.

The lack of correlation between the locking mechanism, or thickness rank, and the clinical wear factor indicates that these parameters have little effect on the wear rate; however, these factors have been associated, by Brien et al. [16] and Learmonth et al. [17], with the fracture and dissociation of the liner. This study included 5 liners of thickness ranking 1, which corresponds to a snaplock-type cup with an outer diameter of 46 or 49 mm, giving a polyethylene thickness at implantation of approximately 1.8 mm at its thinnest point. Clearly, this predisposes the design to early mechanical failure.

Conclusion

The most important conclusion to be drawn from this study is the detrimental effect of the large femoral head size. This accelerates the volumetric wear rate, therefore reducing the components' expected life. An additional consequence of the 32-mm head is the reduction in polyethylene thickness attainable for a given acetabular outer diameter.

The presence of the metal backing was not found to contribute substantially to the high wear rate, and the similar clinical wear factors of the PCA and Charnley designs do not suggest any advantage of either cemented or cementless fixation in terms of wear.

References

1. Astion DJ, Saluan P, Stulberg BN et al: The porous-coated anatomic total hip prosthesis: failure of the metal-backed acetabular component. J Bone Joint Surg 78A:755, 1996

2. Callaghan JJ, Dysart SH, Savory CG: The uncemented porous-coated anatomic total hip prosthesis. J Bone Joint Surg 70A:337, 1988

3. Owen TD, Moran CG, Smith SR, Pinder IM: Results of uncemented porous-coated anatomic total hip replacement. J Bone Joint Surg 76B:258, 1994

4. Howie D, Haynes D, Rogers S et al: The response to particulate debris. Orthop Clin North Am 24:571, 1993

5. Bartel DL, Burstien AH, Toda MD, Edwards DL: The effect of conformity and plastic thickness on contact stresses in metal-backed plastic implants. J Biomed Eng 107:193, 1985

6. Hall RM, Unsworth A, Craig PS et al: Measurement of wear in retrieved acetabular sockets. Proc Inst Mech Eng 209H:233, 1995

7. Kabo JM, Gebhard JS, Loren G, Amstutz HC: In vivo wear of polyethylene acetabular components. J Bone Joint Surg 75B:254, 1993

8. Elloy M: Simulator testing of joint prostheses: the need for realistic simulator testing. p. 79. In Proceedings SERC/IMechE annual expert meeting on the failure of joint prostheses. Mechanical Engineering Publications, London, 1993

9. Dowson D, Wallbridge NC: Laboratory wear tests and clinical observations of the penetration of femoral heads into acetabular cups in total replacement hip joints: 1. Charnley prostheses with polytetrafluoroethylene acetabular cups. Wear 104:225, 1985

10. Wallbridge NC, Dowson D: The walking activity of patients with artificial joints. Eng Med 11:95, 1982

11. Hall RM, Unsworth A, Siney P, Wroblewski BM: Wear in retrieved Charnley acetabular sockets. Proc Inst Mech Eng 210:197, 1996

12. Devane PA, Bourne RB, Rorabeck CH et al: Measurement of polyethylene wear in metal-backed acetabular cups: 2. Clinical application. Clin Orthop 319:317, 1995

13. Hernandez JR, Keating EM, Faris PM et al: Polyethylene wear in uncemented acetabular components. J Bone Joint Surg 76B:263, 1994

14. Atkinson JR, Dowson D, Isaac JH, Wroblewski BM: Laboratory wear tests and clinical observations of the penetration of femoral heads into acetabular cups in total replacement hip joints: 3. The measurement of internal volume changes in explanted Charnley sockets after 2–16 years in vivo and the determination of wear factors. Wear 104:225, 1985

15. Manley MT, Serekian P: Wear debris: an environmental issue in total joint replacement. Clin Orthop 298:137, 1994

16. Brien WW, Salvati EA, Wright TM et al: Dissociation of acetabular components after total hip arthroplasty: report of four cases. J Bone Joint Surg 72A:1548, 1990

17. Learmonth ID, Smith EJ, Cunningham JL: The pathogenesis of osteolysis in two different cementless hip replacements. Proc Inst Mech Eng 211:59, 1997

Surface topography of retrieved PCA acetabular liners: proposal of a novel wear mechanism

A. P. ELFICK, R. M. HALL, A. UNSWORTH
Centre for Biomedical Engineering, University of Durham, DH1 3LE, UK

I. M. PINDER
Freeman Hospital, Newcastle, NE7 7DH, UK
E-mail: A.P.D.Elfick@durham.ac.uk

It is commonly accepted that the long term loosening, and subsequent failure, of a total hip replacement is due an osteolytic response to particulate wear debris [1]. Moreover, this immunological response seems to be dependent on the morphology of the debris produced [2]. Studies on wear debris have indicated that the distribution of particle size may be bimodal with particles of tens of micrometers in size in addition to sub-micrometer particles [3]. Thus, the contribution of the larger particles to the wear volume may be substantial despite a lower frequency [4]. The influence of femoral head roughness on the wear of the socket is widely recognized [5]. However, the effect of the socket surface topography on debris production has had little investigation.

This study assesses the surface of the acetabular liner using a combination of techniques. The use of differential interference contrast (DIC) microscopy and scanning electron microscopy (SEM) allows a qualitative examination, while non-contacting profilometry gives quantitative information on the topography.

The porous coated anatomic (PCA) total hip replacement (Howmedica) was chosen as it gave the opportunity to study the mechanisms of wear without the influence of cement ingression. Twenty explanted acetabular liners were retrieved at revision surgery; ten were of the one-piece design and ten of the modular "snaplock" type. The patient group consisted of 11 men and 9 women with a mean age of 41.2 ± 12.9 y. The mean life of the prosthesis was 5.7 ± 1.9 y. The reasons for primary surgery were rheumatoid arthritis in 8 cases, osteoarthritis in 4 cases, congenital displaysia of the hip (CDH) and ankylosing spondylitis accounted for a further 6 cases, with the remaining being for trauma.

A preliminary study was undertaken using a non-contacting interference profilometer to assess the surface (Zygo NewView 100). A ten times objective lens was used, giving a coverage of 730 μm by 550 μm which represents a horizontal resolution of 2.3 μm per pixel. The vertical resolution of this instrument was 0.1 nm. Form error was removed as twin orthogonal cylinders. The information obtained was used to define a filtering wavelength of 50 μm. The two topographical parameters selected to describe the waviness and roughness of the surface

were the root mean square deviation and maximum peak height values: these are defined in Fig. 1. The explanted liners were measured quantitatively at six positions in the articulating region and three in the periphery.

Descriptive examination of the cups at low magnifications was conducted using a differential interference contrast microscope (Ziess Axiotech). Magnifications of 100 and 200 times allowed the wear features over large areas to be assessed.

Selected cups were gold sputter coated prior to microscopic studies using a Joel JSM IC848 scanning electron microscope. A range of magnifications up to ×10,000 was used to ascertain the nature of the nanometre scale surface features.

Prior to microscopic assessment it was noted that the worn surface exhibited a highly polished nature. The microscopy provided valuable information on the nature of the ultra heavy medium weight polyethylene (UHMWPE) surface. The grain structure of the UHMWPE was easily distinguishable using the DIC microscope (Fig. 2), however the SEM seemed less capable in this regard (Fig. 3). The width of the grains ranged from under 50 μm to approximately 250 μm. No variation in the distribution of grain sizes was observed between the two liner varieties.

Light scratching was observed in the worn region with no dominant orientation. Occasional deep scratches in the worn region were thought to be attributable to damage sustained during surgery. The unworn region often displayed evidence of deep
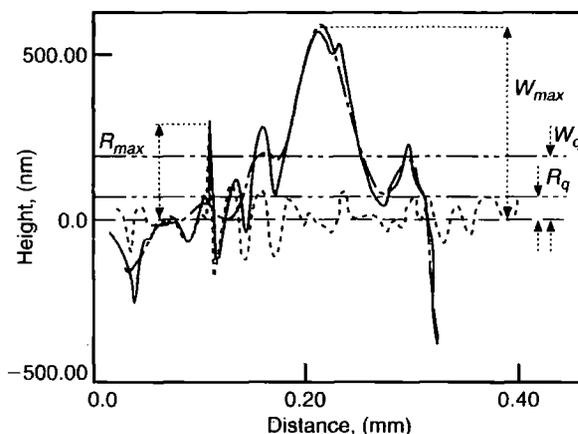

Figure 1 Schematic diagram of roughness parameters.

cycles would be needed to achieve the fatigue limit of the UHMWPE. It is doubtful whether this would happen prior to the removal of this material by microadhesion or abrasion. Cooper's wear model would also be self-limiting in that once the asperities are detached the surface would be devoid of any long wavelength asperities. Therefore, the mechanism by which this mode of wear is created has been removed.

The treatment of UHMWPE as a homogenous continuum by Cooper's model may not be justified. The presence of intergranular defects in both finished components and the bulk UHMWPE prior to manufacture has been reported by many authors [10]. The microscopic investigation reported in this paper clearly shows the grain structure at the surface of the UHMWPE and thus the fatigue model of Cooper *et al.*, which does not exploit the intergranular weaknesses of the UHMWPE, must be limited.

The large particle dimensions are strikingly similar to those of the depressions seen in the topographical studies presented in this paper. This suggests that the depressions observed are caused by the release of a platelet wear particle from the surface. The mechanism by which this would happen is illustrated in Fig. 6. The bulk of the UHMWPE is removed by microadhesion or abrasion, creating the sub-micrometer sized wear particles. However, when only a portion of an individual grain remains it is vulnerable to fatiguing of the grain boundary region by shear stresses. This may quickly result in the failure of the mechanical interlock between the grains which would facilitate the removal of the

remaining portion of the grain by a plucking or rolling motion.

The failure to observe the depressions in all the liners may reflect the random nature of the selection of sites assessed. This mode of wear may be restricted to a certain set of tribological conditions or region of the liner. Alternatively, the variation in the quality and granular integration of the UHMWPE could explain this phenomenon.

This model exploits the granular structure of the UHMWPE by fatiguing the bulk material at its weakest point, it is capable of producing the surface topography observed and the wear debris predicted.

Further work, including wear debris analysis and finite element analysis of the stresses imposed on the UHMWPE asperities, is needed to substantiate this hypothesis.

Acknowledgment

References

1. T. SCHMALZRIED, M. JASTY, A. ROSENBERG and W. HARRIS, *J. App. Biomat.* **5** (1994) 185.
2. D. HOWIE, D. HAYNES, S. ROGERS, M. McGEE and M. PEARCY, *Orthop. Clin. N. Am.* **24** (1993) 571.
3. J. HAILEY, E. INGHAM, M. STONE, B. WROBLEW-

1. Very Smooth. Material removed through abrasion/adhesion. Fatiguing of material close to surface especially at grain boundaries.

2. Weakened at the grain boundaries, the remnants of a grain are plucked from surface as a platelet.

3. Process of abrasion & platelet plucking leaves a polished surface with grain boundary cracks & occasional shallow depressions
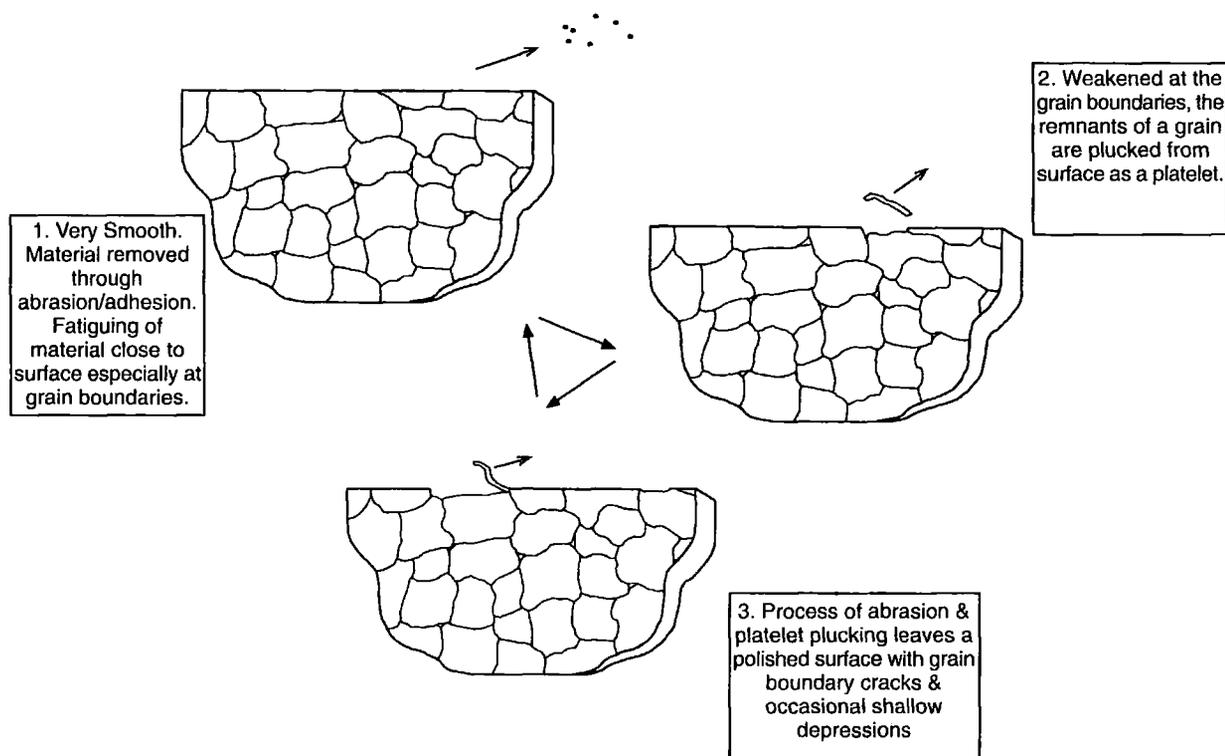
Figure 6 Schematic diagram of a section through part of the UHMWPE acetabular liner. The diagram describes the proposed wear mechanism. Not to scale.

Technical Note

The frictional behaviour of explanted PCA hip prostheses

A P Elfick[1], R M Hall[1]*, I M Pinder[2] and A Unsworth[1]
[1]Centre for Biomedical Engineering, University of Durham
[2]Freeman Hospital, Newcastle

Abstract: The frictional characteristic of 22 explanted and two unused PCA total hip arthoplasties were assessed using the Durham hip simulator. The friction of the explanted joints was not found to be significantly different from that of the unused joints. In contrast, explanted Charnley joints often exhibit increased frictional characteristics. This discrepancy is accounted for by the lack of cement ingression in the PCA design.

NOTATION

f friction factor
L load
r femoral head radius
T frictional torque
u entraining velocity
z Sommerfeld number

η viscosity

1 INTRODUCTION

One of the most commonly employed artificial joint procedures at present is the Charnley low friction arthroplasty. It was designed such that the shear stress at the bone–cement interface of the acetabulum was low, and therefore the life of the prosthesis maximized. Three strategies were employed to achieve these design goals: the materials were chosen to give a low coefficient of friction; the diameter of the femoral head was small (22 mm); and the fixation diameter of the acetabular component was large, thereby keeping the stresses to a minimum [1].

The primary differences between the Charnley and PCA designs are in the fixation methods and the diameter of the articulation. The Charnley is cemented into the bone and has a stainless steel head, while the PCA uses cementless

fixation and a larger diameter (26, 28 or 32 mm) cobalt–chrome–molybdenum alloy (CoCrMo) femoral head.

It has been shown previously [2, 3] that the friction of Charnley joints increases after implantation. Theoretically, the cyclical nature of the torque consequently imposed on the bone–cement interface may well contribute to the loosening of the prosthesis through a fatiguing mechanism. However, Hall et al. [3] showed that the torques were not of sufficient magnitude for friction to have any effect on loosening rate. The aim of this study was to assess the effects of time of implantation on the friction of PCA joints and compare these to those of Charnley joints.

2 EXPERIMENTAL PROCEDURE

2.1 Materials

The 22 hip joints used in this study came from a larger cohort of 100 explanted joints. The selection of joints used was random, though joints were excluded if they showed signs of fracture or delamination of the ultra-high molecular weight of polyethylene (UHMWPE) within the articulating region of the socket. All the joints selected had a femoral head diameter of 32 mm. Two unused joints were also tested for comparison (supplied by Howmedica). The original PCA design utilized a one-piece acetabular component while later examples used a snaplock mechanism to provide modularity of the acetabular component. This study used seven joints of the snaplock type, while the remainder were of the one-piece design. The two new joints tested were of the snaplock type.
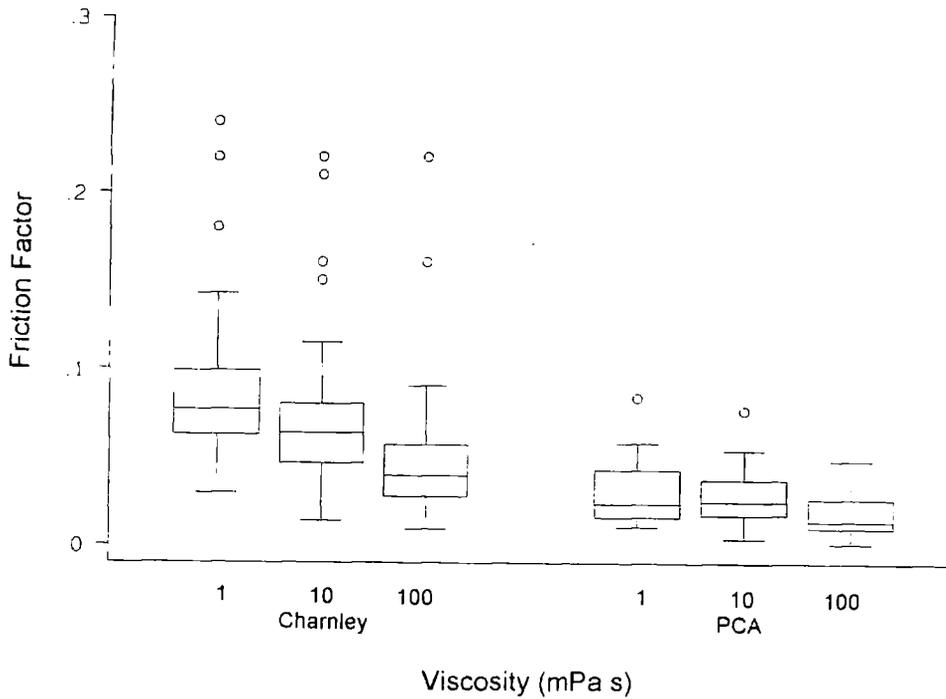
Fig. 1 Box (median and interquartile range) and whisker (upper/lower adjacent values) plots, including individually plotted outliers, of friction factor against viscosity by joint type

5 CONCLUSION

By omitting cement fixation from the PCA design, one source of third-body damage to the femoral head has been removed. This has been shown to reduce the frictional force generated by articulation. However, the large femoral head size of the PCA negates any benefit in terms of frictional torque that may otherwise be attained.

ACKNOWLEDGEMENTS

REFERENCES

1 **Charnley, J.** *Low Friction Arthroplasty of the Hip, Theory and Practice*, 1979 (Springer, New York).
2 **Hall, R. M., Unsworth, A., Wroblewski, B. M.** and **Burgess, I. C.** Frictional characterisation of explanted Charnley hip prostheses. *Wear*, 1994, **175**, 159–166.
3 **Hall, R. M., Unsworth, A., Wroblewski, B. M., Siney, P.** and **Powell, N. J.** The friction of explanted hip prostheses. *Br. J. Rheum.*, 1997, **36**, 20–26.
4 **Hall, R. M., Unsworth, A., Wroblewski, B. M.** and **Hardaker, C.** Long term changes in the frictional behaviour and wear in explanted Charnley hip prostheses. *J. Bone Jt Surg.*, 1993, **75B** (Suppl. 3), 267.
5 **Elfick, A. P., Hall, R. M., Pinder, I. M.** and **Unsworth, A.** A tribological study of explanted PCA total hip replacements. *J. Bone Jt Surg.*, 1997, **79B** (Suppl. 3), 368.
6 **Andersson, G. B. J., Freeman, M. A. R.** and **Swanson, S. A. V.** Loosening of the cemented acetabular cup in total hip replacement. *J. Bone Jt Surg.*, 1972, **54B**, 590–599.

employing the avidin-biotin peroxidase complex. The sections were then counterstained with neutral red (0.5%). Control negative sections were run without primary antibody. The antibodies used were mouse anti-human CS1 fibronectin (Chemicon; 1:100), goat anti human VCAM-1 (R&D systems; 1:200), mouse anti human VLA-4 (alpha 4 beta 1 integrin) (Serotec; 1:100), and chicken anti human TGF-beta 1 and 2 used as a cocktail together (R&D systems,1:60)

Results: The CS1 binding site of fibronectin stained positively around the endothelial cells of blood vessels in the perinodular dupuytren tissue, but also around the myofibroblasts, principally at the periphery of many of the active areas of the Dupuytrens nodule. VCAM-1 stained positively for the endothelial cells of blood vessels surrounding and penetrating the areas of high nodular activity but was only more rarely expressed outwith the blood vessels. VLA4 was expressed by inflammatory cells principally in and around the blood vessels expressing VCAM-1 and CS1 but also on some cells spreading into the nodule. TGF-beta stained positively in principally the inflammatory cells at the perivascular periphery of nodules and these cells often showed VLA4 expression and colocalised with areas of strong CS1 fibronectin production.

Normal palmar fascia was used as control tissue. Only scanty amounts of CS1 fibronectin, virtually no VCAM-1 and only occassional VLA4 or TGF-beta positively stained cell were expresssed in our control tissue.

Discussion: Dupuytren's contracture demonstrates one mechanism for the accumulation of a subgroup of inflammatory cells in a chronic inflammatory condition by the presence of their endothelial adhesion molecules and extracellular matrix ligands, and their subsequent production of TGF-beta. If the differential expression of such integrins and adhesion molecules can be altered then it would represent a therapeutic option.

PREVALENCE OF IMPINGEMENT IN THREE TYPES OF PROSTHESES

R M Hall, P Siney, A Unsworth and B M Wroblewski
Academic Department of Orthopaedic Surgery, Clinical Sciences Building, St James's University Hospital, Leeds, LS9 7TF

The primary cause of loosening in total hip arthroplasty is often reported as being debris induced osteolysis. However, impingement has also been postulated as a cause of loosening1. The aim of this study was to investigate the incidence of impingement, by observing the prevalence of rim damage, in three types of socket design retrieved at revision surgery.

Method: One hundred and eighty McKee-Arden, Howse and Charnley acetabular components were retrieved at the time of revision surgery. One hundred and fifty eight of these sockets were found to be loose at re-operation. The prostheses were ranked depending on the degree of encapsulation; 1 for the McKee-Arden, 2 for the Charnley and 3 for the Howse prostheses. A visual inspection of each of the sockets was undertaken to determine the presence of rim damage due to impingement. The penetration depth and the radius of the femoral neck and head were recorded. Patient details were taken from clinical records. Penetration depth was measured by using the shadowgraphic technique2. The presence of rim damage does not necessarily mean that the socket failed due to the impingement process, though its absence does eliminate impingement as being a cause of loosening.

Results: Seventy-three per-cent (95 % confidence interval; 63-81), 40 % (95 % CI 21-61) and 66 % (95 % CI 46-82) of the sockets were found to have evidence of impingement for the Charnley, McKee-Arden and Howse prostheses, respectively. The differences between means were found to be significant for the Charnley – McKee-Arden comparison (P = 0.004) and marginally so for the Howse – McKee-Arden cohorts (P = 0.09). Modelling using logit regression indicated that the prevalence of rim damage was dependent on the penetration depth (z = 3.86; P < 0.001), the degree of encapsulation (z = 2.65; P = 0.008) and the ratio of the femoral head and neck radius (z = -2.235; P = 0.025).

Discussion: The probability of rim damage was observed to be highly dependent on the depth of penetration and specific design. In particular the degree to which the head is encapsulated by the socket, a measure used to prevent

dislocation, was deemed to be important. The level of impingement-induced loosening occurring *in vivo* across the different cohorts needs close scrutiny. Firstly, fewer than 40 % of the McKee-Arden and 75% of the Charnley sockets showed any incidence of rim damage and, as been alluded to earlier, not all of those sockets that do have rim damage will have failed through impingement. Of additional importance is the result that the level of rim damage is dependent on the penetration depth. This observation favours large femoral head prostheses that have low rates of penetration at the expense of high levels of debris generation. However, such a theoretical advantage is not conferred in practice. Further evidence to support or refute these claims may be forthcoming by comparisons of rim damage in post-mortem retrieved components and the analysis of long-term survivorship studies.

References:
1. BM Wroblewski. *J Bone Joint Surg* 1985:67B:757
2. RM Hall et al. *Proc Inst Mech Eng* 1995:209H:233

TIME AND CONCENTRATION DEPENDENT EFFECTS OF POLYETHYLENE PARTICLES AT THE BONE-IMPLANT INTERFACE

R.A. Brooks, J.R. Sharpe, B.J. Myer, E.N. Dawes and N. Rushton
Orthopaedic Research Unit, University of Cambridge, Box180, Addenbrooke's Hospital, Hills Road Cambridge, CB2 2QQ

Introduction: We have previously described a model of aseptic loosening where a ceramic pin is implanted in a load bearing position in the rat tibia.[1] We subsequently improved our ability to investigate the response of the bone-implant interface to injected particulate materials in this model by developing a method for determining alkaline phosphatase and tartrate-resistant acid phosphatase activities in peri-prosthetic tissues.[2] The study reported here was carried out to investigate the effect of different concentrations of high density polyethylene particles at the bone-implant interface at two time points following their intra-articular injection.

Materials and Methods: Forty eight adult male Sprague Dawley rats were randomly allocated to one of four groups. Pins were implanted unilaterally in the right tibia of all animals and the wound allowed to heal. Intra-articular injections of high density polyethylene particles (mean diameter (s.d.=4.5 (2.6(m) at concentrations of 1(104, 1(106 and 1(108 per joint or saline as a control were given into both hind legs at 8, 10 and 12 weeks following implantation. Six animals from each group were killed 14 weeks after surgery and the remaining animals after 26 weeks. The tibia were fixed and mounted in methyl methacrylate resin. For histomorphometry 200(m longitudinal sections were cut, ground, polished and surface stained using toluidine blue. The area of the gap between bone and pin, including any fibrous tissue, was measured using image analysis to determine quantitatively any response to particle concentration. For enzyme histochemistry, resin was removed from sections by placing them in acetone and sections were re-hydrated. Staining for alkaline phosphatase and tartrate-resistant acid phosphatase was carried out as previously described.[2]

Results: There was a clear trend between increased particle concentration and increased area of the gap between implant and bone at 14 weeks but not at 26 weeks. The mean area of the gap between pin and bone (SEM (mm2) was 0.45 (0.13 (saline control), 0.44 (0.13 (104 particles), 0.70 (0.21 (106 particles) and 1.34 (0.71 (108 particles) at 14 weeks and 0.60 (0.30 (saline control), 0.68 (0.59 (104 particles), 0.61 (0.08 (106 particles) and 0.49 (0.15 (108 particles) at 26 weeks. Tartrate-resistant acid phosphatase activity and alkaline phosphatase activity were found around the implant predominantly at the fibrous tissue/bone boundary immediately below the pin head and around the top of the pin shaft.

Discussion: The increase in gap between implant and bone with increasing particle concentration suggests that there is a concentration dependent osteolytic response in the peri-prosthetic tissues. The fact that this is not seen at 26 weeks indicates that repair of these lesions may subsequently occur. The presence of alkaline phosphatase and tartrate-resistant acid phosphatase activity in the peri-prosthetic tissues shows that active bone remodeling is taking place. It

will be interesting to compare the relative activities of these two enzymes around pins from animals treated with varying particle concentrations and at the two time points.

References:
1. M. Allen, F. Brett, P. Millett, N. Rushton *J Bone Joint Surg* 1996;78B:32-37
2. R.A. Brooks, E.N. Dawes, A. Robertson, B. Myer, N Rushton *J Bone Joint Surg* 1997:79B:SuppIV:463

TRIBOLOGICAL PERFORMANCE OF THE PCA TOTAL HIP REPLACEMENT

A.P.D. Elfick, R.M. Hall, I.M. Pinder* and A Unsworth
Centre for Biomedical Engineering, University of Durham, DH1 3LE
*Freeman Hospital, Newcastle-upon-Tyne, NE7 7DH

The introduction of cementless THRs in the 1980's was in response to the perceived problem of osteolysis due to cement debris. It is now commonly accepted that osteolysis may be promoted as a foreign body reaction to any particulate biomaterial. The PCA THR has been shown to give comparable results to cemented designs in the short term. However, beyond six years results become affected by a tendancy towards osteolysis of the acetabular component1. We present the summarised results of a two year research project into the tribology of the PCA THR: the wear, friction and degradation of the surface finishes.

Methods: One hundred were retrieved at revision surgery. Patient notes were available for 79 of these joints from 68 individuals, 36 of which were men. 40 of the 79 were from the right side. Median age at primary surgery was 44.05 (range 15.8-75.5) years and mean patient mass was 70.1 (SD 14.2)kg. The mean implant duration was 5.89 (SD 3.37) years. Initially the wear was assessed in 82 acetabular components using the shadowgraph technique.[2] Friction testing was conducted on 22 joints using the Durham Hip Function simulator.[3] Also the surface roughness values of both the articulating surfaces (55 femoral heads and 67 acetabular liners) were quantified by non-contacting profilometry.

Results: It was noted that of the snaplock type liners of a combination of 32mm head and 46/49mm diameter backing or 26mm head with 40/43mm backing that were retrieved, 68% had experienced fracture of the UHMWPE at the locking mechanism. The mean total wear volume was found to be 640 (SE 88)mm3. The mean wear rate and clinical wear factor of 99 (SE 12)mm3/year and 2.1 (SE 0.3)x10-6mm3/Nm were calculated using weighted linear regression for a sample of 59 joints all of a 32mm femoral head diameter.[4] The frictional characteristics of the explanted joints were not found to be significantly different from those of unused joints of the same design. The surface topography results showed a deterioration of the femoral head finish. The Rq increased from a median of 3.99 (IQRange 3.09)nm at the periphery to 16.4 (IQRange 18.3)nm in the articulating region. The UHMWPE acetabular liners became very polished in the articulating region. The root mean square deviation of the waviness, Wq, fell from a median of 971 (IQRange 947)nm to 104 (IQRange 206)nm. No correlation was found between any of the surface roughness parameters for head or liner and any wear parameter.

Discussion: The cementless fixation used seems more successful in the femoral component. This may be due to the greater ability of the bone in the intertrochanteric area to create osseointegration5 or the greater ease of debris migration in the acetabular component. The high incidence of liner fracture with combinations of large femoral heads with small acetabular components should come as no surprise. The use of a joint which, at implantation, has an effective UHMWPE thickness of less than 3mm should be avoided. The use of smaller head sizes, or cemented fixation, would allow a thicker acetabular component. In terms of the wear rate the PCA erodes UHMWPE at approximately twice the 55 mm3/year of the Charnley joint.[2] However, the two joints exhibit a similar clinical wear factor suggesting that this difference may be attributed entirely to the larger head size and younger, more active, patients of the PCA joint. Also the Charnley and PCA joints have similar mean wear volumes at retrieval suggesting the existence of a threshold wear volume capable of promoting osteolysis. The lack of cement ingression in the PCA is testified to by the unchanged frictional character-

istic. This contrasts to the Charnley were the friction is observed to rise significantly.[3] This is also reflected by the reduced increase in head roughness seen in the PCA compared with the Charnley.[2]

Conclusions: If used with an equivalent head size and patient group, a cementless system such as the PCA should be capable of delivering comparable results to those of cemented systems such as the Charnley. However, issues such as UHMWPE thickness and the routes provided for debris migration must be given further consideration.

1. Owen et al *JBJS* 76B:258.
2. Hall et al. Part H: *J Eng Med* (210),197.
3. Hall et al. *Wear* 175,159.
4. Elfick et al. accepted for pub. *J.Arth.*
5. Wroblewski Part H: *J Eng Med* (211),109.

The following absracts were presented at the Autumn 1997 meeting.

THE EFFECTS OF CEFUROXIME, CIPROFLOXACIN, FLUCLOXACILLIN AND VANCOMYCIN ON HUMAN OSTEOBLAST-LIKE CELLS *IN VITRO*

M Oyama, ME Emerton, MJO Francis and AHRW Simpson
The Nuffield Department of Orthopaedic Surgery, University of Oxford

Introduction: Prolonged treatment with antibiotic at high dose is often required for the successful management of open fractures, osteomyelitis and of deep infection following joint replacement. However, the effects of high levels of antibiotics on bone cell function is largely unknown. There is one report of Ciprofloxacin having an adverse effect on Osteoblast function *in vitro* at levels close to those seen *in vivo*. (Miclau et al. Proc. ORS 199 p.108). The aim of this study was to examine the effects of the antibiotics most widely used in orthopaedics, on human bone cell function using our established culture methods for human bone derived osteoblast-like cells (HOB).

Methods: HOB were isolated and grown as previously described and 0 - 1 mg/ml of Cefuroxime, Ciprofloxacin, Flucloxacillin and Vancomycin added to first passage HOB cultured in the presence of 100 µg/ml ascorbate-2-phosphate and 10 ng/ml dexamethasone but without the usual penicillin/streptomycin supplements. After 4 days HOB Alkaline Phosphatase Activity (ALP), total DNA content and ³H - Thymidine incorporation were assayed.

Results: Vancomycin had little or no effect on these parameters of HOB metabolism up to 1 mg/ml. ALP activity was largely unaffected by Cefuroxime or Ciprofloxacin even at levels of 100 µg/ml Ciprofloxacin and 1 mg/ml Flucloxacillin. ³H - Thymidine incorporation was significantly decreased (p < 0.05) at 40 µg/ml Ciprofloxacin, 80 µg/ml Cefuroxime and 400 µg/ml Flucloxacillin.

Table 1. Levels at which a significant reduction was found compared with controls

Antibiotic	Alkaline Phosphatase	Total DNA	H Thymidine
Ciprofloxacin	> 100 µg/ml	100 µg/ml	40 µg/ml
Cefuroxime	> 100 µg/ml	200 µg/ml	80 µg/ml
Flucloxacillin	> 1000 µg/ml	1000 µg/ml	400 µg/ml
Vancomycin	> 1000 µg/ml	> 1000 µg/ml	> 1000 µg/ml

Conclusions: Levels of 20 - 40 µg/ml Ciprofloxacin, 40 - 80 µg/ml Cefuroxime and 200 - 400 µg/ml Flucloxacillin are therefore potentially toxic to human bone. Such levels may be achieved in clinical practice particularly with local delivery techniques such as antibiotic impregnated cement or beads. Use of these antibiotics should therefore be considered as potentially deleterious to bone union, regenerate formation or remodelling around arthroplasty.

COMPARISON OF HEALING OF OSTEOCHONDRAL DEFECTS IN MEDIAL AND LATERAL FEMORAL CONDYLES OF RABBITS

YS Qui, BF Shahgaldi, FW Heatley.
Orthopaedic Academic Unit (UMDS), The Rayne Institute, St. Thomas's Hospital, London, SE1 7EH

Introduction: The medial and lateral femoral condyles of the knee joint are different as regards to their anatomy, joint surface contact areas and contact stresses.[1-3] Do these differences affect healing of osteochondral defects is a question often asked at conferences and by reviewers of research papers. To our knowledge it is not known and researcher often fail to draw distinction between the two different condyles. Moreover, if the two condyles are the same one can be used as control for the other. In our

experience this is surgically achievable and economically beneficial. This study compared healing osteochondral defects in femoral condyles of rabbits after 8 and 16 weeks.

Materials and Methods: Osteochondral defects of 3 mm diameter and 3 mm deep were drilled in the medial and lateral femoral condyles of left knees of 24 rabbits. The right knees were kept intact as normal controls. The repair produced was examined after 8 and 16 weeks using microfocal-radiography, histology, electron microscopy, surface indentation and pressure measurements. The thickness of repair tissue replacing cartilage was also measured. Semiquantitative grading of tissues filling defects was carried out using the histological grading scale described by Pineda.[4] *Mann-Whitney U test* was used to demonstrate significance of differences between groups. Unpaired *student t-test* was used to determine significance of differences between mechanical test results.

Results: After 8 weeks, all defects were similarly filled with regenerate tissue in the medial and lateral condyles. Radiographs revealed incomplete healing of the subchondral bone. Microscopically, predominant tissues of repaired surfaces were fibrocartilagenous and fibrous. Subchondral bone plate was not restored. Histological grading scores did not show any significant difference between lateral and medial condyles (p > 0.05) and remained significantly different from that of the normal control cartilage (p < 0.01). At 16 weeks, the amount of bone filling all defects increased from 8 to 16 weeks. The intensity of safranin-O staining decreased during the same period. No significant difference was found in the histological grading and mechanical testing results between medial and lateral condyles (p > 0.05).

Conclusion: No significant difference was found in the quality of osteochondral defect healing between medial and lateral femoral condyles of rabbits.

References:

1. D.B. Kettelkamp and A.W. Jacobs. *JBJS* 1972;54(A): 349-356.
2. K.A. Athanasiou et al. *J Orthop Res* 1991;9:330-340.
3. D.I. Bylski-Austrow et al. *J Orthop Res* 1993;11: 796-804.
4. S. Pineda et al. *Acta Anat* 1992;143:335-340.